

# **Role of N-glycans and Cysteine Residues in the Assembly of Homotrimeric P2X<sub>1</sub> Receptors**

Dissertation  
zur Erlangung des Doktorgrades  
der Naturwissenschaften

vorgelegt beim Fachbereich der chemischen und pharmazeutischen  
Wissenschaften der Johann Wolfgang Goethe-Universität  
in Frankfurt am Main

von  
Sepandarmaz Aschrafi  
aus Teheran

Frankfurt am Main  
2002  
(DF1)

akzeptiert als Dissertation von dem Fachbereich der chemischen und pharmazeutischen Wissenschaften der Johann Wolfgang Goethe-Universität in Frankfurt am Main

Dekan: Prof. Dr. W. Müller

1. Gutachter Prof. Dr. G. Schmalzing

2. Gutachter Prof. Dr. G. Lambrecht

Termin der Disputation: 4. Juli 2002



Die vorliegende Arbeit wurde von Mai 1998 bis März 2001 am Pharmakologischen Institut für Naturwissenschaftler (Fachbereich der chemischen und pharmazeutischen Wissenschaften) der Johann Wolfgang Goethe-Universität in Frankfurt am Main angefertigt.

Mein besonderer Dank gilt meinem Doktorvater Prof. Dr. Günther Schmalzing für die Möglichkeit, diese Dissertation in seinem Arbeitskreis anfertigen zu können, seine wissenschaftliche Betreuung und seine freundschaftliche Unterstützung.

Mein Dank richtet sich außerdem an Prof. Dr. Günther Lambrecht für seine wertvolle wissenschaftliche Diskussion auf dem Gebiet der P2X-Rezeptoren.

Ich möchte mich ganz herzlich bei meinen lieben Kollegen, nämlich Cora Büttner, Mark Lohmann, Jürgen Rettinger, Sven Sadtler, Mathias Ganzo, Michael Sych, Vicky Kostenis und Bernd Failer für die Hilfsbereitschaft und die nette und sehr freundschaftliche Atmosphäre bedanken. Weiter danke ich ihnen für die Geduld, meine Morgenmuffeligkeit ertragen zu haben.

Außerdem danke ich allen Mitgliedern des Pharmakologischen Instituts für die freundschaftliche Gemeinschaft und die vielen kleinen Hilfestellungen.

Mein Dank gilt Bodo Laube für die wissenschaftliche Unterstützung, insbesondere die Fluoreszenzmikroskopie von GFP-P2X<sub>1</sub>.

Ich möchte mich insbesondere bei Anja und Armin Böttcher bedanken, die mich während des Studiums und Promotion immer unterstützt haben sowie für die Bereitstellung ihres Personal Computers zur Anfertigung dieser Arbeit.

Mein spezieller Dank gilt meinen Eltern Afsar Amiri und Ghodrat Aschrafi, sowie meine liebe Schwester Apameh für deren Liebe und Existenz.

Schließlich möchte ich mich bei meiner Lebensgefährtin Angelique Adriana Böttcher bedanken, ohne deren Liebe, Dasein und ständiger Umsorge diese Arbeit hätte nie fertiggestellt werden können.

Ich möchte diese Arbeit meinem Vaterland widmen.

DER MENSCH  
HAT DREI WEGE, KLUG  
ZU HANDELN. ERSTENS  
DURCH NACHDENKEN:  
DAS IST DER EDELSTE.  
ZWEITENS DURCH  
NACHAHMEN: DAS IST  
DER LEICHTESTE.  
DRITTENS DURCH  
ERFAHUNG: DAS IST  
DER BITTERSTE

Konfuzius

---

TABLE OF CONTENTS	I
1. INTRODUCTION AND AIM OF THE THESIS	1
1.1. Ion channels	1
1.1.1. The families of neurotransmitter-gated ion channels	1
1.1.2. The superfamilies of ion channels with two hydrophobic segments	2
1.2. Purinergic receptors (P-Receptors) and the role of ATP in signaling	3
1.2.1. Purinergic receptors	4
1.2.2. P2X receptors	5
1.2.2.1. Molecular physiology of P2X receptor subunits	6
1.2.2.2. Chromosomal localization of human P2X receptor genes	10
1.2.2.3. Pharmacological properties of P2X receptor subunits	12
1.2.2.3. Localization and possible physiological implications of P2X receptors in different tissues	15
1.2.2.4. Therapeutic aspects of P2X receptor function	17
1.3. Aspects of membrane protein synthesis and assembly	19
1.3.1. Assembly and disulfide bond formation of membrane proteins	20
1.3.2. N-glycosylation of membrane proteins	21
1.3.2. 1. Protein folding and core glycosylation in the ER	21
1.3.2.2. Oligosaccharide chains are terminally processed in the Golgi Apparatus	22
1.4. Aim of the thesis	24
2. MATERIAL AND METHODS	26
2.1. Compounds, materials and buffers	26
2.1.1. Compounds and materials	26
2.1.2. Media and buffer solution	28
2.1.2.1. Media and buffers used for cultivation of bacteria and genetic engineering	29
2.1.2.2. Incubation and washing media for oocytes	30
2.1.2.3. Buffers used for protein biochemistry	30
2.2. Animals and cells	32
2.2.1 <i>Xenopus laevis</i>	32

---

2.2.2	<i>E.coli</i> strains	32
2.3.	DNA sources	32
2.4.	Methods	33
2.4.1.	Genetic engineering	33
2.4.1.1.	Construction of cDNAs for tagged and mutant rat P2X <sub>1</sub>	34
2.4.1.2.	Construction of cDNAs for tagged, mutant and truncated rat P2X <sub>2</sub>	40
2.4.1.3.	Construction of cDNAs for tagged rat P2X <sub>5</sub> and rat P2X <sub>6</sub>	40
2.4.1.4.	Construction of cDNAs for P2X receptor chimera	41
2.4.1.5.	cRNA synthesis	42
2.4.2.	Preparation of ovary and maintenance of <i>Xenopus</i> oocytes	43
2.4.3.	Protein biochemistry	44
2.4.3.1.	Radioactive labeling of proteins	44
2.4.3.2.	Purification of His-tagged protein	45
2.4.3.3.	Glycosylation analysis	46
2.4.3.4.	Cross-linking with glutardialdehyde	46
2.4.3.5.	Dissociation of ion channels into lower complexes	46
2.4.3.6.	Sodium dodecylsulfate polyacrylamide gel electrophoresis (SDS-PAGE)	47
2.4.3.7.	Blue native polyacrylamide gel electrophoresis (BN-PAGE)	48
2.4.3.8.	Two-Dimensional Gel Electrophoresis	49
2.4.4.	Electrophysiology	50
3.	<b>RESULTS</b>	51
3.1.	Characterization of P2X receptors in <i>Xenopus laevis</i> oocytes	51
3.1.1.	Characterization of His-tagged P2X <sub>2</sub> subunits after expression in <i>Xenopus</i> oocytes	51
3.1.1.1.	Electrophysiological characterization P2X <sub>2</sub> constructs after expression in <i>Xenopus</i> oocytes	51
3.1.1.2.	Biochemical analysis of the glycosylation status of P2X <sub>2</sub> constructs	52
3.1.1.3.	Investigation of the quaternary structure of the P2X <sub>2</sub> receptor	55
3.1.1.3.1.	Cross-linking analysis	55
3.1.1.3.2.	Blue native PAGE analysis	57

---

3.1.1.4.	Oligomeric state of a His-P2X <sub>2</sub> deletion mutant	60
3.1.2.	Characterization of His-tagged P2X <sub>5</sub> receptors after expression in <i>Xenopus</i> oocytes	63
3.1.2.1.	Electrophysiological characterization P2X <sub>5</sub> receptors after expression in <i>Xenopus</i> oocytes	63
3.1.2.2.	Biochemical characterization of His-P2X <sub>5</sub> polypeptides after expression in <i>Xenopus</i> oocytes by SDS-PAGE	64
3.1.2.3.	Biochemical characterization of P2X <sub>5</sub> constructs after expression in <i>Xenopus</i> oocytes using BN-PAGE	66
3.1.3.	Characterization of His-tagged P2X <sub>6</sub> subunits after expression in <i>Xenopus</i> oocytes	69
3.1.3.1.	Electrophysiological analysis of oocytes expressing rat P2X <sub>6</sub> constructs	69
3.1.3.2.	Biochemical characterization of P2X <sub>6</sub> constructs after expression in <i>Xenopus</i> oocytes using SDS-PAGE	69
3.1.3.3.	Biochemical characterization of the His-P2X <sub>6</sub> protein after expression in <i>Xenopus</i> oocytes by BN-PAGE	71
3.1.4.	Characterization of P2X <sub>1</sub> and P2X <sub>2</sub> subunits after co-expression in <i>Xenopus</i> oocytes	72
3.1.4.1.	Biochemical characterization of P2X <sub>1</sub> and P2X <sub>2</sub> polypeptides after co-expression in <i>Xenopus</i> oocytes by SDS-PAGE	72
3.1.4.2.	Investigation of the quaternary structure of the P2X <sub>2</sub> /P2X <sub>1</sub> complex	75
3.1.4.2.1.	Cross-linking analysis	75
3.1.4.2.2.	BN-PAGE analysis of the P2X <sub>2</sub> /P2X <sub>1</sub> complex	76
3.1.5.	Characterization of P2X <sub>1</sub> subunits tagged with green fluorescent protein after expression in <i>Xenopus</i> oocytes	80
3.1.5.1.	Electrophysiological characterization GFP tagged His-P2X <sub>1</sub> constructs after expression in <i>Xenopus</i> oocytes	80
3.1.5.2.	Visualization of <i>Xenopus</i> oocytes expressing GFP tagged His-P2X <sub>1</sub> constructs by confocal fluorescence microscopy	81
3.1.5.3.	Biochemical characterization of GFP tagged His-P2X <sub>1</sub> constructs after expression in <i>Xenopus</i> oocytes by SDS-PAGE	82
3.1.5.4.	Investigation of the quaternary structure of the GFP-tagged P2X <sub>1</sub> fusion proteins	84
3.1.5.4.1.	Cross-linking analysis	84
3.1.5.4.2.	BN-PAGE analysis	85
3.1.6.	Characterization of P2X subunit chimeras after expression in <i>Xenopus</i> oocytes	88



---

3.1.6.1.	Biochemical characterization of P2X subunit chimeras by SDS-PAGE	89
3.1.6.2.	Blue native PAGE analysis of P2X subunit chimeras	91
3.1.6.3	Electrophysiological characterization of P2X subunit chimeras after expression in <i>Xenopus</i> oocytes	93
3.2.	Studies on the role of asparagines-linked glycosylation in the rat P2X <sub>1</sub> receptor function and expression	95
3.2.1.	Identification of the sites of N-linked glycosylation of rat P2X <sub>1</sub> receptor after expression in <i>Xenopus</i> oocytes	95
3.2.2.	Importance of N-glycans for P2X <sub>1</sub> receptor function and assembly	97
3.2.2.1.	BN-PAGE analysis of P2X <sub>1</sub> mutants lacking one or several consensus sequences for N-glycosylation	97
3.2.3.	Electrophysiological analysis of oocyte-expressed P2X <sub>1</sub> mutants lacking one or several consensus sequences for N-glycosylation	101
3.3.	Role of conserved cysteine residues for the function and expression of rat P2X <sub>1</sub> receptor	104
3.3.1.	P2X <sub>1</sub> receptor expression, subunit folding, and intracellular transport: effects of DTT in <i>Xenopus</i> oocytes	104
3.3.2.	Mutational analysis of the importance of conserved cysteine residues for the generation of P2X <sub>1</sub> receptors in <i>Xenopus</i> oocytes	106
3.3.2.1.	Effects of single cysteine substitutions on P2X <sub>1</sub> receptor expression and processing	106
3.3.2.2.	BN-PAGE analysis of P2X <sub>1</sub> mutants lacking one cysteine residue.	110
3.3.2.3.	Analysis of cell surface expressed P2X <sub>1</sub> receptor mutants lacking two or three cysteine residues	113
3.3.2.4.	BN-PAGE analysis of P2X <sub>1</sub> mutants lacking two or three cysteine residues	115
3.3.2.4.	Functional analysis of P2X <sub>1</sub> receptor mutants lacking one, two, or three cysteine residues	118
3.3.2.4.1.	Effects of cysteine substitution on ATP concentration response of P2X <sub>1</sub> Receptors	119
4.	<b>DISCUSSION</b>	121
4.1.	Investigation of P2X receptors after expression in <i>Xenopus</i> oocytes	121
4.1.1.	Homomeric assembly of P2X receptors after expression in <i>Xenopus</i> oocytes	121
4.1.2.	Role of carboxyl-terminal domain for the assembly of the P2X <sub>2</sub> receptor	122
4.1.3.	Heteropolymerization of P2X <sub>1</sub> and P2X <sub>2</sub> subunits in <i>Xenopus</i> oocytes	123
4.1.4.	Investigation of P2X <sub>6</sub> after expression in <i>Xenopus</i> oocytes	126
4.1.5.	Factors that regulate assembly and folding of P2X receptors	127

---

4.1.6.	Methods used to investigate the quaternary structure of P2X receptors	128
4.1.6.1.	Cross-linking of P2X receptors	128
4.1.6.2.	Biochemical analysis of the P2X receptor complexes by BN-PAGE	129
4.1.7.	Identification of regions that regulate desensitization of P2X receptors	130
4.2.	Investigation of P2X <sub>1</sub> -GFP fusion proteins	132
4.2.1.	Clustering of His-P2X <sub>1</sub> -GFP receptors	132
4.2.2.	Anchoring of P2X receptors in the membrane	133
4.3.	Role of N-glycans for the functional expression and assembly of the rat P2X <sub>1</sub> receptor	134
4.3.1.	N-glycans and membrane folding of P2X <sub>1</sub>	135
4.3.2.	Positional effects of N-glycans on surface expression of P2X <sub>1</sub> receptor	135
4.3.3.	Conservation of N-glycosylation sites among P2X isoforms	136
4.3.4.	N-glycans and ligand recognition	137
4.4.	Role of individual cysteine residues for the functional expression and assembly of the rat P2X <sub>1</sub> receptor	138
4.4.1.	Effects of the reducing agent DTT on His-P2X <sub>1</sub> expression and assembly	138
4.4.2.	Investigation of P2X <sub>1</sub> receptor mutants lacking cysteine residues	139
5.	<b>SUMMARY</b>	142
6.	<b>ZUSAMMENFASSUNG</b>	144
7.	<b>REFERENCES</b>	147
8.	<b>APPENDIX</b>	164
8.1.	Oligodeoxynucleotides	164
8.1.1.	Oligodeoxynucleotide primers used for site-directed mutagenesis	164
8.1.2.	Oligodeoxynucleotide primers used for sequencing	165
8.1.3.	Oligodeoxynucleotide primers used for insertion or deletion of a restriction site into constructs	166
8.1.4.	Oligodeoxynucleotide primers inserted into constructs	167
8.2.	Glossary of Abbreviation	167
9.	<b>BIBLIOGRAPHY</b>	170
10.	<b>CURRICULUM VITAE</b>	172

## 1. Introduction and Aim of the Thesis

### 1.1. Ion channels

Ion channels constitute a class of proteins that is ultimately responsible for generating and orchestrating the electrical signals passing through the thinking brain, the beating heart, and the contracting muscle (Ackerman & Clapham, 1997). They are macromolecular protein tunnels that span the lipid bilayer of the cell membrane. Small conformational changes gate a single channel from closed to open, allowing up to 10 million ions to flow into or out of the cell each second. A few pico amps ( $10^{-12}$  A) of current are generated by the flow of highly selected ions each time the channel opens. Since ion channels are efficient, their numbers per cell are relatively low; a few thousand of a given type is usually sufficient. Ion channels are usually classified according to the type of ion they allow to pass - sodium, potassium, calcium, or chloride - although some are less selective. They may be gated by extracellular ligands such as neurotransmitters (ligand-gated ion channels), or changes in transmembrane voltage (voltage-gated ion channels).

#### 1.1.1. The families of neurotransmitter-gated ion channels

Neurotransmitter-gated ion channels are receptors that rapidly mediate signaling across the synapse of the central and peripheral nervous system (Leite & Cascio, 2001). These ionotropic receptors are divided into families based on their high sequence homology and are classified as the ligand-gated ion channel superfamily (LGICS). One such subset is the nicotinic acetylcholine receptor family (Le Novere & Changeux, 1999), which includes the glycine receptors (GlyRs), the nicotinic acetylcholine receptors (nAChRs), the 5-HT<sub>3</sub> receptors, and the GABA receptors. Typically, these receptors assemble as heteropentamers of different gene products and/or splice variants. Biochemical analysis revealed that each of the ion channel subunits from this family share several features such as a conserved cysteine loop in the extracellular N-domain, four putative transmembrane regions (M1-M4), and a short extracellular C-terminus (Karlin, 1993). The second of the transmembrane

regions (M2) is the main contributor to the ion channel (Hucho *et al.*, 1986). Another family, the glutamate receptors (GluRs) are grouped into kainic acid,  $\alpha$ -amino-3-hydroxy-5-methyl-4-isoxazole propionic acid (AMPA), and N-methyl-D-aspartic acid (NMDA) subtypes based on amino-acid sequence and agonist pharmacology (Hollmann & Heinemann, 1994). The ionotropic glutamate receptors share similar channel properties and have analogous transmembrane domains like the nicotinic acetylcholine receptors, but the extracellular domain is bigger and has no obvious sequence identity with the nicotinic acetylcholine receptor family (Cockcroft *et al.*, 1993). The third family of ligand-gated ion channels, the P2X receptor family, has neither structural nor sequence homology with the first two superfamilies, but shares structural similarities with a family of ion channels with two hydrophobic segments as described in the next chapter (Nicke *et al.*, 1999).

### 1.1.2. The superfamilies of ion channels with two hydrophobic segments

Ion channels with two membrane-spanning domains per subunit fall into four main structural families (North, 1996). These are the inward-rectifier potassium channels (Kirs), epithelial sodium channels (ENaCs), the mechanosensitive channel of *Escherichia coli* (mscL), and the P2X receptors (reviewed in chapter 1.2). Inward-rectifier potassium channels comprise a large ion channel family. They have relatively long intracellular amino and carboxyl termini, short extracellular loops, and a pore-forming (P) region between the two transmembrane domains (Doupnik *et al.*, 1995). ENaC subunits have about 650–700 amino acids each, and contain two extended hydrophobic regions (M1 and M2) separated by a region of about 450 amino acids which contains 16 conserved cysteine residues (Garty, 1994). Quantitative analysis of cell surface expression of EnaC  $\alpha$ ,  $\beta$ , and  $\gamma$  subunits has indicated a tetrameric structure in which two  $\alpha$  subunits are separated by the  $\beta$ , and  $\gamma$  subunits (Firsov *et al.*, 1998). The mscL protein is 136 amino acids long, with two hydrophobic domains and a hydrophilic C-terminal domain. Its extracellular domain is extremely short and it does not have any significant sequence homology with members of the extended ENaC family, or with P2X receptors (Sukharev *et al.*, 1994). While previous data had suggested that the functional MscL complex might be a hexamer, a recent crystallographic study of the MscL homologue from *M.*

*tuberculosis* revealed a pentameric structure (Chang *et al.*, 1998). Additionally, in another study, MscL in the membrane could be chemically cross-linked. The cross-linking agents used at saturating concentrations invariably generated pentamers as the largest product (Sukharev & McCaslin, 1999).

## 1.2. Purinergic receptors (P receptors) and the role of ATP in signaling

The concept of chemical synaptic transmission began to develop over a century ago, when researchers showed that stimulation of certain peripheral nerves produced responses in their target organs. In most cases, the release of acetylcholine or noradrenaline mediated these responses in their target organs (Khakh, 2001). A role for extracellular purines had been described by Drury and Szent-Györgyi in 1929 (Drury & Szent-Györgyi, 1929) soon after the discovery of ATP (Embden & Zimmerman, 1927). ATP is an amphiphilic compound showing both hydrophilic and strong hydrophobic interfaces. Autonomic nonadrenergic and noncholinergic nerves (Burnstock *et al.*, 1963) were proposed to contain ATP, and a tentative model of storage and release was proposed (Burnstock, 1972). Nerve cells that employ ATP as their principal transmitter were termed “purinergic”. Adenine nucleotides are continually present in inconsistent amounts in the extracellular space of many organs. There is strong evidence supporting the idea that ATP is a cotransmitter in sympathetic nerves. Other possible sources of the nucleotide include the following: 1) ischemic myocytes (Williams & Forrester, 1983), 2) activated platelets (Holmsen, 1985), 3) nerve terminals (Holton, 1995), 4) inflammatory cells (Di Virgilio *et al.*, 1996), 5) erythrocytes (Bergfeld & Forrester, 1992), 6) endothelial cells (Bodin & Burnstock, 1996), and 7) smooth muscle cells (Katsuragi *et al.*, 1991). The mechanism by which ATP is transported across the cell membrane or released from muscle cells is not fully understood. In living cells, the electrochemical gradient supporting ATP efflux is near nine orders of magnitude (versus 6 for  $\text{Ca}^{2+}$ ) considering intra- and extracellular ATP concentrations to be 10 mM and 10 nM, respectively. Thus, membrane permeability to ATP should be very low, which is in agreement with the negative charge of ATP (Vassort, 2001). ATP can be released by exocytosis from platelets and nerves like other neurotransmitters. It can also leak out during cell lysis (Gordon, 1986; Dubyak *et al.*, 1993).

### 1.2.1. Purinergic receptors (P receptors)

In 1971, Burnstock proposed the existence of nerves that use purines as a transmitter. Meanwhile it is widely accepted that purines (ATP, ADP and adenosine) and pyrimidines (UTP and UDP) act as extracellular messengers via plasma membrane receptors termed purinergic receptors (P receptors) (Stojilkovic, 2001). There are two main groups of purinergic receptors: adenosine-activated P1-receptors (also called A receptors) and ATP-, ADP-, UTP- and/or UDP-activated P2 receptors (P2 receptors). This classification was originally introduced by Burnstock (1978). Molecular, physiological and pharmacological data propose the existence of four mammalian A-receptor subtypes (denoted A1-, A2A-, A2B-, and A3-receptors), which all signal through G-protein-dependent pathways.

P2 receptors belong to one of two families: G-protein-coupled receptors (P2Y receptors), originally identified by Dubyak (1991), and ligand-gated P2X ion channels (P2X receptors), identified by Benham & Tsien (1987). P2Y receptors are seven-membrane-spanning proteins, 328 to 379 amino acids long corresponding to molecular masses of 41 to 53 kD after glycosylation (Ralevic & Burnstock, 1998; Webb *et al.*, 1993). The N-terminal domain is located on the extracellular environment, and the C terminus is on the cytoplasmic side of the plasma membrane. Signal transduction takes place via the pathways used also by other seven-membrane-spanning receptors: activation of phospholipase C and/or stimulation/inhibition of adenylate cyclase. All of the P2Y receptors are triggered by ATP, but at two of them, P2Y<sub>4</sub> and P2Y<sub>6</sub>, UTP is more potent (Communi *et al.*, 1996 a & b; Chang *et al.*, 1995), and at P2Y<sub>2</sub> ATP and UTP are equipotent (Lustig *et al.*, 1993). At P2Y<sub>1</sub> receptor, UTP is inactive and ADP is reported to be equipotent or even more potent than ATP (Henderson *et al.*, 1995), at P2Y<sub>11</sub> receptor ATP is more potent than ADP and UTP is inactive (Communi *et al.*, 1997). With respect to the signal transduction pathway, P2Y<sub>1</sub> and P2Y<sub>2</sub> receptors are coupled to stimulation of phospholipase C and inhibition of adenylate cyclase via G<sub>q/11</sub> and G<sub>i</sub> proteins, respectively (Ralevic & Burnstock, 1998). P2Y<sub>4</sub> and P2Y<sub>6</sub> receptors appear to only couple to phosphoinositide breakdown, whereas P2Y<sub>11</sub> receptor rather stimulates activation of both the phosphoinositide and the adenylate cyclase pathways (Qi *et al.*, 2001).

## 1.2.2. P2X receptors

P2X receptors are ATP-gated ion channels first characterized in and cloned from excitable cells (Brake *et al.*, 1994; Valera *et al.*, 1994) and then reported to be nearly ubiquitous expressed (Soto *et al.*, 1997). P2X receptors mediate fast permeability changes to monovalent and divalent cations ( $\text{Na}^+$ ,  $\text{K}^+$ , and  $\text{Ca}^{2+}$ ).

### 1.2.2.1. Molecular physiology of P2X receptor subunits

Currently, seven ATP-gated P2X receptor subunits are known (Table 1.1), which are encoded by different genes (Buell *et al.*, 1996). Each subunit has a topology that is different from that of other identified ligand-gated channels. The seven P2X isoforms comprise 379–595 amino acids in length.

**Subunit topology.** The P2X polypeptides possess two hydrophobic transmembrane domains with a large extracellular hydrophilic loop and two intracellularly located termini (Fig. 1.1). The extracellular domain starts approximately at position 52 and ends near the proline at position 329.

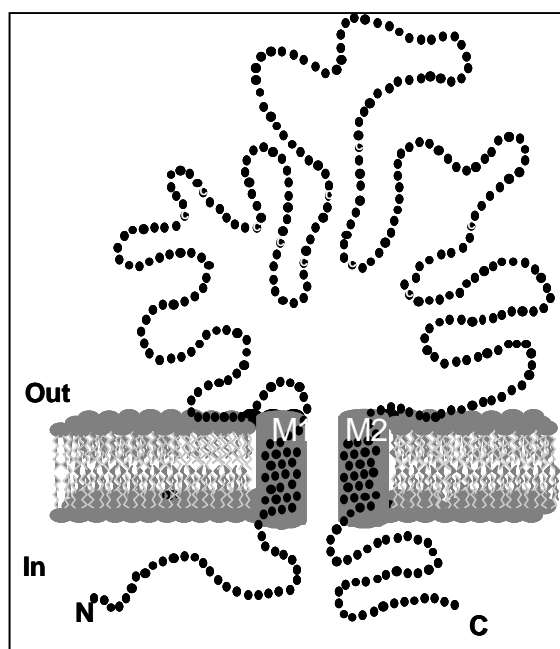


**Fig. 1.1:** Schematic representation of a P2X receptor subunit comprising intracellular N- and C-termini, two transmembrane spanning domains (M1 and M2) and a large extracellular loop containing 10 conserved cysteine residues, which may form disulfide bonds.

**The N-terminal domain.** The amino-terminal tails of P2X subunits are relatively short, comprising about 20-30 amino acids. All of the P2X subunits contain in their N-domain a protein kinase C site, which was shown to be important for P2X<sub>2</sub> function=([Boue-Grabot et al., 2000](#)).

**The C-terminal domain.** The C-terminal domain of P2X subunits differs markedly in length from 28 (P2X<sub>4</sub>) to 242 (P2X<sub>7</sub>) residues. Deletions, mutations or splicing of this region have been shown to affect the kinetics, permeations and desensitization of P2X channels ([Brandle et al., 1997](#); [Smith et al., 1999](#)).

**The extracellular domain.** Between the transmembrane segments, there is an extracellular region with ten cysteine residues (Fig 1.2), which are fully conserved among all seven P2X isoforms ([Newbolt et al., 1998](#); [Torres et al., 1998 a](#)). 63 residues are fully conserved, of which 15 are glycine residues (Fig 1.3). In addition, many residues are almost completely conserved. The extracellular domain is separated into two disulfide cross-linked domains ([Hansen et al., 1997](#)). Alterations in ATP potency was observed upon by systematic mutagenesis of extracellularly located, positively charged amino acids of human P2X<sub>1</sub> receptor and a subset of basic amino acids (<sup>68</sup>K, <sup>70</sup>K, <sup>292</sup>R) were found to contribute to the ATP potency ([Ennion et al., 2000](#)). Additional analysis proposes that the ATP binding site is located in a region near the lysine residues at positions 69 and 71 ([Jiang et al., 2000](#)). Consensus sites for N-linked glycosylation (Asn-X-Ser/Thr) are found in the extracellular loop of all P2X isoforms. Interestingly, some of these sites are well conserved in mouse, rat, and human clones of the P2X family ([Rettinger et al., 2000](#)), suggesting that the binding of carbohydrate moieties to the protein may be important for the expression or the function of the channel. Nicke (1998) reported that only four of the five putative N-glycosylation sites are used when of the rat P2X<sub>1</sub> subunit is expressed in *Xenopus* oocytes (Fig. 1.2).



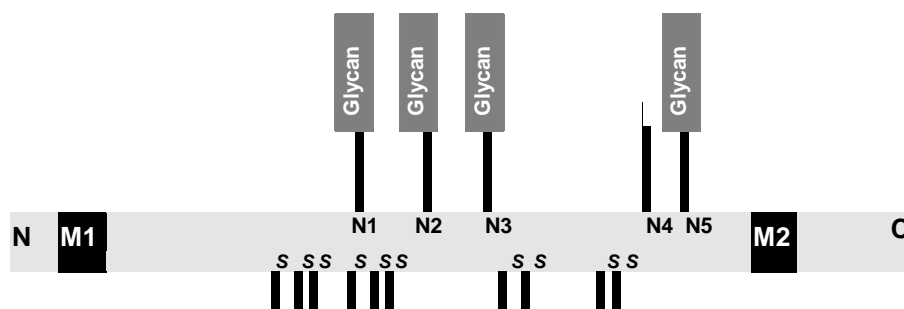


**Fig.1.2: Linear model of rat P2X<sub>1</sub> showing approximate positions of N-glycosylation sequons and cysteine residues.** N, cytoplasmic N terminus; M1 and M2, membrane spanning segments; N1-N5, asparagine residues of NXT/S tripeptides at position 153 (N1), 184 (N2), 210 (N3), 284 (N4), and 300 (N5). The 10 cysteine residues (S) which are conserved among all seven P2X isoforms and which are assumed to form five intra-molecular disulfide linkages are also indicated; an additional conserved cysteine residue (not shown) is located in M2 (Rettinger *et al.*, 2000).

**The P2X receptor pore.** P2X receptors are generally cation-selective channels with significant permeability to Ca<sup>2+</sup> and equal permeability to Na<sup>+</sup> and K<sup>+</sup> (Evans *et al.*, 1996). The substituted cysteine accessibility method has been employed to identify parts of the molecule that contribute to the ionic pore of the P2X<sub>2</sub> receptor (Rassendren *et al.*, 1997). <sup>338</sup>L and <sup>349</sup>D, amino acid residues conserved among all the seven P2X receptors, are on either side of the channel gate with <sup>349</sup>D positioned near the middle of the channel (Fig. 1.3). Thus, it might be possible that <sup>349</sup>D is the site of permeant cation binding and responsible for ionic selectivity (Ding & Sachs, 1999). The asparagine residue <sup>333</sup>N was shown to regulate the conductance. The unitary conductance of 80 pS in 100 μM Na<sup>+</sup> was approximately halved when this asparagine was substituted by isoleucine (N<sup>333</sup>I) (Nakazawa *et al.*, 1998). In P2X<sub>2</sub> receptors, the second transmembrane domain (TM2), which appears to line the pore, has a α-helical conformation (Egan *et al.*, 1998).

Remarkable permeation properties were observed for P2X<sub>7</sub> receptors, that change their permeability to organic cations on a timescale of seconds (Suprenant *et al.*, 1996). Changes in permeability are further observed for heterologously expressed P2X<sub>2</sub> and P2X<sub>4</sub> receptors or native P2X receptors in neurons, as measured electrophysiologically or with dye uptake studies (Khack *et al.*, 1999; Rassendren *et al.*, 1997)

**The stoichiometry of P2X receptors.** P2X<sub>2</sub> and P2X<sub>3</sub> subunits co-assemble to form a distinct heteromeric channel (Lewis *et al.*, 1995; Radford *et al.*, 1997) with specific properties (Virginio *et al.*, 1997 & 1998). Likewise, heteromeric assembly was suggested by *in situ* hybridization studies for P2X<sub>1</sub> and P2X<sub>5</sub> isoforms, P2X<sub>2</sub> and

P2X<sub>6</sub> isoforms, and P2X<sub>4</sub> and P2X<sub>6</sub> isoforms (Torres *et al.*, 1998 a; Collo *et al.*, 1996; King *et al.*, 2000). P2X<sub>4</sub> and P2X<sub>7</sub> subunits do not form heteromers, whereas P2X<sub>6</sub> subunit needs to be associated in heteromers either with P2X<sub>1, 2, 4, 5</sub> subunits to form an active channel.

From gel filtration experiments with the recombinant P2X<sub>2</sub> extracellular loop, it has been deduced that the P2X<sub>2</sub> receptor exists as a tetramer (Kim *et al.*, 1997). In contrast, using cross-linkers and the blue native PAGE analysis, it was shown that full length P2X<sub>1</sub> and P2X<sub>3</sub> receptors form stable trimers (Nicke *et al.*, 1998). By investigating single channel properties of P2X<sub>2</sub> receptor, Ding & Sachs (1999) found that the channel proceeds through three ATP binding steps before opening and that the three ATP binding sites are not independent, but positively cooperative, supporting the view for a trimeric structure for this receptor.

**M1**

rP2x1 -MARRLQDELSAFFFEYDTPRMVLVRNKKVGVIFRLIQLVVLVYVIGWVVFVEKGYQTSS-DLISSVSVKLGAVTQL-----QGLGPQVWDVADYV 91  
 rP2x2 -MVRRLARGCWSAFWDYETPKVIVVRNRRLGFVHRMVLQLLIIILLYFVWYVFIQKSYQDSETPPESSIIITKVKGITMS-----EDKVWDVEEYV 87  
 rP2x3 -----MNCISDFFTYETTKSVVVKSWTIGIINRAVQLLIISYFVGVWFLHEKAYQVRDTAIESSVVTKVKGFGR-----YANRVMDVSDYV 81  
 rP2x4 --MAGCCSVLGSFLFEYDTPRIVLIRSRKVGMLNRAVQLLILAYVIGWVFWVEKGYQETD-SVSSVTTKAKGVAVTNT-----SQLGFRIDWDVADYV 90  
 rP2x5 -MGQAAWKGFVLSLFDYKTAKFVVAKSKKVGLLYRVLQLIILLYLLIIVVFLIKKSYQDIDTSLQSAVVTKVKGVAYTNT-----TMLGERLWDVADFV 92  
 rP2x6 MASAVAAALVSWGFLDYKTEKYVMTRNCWVGISQRLQLQGVVYVIGWALLAKKGYQEWDMDPQISVITKLGVSVTQV-----KELEKRLWDVADFV 93  
 rP2x7 ----MPACCSWNDVFQYETNKVTRIQSVNYGTIKWILHMTVFSYVS-FALMSDKLYQRKE-PLISSVHTKVKGVAEVTENVTEGGVTKLVHGFIDTADYT 94

rP2x1 FPAHGDSSFFVMTNFIVTPQQTQGHCAENP-EGG-ICQDDSGCTPGKAERKAQGIRTGNCVPFNGTVK-TCEIFGWCPVEVDDKIPSPALLREAENFTLF 188  
 rP2x2 KPPEGGSVVSIITRIEVTSPQTLGTCPESEMRVHSSTCHSDDDCIAGQLDMQNGIRTGHCVYYHGDSKTCEVSAWCPVEDGTSDN-HFLGKMAPNFTIL 187  
 rP2x3 TBPQGTSVFVITTKIIVTENQMQGFCPENE--EKYRCVSDSQC--GPERFPGGGILTGRVCNYSSVLR-TCEIQGWCPTEVDTVEM--PIMMEAENFTIF 176  
 rP2x4 IPAQEENSLFIMTNMIVTVNQTSQTCPEIP-DKTSICNSDADCTPGLRDTHSSGVATGRCPVFNESVK-TCEVAAWCPVENDVGVPPTPAFLKAAENFTLL 188  
 rP2x5 IPSQGENVFFLVNLIIVTPNQQRQICAEEREGIPDGECSDDCHAGESVVAHGHLKTRCLRVGNSTRGTCEIFAWCPVETKSMPTD-PLLKDAESFTIF 192  
 rP2x6 RPSQGENVFFLVNLIIVTPAQVQGRCPPEHPSVPLANCWADEDCPEGEMGTYSHGIKTGQCVAFNGTHR-TCEIWSWCPVESAVPRK-PLLAQAKNFTLF 192  
 rP2x7 LPLQG-NSFFVMTNYLKSEGQEQKLCPEYP-SRGKQCHSDQGCICKGWMDPQSKGIQTGRICIPYDQKRK-TCEIFAWCPAEEGKEAPRPALLRSAENFTVL 191

rP2x1 IKNSISFPRFKVNRNRLVEEVNGTYMKKCLYHKIQHPLCPVFNLGYVVRESQDFRSLAEKGGVVGITIDWKCDLDWHVRHCKPIYQFHGLYG---EKNL 288  
 rP2x2 IKNSIHYPKFKFKSGKNIASQKSD-YLKHCTFDQSDPYCPIFRLGFIVEKAGENFTELAHKGGVIGVIINWNCDDLSESECNPKYSFRRLDP--KYDPA 285  
 rP2x3 IKNSIRFPLFNFEKGNLLPNLTDKDIKRCRFHPEKAPFCPIILRVGDVVKFAGDFAKLRTGGVGLGKIGWCDLDKAWDQCIPKYSFTRLDGVSEKSSV 274  
 rP2x4 VKNNIWPYKFNFSKRNILPNITTSYLKSCIYNAQTDPFPCPIFRLGTIVEDAGHSFQEMAVEGGIMGIQIKWDCNLDRAASLCLPRYSFRRLDTRDLEHNV 288  
 rP2x5 IKNFIRFPKFNFSKANVLETDNKHFLKTCFSSSTN-LYCFIFRLGSIWRWAGADFQDIALKGGVIGIYIEWDCDLKAASKCNPHYYFNRLDNK-HTHSI 290  
 rP2x6 IKNTVTFNKFNFSTRNALDNTYFKYCLYDSLSSPYCPVFRIGDLVAMTGGDFEDLALLGGAVGINIHWCNLDTKGSDCSPQYSFQ-LQE----- 291  
 rP2x7 IKNNIDFPGHNYTTRNILLPGMNI--S--CTFHKTWNPQCPPIFRLGDIQFQIENFTEVAVQGGIMGIEIYWDNLDNSWSHRQPKYSFRRLDDKYTNESL 287

**M2**

rP2x1 SPGFNFRFARHFVQNG-TNRRHLFKVFGIHFIDLVDGKAGKFDIIPMTTIGSGIGIFGVATVLCDLLLHILP-----KRHYKQK 384  
 rP2x2 SSGYNFRFAKYKINGTTTTTRTLIKAYGIRIDVIVHGQAGKFSLIPTIINLATALTSIGVGSFLCDWILLTFMN-----KNKLYSHK 383  
 rP2x3 SPGFNFRFAKYKMEGSEYRLLKAFGIRFDVLVYGNAGKFNIIPTIISVAAFTSVGVGTVLCDIILLNFK-----GADHYKAR 374  
 rP2x4 SPGFNFRFAKYRDLAGKEQRTLTKAYGIRFDIIVFGKAGKFDIIPMTINVGSGLALLGVATVLCDIVILYCMK-----KKYYYRDK 388  
 rP2x5 SSGYNFRFARYRDPNGVEFRDLMKAYGIRFDVIVNGKAGKFSIIPTVINIGSGLALMGAGAFFCDLVLIYLIR-----KSEFYRDK 389  
 rP2x6 -RGYNFRTANYWAAAGVESRSLKLYGIRFDILVTGQAGKFAIPTAITVGTGAAWLGMVTFLCDLLELLYVDR-----EAGFYWRT 382  
 rP2x7 FPGYNFRYAKYKENG-MEKRTLKAFGVRFDILVFGTGGKFDIQLVYVIGSTLSYFGLATVCIDLINTYASTCCRSRVYPSCKCCEPCAVNEYRYRK 386

rP2x1 KFKYAEDMGPGEGEHDPVATSSTLGLQENMRTS **399**  
 rP2x2 KFDKVRTPKHP **SSRW**PVTL**ALVLGQIPPPP**SHYSQD**PPSP**SGEGPTLGEGAEPLAV**QSPR**PCISALTEQVVDTLGQHMGQRPPVPEPSQDSTSTDPKGLAQL **472**  
 rP2x3 KFEVETETTLKGTASTNPVFASDQATVEKQSTDSGAYSIGH **397**  
 rP2x4 KYKYVEDYEQQLSGEMNQ . **388**  
 rP2x5 KFEKVRGQKEDANVEVEANEME**QE**QPEDEPLERVRQDEQS**QEL**AQSGRKQNSNCQVLLPARFGLRENAIVNVK**QS**QILHPVKT **455**  
 rP2x6 KYEEARAPKATNSA **379**  
 rP2x7 KCEPIVEPKPTLKYSVDFVDEPHIWMVDQQLLGKSLQDVKGQEVPRPQTD**FLE**LSRLSLSLHHSPP**IP**GQPEEM**QL**LQIEAVPRSRD**SP**WCQCGNCLPSQ 436  
 rP2x7 LPENRRAL**EEL**CCRRKPGQCITTS**EL**FSKIVLSREAL**QL**LLLYQ**EP**LLALEGEAINSKLRHCAYRSYATWR**FV**SQDMAD**FA**IL**PS**CCR**WK**IRKE**FP**KTQ**G**QYS**G**FKYPY **595**

**Fig. 1.3: Amino acid sequence alignment of the cloned rat P2X receptor subunits.** The alignment was made using ClustalW software (<http://searchlauncher.bcm.tmc.edu>). Identical amino acids are highlighted by shaded boxes. The triangles indicate the conserved cysteine residues. The rectangle indicates the sole consensus sequence for N-glycosylation that is conserved among all isoforms except P2X<sub>5</sub>. The two putative transmembrane domains (M1 and M2) are indicated by horizontal bars. Proposed recognition sequences for serine kinases and two proline rich sequences that could associate with the SH3 domains are dark shaded.

### 1.2.2.2. Chromosomal localization of human P2X receptor genes

The genes for the cloned human P2X receptors have been mainly mapped to three distinct chromosomes (for review see Soto *et al.*, 1997). Some of the P2X genes appear in clusters in a similar manner to several nAChR and GABA receptor subunit genes (Boulter *et al.*, 1990; McLean *et al.*, 1995). The hP2X<sub>3</sub> gene has been localized on chromosome 11, region q12 (Garcia-Guzman *et al.*, 1997). The hP2X<sub>5</sub> and the hP2X<sub>1</sub> genes are located on chromosome 17, region p13.3 (Valera *et al.*, 1995). The hP2X<sub>4</sub> and hP2X<sub>7</sub> genes are located on chromosome 12, region p24 (Garcia-Guzman *et al.*, 1997; Talabot *et al.*, 1997). By applying radiation hybridization mapping, it was attempted to correlate mutations in P2X receptors with human diseases and the localization of hP2X<sub>1</sub>, hP2X<sub>4</sub>, hP2X<sub>5</sub> and hP2X<sub>7</sub> genes has been linked to several polymorphic markers (Talabot *et al.*, 1997).

**Table 1.1: Listing of cloned P2X isoforms.** \* indicates splicing variants  
(Soto *et al.*, 1997)

Gene	Species / Tissue of cloning	Number of amino acids	Potential N-glycosylation sites	Accession numbers (GenBank)	Reference
P2X <sub>1</sub>	Rat vas deferens	399	5	X80477	Valera <i>et al.</i> , 1994
	Human urinary bladder	399	5	X83688	Valera <i>et al.</i> , 1995
	Human platelets	399	5	AF020498	Sun <i>et al.</i> , 1998
	Human heart*	348	5		Soto <i>et al.</i> , 1997
	Mouse urinary bladder	399	5	X84896	Valera <i>et al.</i> , 1995
P2X <sub>2</sub>	Rat PC12 cells	472	3	U14414	Brake <i>et al.</i> , 1994
	Rat pituitary*	361	3	L43511	Housley <i>et al.</i> , 1995
P2X <sub>3</sub>	Rat dorsal root ganglia	397	4	X90651	Chen <i>et al.</i> , 1995
	Human heart	397	4	Y07683	Garcia-Guzman <i>et al.</i> , 1997
	Mouse	397	4		Souslave <i>et al.</i> , 1997
P2X <sub>4</sub>	Rat hippocampus	388	5	X91200	Bo <i>et al.</i> , 1995
	Rat superior cervical ganglia	388	5	X87763	Buell <i>et al.</i> , 1996
	Rat brain	388	5	U32497	Seguela <i>et al.</i> , 1996
	Rat brain	388	5	X93565	Soto <i>et al.</i> , 1996
	Rat pancreatic islets	388	5	U47031	Wang <i>et al.</i> , 1996
	Human brain	388	5	Y07684	Garcia-Guzman <i>et al.</i> , 1997
	Human placenta	388	5		Talabot <i>et al.</i> , 1997
P2X <sub>5</sub>	Rat celiac ganglia	455	3	X92070	Collo <i>et al.</i> , 1996
	Rat heart	455	3	X97376	Garcia-Guzman <i>et al.</i> , 1996
	Human fetal brain	398	2		Talabot <i>et al.</i> , 1997
P2X <sub>6</sub>	Rat superior cervical ganglia	379	3	X92070	Collo <i>et al.</i> , 1996 b
	Rat brain	379	3	X97376	Soto <i>et al.</i> , 1996
P2X <sub>7</sub>	Rat autonomic ganglia	595	6	X95882	Surprenant <i>et al.</i> , 1996

### 1.2.2.3. Pharmacological properties of P2X receptor subunits

P2X receptors can be divided into two broad groups according to whether they show fast desensitization within 100–300 ms or no desensitization (Table 1.1). Rapidly desensitizing P2X receptors are activated by ATP,  $\alpha,\beta$ -met-ATP, and 2-MeSATP. They comprise recombinant P2X<sub>1</sub> and P2X<sub>3</sub> receptors. The nondesensitizing  $\alpha,\beta$ -met-ATP-insensitive P2X receptors are the expressed cloned P2X<sub>2</sub>, P2X<sub>4</sub>, P2X<sub>5</sub>, and P2X<sub>7</sub> receptors.

**P2X<sub>1</sub> Receptor**. In 1994, two papers reported the cloning of two members of a novel family of ligand-gated ion channels, one of which was the 399 amino acid-long P2X<sub>1</sub> receptor (Brake *et al.*, 1994; Valera *et al.*, 1994). The P2X<sub>1</sub> receptor, heterologously expressed in *Xenopus* oocytes, activates and desensitizes rapidly (50–150 ms) and shows a relative high permeability for Ca<sup>2+</sup>. The order of agonist potency is 2-MeSATP  $\geq$  ATP >  $\alpha,\beta$ -met-ATP > ADP, UTP, GTP (Vassort, 2001). Both suramin and pyridoxalphosphate-6-azophenyl-2',4'-disulfonic acid (PPADS), but not amiloride, block this current (Lambrecht, 2000). The conductance, 19 pS at negative potential, shows anomalous inward rectification (Surprenant, 1996). These electrophysiological properties are close to those observed for a native ATP-activated channel in smooth muscle (Bean, 1992).

**P2X<sub>2</sub> Receptor**. The P2X<sub>2</sub> receptor was first cloned by Brake *et al.* (1994) from a DNA library constructed from the mRNA of PC12 cells and examined in *Xenopus* oocytes. The homomeric P2X<sub>2</sub> channel is characterized by its insensitivity to  $\alpha,\beta$ -met-ATP and its lack of desensitization during ATP applications of up to 10 s. Its conductance is 21 pS at -100 mV in 150 mM NaCl (Surprenant, 1996). Desensitization of P2X<sub>2</sub> receptors expressed in either *Xenopus* oocytes or HEK cells is obviously accelerated by increasing ATP concentrations (Zhou *et al.*, 1998). Desensitization of P2X<sub>2</sub> receptor is suggested to be controlled by alternative splicing (Brandle *et al.*, 1997). The splice isoform P2X<sub>2b</sub> or P2X<sub>2-2R</sub>, which lacks a stretch of C-terminal amino acids (<sup>370</sup>V-<sup>438</sup>Q), displays rapid and complete desensitization, whereas the wild-type channel desensitizes slowly (Simon *et al.*, 1997). The <sup>373</sup>P-<sup>376</sup>P sequence of P2X<sub>2R</sub> isoform represents a functional motif that is crucial for the development of the slow desensitization profile (Koshimizu *et al.*, 1999). The

behavior of the P2X<sub>2</sub> receptor approximates native P2X receptors of PC12 cells, but differs from those on vascular smooth muscle and vas deferens, where  $\alpha,\beta$ -met-ATP acts as a potent agonist. ATP $\gamma$ S, and 2-MeSATP are roughly equipotent agonists. CTP and 2'-deoxy-ATP (dATP) elicit small currents, whereas UTP, GTP, ADP, and AMP are inactive. In neurons, extracellular Zn<sup>2+</sup> potentiates the ATP effect on the recombinant receptor by changing the EC<sub>50</sub> for ATP to 15  $\mu$ M (Cloues, 1995).

**P2X<sub>3</sub> Receptor.** The P2X<sub>3</sub> receptor cDNA was cloned from rat dorsal root ganglion cDNA library (Chen *et al.*, 1995). Both ATP and  $\alpha,\beta$ -met-ATP evoke fast-activating and rapidly desensitizing currents. Direct evidence for heteromeric assembly of P2X<sub>2</sub> and P2X<sub>3</sub> subunits is presented by co-purification of the two subunits from Baculovirus-infected SF9 cells (Radford *et al.*, 1997). This co-expression yields ATP-activated currents, which closely resemble the  $\alpha,\beta$ -met-ATP-sensitive, non-desensitizing current that are detected in sensory neurons.

Expression of a truncated P2X<sub>3</sub> clone lacking the intracellular N-domain yield functional channels that do not desensitize in oocytes (King *et al.*, 1997 a). Desensitization of the ATP-gated cation channel P2X<sub>3</sub> is abolished by removal of external Ca<sup>2+</sup> or by cyclosporin pretreatment (King *et al.*, 1997 b). The rate of desensitization is also decreased by injection of the autoinhibitory peptide CaNA457–481 in the oocyte. Thus, it is thought that P2X<sub>3</sub> desensitizes through a Ca<sup>2+</sup>–dependent calcineurin-mediated phosphorylation on N–terminal residues (King *et al.*, 1997 b).

**P2X<sub>4</sub> Receptor.** The P2X<sub>4</sub> subunit was initially cloned from rat brain (Bo *et al.*, 1995) and shown to be distantly related to P2X<sub>1</sub>, P2X<sub>2</sub>, and P2X<sub>3</sub> subunits (Soto *et al.*, 1996). Its expression leads to an ATP-activated cation-selective channel that is highly sensitive to Ca<sup>2+</sup> and whose agonist sensitivity is potentiated by Zn<sup>2+</sup> without altering maximal response (Soto *et al.*, 1996). Its conductance is nine pS. This ligand-gated channel is activated by ATP > ATP $\gamma$ S > 2-MeSATP > ADP ~  $\alpha,\beta$ -met-ATP. A particular feature is its insensitivity to the presently used P2X receptor antagonists, suramin, PPADS, and reactive blue 2 (RB2). The agonist response of the mouse ortholog of the P2X<sub>4</sub> receptor (mP2X<sub>4</sub>) is potentiated by suramin, RB2, and in part by PPADS (Townsend-Nicholson *et al.*, 1999).

**P2X<sub>5</sub> Receptor**. The ATP-induced current after expression of the P2X<sub>5</sub> receptor in HEK-293 cells showed rapid activation with minimal desensitization and a lack of effect of  $\alpha,\beta$ -met-ATP (Collo *et al.*, 1996). Like with P2X<sub>1</sub> and P2X<sub>2</sub> receptors, this current was inhibited by suramin and PPADS (Torres *et al.*, 1999).

**P2X<sub>6</sub> Receptor**. When heterologously expressed in HEK 293 cells, only very small ATP-evoked currents were observed (Collo *et al.*, 1996). Currently, there is general agreement that homomeric P2X<sub>6</sub> channels are not formed in *Xenopus* oocytes (Le *et al.*, 1998; Torres *et al.*, 1999).

**P2X<sub>7</sub> Receptor**. The P2X<sub>7</sub> receptor was originally cloned from rat and human macrophages and brain (Surprenant *et al.*, 1996; Rassendren *et al.*, 1997). The P2X<sub>7</sub> receptors shows exclusive characteristics, which have been attributed to its 240 amino acids long intracellular C-terminal tail, of which at least 177 are involved in the induction of the nonselective cation channel and do not contain any known signaling motifs. P2X<sub>7</sub> receptors share many characteristics with receptors previously named P2Z receptors, through which ATP permeabilizes macrophages and other cells and leads to cell death (Di Virgilio, 1995). Thus, P2X<sub>7</sub> and P2Z receptors show both high sensitivity to BzATP relative to ATP and marked potentiation of the responses at reduced external divalent cation concentration, suggesting that ATP<sup>4-</sup> rather than MgATP acts as an agonist (Cockcroft & Gomperts, 1979). Indeed, the binding of ATP<sup>4-</sup> to P2X<sub>7</sub> receptors induces within milliseconds the opening of a channel selective for small cations and within seconds a larger pore whose single-channel conductance is 409 pS in macrophages and which is permeable to molecules up to 900 D (Coutinho-Silva & Persechini, 1997; Surprenant *et al.*, 1996). These effects of ATP are antagonized by PPADS, but not by suramin (Chessell *et al.*, 1997).



**Table 1.2: Selected properties of recombinant rat P2X receptors.**(Dunn, Zhong, & Burnstock, 2001; Soto *et al.*, 1997)

Isoform	Kinetics		ATP (EC <sub>50</sub> )	Agonist $\alpha\beta$ - MetATP (EC <sub>50</sub> )	Antagonist		Modulator	
	Activation	Desensitization			Suramin (IC <sub>50</sub> )	PPADS (IC <sub>50</sub> )	H <sup>+</sup>	Zn <sup>2+</sup>
P2X <sub>1</sub>	Fast	Fast	1 $\mu$ M	1-3 $\mu$ M	1 $\mu$ M	< 30 $\mu$ M	Inhibition	-
P2X <sub>2</sub>	Fast	Slow	60 $\mu$ M	> 100 $\mu$ M	10 $\mu$ M	1-5 $\mu$ M	Potentialiation	Increase
P2X <sub>3</sub>	Fast	Fast	0.5 $\mu$ M	1 $\mu$ M	3 $\mu$ M	1.5 $\mu$ M	Inhibition	
P2X <sub>4</sub>	Biphasic	Moderately slow	10 $\mu$ M	>> 100 $\mu$ M	> 300 $\mu$ M	>50 $\mu$ M	Inhibition	Increase (< 10 $\mu$ M)
P2X <sub>5</sub>	Fast	Slow	15 $\mu$ M	>> 100 $\mu$ M	4 $\mu$ M	3 $\mu$ M	-	-
P2X <sub>7</sub>	Biphasic	None	115 $\mu$ M	>> 300 $\mu$ M	~ 500 $\mu$ M	45 $\mu$ M	Inhibition	Decrease
P2X <sub>2/3</sub>	Fast	Slow	1 $\mu$ M	1 $\mu$ M	-	2 $\mu$ M	Potentialiation	-
P2X <sub>1/5</sub>	Fast	Biphasic	10 $\mu$ M	5 $\mu$ M	-	-	Inhibition	-
P2X <sub>4/6</sub>	Fast	Moderately slow	15 $\mu$ M	30 $\mu$ M	-	-	Inhibition	Increase (10 $\mu$ M)
P2X <sub>2/6</sub>	Biphasic	Biphasic	30 $\mu$ M	Inactive	6 $\mu$ M	-	Potentialiation	Increase

### 1.2.2.3. Localization and possible physiological implications of P2X receptors in different tissues

#### P2X receptors in muscle tissue

**Smooth muscle.** The presence of P2X receptors has been demonstrated in several smooth muscle containing tissues, such as arteries, vas deferens, and urinary bladder of a variety of species (Dubyak & El-Moatassim, 1993). The ATP-elicited contractions in these tissues are short-lasting due to rapid desensitization of the P2X receptors subtypes. ATP is released as a cotransmitter together with noradrenaline or acetylcholine, suggesting that ATP might only have a modulatory function by potentiating the effect of other neurotransmitters.

**Skeletal muscle.** P2X receptors have been functionally determined in embryonic myoblasts and myotubes of the chick (Henning *et al.*, 1993). In these tissues, ATP activates P2X receptors as a fast excitatory cotransmitter of acetylcholine with similarities in the effects elicited by acetylcholine.

**Heart muscle.** RT-PCR on micro-dissected tissues from various areas of the heart confirms the presence of P2X<sub>1</sub>, P2X<sub>2</sub>, P2X<sub>3</sub> subunit mRNAs (Nori *et al.*, 1998). Furthermore, two splice variants of the P2X<sub>2</sub> subunit were identified. Northern blot and RT-PCR analysis demonstrate P2X<sub>4</sub> transcripts in many tissues of the rat including blood vessels and heart (Soto *et al.*, 1996). Moreover, the P2X<sub>5</sub> receptor was cloned from rat heart (Garcia-Guzman *et al.*, 1996).

### Functional responses in the CNS

**Postsynaptic.** Patch-clamp recording of P2X-mediated synaptic currents has been reported in neurons in six different central regions: medial habenula (Edwards *et al.*, 1992) lamina II cervical dorsal horn (Bardoni *et al.*, 1997), superficial spinal cord dorsal horn (Jo & Schlichter, 1999), hippocampal CA1 (Pankratov *et al.*, 1998) hypothalamus (Jo & Schlichter, 1999) and CA3 (Nieber *et al.*, 1997). Furthermore, intracellular voltage recordings of a synaptic current in locus coeruleus have been reported to show a PPADS-sensitive and a suramin-sensitive component (Nieber *et al.*, 1997). In recent years, the development of selective antibodies against P2X subtypes has also allowed visualization of these receptors in specific synapses within the CNS (Atkinson *et al.*, 2000).

**Presynaptic.** Presynaptic modulation of transmitter release is evidently a central component of P2X receptor function in the CNS. The existence of such presynaptic receptors has been established electrophysiologically (Pintor *et al.*, 1999) with Ca<sup>2+</sup> imaging (Trodec *et al.*, 1998), and structurally using selective antibodies against the receptors (Atkinson *et al.*, 2000). Activation of P2X receptors has been shown to modulate the release of glutamate, GABA, glycine and vasopressin (Khakh & Henderson, 2000)

**Glial responses.** It has been revealed that glia has a wide variety of voltage and ligand-gated channels as well as metabotropic receptors (Verkhatsky *et al.*, 1998), which can contribute to the cellular communication pathways. Glial cells are considered to use the phenomenon of calcium waves to communicate with each other and to modulate neuronal activity. ATP has been shown to act as an extracellular signal, which mediates this form of communication both in the peripheral nervous system (Robitaille, 1995; Stevens & Fields, 2000), and in cultured glia from the CNS (Newman & Zahs, 1997). A recent review outlines the actions of

P2 receptors on glia-neuron communication both in the CNS and PNS (Fields & Stevens, 2000).

#### 1.2.2.4. Therapeutic aspects of P2X receptor function

**Auditory function.** P2 receptors are found in the vestibular system, and some P2X<sub>2</sub> receptor splice variants are present in rat and guinea pig cochlea (Housley *et al.*, 1995). The latter are present on the endolymphatic surface of the rat cochlear endothelium, an area associated with sound transduction (Vlajkovic *et al.*, 1996). ATP has the potential to regulate fluid homeostasis, hearing sensitivity, and development. Perilymphatic ATP lowers the sound-evoked gross compound action potential of the auditory nerve and the distortion product otoacoustic emission, the latter being a measure of the active process of the outer hair cells (Kujawa *et al.*, 1984).

**Pain.** ATP is implicated in the processing of nociceptive sensory information and may be directly involved in the pain associated with causalgia, reflex sympathetic dystrophy, angina, migraine, and cancer (Burnstock, 1996). ATP is also a mediator of neurogenic inflammation, acting via P2 receptors on neutrophils, macrophages, and monocytes to provoke cytokine and prostaglandin release (Dubyak & El Moatassim, 1993). Peripheral administration of ATP produces pain at the site of administration (Bland-Ward & Humphrey, 1997), and assists nociceptive responses to other noxious stimuli (Driessen *et al.*, 1994; Hamilton, Wade & McMahon, 1999). These effects are blocked by the P2 antagonists suramin and PPADS (Sawynok & Reid, 1997). ATP released in response to a tissue trauma can activate P2X<sub>3</sub> receptors that initiate and contribute to the peripheral and central sensitization associated with cutaneous and visceral nociception (Driessen *et al.*, 1994; Hamilton, Wade & McMahon, 1999). Homomeric P2X<sub>3</sub> and heteromeric P2X<sub>2/3</sub> receptors are highly restricted on sensory ganglia (Guo *et al.*, 1999; Vulchanova *et al.*, 1997) and can be regulated by extracellular Ca<sup>2+</sup> concentrations (Cook *et al.*, 1998). P2X<sub>3</sub> receptor expression is up-regulated in sensory afferents and spinal cord following damage to peripheral sensory fibers (Kassotakis *et al.*, 1996), whereas neonatal capsaicin treatment diminishes P2X<sub>3</sub> message in the dorsal root ganglion

(Ralevic & Burnstock, 1998) and abolishes ATP-mediated acute nociceptive responses (Chen *et al.*, 1995). P2X<sub>3</sub> receptor antagonists thus have potential as novel analgesics.

**Trophic actions of ATP and neurodegenerative disorders.** Trophic factors ensure neuronal viability and regeneration and are increased following neural injury (Neary *et al.*, 1996). ATP can proceed synergistically with growth factors to excite astrocyte proliferation, contributing to the process known as reactive astrogliosis, a hypertrophic/hyperplastic response related with brain trauma, stroke/ischemia, seizures, and neurodegenerative disorders. In reactive astrogliosis, astrocytes undergo process elongation and express the transitional filament protein, glial fibrillary acidic protein, with an increase in astroglial cellular proliferation. ATP, like basic fibroblast growth factor, increases astrocyte glial fibrillary acidic protein and AP-1 complex formation (Neary *et al.*, 1996). ATP and GTP provoke trophic factor (nerve growth factor, neurotrophin-3, fibroblast growth factor) synthesis in astrocytes and neurons, an effect that is not consistent with the profile of any known P2 receptor. The P2X<sub>7</sub> receptor is a unique member of the P2X receptor family that functions as a non-selective ion pore in mast cells, platelets, macrophages, and lymphocytes (Dubyak *et al.*, 1996). P2X<sub>7</sub> receptor activation triggers apoptosis and stimulates the release and maturation of interleukin-1b from macrophages by activating interleukin-1b convertase. P2X<sub>7</sub> receptors are present in the microglia within the superior cervical ganglia and spinal cord, and cerebral artery occlusion increases P2X<sub>7</sub> immunoreactive cells in the stroke penumbra (Collo *et al.*, 1997). ATP also induces P2X<sub>7</sub> receptor-mediated cytolysis in macrophages infected with *Mycobacterium* via both apoptotic and necrotic events (Lammas *et al.*, 1997). This anti-microbial activity of ATP may have potential use in the treatment of tuberculosis and also may provide a more fundamental understanding of P2X<sub>7</sub> receptor-mediated apoptotic events than can be observed in more complex mammalian cell systems.

**Neurourology.** The urinary bladder is controlled by both sympathetic and parasympathetic nervous system input. ATP mimics the effects of parasympathetic stimulation, resulting in bladder contraction (Burnstock *et al.*, 1978; Dean & Downie, 1978) via activation of P2X receptors present in the smooth muscle of the urinary bladder detrusor muscle implicated in bladder emptying (Chancellor *et al.*, 1992).

Detrusor malfunction can lead to urge urinary incontinence (UUI), a major health problem in the aging female population. Micturition involves urethral relaxation, in which ATP operates as a co-transmitter with NO. NO mediates the first stage of relaxation (Pinna, Puglis & Burnstock, 1998) and ATP the second, acting via P2 receptors. P2X receptors are also present in the bladder urothelium, and serosal ATP release occurs in the rabbit bladder because of the hydrostatic pressure changes associated with bladder filling (Yoshimura & de Groat, 1997). Muscarinic receptors mediate 15% of rat urinary bladder neurogenic contraction, and another 50% is mediated by P2X receptor mechanisms (Hashimoto *et al.*, 1995). Muscarinic antagonists such as oxybutynine and tolteridone are the mainstay treatment for UUI and have typical muscarinic side effects. P2X receptor antagonists may be potentially superior agents for the treatment of UUI, if their side-effect profile is tolerable.

**P2X and male fertility.** Mulryan *et al.* (2000) produced a “knockout” mouse lacking the gene for the P2X<sub>1</sub> receptor. The obvious effect of this gene deletion was a 90% decrease in the fertility of the male animals, which was caused by a low sperm count in the ejaculated semen. Thus, mutant females did not become pregnant when mated with mutant males, but normal rates of conception were observed when they mated with wild type or heterozygous males. The sperm from the mutant male mice were, however, viable and able to fertilize ova in vitro. The authors have therefore suggested that the selective pharmacological blockade of P2X<sub>1</sub> receptors should generate a similar effect, and might thus present a means for developing a non-hormonal male contraceptive pill.

### 1.3. Aspects of membrane protein synthesis and assembly

Multimeric transmembrane proteins, including ligand-gated ion channels represented by P2X receptors, generally require subunit assembly to be transported beyond the endoplasmic reticulum (ER) in the secretory pathway leading to the cell surface. The P2X polypeptide is classified as a type II multi-spanning membrane protein, because it lacks a cleavable signal sequence and the C-terminal portion of the first transmembrane segment is located in the ER lumen (Nicke *et al.*, 1998). The lumen

of the ER is the site where translocated proteins assume their secondary and tertiary structure and where assembly of oligomeric complexes occurs. Additionally, newly synthesized proteins undergo co-translational and posttranslational modifications in the lumen of the ER, some of which allow transient interactions of the folding polypeptide chains with a set of ER-resident proteins (Hammond & Helenius, 1995). Only after acquiring a fully folded, native conformation can proteins complete their passage through the secretory pathway (Hurtley & Helenius, 1989).

### 1.3.1. Assembly and disulfide bond formation of membrane proteins

A polypeptide chain can adopt many conformations. Yet, the sequence of its amino-acid residues directs folding to a particular native state (Anfinsen, 1973). The loss of conformational entropy associated with folding destabilizes the native conformation. This destabilization is overcome by the hydrophobic effect, hydrogen bonds, other noncovalent interactions, and (for many proteins) disulfide bonds (Dill, 1990). The extracellular domains of many transmembrane proteins include intrachain disulfide bonds, which are considered to contribute to the formation and stabilization of their mature conformation (Jaenicke, 1991). In some cases these bonds are established co-translationally, as soon as the participating cysteine residues appear in the lumen of the endoplasmic reticulum (ER), while in other cases the arrangement of disulfide bonds does not occur until a substantial interval after translation (Huth *et al.*, 1992), or even after assembly of monomers (Segal *et al.*, 1992). The oxidizing microenvironment required for this modification is offered by the lumen of the ER. This organelle also holds the enzymes that assist formation of disulfide bonds and support in protein folding including “foldases” such as protein disulfide isomerase and peptidylprolyl isomerase, and molecular chaperones such as calnexin and calreticulin (Hurtley & Helenius, 1989). In addition, the ER is the location of assembly of most oligomeric membrane and secretory proteins, which exit to the Golgi complex and are transported to the cell surface only after the completion of assembly.

### 1.3.2. N-glycosylation of membrane proteins

#### 1.3.2.1. Protein folding and core glycosylation in the ER

N-Glycan processing was shown to be an important event in the folding of the nascent protein chain. N-glycosylation starts in the ER compartment by the co-translational *en bloc* attachment of the core glycan,  $\text{Glc}_3\text{Man}_9\text{GlcNAc}_2$  to an Asn residue in the Asn-X-Ser(Thr) consensus sequence of a nascent protein, where X can be any amino acid other than proline (Kobata, 1992). These glycoproteins carrying three glucose residues on each glycan are co-translationally trimmed by the sequential action of ER glucosidases II and I. Monoglucosylated glycoproteins then bind type I membrane protein calnexin and/or the soluble protein calreticulin (Chevet *et al.*, 1999; Michalak, 1999). These two lectins share the same glycan specificity and bind monoglucosylated N-linked oligosaccharides with a  $\text{GlcMan}_9\text{GlcNAc}_2$  structure (Vassilakos *et al.*, 1998). Calnexin and calreticulin operate as chaperones in the quality control of newly synthesized glycoproteins in two opposing ways. They ensure that correctly folded glycoproteins leave the ER, but they can also mediate glycoprotein degradation in cases where correct protein folding is not possible (Trombetta & Helenius, 1998). The lectin-assisted glycoprotein folding involves a cycle of de- and reglycosylation (Ellgaard, Molinari & Helenius, 1999). Monoglucosylated glycoproteins bind calnexin and calreticulin and are presented to Erp57. Glucosidase II removes the remaining glucose residue such that the lectin-glycoprotein interaction becomes abolished. If the glycoprotein is correctly folded, it will leave the ER, if not, it will be recognized by the ER enzyme UDP-glucose:glycoprotein glucosyltransferase (GT) and reglycosylated. The deglycosylation and reglycosylation rounds continue until the properly folded glycoprotein is able to leave the cycle (Trombetta & Helenius, 1998). GT functions as a folding sensor, because it recognizes glycoproteins in their non-native but not in their native conformation (Parodi, 1999). GT is able to distinguish between different non-native conformations with a distinct preference for partially structured folding intermediates (Trombetta & Helenius, 2000). The deglycosylation and reglycosylation cycle continues until correct folding is achieved (Fig. 1.4).

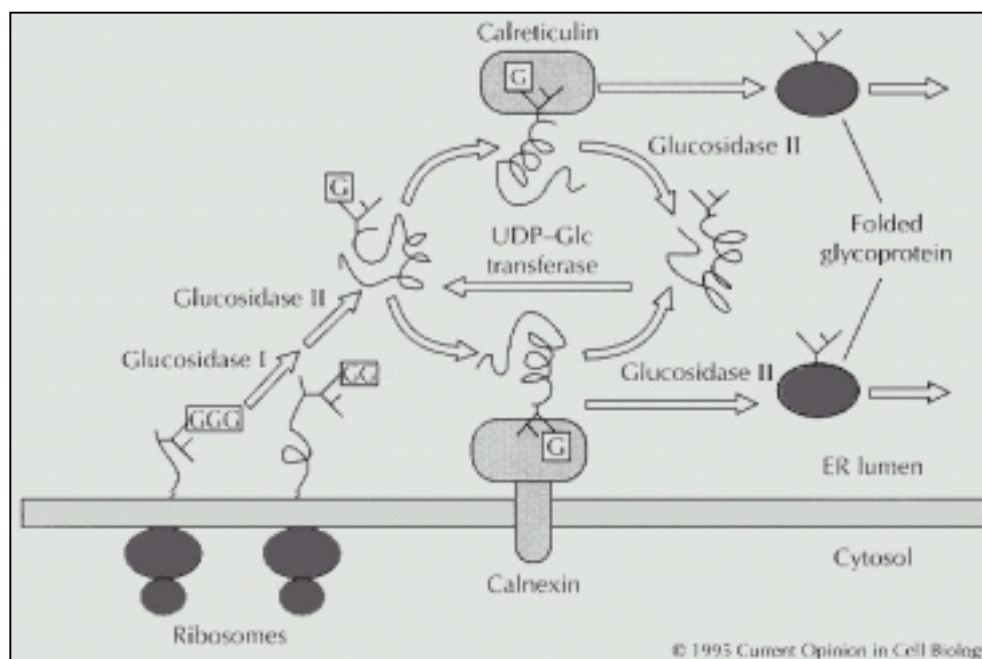


**Fig. 1.4: A model for a calnexin/calreticulin binding cycle involved in protein folding and quality control.** Trimming of glucose residues (G) from the N-linked oligosaccharides of newly synthesized proteins by glucosidases II and I allows binding of proteins to calnexin and calreticulin, lectins that recognize monoglucosylated oligosaccharides. Glucosidase II removes glucose residues and allows the protein to dissociate. Partially folded proteins are reglycosylated by UDP-glucose: glycoprotein glucosyltransferase (UDP-Glc transferase), which allows rebinding to calnexin/calreticulin and retention. Once a protein is folded correctly, it is no longer recognized by the glucosyltransferase and is released from the cycle by glucosidase II (scheme taken from: [Trombetta & Helenius, 1998](#)).

### 1.3.2.2. Oligosaccharide chains are terminally processed in the Golgi apparatus

The N-linked oligosaccharides are attached *en bloc* to the glycoproteins in the ER and this N-glycan is then trimmed, while the protein is still in the ER. Further modifications and additions occur in the Golgi apparatus. In the *cis*-Golgi, mannosidase I first removes three mannoses, and in the *medial*-Golgi *N*-acetylglucosamine transferase I then adds an *N*-acetylglucosamine, which enables mannosidase II to remove two additional mannoses in the *medial*-Golgi ([Alberts et al., 1994](#)). At this stage, the bond between the two *N*-acetylglucosamine in the core becomes resistant to digestion by the highly specific endoglucosidase (Endo H). Since all later structures in the pathway are also Endo H-resistant, treatment with this enzyme is generally used to differentiate complex from core-type and high mannose oligosaccharides. The enzymatic actions illustrated initiate “branches”,



which are then elongated in the *trans*-Golgi, to create much of the observed structural diversity of mature complex-type N-glycans (Fig 1.5). In addition to tissue-specific expression of Golgi enzymes, variability in glycan chain elongation and completion results in further structural heterogeneity (Dennis *et al.*, 1999). Figure 1.5 illustrates some of the key elements in the N-glycosylation pathways.

After acquisition of complex-type carbohydrates in the Golgi apparatus, the membrane proteins are transported from *trans*-Golgi to the cell surface and integrated into the plasma membrane by vesicle fusion by vesicle fusion.

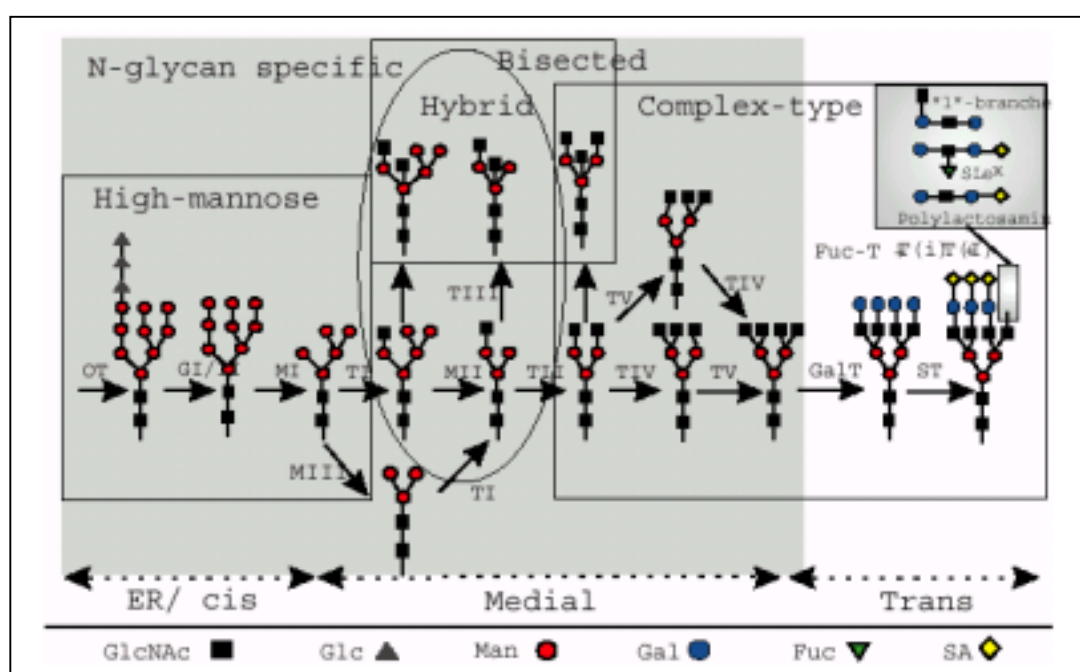


**Figure 1.5: Schematic drawing of N-linked glycan biosynthesis showing the Golgi compartments and the four classes of N-glycans: high-mannose-, hybrid-, bisected-, and complex-type.** Abbreviations: OT, oligosaccharyltransferase; GI and GII,  $\alpha$ -glucosidases I and II; TI, TII, TIII, TIV, T(i), T(l),  $\beta$ -N-acetylglucosaminyltransferases; MI,  $\alpha$ 1,2mannosidase; MII, MIII,  $\alpha$ 1,3/6mannosidases; Gal-T,  $\beta$ 1,4-galactosyltransferases; Fuc-T,  $\alpha$ -fucosyltransferase; ST,  $\alpha$ -sialyltransferase. The terminal sequences are added to N-glycans by  $\beta$ 1,4Gal-T;  $\beta$ 1,3GlcNAc-T(i);  $\beta$ 1,6GlcNAc-T(l);  $\alpha$ 2,3ST,  $\alpha$ 1,3Fuc-T. A number of substrate-product relationships govern N-glycan biosynthesis. Briefly, the GlcNAc-TI product is required for substrate recognition by  $\alpha$ -mannosidase II and GlcNAc-TII, and necessary for biosynthesis of the complex-type glycans. GlcNAc-TIII substitutes the core  $\beta$ -mannose residue, redirects the pathway into “bisected glycans” (Dennis *et al.*, 1999).

#### 1.4. Aim of the thesis

The P2X receptor family of ligand-gated cation channels currently comprises seven isoforms (P2X<sub>1</sub> – P2X<sub>7</sub>) that are products of seven distinct genes (Rettinger *et al.*, 2000). The heterologously expressed P2X receptors form functional homomeric or heteromeric complexes. By using biochemical techniques, Dr. A. Nicke had shown that trimers represent an essential structural element of P2X<sub>1</sub> and P2X<sub>3</sub> receptors (Nicke *et al.*, 1998). In addition, a trimeric structure was shown for the P2X<sub>1</sub>, P2X<sub>4</sub> and P2X<sub>7</sub> receptors that were cloned from human B-lymphocytes (Büttner, 2001). In this thesis, it was aimed to determine the quaternary structure of the remaining P2X receptor subtypes, namely P2X<sub>2</sub>, P2X<sub>5</sub>, and P2X<sub>6</sub>. The expression of these P2X receptors in *Xenopus* oocytes was verified by SDS-PAGE and their function was examined by two-electrode voltage-clamp analysis. The quaternary structure of the oocyte-expressed and either metabolically labeled or radio-iodinated P2X receptors was investigated by two different biochemical techniques: chemical cross-linking and blue native PAGE analysis.

To examine whether N-glycans are important for P2X<sub>1</sub> receptor assembly, surface expression, or ligand recognition, the respective N-glycosylation sites located on the ectodomain of the receptor subunit were eliminated by site-directed mutagenesis and the oligomerization and ATP-gated currents were analyzed in *Xenopus* oocytes by SDS-PAGE, blue native PAGE, and two-electrode voltage clamp measurements, respectively. An additional aim of the study was to examine the effect of N-glycans on the migration of P2X receptor complexes in the blue native PAGE system.

The P2X<sub>1</sub> receptors are membrane proteins with large ectodomains that fold inside the ER lumen. The ectodomain of P2X receptor family proteins is characterized by the existence of two cysteine-rich domains (Hanson, 1997), consisting of ten highly conserved cysteine residues that may contribute to the formation of five intrachain disulfide bonds. In this study, it was aimed to verify whether disulfide bonds affect the expression or function of the P2X<sub>1</sub> receptor. Therefore, various single, double and triple cysteine deletion mutants of His-P2X<sub>1</sub> receptors were constructed by site-directed mutagenesis, and their synthesis and function was analyzed in *Xenopus* oocytes by SDS-PAGE, blue native PAGE, and two-electrode voltage clamp measurements, respectively. In addition, the reducing

agent dithiothreitol (DTT) was applied to study the contribution of the ER redox environment to the posttranslational processing and intracellular transport of oocyte-expressed P2X<sub>1</sub> receptors.

In addition, the hetero-oligomeric assembly of P2X<sub>1</sub> and P2X<sub>2</sub> subunits was examined. Therefore, a co-purification assay was exploited, in which the hexahistidyl-tagged rat P2X<sub>2</sub> subunit was co-expressed with non-tagged P2X<sub>1</sub> subunit and *vice versa* in *Xenopus* oocytes. The isolated polypeptides were analyzed by SDS-PAGE and their oligomeric state was examined by blue native PAGE analysis and by chemical cross-linking using glutardialdehyde.

To observe the subcellular localization and membrane targeting of P2X<sub>1</sub> receptor, the His-P2X<sub>1</sub> receptor subunit was tagged N- or C-terminally with the green fluorescent protein (GFP). These fusion proteins were then expressed in *Xenopus* oocytes and visualized by the use of a confocal laser-scanning microscope. In addition, the fusion proteins were biochemically analyzed by SDS-PAGE and BN-PAGE.

Furthermore, various non-desensitizing P2X receptor chimeras were constructed and studied by SDS-PAGE, BN-PAGE, and two-electrode voltage clamping. The aim of these studies was to prove or disprove whether P2X receptors with non-desensitizing phenotype ([Werner et al., 1996](#)) have a propensity to assemble to hexamers rather than to trimers.

## 2. Material and Methods

### 2.1. Compounds, materials, and buffers

#### 2.1.1. Compounds and materials

##### Detergents, cross-linkers and amino-reactive compounds

- Digitonin, water soluble (serva, Heidelberg, Germany), (Sigma-Aldrich, Steinheim, Germany)
- *n*-Dodecyl- $\beta$ -D-maltoside (Biomol, Hamburg, Germany)
- Lithium dodecyl sulfate for biochemical use [LiDS] (Merck, Darmstadt, Germany)
- Sodium dodecyl sulfate, electrophoresis purity reagents [SDS] (Biorad Laboratories, München, Germany)
- *n*-Octyl- $\beta$ -D-glucopyranoside (Biomol, Hamburg, Germany)
- Glutardialdehyde (Roth, Karlsruhe, Germany)
- Sulfosuccinimidyl-3-(4-hydroxyphenyl)propionate [Sulfo-SSHP] (Pierce, Rockford, IL, USA)

##### Enzymes for protein biochemistry and oocyte preparation

- Collagenase (serva, Heidelberg, Germany)
- Endoglycosidase H [endo H] (New England Biolabs, Schwalbach, Germany)
- Peptide:N-glycosidase F [PNGase F] (New England Biolabs, Schwalbach, Germany)

##### Reagents for protein purification and polyacrylamide gel electrophoresis

- 6-Amino-*n*-caproic acid (Merck, Darmstadt, Germany)
- Ammonium persulfate [APS] (Sigma-Aldrich, Steinheim, Germany)
- Combitheck<sup>®</sup> Calibration proteins: aldolase, bovine Serum albumin, catalase, ferritin, hen's egg albumin (Boehringer Mannheim, Germany)
- Coomassie Brilliant blue G-250 (Serva, Heidelberg, Germany)
- Dithiothreitol [DTT] (Roth, Karlsruhe, Germany)

- Iodoacetamide (Sigma, St. Louis, MO, USA)
- Ni<sup>2+</sup>-Nitriloacetic acid agarose [Ni<sup>2+</sup> NTA agarose] (Qiagen, Hilden, Germany)
- Pefabloc (Merck, Darmstadt, Germany)
- Antipain (Biomol, Hamburg, Germany)
- Pepstain (Biomol, Hamburg, Germany)
- Rainbow™ coloured protein molecular weight markers 14,300-220,000 D (Amersham Buchler, Braunschweig, Germany)
- N, N, N', N'-Tetramethylethylenediamin [TEMED] (Merck, Darmstadt, Germany)
- Urea (Sigma, St. Louis, MO, USA)

### Radioactive compounds

- <sup>125</sup>Iodine sodium salt (Amersham Buchler, Braunschweig, Germany)
- L-[<sup>35</sup>S]Methionine (Amersham Buchler, Braunschweig, Germany)
- Rainbow™ [<sup>14</sup>C]methylated protein molecular weight markers 14,300-220,000 D (Amersham Buchler, Braunschweig, Germany)

### Equipment

- Autoclave: Bioclav (KSG, Olching, German)
- Centrifuge 5430 (Eppendorf, Hamburg, Germany)
- Sequi-Gen® Sequencing Cell (Biorad Laboratories, München, Germany)
- Power supply for Sequencing cell: Power Pac 3000 (Biorad Laboratories, München, Germany)
- Power supplies for gel electrophoresis: Phero-stab.300 (Biotec Fischer, Reiskirchen), Power supply 250/250 (Desaga, Heidelberg, Germany)
- Microinjector: Drummond "Nanoject" (Drummond Scientific, Broomall, PA, USA; Bachofer Laboratoriumsgeräte, Reutlingen, Germany)
- Micropipette puller: Model PP-830 (Narishige, Japan)
- Sample cups for metabolic labeling and binding (Sarstedt, Nürmbrecht, Germany)
- Tissue culture dishes for oocyte cultivation: Cell+ (Sarstedt, Nürmbrecht, Germany)
- Incubator: Kelvitron kl (Heraeus, Hanau, Germany)

- Vertical slab gel electrophoresis apparatus 8 x 16 cm (Phase, Lübeck, Germany)
- X-ray films: Biomax™ MR films for gels with <sup>35</sup>S samples, Biomax™ MS films for gels with <sup>125</sup>I samples or <sup>35</sup>S samples in combination with screen (Eastman Kodak, Rochester, New York, USA)
- Biomax TransScreen-LE (Eastman Kodak, Rochester, New York, USA)
- Developer, Replenisher: GBX reagents (Eastman Kodak, Rochester, New York, USA)
- Microwave R-3V10 (Sharp, Hamburg, Germany)
- Thermocycler: Thermal reactor (Hybaid, Heidelberg, Germany)
- pH-meter: PHM 62 (Radiometer, Copenhagen, Denmark)
- Pipettes: Pipetman (Abimed, Langenfeld, Germany)
- Shaker: Vibrax (IKA, Staufen, Germany)
- Thermal shaker for bacterial cultures: Controlled Environmental Incubator Shaker (New Brunswick Scientific, USA)
- Vacuum pump: Vapor Trap (Biorad, München, Germany)
- Gel dryer, Model 583 (Biorad, München, Germany)
- Water bath (GFL, Burgwedel, Germany)
- Weighing-machine: PR 503 Delta Range (Mettler Toledo, Greifensee, Switzerland)

### 2.1.2. Media and buffer solution

Unless otherwise noted, all media, buffers and solutions were made from commercially available chemicals of analytical grade purity and purified water (Millipore Milli-Qplus) or double distilled water. Reaction buffers for modification of DNA or RNA and elution/storage buffers for samples of DNA, RNA, and purified protein were prepared from ultra pure water (Gibco, Karlsruhe, Germany). Media and buffer solutions were either autoclaved or sterile filtered.

### 2.1.2.1. Media and buffers used for cultivation of bacteria and genetic engineering

#### *LB<sub>amp</sub>-medium (Luria-Bertani medium)*

20 g of broth base (Gibco BRL Life Technologies, Berlin, Germany) was solubilized in 1 liter of deionized water. A pH of 7.0 is adjusted without manipulation. The solution was autoclaved. Ampicillin with the final concentration of 50 mg/l was added to the LB-medium just before use.

#### *LB<sub>amp</sub>-agar plates*

1.5% Agar Bacteriological Grade (Gibco BRL Life Technologies, Berlin, Germany) was added to the previously prepared LB-medium. The solubilization of agar was achieved by autoclaving the media. Ampicillin with the final concentration of 100 mg/l was added to the chilled (< 50°C) medium. The solution was poured into petri dishes and the solution was left to solidify.

#### *Tris-acetate-EDTA-buffer for agarose gel electrophoresis (TAE-buffer)*

50 x TAE-buffer	
Tris base	242 g
Acetic acid	57.1 ml
EDTA (0.5 M), pH 8.0	100 ml
Filled up to 1 liter with Milli-Qplus water	

**The solution was diluted 1:50 with Milli-Q plus water before use.**

#### *Tris-EDTA-buffer (TE-buffer)*

100 x TE-buffer	
Tris base	1 M
EDTA	0.1 M
In Milli-Qplus water, adjusted to pH 8.0 with 1 M HCl and autoclaved	

**The solution was diluted 1:100 with Milli-Q plus water before use.**

## 2.1.2.2. Incubation and washing media for oocytes

Oocyte Ringer solution (ORi)		Ca <sup>2+</sup> -free Oocyte Ringer solution (Ca <sup>2+</sup> -free ORi)		Oocyte phosphate-buffered saline (Oocyte PBS)	
NaCl	90 mM	NaCl	90 mM	NaCl	70 mM
KCl	1 mM	KCl	1 mM	Na <sub>2</sub> HPO <sub>4</sub>	30 mM
CaCl <sub>2</sub>	1 mM	MgCl <sub>2</sub>	2 mM	MgCl <sub>2</sub>	1 mM
MgCl <sub>2</sub>	1 mM	HEPES	5 mM	CaCl <sub>2</sub>	0.1 mM
HEPES	5 mM				
Gentamycin (optional)	50 µg/ml				
In Milli-Qplus water, adjusted to pH 7.4 with 1 M NaOH and autoclaved				In Milli-Qplus water, adjusted to pH 8.0 with 1 M NaH <sub>2</sub> PO <sub>4</sub> and autoclaved	

## 2.1.2.3. Buffers used for protein biochemistry

*Buffers used for purification of His-tagged protein*

Ni <sup>2+</sup> -NTA binding buffer (0.1 M phosphate buffer, pH 8.0)	
Na <sub>2</sub> HPO <sub>4</sub>	93.2 mM
NaH <sub>2</sub> PO <sub>4</sub>	6.8 mM

Non-denaturing elution buffer	
Tris/HCl (pH 7.4)	20 mM
Imidazole	200 mM

*Buffers used for SDS-PAGE*

5 X SDS-PAGE sample buffer	
Tris/HCl (pH 6.8)	0.3 M
SDS	5%
Glycerol	50%
Bromphenol blue	1%
DTT (optional)	100mM

10 X SDS-PAGE running buffer	
Tris/HCl (pH 8.3)	0.25 M
Glycin	1.92 M
SDS	1 %



*Buffers used for Blue Native-PAGE*

5 X Blue Native-PAGE sample buffer	
Na-aminocaproate	100 mM
Coomassie Serva	1%
Blue G	
Glycerol	50%

Staining solution	
Coomassie blue R250	0.1%
Methanol	45%
Water	45%
Acetic acid	10%

3 X Blue Native-PAGE gel buffer	
Na-aminocaproate	1.5 M
BisTris pH 7.0	150 mM

Destaining solution	
Methanol	10%
Water	80%
Acetic acid	10%

1 X Blue Native-PAGE anode buffer	
BisTris pH 7.0	50 mM

1X Blue Native-PAGE cathode buffer	
Tricine	50 mM
BisTris pH 7.0	15 mM
Serva blue G	0.005%

## 2.2. Animals and cells

### 2.2.1. *Xenopus laevis*

*Xenopus laevis* (South African clawed frog) females were imported directly from the African *Xenopus* facility, Noordhoeck, Republic of South Africa. They were kept in water tanks at a temperature of 16-20°C. Fresh tap water was delivered twice daily for 2 h. An artificial 12-hour light-dark cycle was installed. The frogs were fed twice per week with raw bovine heart cut into small pieces and supplemented with Multisanostol<sup>®</sup> (Roland, Hamburg, Germany).

### 2.2.2. *E.coli* strains

Competent cells of the bacterial strains Top 10 and XL-1 Blue (Invitrogen, Groningen, Netherlands) prepared by the CaCl<sub>2</sub> method (according to Sambrook, Fritsch, & Maniatis, 1989) were used for plasmid DNA amplification and cDNA cloning.

## 2.3. DNA sources

- Vectors pNKS2, pNKS4 (Prof. G. Schmalzing, Technical University Aachen, Dept. of Pharmacology and Toxicology), ([Gloor, Pongs, & Schmalzing, 1995](#))
- cDNA encoding N-terminally hexahistidyl-tagged rat P2X<sub>1</sub> (His-rP2X<sub>1</sub>) in pNKS<sub>2</sub>, rat P2X<sub>2</sub> in pNKS2 vector, rat P2X<sub>3</sub>-pNKS2, and human P2X<sub>4</sub>-pNKS2 (Prof. G. Schmalzing, Technical University Aachen, Dept. of Pharmacology and Toxicology)
- cDNA encoding rat P2X<sub>5</sub> and rat P2X<sub>6</sub> in vector pSP64 (Dr. F. Soto, Max-Planck-Institute for Experimental Medicine, Göttingen, Germany)
- His-P2X<sub>1</sub>-GFP-pSPS64polyA (Dr. Helmut Reiländer, Max-Planck-Institute for Biophysics, Department of Molecular Membrane Biology, Frankfurt, Germany)
- Vector pEGFP-pCMV (Clontech, SanDiego, USA)
- Oligonucleotides were purchased from Sigma-ARK Scientific (Darmstadt, Germany) or MWG Biotec (Ebersberg, Germany). For sequences of the

numbered oligonucleotides described under genetic engineering, see appendix.

## 2.4. Methods

### 2.4.1. Genetic engineering

cDNA constructs were generated by using standard molecular biology techniques (Sambrook, Fritsch, & Maniatis, 1989). Enzymes for genetic engineering of plasmid DNA were purchased from New England Biolabs (Schwalbach, Germany) and utilized as recommended by the supplier. If a change of buffer was necessary between enzymatic reactions, the samples were desalted by using MicroSpin S-50 columns (Pharmacia Biotech, Freiburg, Germany). DNA fragments were extracted from a preparative 1% agarose gel using the Qiaex DNA Extraction kit (Qiagen, Hilden, Germany). Oligonucleotides and plasmid DNA were stored in 1 x TE buffer (pH 8.0) at -20°C.

Plasmid DNA was purified from bacterial culture by using the SeqLab (Göttingen, Germany) or the GFX™ Micro Plasmid prep kit (Pharmacia Biotech, Freiburg, Germany).

To generate double-stranded oligonucleotides, the single-stranded oligonucleotides were combined and diluted to a final concentration of 5 μM of each oligonucleotide. After heating this mixture at 95°C for 5 min, it was cooled down slowly (1°C per min) to allow for annealing of the oligonucleotides. 0.5 μl of the annealed oligonucleotide mixture was used for ligation with about 200 ng of vector in a final volume of 20 μl. Ligations were performed using the T4 DNA ligase (New England Biolabs Schwalbach, Germany) according to the protocol of the supplier.

cDNA constructs were sequenced either by the dideoxynucleotide method (T7 Sequencing kit, Pharmacia Biotech, Freiburg, Germany) using a 6% sequencing gel (Acrylamide 4K Sequencing kit, Applichem, Darmstadt, Germany), or by cycle sequencing (ABI PRISM Dye Terminator Cycle Sequencing Ready Reaction kit; 377 Sequencer Perkin Elmer/Applied Biosystems; Institute of Pharmaceutical Biology, University of Frankfurt).

### **Construction of cDNAs in vector pNKS2 with an optimized 5'-non-translated region.**

Some of the constructs were optimized in the 5'-non-translated sequence of vector pNKS2 just prior to the open reading frame of the gene of interest. To this end, a double-stranded oligonucleotide (#423 and #424) encoding the optimized 5'-non-translated region followed by an *Aat* II site was introduced in frame between the unique *Hind* III and *Nco* I sites of the vector pNKS2. The cDNA sequence used has been reported to support efficient protein synthesis because of lack of secondary structure (Kozak, 1994). The vector pNKS2 was renamed into pNKS2\* after the optimization of the 5'-non-translated region. This optimization step was conducted for all pNKS2 constructs except the cysteine and N-glycan mutants of His-rP2X<sub>1</sub>-pNKS2.

#### **2.4.1.1. Construction of cDNAs for tagged and mutant rat P2X<sub>1</sub>**

In general the Quick Change™ mutagenesis Kit (Stratagene, Heidelberg, Germany) was used for site-directed mutagenesis. The kit can be used to make point mutations, switch amino acids, and delete or insert single or multiple amino acids. The mutagenesis method is performed using *Pfu* DNA polymerase, which replicates both plasmid strands with high fidelity, the mutant oligonucleotide primers, and a thermal cycler. The procedure utilizes a supercoiled, double-stranded DNA vector with an insert of interest and two synthetic oligonucleotide primers containing the desired mutation. The oligonucleotide primers, each complementary to opposite strands of the vector, extend during temperature cycling by means of *Pfu* DNA polymerase. On incorporation of the oligonucleotide primers, a mutated plasmid containing staggered nicks is generated. Following temperature cycling, the product is treated with *Dpn* I. The *Dpn* I endonuclease (target sequence: 5'-G<sup>m6</sup>ATC-3') is specific for methylated and hemimethylated DNA and is used to digest the parental DNA template and to select for mutation-containing DNA. The nicked vector DNA incorporating the desired mutation is then transformed into *E. coli* (XL-1 Blue supercompetent cells).

**Rat P2X<sub>1</sub> mutants lacking one or several consensus sequences for N-glycosylation.** His-P2X<sub>1</sub> mutants lacking one or several consensus sequences for N-glycosylation were generated by changing the asparagine of existing NXS/T codons to glutamine using site directed mutagenesis (Table 2.1). All mutations were verified by dideoxynucleotide sequencing. The final mutant in this table describes a substitution of a proline residue following the consensus sequence <sup>284</sup>NLS by an alanine residue.

Table 2.1: Mutants lacking one or several consensus sequences for N-glycosylation.

Mutated construct (Sequenced cDNA construct)	Parent construct	Abbreviated name of construct	Primer used
His-P2X <sub>1</sub> -N <sup>153</sup> Q-pNKS2 (2-1907)	His-P2X <sub>1</sub> -pNKS2	ΔN1	492 / 493
His-P2X <sub>1</sub> -N <sup>184</sup> Q-pNKS2 (1-0606)	His-P2X <sub>1</sub> -pNKS2	ΔN2	494 / 495
His-P2X <sub>1</sub> -N <sup>210</sup> Q-pNKS2 (1-1407)	His-P2X <sub>1</sub> -pNKS2	ΔN3	506 / 507
His-P2X <sub>1</sub> -N <sup>284</sup> Q-pNKS2 (2-2206)	His-P2X <sub>1</sub> -pNKS2	ΔN4	508 / 509
His-P2X <sub>1</sub> -N <sup>300</sup> Q-pNKS2 (1-2705)	His-P2X <sub>1</sub> -pNKS2	ΔN5	519 / 520
His-P2X <sub>1</sub> -N <sup>184</sup> Q / N <sup>210</sup> Q-pNKS2 (1-1709)	ΔN3	ΔN23	494 / 495
His-P2X <sub>1</sub> -N <sup>184</sup> Q / N <sup>284</sup> Q-pNKS2 (3-2007)	ΔN4	ΔN24	494 / 495
His-P2X <sub>1</sub> -N <sup>184</sup> Q / N <sup>300</sup> Q-pNKS2 (1-1809)	ΔN5	ΔN25	494 / 495
His-P2X <sub>1</sub> -N <sup>210</sup> Q / N <sup>300</sup> Q-pNKS2 (1-2009)	ΔN3	ΔN35	519 / 520
His-P2X <sub>1</sub> -N <sup>153</sup> Q / N <sup>210</sup> Q-pNKS2 (1-1904)	ΔN3	ΔN13	492 / 493
His-P2X <sub>1</sub> -N <sup>153</sup> Q / N <sup>300</sup> Q-pNKS2 (1-2104)	ΔN5	ΔN15	492 / 493
His-P2X <sub>1</sub> -N <sup>153</sup> Q / N <sup>184</sup> Q-pNKS2 (1-2410)	ΔN2	ΔN12	492 / 493
His-P2X <sub>1</sub> -N <sup>153</sup> Q / N <sup>184</sup> Q / N <sup>210</sup> Q- pNKS2 (1-2510)	ΔN23	ΔN123	492 / 493
His-P2X <sub>1</sub> -N <sup>153</sup> Q / N <sup>184</sup> Q / N <sup>284</sup> Q- pNKS2 (2-1408)	ΔN24	ΔN124	492 / 493
His-P2X <sub>1</sub> -N <sup>184</sup> Q / N <sup>210</sup> Q / N <sup>300</sup> Q- pNKS2 (1-3003)	ΔN23	ΔN235	519 / 520

<b>Mutated construct (Sequenced cDNA construct)</b>	<b>Parent construct</b>	<b>Abbreviated name of construct</b>	<b>Primer used</b>
<b>His-P2X<sub>1</sub>-N<sup>153</sup>Q / N<sup>184</sup>Q / N<sup>210</sup>Q / N<sup>284</sup>Q-pNKS2 (2-0809)</b>	ΔN124	ΔN1234	506 / 507
<b>His-P2X<sub>1</sub>-N<sup>153</sup>Q / N<sup>184</sup>Q / N<sup>210</sup>Q / N<sup>284</sup>Q / N<sup>300</sup>Q-pNKS2 (1-1909)</b>	ΔN1234	ΔN12345	519 / 520
<b>His-P2X<sub>1</sub>-P<sup>287</sup>A-pNKS2 (1-3011)</b>	His-P2X <sub>1</sub> -pNKS2	+N4	606 / 607

In column one, the name of the mutant and the sequenced clone are indicated. The positions of the asparagine residues are derived from the sequence of the wild type rat P2X<sub>1</sub> sequence. The oligonucleotide numbers used for site-directed mutagenesis are indicated in column four.

**Rat P2X<sub>1</sub> mutants lacking one or several cysteine residues.** His-P2X<sub>1</sub> mutants lacking one or several cysteine residues were generated by changing the cysteine residue to serine by site-directed mutagenesis (Table 2.2).

**Table 2.2: Mutants lacking one or several cysteine residues.**

<b>Mutated construct (Sequenced cDNA construct)</b>	<b>Parent construct</b>	<b>Abbreviated name of construct</b>	<b>Primer used</b>
<b>His-rP2X<sub>1</sub>-C<sup>117</sup>S-pNKS2 (1-0704)</b>	His-P2X <sub>1</sub> -pNKS2	ΔC1	642 / 643
<b>His-rP2X<sub>1</sub>-C<sup>126</sup>S-pNKS2 (1-1405)</b>	His-P2X <sub>1</sub> -pNKS2	ΔC2	652 / 653
<b>His-rP2X<sub>1</sub>-C<sup>132</sup>S-pNKS2 (1-1505)</b>	His-P2X <sub>1</sub> -pNKS2	ΔC3	654 / 655
<b>His-rP2X<sub>1</sub>-C<sup>149</sup>S-pNKS2 (2-2805)</b>	His-P2X <sub>1</sub> -pNKS2	ΔC4	656 / 657

<b>Mutated construct (Sequenced cDNA construct)</b>	<b>Parent construct</b>	<b>Abbreviated name of construct</b>	<b>Primer used</b>
<b>His-rP2X<sub>1</sub>-C<sup>159</sup>S-pNKS2 (1-1605)</b>	His-P2X <sub>1</sub> -pNKS2	ΔC5	658 / 659
<b>His-rP2X<sub>1</sub>-C<sup>165</sup>S-pNKS2 (1-1705)</b>	His-P2X <sub>1</sub> -pNKS2	ΔC6	660 / 661
<b>His-rP2X<sub>1</sub>-C<sup>217</sup>S-pNKS2 (1-0906)</b>	His-P2X <sub>1</sub> -pNKS2	ΔC7	678 / 679
<b>His-rP2X<sub>1</sub>-C<sup>227</sup>S-pNKS2 (1-1106)</b>	His-P2X <sub>1</sub> -pNKS2	ΔC8	680 / 681
<b>His-rP2X<sub>1</sub>-C<sup>261</sup>S-pNKS2 (1-1206)</b>	His-P2X <sub>1</sub> -pNKS2	ΔC9	682 / 683
<b>His-rP2X<sub>1</sub>-C<sup>270</sup>S-pNKS2 (1-1006)</b>	Hi-P2X <sub>1</sub> -pNKS2	ΔC10	684 / 685
<b>His-rP2X<sub>1</sub>-C<sup>353</sup>S-pNKS2 (1-1306)</b>	Hi-P2X <sub>1</sub> -pNKS2	ΔC11	686 / 687
<b>His-rP2X<sub>1</sub>-C<sup>117</sup>S / C<sup>126</sup>S-pNKS2 (B1-2710)</b>	ΔC1	ΔC1+2	652 / 653
<b>His-rP2X<sub>1</sub>-C<sup>117</sup>S / C<sup>165</sup>S-pNKS2 (C61-1008)</b>	ΔC1	ΔC1+6	660 / 661
<b>His-rP2X<sub>1</sub>-C<sup>126</sup>S / C<sup>132</sup>S-pNKS2 (C23-0908)</b>	ΔC3	ΔC2+3	652 / 653
<b>His-rP2X<sub>1</sub>-C<sup>126</sup>S / C<sup>149</sup>S-pNKS2 (A1-2710)</b>	ΔC4	ΔC2+4	652 / 653
<b>His-rP2X<sub>1</sub>-C<sup>126</sup>S / C<sup>159</sup>S-pNKS2 (E1-2109)</b>	ΔC2	ΔC2+5	658 / 659
<b>His-rP2X<sub>1</sub>-C<sup>132</sup>S / C<sup>149</sup>S-pNKS2 (B1-2109)</b>	ΔC3	ΔC3+4	656 / 657
<b>His-rP2X<sub>1</sub>-C<sup>132</sup>S / C<sup>159</sup>S-pNKS2 (D1-2508)</b>	ΔC3	ΔC3+5	658 / 659
<b>His-rP2X<sub>1</sub>-C<sup>149</sup>S / C<sup>159</sup>S-pNKS2 (C1-2109)</b>	ΔC5	ΔC4+5	656 / 657



Mutated construct (Sequenced cDNA construct)	Parent construct	Abbreviated name of construct	Primer used
His-rP2X <sub>1</sub> -C <sup>117</sup> S / C <sup>126</sup> S / C <sup>165</sup> S- pNKS2 (A1-2003)	ΔC1+6	ΔC1+2+6	652 / 653
His-rP2X <sub>1</sub> -C <sup>126</sup> S / C <sup>132</sup> S / C <sup>149</sup> S- pNKS2 (B2-2003)	ΔC3+4	ΔC2+3+4	652 / 653
His-rP2X <sub>1</sub> -C <sup>126</sup> S / C <sup>149</sup> S / C <sup>159</sup> S- pNKS2 (C1-2003)	ΔC4+5	ΔC2+4+5	652 / 653
His-rP2X <sub>1</sub> -C <sup>159</sup> S / C <sup>165</sup> S-pNKS2 (C1-2710)	ΔC6	ΔC5+6	658 / 659

In column one, the name of the mutant and the sequenced clone are indicated. The positions of the cysteine residues are derived from the sequence of the wild type rat P2X<sub>1</sub> sequence. The oligonucleotide numbers used for site-directed mutagenesis are indicated in column four.

### **Construction of cDNAs for GFP-tagged His-P2X<sub>1</sub>.**

#### *His-rP2X<sub>1</sub>-GFP in vector pNKS2\**

The cDNA of His-P2X<sub>1</sub> with a C-terminal GFP-tag in pSP64polyA was provided by Dr. Helmut Reiländer (Max-Planck-institute for Biophysics, Frankfurt, Germany). His-rP2X<sub>1</sub>-GFP-pSP64polyA was first cut with *Not* I, blunted by T4 DNA polymerase treatment, and then cut with *Bam*H I. Finally, this cDNA fragment including the entire coding region was sub-cloned between the *Bam*H I and *Sma* I cleavage sites of the oocyte expression vector pNKS2.

#### *GFP-His-rP2X<sub>1</sub> in vector pNKS2\**

cDNA encoding an N-terminal GFP sequence fused in frame with a hexahistidyl-tagged rat P2X<sub>1</sub> was constructed as follows: using overlap extension polymerase chain reaction (PCR) (flanking primers # 886 and # 887), an *Aat* II site in the 5'-non-translated region 12 nucleotides upstream the initiation ATG and a *Nco* I site at the C-terminus of GFP were introduced. Subsequently, this fragment was ligated in frame between *Aat* II and *Nco* I cleavage sites of the His-P2X<sub>1</sub>.pNKS2\*.

#### 2.4.1.2. Construction of cDNAs for tagged, mutant, and truncated rat P2X<sub>2</sub>

##### *His-rP2X<sub>2</sub>-pNKS2\**

To generate a cDNA encoding N-terminally hexahistidyl-tagged rat P2X<sub>2</sub> (His-rP2X<sub>2</sub>) in vector pNKS2\*, the endogenous *Nco* I site within the coding region of the rat P2X<sub>2</sub> cDNA was deleted by site-directed mutagenesis using oligonucleotides # 488 and # 489 without changing the respective amino acid, <sup>184</sup>H. Then, the double-stranded oligonucleotide (# 423 and # 424) encoding the optimized 5'-non-translated region followed by an *Aat* II site was introduced between the *Hind* III of the vector pNKS2 and the *Nco* I cleavage site at the starting ATG of the rP2X<sub>2</sub> cDNA. Finally, the hexahistidyl-tag was directionally inserted using double-stranded oligonucleotides (#496 and #497) between the *Aat* II and *Nco* I sites of r2X<sub>2</sub>-pNKS2\*.

##### *His-rP2X<sub>2</sub>-N<sup>239</sup>Q-pNKS2\**

Using site-directed mutagenesis, a His-rP2X<sub>2</sub> mutant lacking one of the three existing consensus sequences for N-glycosylation was generated by changing the asparagine at the position 239 to glutamine, using the oligonucleotides # 947 and # 948.

##### *His-rP2X<sub>2</sub><sup>1-409</sup>-pNKS2\**

For construction of a C-terminally truncated rat P2X<sub>2</sub> receptor with a N-terminal hexahistidyl sequence, the coding sequence of rat P2X<sub>2</sub> after the amino acid <sup>409</sup>G was deleted using singular *Eco* NI and *Xba* I cleavage sites. Then, a double-stranded oligonucleotide (# 719 and # 720) was ligated in frame between the *Eco* NI and the *Xba* I sites of His-rP2X<sub>2</sub> in vector pNKS2\* to introduce a stop codon after the amino acid <sup>409</sup>G.

#### 2.4.1.3. Construction of cDNAs for tagged rat P2X<sub>5</sub> and rat P2X<sub>6</sub>

##### *His-rP2X<sub>5</sub> in vector pNKS4\**

The complete coding sequence of rat P2X<sub>5</sub> was first subcloned from the original pBSK vector into the pNKS4 vector. To this end, a unique *Nco* I recognition site was introduced at the start codon of rat P2X<sub>5</sub> by site-directed mutagenesis (oligonucleotides # 535 and # 536). The P2X<sub>5</sub> coding sequence could then be

excised with *Nco* I and *Apa* I, and subcloned into the corresponding sites of vector pNKS4. To insert a N-terminal hexahistidyl-tag into rP2X<sub>5</sub>-pNKS4, a double stranded oligonucleotide (# 547 and # 548) encoding the optimized 5'-non-translated region followed by six histidine residues was directionally inserted between the unique *Hind* III and *Nco* I sites of rP2X<sub>5</sub>-pNKS2\*.

#### *His-rP2X<sub>6</sub> in pNKS2\**

The coding sequence of rat P2X<sub>6</sub> was isolated by using endogenous *Nco* I and *Xho* I cleavage sites and subcloned into the pNKS2\* vector. To generate a cDNA encoding N-terminally hexahistidyl-tagged P2X<sub>6</sub>, the annealed oligonucleotides # 496 and # 497 encoding six histidine residues were directionally inserted between the unique *Aat* II and *Nco* I sites of P2X<sub>6</sub>-pNKS2\*.

#### 2.4.1.4. Construction of cDNAs for P2X receptor chimera

##### *His-rP2X<sub>2</sub>/rP2X<sub>1</sub>-pNKS2*

A chimeric cDNA encoding a hexahistidyl-tag followed by the first 47 N-terminal amino acids of rat P2X<sub>2</sub> joined with 352 amino acids of the C terminus of the rat P2X<sub>1</sub> polypeptide was constructed by first introducing a unique *Sna*B I site at codon <sup>48</sup>V of the rat P2X<sub>1</sub>-pNKS2 plasmid by site-directed mutagenesis (oligonucleotides # 502 and # 503). Then, a *Sna*B I site at codon <sup>47</sup>V of the N-terminally hexahistidyl-tagged rat P2X<sub>2</sub> was introduced by site-directed mutagenesis (oligonucleotides # 503 and # 504). Finally, the N-terminal His-rP2X<sub>2</sub> sequence was excised with *Hind* III and *Sna*B I and ligated in frame between the *Hind* III of the vector and engineered *Sna*B I cleavage sites of rat P2X<sub>1</sub>-pNKS2.

##### *His-rP2X<sub>1</sub>[TM(1)P2X<sub>2</sub>]-pNKS2*

To generate a chimeric cDNA encoding a N-terminally hexahistidyl-tagged rat P2X<sub>1</sub> subunit with the sequence for the predicted first transmembrane region of the rat P2X<sub>2</sub> subunit, a unique *Bsp*E I site at position <sup>25</sup>R (oligonucleotides # 525 and # 526) and a unique *Sna*B I site at position <sup>48</sup>V of the His-rP2X<sub>1</sub>-pNKS2 (oligonucleotides # 502 and # 503) were introduced by site-directed mutagenesis. No amino acid of the coding sequence was changed by introduction of the restriction sites. Finally, a double stranded oligonucleotide (# 529 and # 530) derived from the first

transmembrane region of rat P2X<sub>2</sub> encoding the amino acids <sup>43</sup>NRRLGFVHRMVQLLILLYFVWY<sup>65</sup> were directionally inserted between the engineered *BspE* I and *SnaB* I sites.

#### *His-rP2X<sub>2</sub>/rP2X<sub>3</sub>-pNKS2\**

A chimeric cDNA encoding a hexahistidyl-tag followed by the first 47 N-terminal amino acids of the rat P2X<sub>2</sub> subunit and joined with 356 amino acids of the C terminus of the P2X<sub>3</sub> polypeptide was constructed as follows: to delete the endogenous *SnaB* I site in the 3'-non-translated region of the rat P2X<sub>3</sub> gene in pNKS2 the construct was opened with *Apa* I and *SnaB* I, blunted by T4 DNA polymerase treatment and religated. Then, a *SnaB* I site at the position <sup>41</sup>V was introduced into rat P2X<sub>3</sub>-pNKS2 by site-directed mutagenesis (oligonucleotides # 527 and # 528). Finally, the rat P2X<sub>3</sub> fragment between the engineered *SnaB* I and *EcoR* I site was excised and the rat P2X<sub>1</sub> fragment of the construct His-rP2X<sub>2</sub>/rP2X<sub>1</sub>-pNKS2 was replaced directionally by the *SnaB* I / *EcoR* I-isolated rat P2X<sub>3</sub> fragment.

#### *His-hP2X<sub>4</sub>/rP2X<sub>1</sub>-pNKS2\**

For construction of a chimeric cDNA encoding a hexahistidyl-tag followed by the first 45 N-terminal amino acids of the human P2X<sub>4</sub> subunit connected with 352 amino acids of the C terminus of rat P2X<sub>1</sub> polypeptide, a unique *SnaB* I site was introduced by site-directed mutagenesis at the position <sup>45</sup>V of the His-hP2X<sub>4</sub>-pNKS2\* construct (oligonucleotides # 513 and # 514). Subsequently, the human P2X<sub>4</sub> fragment between the *SnaB* I and *Hind* III site was excised and the rat P2X<sub>2</sub> fragment of the construct His-rP2X<sub>2</sub>/rP2X<sub>1</sub>-pNKS2 was replaced by the *Hind* III / *SnaB* I-isolated hP2X<sub>4</sub> fragment.

#### 2.4.1.5. cRNA synthesis

For synthesis of run-off cRNA, plasmids were usually linearized at the unique *EcoR* I cleavage site at the 5' end of the polyA tail (vector pNKS2). If an additional *EcoR* I site was present in the plasmid (P2X<sub>2</sub>, and P2X<sub>5</sub>), *Not* I was used for linearization. Linearized plasmid cDNAs were purified by using the QIAquick Nucleotide Removal Kit (Qiagen, Hilden, Germany), and dissolved in 0.5 x TE. Capped cRNAs were synthesized from these templates with SP6 RNA polymerase (Pharmacia Biotech,

Freiburg, Germany), purified with Sepharose G50 (Stratagene, Heidelberg, Germany) chromatography and phenol-chloroform extraction, and dissolved in 5 mM Tris/HCl, pH 7.2, using the optical density reading at 260 nm for quantification (OD 1.0 = 40 µg/µl, Hitachi U-2000 spectral photometer).

#### 2.4.2. Preparation of ovary and maintenance of *Xenopus* oocytes

*Xenopus leavis* females were anaesthetized by 15-30 min immersion in a 0.2% solution of 3-aminobenzoic acid ethyl ester (Tricaine, MS 222, Sigma, St.Louis, MO, USA) in water (adjusted with HEPES to pH 7.4). The anaesthetized frog was placed on a flat surface and an incision of approximately 1 cm was made through skin and muscle in the lateral of the abdomen. The desired amount of ovary was carefully teased out of the abdomen, excised, and immediately transferred into ORi. The incisions in the body wall and in the skin were sutured separately. Frogs were left overnight to recover and kept in a separate tank for approximately half a year for complete regeneration.

For isolation of oocytes, the ovary lobes were separated into small pieces and incubated for about 15 hours at 19°C with collagenase at a concentration of 1.5 mg per ml of ORi (sterile filtered) (Schmalzing *et al.*, 1991). Subsequently, oocytes were washed and incubated in Ca<sup>2+</sup>-free ORi for 10 min to remove the adherent follicle cells and then placed in ORi. A homogenous group of follicle cell-free oocytes of oogenesis stages V and IV (Colman, 1984) was selected soon thereafter and injected with 50 nl aliquots of cRNA (0.5 µg/µl). Injected oocytes and non-injected controls were cultured at 19°C in ORi using petri dishes with modified surface (Greiner, Germany).

### 2.4.3. Protein biochemistry

#### 2.4.3.1. Radioactive labeling of proteins

##### *Metabolic labeling with [<sup>35</sup>S] methionine*

In general, metabolic labeling was achieved by the overnight incubation of the total protein of cRNA-injected *Xenopus* oocytes and non-injected controls with L-[<sup>35</sup>S]methionine at ~100 MBq/ml with ~0.2 MBq/oocyte. Incubation with [<sup>35</sup>S]methionine was performed at 19°C in closed sample cups that had been pre-treated with oocyte homogenate to prevent adhesion of oocytes. Incorporation of radioactivity was stopped by an overnight chase period in ORi. During this chase interval, oocytes were kept in tissue culture dishes.

##### *Cell surface iodination with <sup>125</sup>I-sulfo-SHPP*

For selective labeling of cell surface proteins, oocytes were cultured for three days after cRNA injection. Then 12 to 15 intact oocytes per group were selected, washed in chilled oocyte PBS, and placed on ice in 0.5 ml reaction tubes that had been pre-treated with oocyte homogenate. Sulfosuccinimidyl-3-(4-hydroxyphenyl)-propionate [sulfo-SHPP] was radio-iodinated by a modification of the method described by Thompson *et al.* (Thompson, Lau, & Cunningham, 1986): at ambient temperature the reagents were rapidly and subsequently added as described in Table 2.3. All solutions were freshly prepared. 15 µl aliquots were immediately added per 12-15 oocytes. After 60 min incubation on ice with occasional gentle mixing, oocytes were washed in Ca<sup>2+</sup>-free ORi with 5.5 mM lysine-monohydrochloride and the labeled protein was purified as described.

Table 2.3: Reaction mix for cell surface iodination with  $^{125}\text{I}$ -sulfo-SHPP.

Reagent	Concentration of stock solution	Volume in reaction mix
Sulfo-SHPP (Pierce, Rockford, USA)	40 $\mu\text{g}/\text{ml}$ in DMSO	0.05 $\mu\text{l}$
$\text{Na}^{125}\text{I}$ (Amersham Buchler, Braunschweig)	4 MBq/ $\mu\text{l}$	0.25 $\mu\text{l}$
Chloramin T (Sigma Chemicals, St. Louis, USA)	5 mg/ml in 0.5 M Na-phosphate pH 7.4	1 $\mu\text{l}$
D,L- $\alpha$ -hydroxy-Phenyl acetic acid (Sigma Chemicals, St. Louis, USA)	1 mg/ml in 0.1 M NaCl	13 $\mu\text{l}$
Sodium meta-bisulfite (Sigma Chemicals, St. Louis, USA)	12 mg/ml in 0.05 M Na-phosphate pH 7.4	1 $\mu\text{l}$

#### 2.4.3.2. Purification of His-tagged protein

Prior to protein purification, radio-labeled oocytes were washed in  $\text{Ca}^{2+}$ -free ORi to avoid activation of  $\text{Ca}^{2+}$ -dependent peptidases. If otherwise not noted, all samples and buffers were kept on ice during protein purification. Oocytes were homogenized in 0.1 M phosphate buffer, pH 8.0 (20  $\mu\text{l}$  per oocyte), containing 1% digitonin, the antipeptidases Pefabloc (1 mM), antipain (100  $\mu\text{l}$ ), and pepstain (100 $\mu\text{l}$ ). In addition, 10 mM iodacetamide was added to avoid artificial disulfide bond formation. The homogenate was incubated on ice for 15 min and occasionally vortexed. The extract was then cleared by two centrifugation steps, each for 10 min at 15,000 rpm and 4°C. 200  $\mu\text{l}$  of the clear supernatant was diluted with 300  $\mu\text{l}$  of the 0.1 M phosphate buffer and supplemented with 30  $\mu\text{l}$  of  $\text{Ni}^{2+}$ -NTA agarose beads and 10 mM imidazole. After 30 min of incubation under continuous end-over-end mixing at ambient temperature, the agarose-bound protein was washed five to six times with 1 ml phosphate buffer containing 0.2% digitonin, 100  $\mu\text{M}$  Pefabloc, and imidazole to reduce the background of endogenous oocyte proteins. A concentration of 25 mM and 15 mM imidazole for metabolically labeled proteins and iodinated proteins,

respectively, was found to be optimal. After washing, the protein was released from the agarose beads by a non-denaturing elution buffer containing 1% digitonin with 200 mM imidazole containing 20 mM Tris/HCl (pH 7.4). Elution was performed under continuous shaking at ambient temperature with 2 x 50  $\mu$ l elution buffer (each step for 10 min). Eluted protein was kept at 0°C until analyzed.

#### **2.4.3.3. Glycosylation analysis**

For analysis of the glycosylation status, 10  $\mu$ l aliquots of purified protein in reducing SDS sample buffer were incubated for 2 hours (occasionally over night) at 37°C with Endo H or PNGase F. For incubation with PNGase F, the samples were supplemented with 1% octylglucoside (added from a 10% stock solution) to prevent inactivation of the enzyme by SDS in the sample buffer.

#### **2.4.3.4. Cross-linking with glutardialdehyde**

Cross-linking was performed after the cell surface iodination with  $^{125}$ I-sulfo-SHPP on intact oocytes. Groups of 12-15 intact radio-iodinated oocytes were washed twice in oocyte PBS. Oocytes were then incubated for 30-60 min (as indicated) with glutardialdehyde. The glutardialdehyde was freshly prepared from a 10fold concentrated stock solution (stock solutions were prepared in oocyte PBS, pH 8.0). After incubation time was finished, the cross-linker was quenched with 500 mM lysine in oocyte PBS and the cells were washed twice in  $\text{Ca}^{2+}$ -free ORi and the labeled protein was purified as described.

#### **2.4.3.5. Dissociation of ion channels into lower complexes**

Different conditions were needed depending on the stability of the ion channel: for dissociation of P2X<sub>1</sub> and P2X<sub>3</sub> receptors, usually 10  $\mu$ l of the protein sample isolated under non-denaturing conditions were supplemented with 2.5  $\mu$ l of the native sample buffer (5x) and 1  $\mu$ l of DTT (1M) and then incubated for 30-60 min at 37°C. For



dissociation of P2X<sub>2</sub>, P2X<sub>5</sub> receptors, and the hetero-multimeric P2X<sub>1</sub>/P2X<sub>2</sub> and P2X<sub>2</sub>/P2X<sub>3</sub> receptors addition of 4 M or 8 M urea (added as solid: 2.5 or 5 mg per 10 µl sample) was required for effective denaturation. By increasing the incubation time, better dissociation efficiency could be achieved.

#### 2.4.3.6. Sodium dodecylsulfate polyacrylamide gel electrophoresis (SDS-PAGE)

For SDS-PAGE, 10 µl of the protein samples were supplemented with 2.5 µl of SDS-sample buffer (5x) after elution under non-denaturing conditions, If not indicated otherwise. DTT was added at a final concentration of 20 mM and samples were incubated at 37°C for 15 min to allow for denaturation and reduction of disulfide bonds. Samples were subsequently electrophoresed in parallel with [<sup>14</sup>C]-labeled molecular mass markers on vertical slab SDS-polyacrylamide gels. Homogenous gels (0.5 mm) or linear gradient gels (1 mm) were cast as indicated, according to the protocol of Biorad, bulletin 1156 (1984). To minimize convective disturbances by heat generation during polymerization of 4-10% gradient gels, 75% of the water in the 10% acrylamide solutions was replaced by a 40% sucrose solution. Electrophoresis was started at 100 V until the buffer front entered the separating gel; voltage was then set to 130 V. The running time was about 1.5 hours.

**Table 2.4 A: Preparation of the SDS-PAGE separating gel.**

Reagents	Final concentration
Separating gel buffer	375 mM Tris/ HCl pH 8.8; LiDS 0.1%
40% acrylamide (19 : 1)	8%; 10%; 12%
APS	0.01%
TEMED	0.5 µl/ml

**Table 2.4 B: Preparation of the SDS-PAGE stacking gel.**

Reagents	Final concentration
Separating gel buffer	375 mM Tris/ HCl pH 8.8; LiDS 0.1%
40% acrylamide (19 : 1)	4%
APS	0.05%
TEMED	1.2 µl/ml

#### 2.4.3.7. Blue native polyacrylamide gel electrophoresis (BN-PAGE)

For BN-PAGE analysis, purified protein was eluted in non-denaturing elution buffer supplemented with 1% digitonin. Samples were stored on ice until electrophoresis.

Blue native PAGE was performed according to the method of Schägger and von Jagow (Schägger & von Jagow, 1991) with slight modifications. 10 µl of the protein sample were supplemented with 2.5 µl of blue native sample buffer (5 X concentrated). 1 mm separating gels with linear polyacrylamide gradients (30% acrylamide mix 37.5:1, Biorad, München, Germany) were cast by a conventional two-chamber gradient mixer and a magnetic stirrer. A 4% polyacrylamide stacking gel (30% acrylamide mix 37.5:1, Biorad, München, Germany) was cast to get sharper protein bands. Molecular mass markers (a mixture of aldolase, bovine serum albumin, ferritin, catalase, and ovalbumin, each 10 µg per lane) were run at either side of the gel. Electrophoresis was performed at 100 V, using the buffers described by Schägger (Schägger & von Jagow, 1991) (for description see section 2.1.2.3). The running time was about 2.5 hours. To further enhance the staining of the molecular weight markers after electrophoresis, the gel was incubated in a staining solution containing Coomassie dye.

**Table 2.5 A: Preparation of the of linear gradient gels (0.1 x 8 x 16 cm) for BN-PAGE (separating gel).**

Reagents	4%	10%	13%
Aqua dest.	3.2 ml	1.03 ml	0.43
3 x gel buffer	1.9 ml	1.90 ml	1.9 ml
Acrylamide 30% (37.5:1)	0.8 ml	1.97 ml	2.57 ml
Glycerol	-	1.0 ml	1.0 ml
TEMED	4 $\mu$ l	4 $\mu$ l	4 $\mu$ l
APS (10%)	20 $\mu$ l	20 $\mu$ l	20 $\mu$ l

**Table 2.5 B: Preparation of the of stacking gel for BN-PAGE (separating gel).**

Reagents	Final concentration
3 x gel buffer	1.67 ml
Acrylamide 30% (37.5:1)	0.667 ml
Aqua dest.	2.64 ml
APS (10%)	20 $\mu$ l
TEMED	4 $\mu$ l

#### 2.4.3.8. Two-dimensional gel electrophoresis

The protein complexes separated in the first dimension by BN-PAGE were further resolved into their individual subunits by denaturing SDS-PAGE in the second dimension. Two-dimensional gel electrophoresis (2-D gel electrophoresis) was performed according to the method of Schagger and von Jagow ([Schagger & von Jagow, 1994](#)) with slight modifications. BN-PAGE for 4%-10% acryl amide BN-PAGE (as described above) was always used in the first dimension of two-dimensional PAGE. SDS-PAGE then followed in the second dimension. The transition from first to second dimension was performed as follows: one "lane" (0.3-0.5 cm) of BN-PAGE was cut out and the gel slice carrying the dissociated proteins separated during the

BN-PAGE was soaked with stacking gel buffer (1x) and 1% mercaptoethanol for 2 hours. Mercaptoethanol was then removed as completely as possible since it inhibits polymerization of acrylamide. The gel slice was then placed on a glass plate at the usual position for stacking gels. Spacers were positioned (0.1 mm), and the second glass plate was put on top. A separating gel mixture for 8% acrylamide SDS-PAGE was poured between the glass plates leaving a 1 cm gap to the first-dimensional gel strip. After polymerization of the separating gel, the gel strip was embedded in a 4% acrylamide stacking SDS gel so that the strip of gel was covered. High APS and TEMED concentrations (50  $\mu$ l of APS (10%) and 10  $\mu$ l of TEMED per 5 ml) were necessary to allow complete polymerization within 60 min despite the presence of traces of mercaptoethanol. Electrophoresis was started using the SDS-PAGE running buffer at 100 V until the buffer front entered the separating gel; voltage was then set to 130 V. The running time was about 1.5 hours.

#### 2.4.4. Electrophysiology

Dr. J. Rettinger performed functional analysis of ion channel constructs. Current responses were measured by using the two-electrode voltage-clamp technique on *Xenopus laevis* oocytes injected with respective cRNA one to three days earlier. The electrodes contained 3 M KCl and had resistances of 0.5 – 2 M $\Omega$ . The superfusion solution consisted of 90 mM NaCl, 1 mM KCl, 2 mM MgCl<sub>2</sub> and 5 mM Hepes/NaOH, pH 7.4. Calcium salts were omitted to avoid activation of endogenous Ca<sup>2+</sup>-dependent Cl<sup>-</sup> channels. A fast and reproducible solution exchange was achieved by using a 10  $\mu$ l experimental oocyte chamber combined with a fast solution flow (150  $\mu$ l/s) fed through a glass capillary mounted close above the oocyte. Current signals were low pass filtered at 100 Hz, and sampled at 200 Hz using the Turbo TEC-05 amplifier (NPI electronics, Germany). All measurements were performed at room temperature (20-22°C).

For analysis of P2X receptor-mediated responses, 1  $\mu$ M ATP was applied for 5 s at 1 min intervals. Between measurements at different holding potentials, control responses to 1  $\mu$ M ATP for 5 s at -60 mV were recorded and only oocytes with less than 10% change in control responses at -60 mV throughout the experiment were included for analysis.

## 3. Results

### 3.1. Characterization of P2X receptors in *Xenopus laevis* oocytes

#### 3.1.1. Characterization of His-tagged P2X<sub>2</sub> subunits after expression in *Xenopus* oocytes

The rat P2X<sub>2</sub> subunit was N-terminally tagged with a hexahistidyl sequence to allow for the purification of the rat P2X<sub>2</sub> protein (His-rP2X<sub>2</sub>) after expression in *Xenopus* oocytes. The isolation of the protein was achieved using Ni<sup>2+</sup>-NTA agarose affinity chromatography. This purification method has the advantage that proteins can be released from the agarose beads under non-denaturing conditions.

##### 3.1.1.1. Electrophysiological characterization of rP2X<sub>2</sub> constructs after expression in *Xenopus* oocytes

In order to first confirm that the hexahistidyl tag does not disturb the function of the rP2X<sub>2</sub> receptor, electrophysiological measurements on cRNA-injected oocytes were performed to compare the electrophysiological phenotype of the non-tagged and the hexahistidyl-tagged P2X<sub>2</sub> receptors. Two days after injection, oocytes expressing the His-P2X<sub>2</sub> subunit were exposed to ATP under two-electrode voltage clamp and the rates of desensitization were compared with those of oocytes expressing the wild-type P2X<sub>2</sub> receptor. In oocytes expressing the His-rP2X<sub>2</sub> or the wild type rP2X<sub>2</sub> receptor, prolonged application of ATP (30 μM) elicited a large inward current with a rapid onset and slow rate of desensitization (Fig. 3.1 A and B). In addition, concentration response curves for ATP of the wild type P2X<sub>2</sub> and the His-rP2X<sub>2</sub> receptor were recorded (Fig. 3.1 C). Fitting the Hill equation to the data for the wild type rP2X<sub>2</sub> receptor and the His-rP2X<sub>2</sub> receptor yielded EC<sub>50</sub> values for ATP of 25.0 ± 1.9 μM (n=12), and 25.9 ± 1.9 μM (n=10), respectively, i.e. an virtually identical potency for ATP. This observation indicates that the N-terminal His-tag has no effect on the function of the rat P2X<sub>2</sub> receptor.

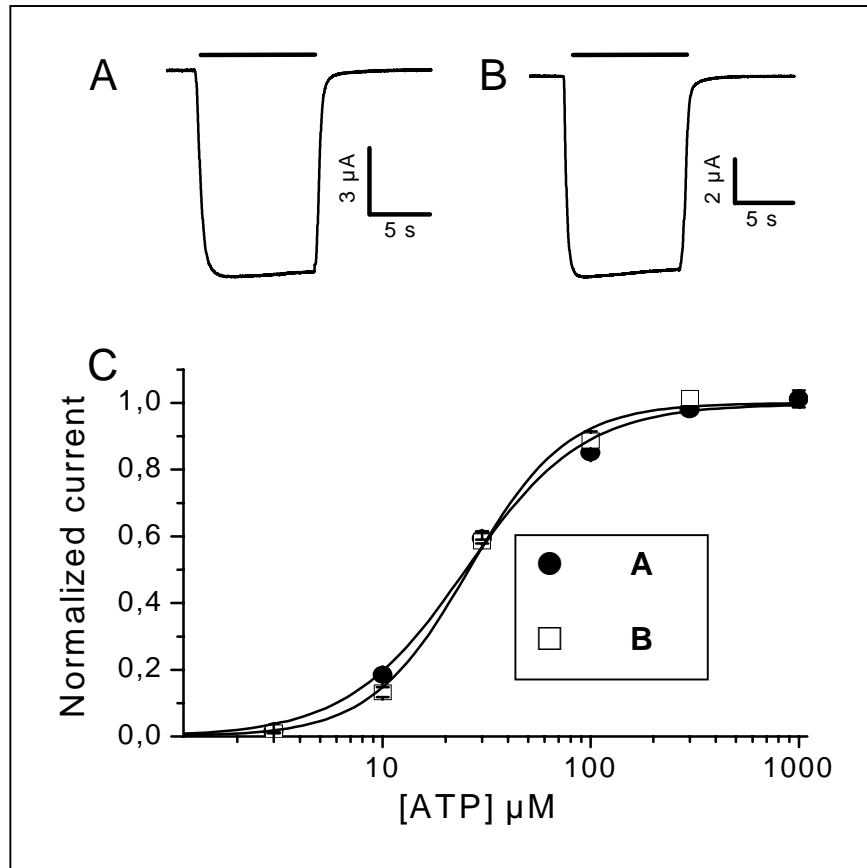


**Fig. 3.1: Comparison of electrophysiological responses to activation of the wild type or the hexahistidyl-tagged P2X<sub>2</sub> receptor.** Oocytes were injected with 0.25 ng of cRNA for the wild type P2X<sub>2</sub> (A) or the His-rP2X<sub>2</sub> subunit (B). Two days after injection current responses elicited by 30 μM ATP were measured at a holding potential -60 mV. The duration of agonist activation is shown by the horizontal bar. (C) ATP dose-response curves for the wild type P2X<sub>2</sub> (□) and the His-rP2X<sub>2</sub> receptor (●). Currents were elicited by the respective ATP concentration in 1-min intervals. The experiment was performed by Dr. Jürgen Rettinger.

### 3.1.1.2. Biochemical analysis of the glycosylation status of P2X<sub>2</sub> constructs

For biochemical analysis, oocytes injected with the cRNA for the His-P2X<sub>2</sub> subunit were metabolically labeled by overnight incubation with [<sup>35</sup>S]methionine. Directly after the labeling or after an additional 24h chase interval, digitonin extracts were prepared. His-P2X<sub>2</sub> was isolated by Ni<sup>2+</sup>-NTA agarose affinity chromatography, eluted with non-denaturing elution buffer, and then supplemented with SDS sample buffer. Samples were incubated in the presence of Endo H or PNGase F and then analyzed by SDS-PAGE followed by autoradiography.

SDS-PAGE analysis of the [<sup>35</sup>S]methionine-labeled His-rP2X<sub>2</sub> subunit after the overnight pulse period yielded two bands with approximate molecular masses of 61 kD and 50 kD (Fig. 3.2, lane 1), respectively. The smaller band, possibly a proteolytic

cleavage product generated within the ER, almost disappeared within the 20h chase period (Fig. 3.2, lane 4). Treatment with PNGase F reduced the molecular mass by 6-8 kD, yielding a 53 kD band (Fig. 3.2, lane 6), close to the mass of the His-tagged protein core computed from the cDNA-deduced protein sequence (52.5 kD). Since 6-8 kD corresponds to the mass of three N-linked oligosaccharide side chains, this finding implies that each of the three consensus sequences for N-linked glycosylation at positions <sup>182</sup>NFTI, <sup>239</sup>NFTE, and <sup>298</sup>NGTT of the rP2X<sub>2</sub> subunit is occupied by an N-glycan.

Glycoproteins carrying fully processed complex-type carbohydrates are resistant to Endo H digestion. As shown in Fig. 3.2, lane 5, the His-rP2X<sub>2</sub> subunit was partially resistant to Endo H after the chase period, indicating that a significant portion of the His-rP2X<sub>2</sub> receptor is able to leave the ER within 20h, and that possibly all of the three N-linked carbohydrate chains become complex glycosylated in the Golgi apparatus.

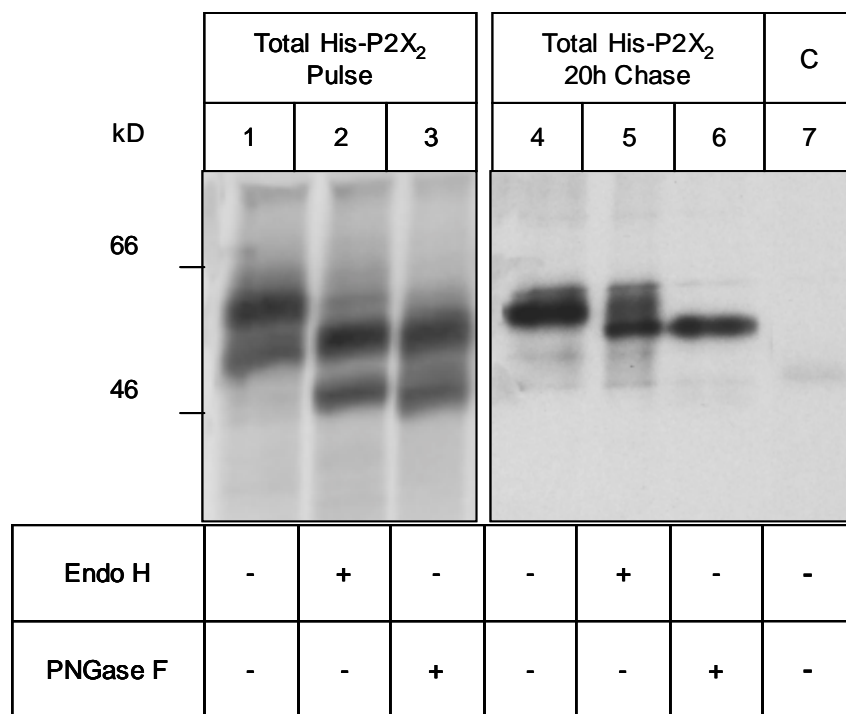


**Fig. 3.2: Glycosylation status of the His-rP2X<sub>2</sub> polypeptide after metabolic labeling.** Oocytes injected with 25 ng of cRNA for His-rP2X<sub>2</sub> were metabolically labeled overnight. Cells were either directly extracted with 1% digitonin or after a 20 h chase period. His-rP2X<sub>2</sub> was purified by Ni<sup>2+</sup>-NTA affinity chromatography. Samples were eluted in 200 mM imidazole, 20 mM Tris and 1% digitonin (pH 7.4), and treated with PNGase F (5 IUB, milliunits per 10  $\mu$ l sample) or Endo H (5 IUB milliunits per 10  $\mu$ l sample) and analyzed by SDS-PAGE (8% acrylamide). C, non-injected oocytes.

To further explore the glycosylation status of His-rP2X<sub>2</sub> at the cell surface, the N-glycosylation site at <sup>239</sup>N was eliminated by site-directed mutagenesis. Oocytes expressing the parent His-rP2X<sub>2</sub> or the mutant His-rP2X<sub>2</sub>-N<sup>239</sup>Q subunit were surface radio-iodinated with <sup>125</sup>I-sulfo-SHPP three days after cRNA injection. The radio-iodinated proteins were then isolated by Ni<sup>2+</sup>-NTA chromatography under non-denaturing conditions from digitonin extracts, denatured with SDS sample buffer, then treated with Endo H and PNGase F. SDS-PAGE analysis of <sup>125</sup>I-labeled parent His-P2X<sub>2</sub> subunit revealed a band with an approximate molecular mass of 61 kD (Fig. 3.3, lane 1). Treatment with Endo H did not induce a decrease of the mass of the His-rP2X<sub>2</sub> subunit (Fig. 3.3, lane 2), indicating that none of the N-glycans is sensitive to Endo H. After treatment with PNGase F, the radiolabeled His-rP2X<sub>2</sub> polypeptide migrated at 53 kD (Fig. 3.3, lane 3). Since this reflects a mass difference compatible with three Endo H resistant N-glycans compared to the mass of the non-treated glycoprotein, it can be concluded that the His-rP2X<sub>2</sub> subunit acquires three complex-type carbohydrates during transit of the Golgi apparatus.

Next, the role of N-glycans for surface expression of the His-rP2X<sub>2</sub> receptor was determined. To this end, the glycan minus mutant His-rP2X<sub>2</sub>-N<sup>239</sup>Q was analyzed by SDS-PAGE. The <sup>125</sup>I-labeled His-rP2X<sub>2</sub>-N<sup>239</sup>Q was isolated from the cell surface as a glycoprotein that had a 2-3 kD lower mass than the parent P2X<sub>2</sub> glycoprotein (Fig. 3.3, lane 4), indicating that the replaced asparagine is occupied by an N-glycan in the wild type P2X<sub>2</sub> subunit. Treatment with Endo H failed to alter the mobility of the mutant glycoprotein (Fig. 3.3, lane 5), indicating that His-rP2X<sub>2</sub>-N<sup>239</sup>Q is only in the complex-glycosylated form. The elimination of the glycan at <sup>239</sup>N resulted in a decrease of the expression level.



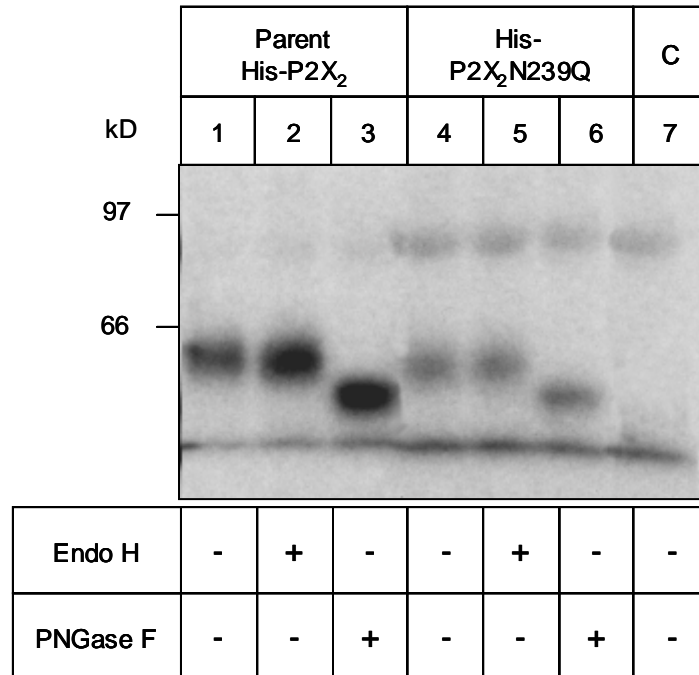


**Fig. 3.3: Glycosylation status of His-rP2X<sub>2</sub> and His-rP2X<sub>2</sub>N<sup>239</sup>Q on the cell surface.** Oocytes injected with 2.5 ng of cRNA for His-P2X<sub>2</sub> or His-P2X<sub>2</sub>N<sup>239</sup>Q were left for 3 days at 19°C and then labeled with membrane-impermeant <sup>125</sup>I-sulfo-SHPP. His-rP2X<sub>2</sub> and His-rP2X<sub>2</sub>N<sup>239</sup>Q were purified by Ni<sup>2+</sup>-NTA affinity chromatography from 1% digitonin extracts of each oocyte group, and eluted with non-denaturing elution buffer. Aliquots of these samples were supplemented with SDS sample buffer, 20 mM DTT, and PNGase F in 1% octylglycoside (5 IUB, milliunits per 10 µl sample) or Endo H (5 IUB milliunits per 10 µl sample). After 2 h incubation at 37°C, proteins were resolved by SDS-PAGE (8% acrylamide) followed by autoradiography. C, non-injected control oocytes.

### 3.1.1.3. Investigation of the quaternary structure of the rat P2X<sub>2</sub> receptor

#### 3.1.1.3.1. Cross-linking analysis

The cross-linker glutardialdehyde was used to investigate the quaternary structure of P2X<sub>2</sub> receptors in the plasma membranes of intact *Xenopus* oocytes. The aldehyde groups of glutardialdehyde are able to form a Schiff base with lysine residues. Therefore, this cross-linker may be suited to investigate the oligomeric state of protein complexes. His-rP2X<sub>2</sub> cRNA-injected oocytes were surface-labeled with <sup>125</sup>I-sulfo-SHPP and then incubated with 100 µM glutardialdehyde for 30 min and 60 min. After the cross-linking reaction, His-rP2X<sub>2</sub> receptor was purified from a digitonin extract of the oocytes by Ni<sup>2+</sup> NTA agarose affinity chromatography and subjected to reducing SDS-PAGE analysis. In addition to the rat P2X<sub>2</sub> monomer, two bands of higher molecular masses were observed in cross-linker treated oocytes (Fig. 3.4, lanes 3 and 4). These bands corresponded in size to the calculated molecular

masses of the rat P2X<sub>2</sub> dimer and trimer. In all experiments, the intensity of the bands strongly declined when the incubation time with glutardialdehyde was increased.

The results of this experiment cannot entirely exclude the generation rP2X<sub>2</sub> complexes higher than the trimer. Such complexes may have remained undetected due to the reduced amount of isolated protein after the cross-linking reaction. Therefore, the blue native polyacrylamide gel electrophoresis (BN-PAGE) was used as an alternative approach to investigate the oligomeric state of rP2X<sub>2</sub> receptor complex.

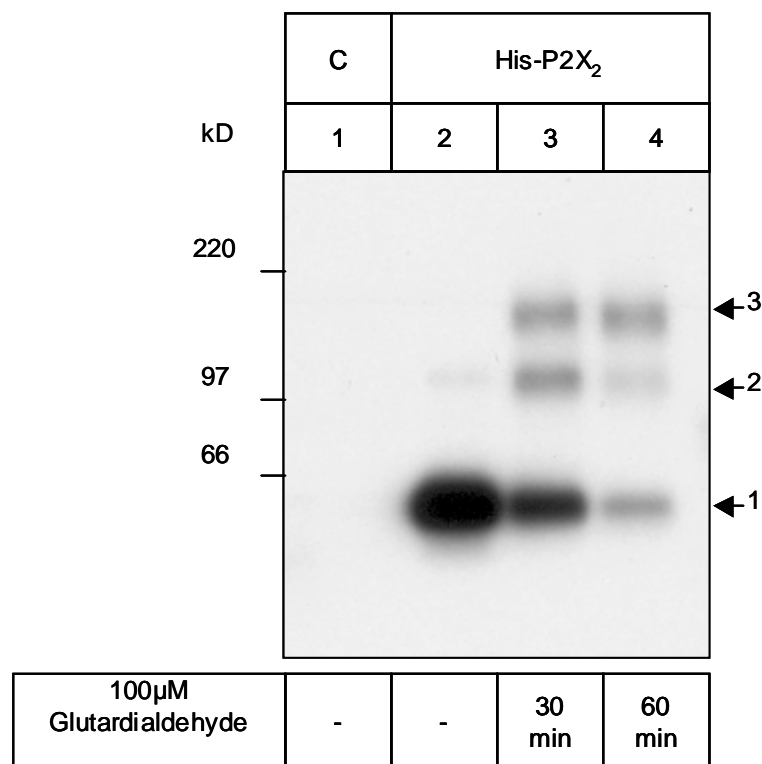


**Fig. 3.4: Cross-linking of the His-rP2X<sub>2</sub> receptor with glutardialdehyde in intact *Xenopus* oocytes.** Oocytes injected with 2.5 ng of cRNA for His-P2X<sub>2</sub> were surface iodinated with <sup>125</sup>I-sulfo-SHPP three days after injection. Immediately after removal of unbound <sup>125</sup>I-sulfo-SHPP by washing, the cross-linking reaction was inhibited by adding 100 μM glutardialdehyde to the intact oocytes for 30 min or 60 min at 4°C. After removing of excess glutardialdehyde by washing with oocyte-PBS, the oocytes were homogenized in 1% digitonin. His-P2X<sub>2</sub> was purified by Ni<sup>2+</sup>-NTA agarose affinity chromatography, eluted with non-denaturing elution buffer, and analyzed by reducing SDS-PAGE (4-10% acrylamide gradient gel). C, non-injected control oocytes.

### 3.1.1.3.2. Blue native PAGE analysis

It was previously reported that the His-tagged rat P2X<sub>1</sub> receptor migrates at 240 kD when resolved by blue native PAGE (Fig. 3.6, lane 1). The exposure of the natively eluted rat P2X<sub>1</sub> receptor to DTT and urea in the presence of Coomassie blue and sodium 6-amino-*n*-caproate caused a partial dissociation of the His-rP2X<sub>1</sub> receptor complex into a monomer and a dimer of apparent masses similar to 80 kD and 170 kD, respectively (Fig. 3.6, lanes 2-4), indicating that the non-denatured 240 kD protein band is a homo-trimer (Nicke *et al.*, 1998).

To investigate the assembly of rat P2X<sub>2</sub> subunits, oocytes injected with the cRNA for the His-rP2X<sub>2</sub> subunit were metabolically labeled with [<sup>35</sup>S]methionine. His-rP2X<sub>2</sub> protein complexes were then isolated under non-denaturing conditions from a digitonin extract of the oocytes directly after the metabolic labeling or after a subsequent 20 h chase period and analyzed by BN-PAGE. Metabolically labeled His-P2X<sub>2</sub> protein isolated after the overnight pulse period migrated at a broad range of masses well above the 250 kD band of the rP2X<sub>1</sub> homo-trimer when analyzed by BN-PAGE (Fig. 3.5, lane 1). Most likely, this large excess of undefined protein complexes represents aggregates of His-rP2X<sub>2</sub> subunits. Treatment with urea did not lead to a marked dissociation of the aggregates into lower order intermediates (Fig. 3.5, lanes 2 and 3).

When the digitonin-solubilized His-rP2X<sub>2</sub> protein was purified under non-denaturing conditions from metabolically labeled oocytes after an additional 20 h chase period and analyzed by BN-PAGE, not only aggregates in the high molecular mass range, but also two weak protein bands of approximately 220 kD and 380 kD were observed (Fig. 3.5, lane 4). Incubation prior to BN-PAGE of the natively eluted His-rP2X<sub>2</sub> receptor with urea in the presence of the blue native sample buffer intensified the visibility of these two bands and induced the appearance of a third band of ~120 kD (Fig. 3.5, lanes 5 and 6). In conclusion, these observations demonstrate that the majority of metabolically labeled His-rP2X<sub>2</sub> subunit did not assemble within the first 15h after the cRNA injection. While the trimeric complex of His-rP2X<sub>2</sub> receptor is weakly visible at 380 kD, also intermediate dimers and a large amount of aggregated proteins are observed by BN-PAGE analysis.

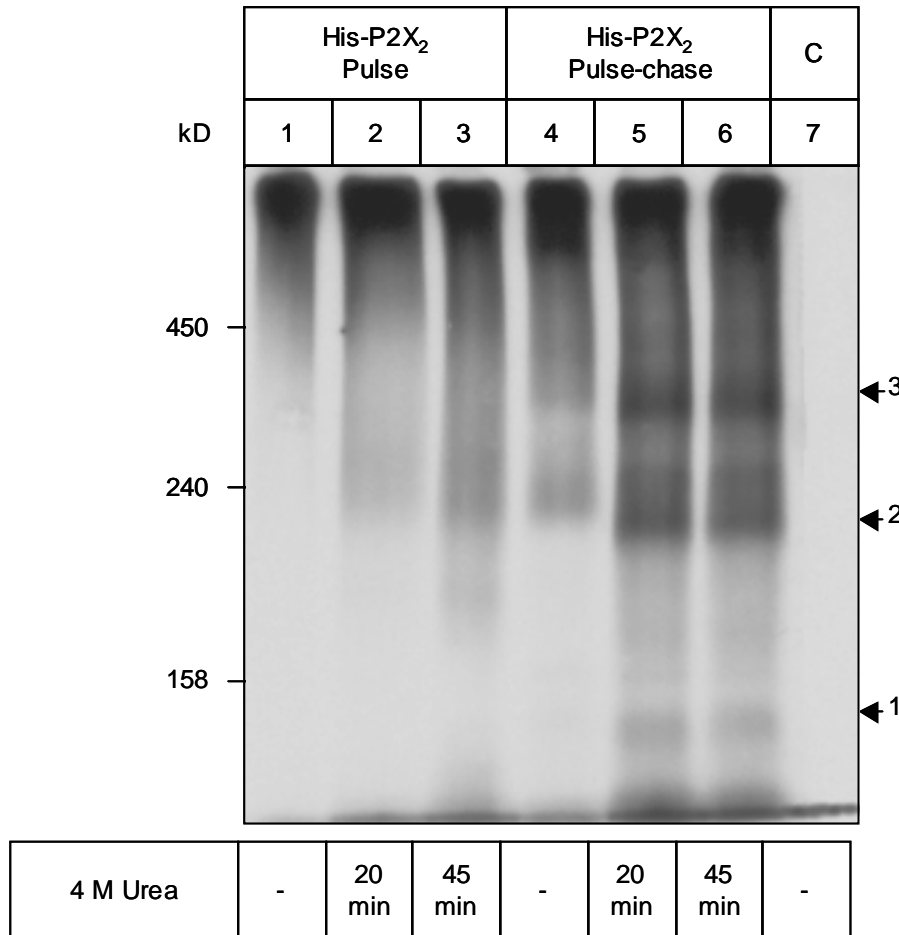


**Fig. 3.5: His-rP2X<sub>2</sub> receptor complexes resolved on a blue native polyacrylamide gel.** Oocytes injected with 2.5 ng of cRNA for His-rP2X<sub>2</sub> protein were metabolically labeled overnight. Cells were either immediately extracted with 1% digitonin (pulse) or first chased for 20 h and then extracted. The His-rP2X<sub>2</sub> protein was purified by Ni<sup>2+</sup>-NTA affinity chromatography under non-denaturing conditions. Digitonin solubilized His-rP2X<sub>2</sub> receptor was either non-treated or dissociated by incubation with increasing concentration of urea in the presence of blue native sample buffer (45 min, 37°C). Samples were analyzed by BN-PAGE (4-13% acrylamide gradient gel). C, non-injected control oocytes.

Cross-linking analysis of radio-iodinated His-P2X<sub>2</sub> subunits in the plasma membranes of intact oocytes revealed a trimeric structure for this receptor. However, investigation of the glycosylation status of total His-P2X<sub>2</sub> protein from the [<sup>35</sup>S]methionine labeled oocytes revealed that part of the synthesized protein was retained in the ER one day after injection (Fig. 3.2, lane 3). This retention of His-rP2X<sub>2</sub> receptor in the ER may reflect 'quality control' (Hammond & Helenius, 1995). In addition, when resolved by BN-PAGE, the metabolically labeled His-rP2X<sub>2</sub> protein appeared as two bands representing dimers and trimers and a diffuse smear of aggregated protein (Fig. 3.5, lane 4). These results indicate an incomplete folding and partial assembly of His-P2X<sub>2</sub> receptor. To visualize the plasma membrane form of the His-P2X<sub>2</sub> receptor with BN-PAGE, oocytes injected with His-rP2X<sub>2</sub> cRNA were surface radio-iodinated, and the <sup>125</sup>I-labeled His-rP2X<sub>2</sub> receptor was isolated by Ni<sup>2+</sup>

-NTA chromatography under non-denaturing conditions. Blue native PAGE analysis of the surface expressed His-rP2X<sub>2</sub> receptor revealed three bands at 380 kD, 550 kD and a band that did not enter the separating gel. The bands at 380 kD and 550 kD correspond in size to the trimeric and hexameric form of His-rP2X<sub>2</sub> receptor (Fig. 3.6, lane 5). Tetrameric or pentameric complexes between the two bands were not detected. The protein band of higher molecular mass, which did not enter the acrylamide gel, might correspond to the nanomeric form of His-rP2X<sub>2</sub> protein. The 380 kD protein band corresponded in mass to the metabolically labeled His-rP2X<sub>2</sub> trimer (Fig. 3.5, lane 4). Exposure of the natively eluted His-rP2X<sub>2</sub> receptor to urea at 37°C prior to the blue native PAGE induced the appearance of two additional bands beside the non-denatured His-rP2X<sub>2</sub> trimeric complex (Fig. 3.6, lane 6). These protein bands of apparent masses of 220 kD and 120 kD represent the intermediate His-rP2X<sub>2</sub> dimer and monomer, respectively.

To analyze the number of subunits of the rat P2X<sub>2</sub> receptor, also the strong reductant DTT in the presence of blue native sample buffer was applied. This investigation revealed that the radio-iodinated His-P2X<sub>2</sub> receptor in contrast to the His-rP2X<sub>1</sub> complex almost completely resisted dissociation by exposure to DTT (Fig.3.6, lane 7). It turned out that DTT intensified the dissociation of the His-rP2X<sub>2</sub> complex when used in combination with urea (Fig. 3.6, lane 8).

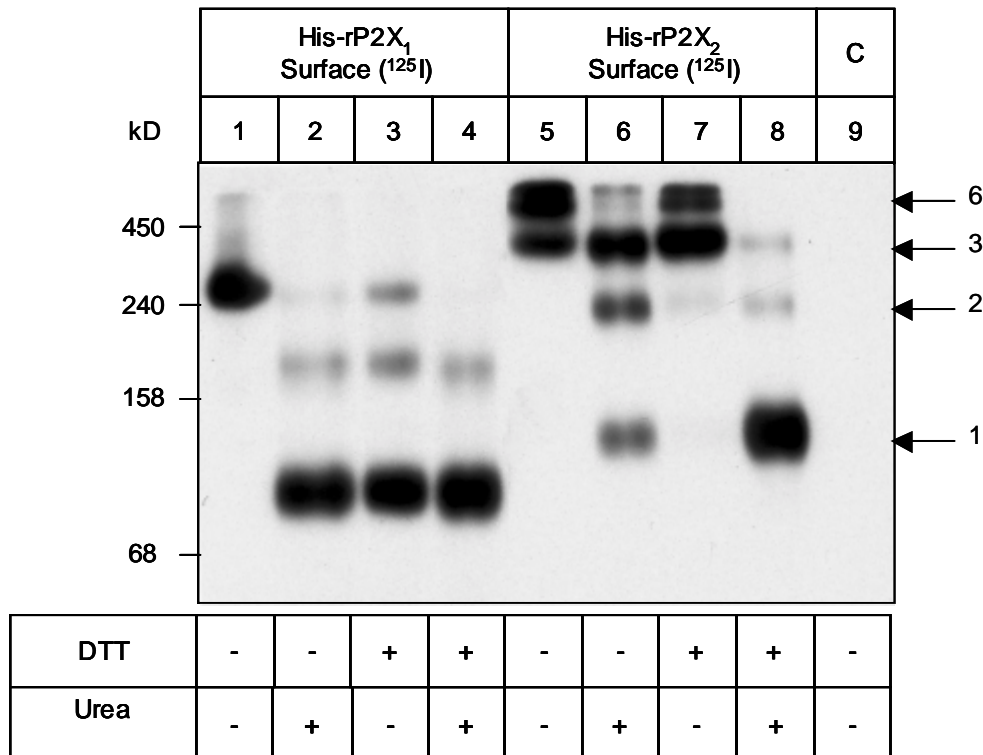


**Fig. 3.6: Dissociation of surface-iodinated His-rP2X<sub>1</sub> and His-rP2X<sub>2</sub> receptors.** Oocytes injected with 25 ng of cRNA for His-rP2X<sub>1</sub> or 2.5 ng of cRNA for His-rP2X<sub>2</sub> were left for 3 days at 19°C and then surface-labeled with membrane-impermeant <sup>125</sup>I-sulfo-SHPP. His-rP2X<sub>1</sub> or His-rP2X<sub>2</sub> receptors were purified by Ni<sup>2+</sup>-NTA agarose affinity chromatography from 1% digitonin extracts of each oocyte group, and eluted with non-denaturing elution buffer. His-rP2X<sub>1</sub> or His-rP2X<sub>2</sub> receptors were either non-treated or dissociated by incubation with 8 M urea, dissociated by incubation with 100 mM DTT, dissociated by incubation with both 8 M urea and 100 mM DTT in the presence of blue native sample buffer (45 min, 37°C). Samples were analyzed by BN-PAGE (4-13% acrylamide gradient gel). C, non-injected control oocytes.

#### 3.1.1.4. Oligomeric state of a His-rP2X<sub>2</sub> deletion mutant

All members of the P2X receptor family are produced by the oligomeric assembly of two-transmembrane domain subunits with both their N and C termini located intracellularly (Chow, 1998). Rat P2X<sub>2</sub> subunits have a large intracellular C-terminal domain. In an attempt to determine the role of this region in the P2X<sub>2</sub> receptor oligomerization, a truncated form of the wild-type P2X<sub>2</sub> subunit was produced, lacking 63 amino acid residues of the C-terminus of His-P2X<sub>2</sub> (His-P2X<sub>2</sub><sup>1-409</sup>). The truncation of the P2X<sub>2</sub> subunit produced a protein consisting of 409 amino acids that had approximately the same size like the wild type P2X<sub>1</sub> subunit (399 amino acids). It is known that His-rP2X<sub>1</sub> migrates at 240 kD when analyzed by BN-PAGE. The intention of the investigation was also to compare the migration of the truncated P2X<sub>2</sub> with the migration of His-P2X<sub>1</sub> in the BN-PAGE. A further intention was to

reveal the role of the C terminal end of the rat P2X<sub>2</sub> subunit in the assembly of the His-rP2X<sub>2</sub> receptor.

BN-PAGE analysis of the radio-iodinated His-rP2X<sub>2</sub><sup>1-409</sup> mutants revealed that the truncated His-P2X<sub>2</sub> was detectable on the surface of *Xenopus* oocytes. Like the parent His-rP2X<sub>2</sub> receptor, the His-rP2X<sub>2</sub><sup>1-409</sup> construct appeared as a distinct protein band, but with a lower apparent molecular mass of about 270 kD (Fig. 3.7, lane1). This protein band corresponded in mass approximately to the mass of the protein band of the His-rP2X<sub>1</sub> complex resolved by BN-PAGE and can hence be considered to possess a trimeric structure.

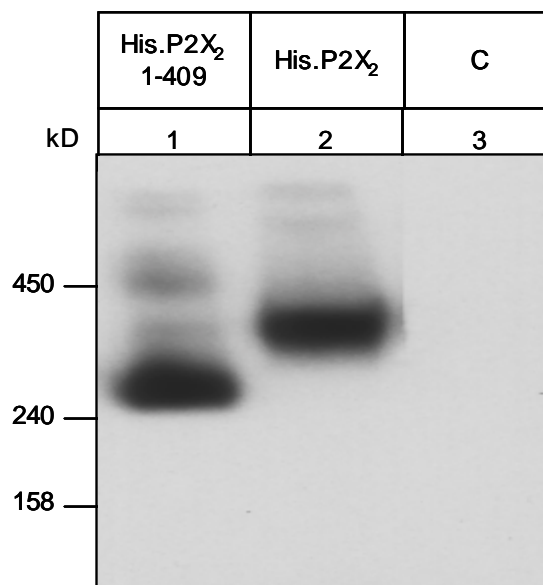


**Fig. 3.7: BN-PAGE analysis of a C-terminally truncated His-rP2X<sub>2</sub> subunit on the cell surface.** Oocytes injected with 2.5 ng of cRNA for the His-rP2X<sub>2</sub> subunit or His-rP2X<sub>2</sub><sup>1-409</sup> mutant were left for 3 days at 19°C and then surface-labeled with membrane-impermeant <sup>125</sup>I-sulfo-SHPP. Protein was isolated under non-denaturing conditions (1% digitonin) and analyzed by BN-PAGE on a 4-10% acrylamide gradient gel. C, non-injected control oocytes.

When the metabolically labeled His-P2X<sub>2</sub><sup>1-409</sup> protein was purified under non-denaturing conditions and analyzed by BN-PAGE, mainly undefined protein complexes in form of aggregates in the high molecular mass rang and a very weak protein band of approximately 270 kD were observed (Fig. 3.8, lane 2). Partial dissociation with 4 M urea in the presence of blue native sample buffer prior to BN-PAGE intensified the protein band at 270 kD, but this band was still very poorly visible (Fig. 3.8, lane 3). Treatment with 8 M urea reduced the amount of the aggregated protein and induced the appearance of two additional bands at 100 kD and 190 kD (Fig. 3.8, lane 4). Most of the aggregated protein was dissociated into

the monomeric form at 100 kD when treated by 8 M urea. This indicates that like parent His-P2X<sub>2</sub>, the majority of metabolically labeled His-P2X<sub>2</sub><sup>1-409</sup> did not assemble within the first two days after the cRNA injection. While the trimeric form of the His-rP2X<sub>2</sub><sup>1-409</sup> protein complex could be detected on the cell surface, most of the intracellular located His-P2X<sub>2</sub><sup>1-409</sup> subunits existed as aggregated protein as visualized by BN-PAGE.

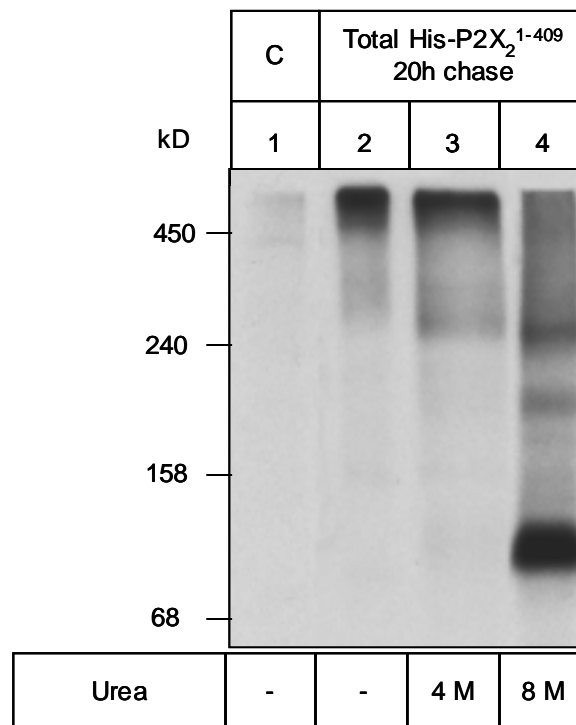


**Fig. 3.8: C-terminally truncated His-rP2X<sub>2</sub> protein complex resolved on a blue native polyacrylamide gel.** Oocytes injected with 2.5 ng of cRNA for His-rP2X<sub>2</sub><sup>1-409</sup> mutant were metabolically labeled overnight. Cells were chased for 20 h and then extracted with 1% digitonin. The His-rP2X<sub>2</sub><sup>1-409</sup> protein was purified by Ni<sup>2+</sup>-NTA affinity chromatography under non-denaturing conditions. Digitonin solubilized His-rP2X<sub>2</sub><sup>1-409</sup> was either non-treated or dissociated by incubation with increasing concentration of urea in the presence of blue native sample buffer (45 min, 37°C). Samples were analyzed by BN-PAGE (4-13% acrylamide gradient gel) followed by autoradiography. C, non-injected control oocytes.



### 3.1.2. Characterization of His-tagged rat P2X<sub>5</sub> receptors after expression in *Xenopus* oocytes

Like the rat P2X<sub>2</sub> subunit, also the rat P2X<sub>5</sub> subunit was N-terminally tagged with a hexahistidyl sequence to allow for affinity chromatography-mediated purification of the His-rP2X<sub>5</sub> protein after expression in *Xenopus* oocytes.

#### 3.1.2.1. Electrophysiological characterization rat P2X<sub>5</sub> receptors after expression in *Xenopus* oocytes

In order to confirm that the hexahistidyl tag does not disturb the function of the rat P2X<sub>5</sub> receptor, electrophysiological measurements on cRNA-injected oocytes were performed to compare the current-carrying properties of the non-tagged and the hexahistidyl-tagged rat P2X<sub>5</sub> receptors. Two days after injection, oocytes expressing the His-rP2X<sub>5</sub> subunit were exposed to ATP under two-electrode voltage clamp and the current amplitudes as well as the rates of desensitization were compared with those of oocytes expressing the wild-type P2X<sub>5</sub> receptor. Fig. 3.9 A and B show current responses of wild type rP2X<sub>5</sub> and His-rP2X<sub>5</sub>, respectively, elicited at the holding potential –60 mV by application of 10 μM ATP. In oocytes expressing the His-P2X<sub>5</sub> or the wild type rP2X<sub>5</sub> receptor, ATP applied for 10 sec evoked a sustained nondesensitizing current. Simultaneously, a second non-desensitizing current was observed in response to 10 μM ATP from oocytes injected with cRNA for the wild type rP2X<sub>5</sub> or His-rP2X<sub>5</sub> receptors. This non-desensitizing current component results possibly from the activation of endogenous ion channels of *Xenopus* oocytes that interact with the heterologously expressed wild type rP2X<sub>5</sub> or His-rP2X<sub>5</sub> receptors, since this current component was not observed when the rP2X<sub>5</sub> receptor was functionally analyzed in HEK-293 cells (Ruppelt *et al.*, 2001). Taken together, the results obtained from the electrophysiological analysis of both constructs suggested that N-terminal His-tag has no effect on the function of the rP2X<sub>5</sub> receptor.

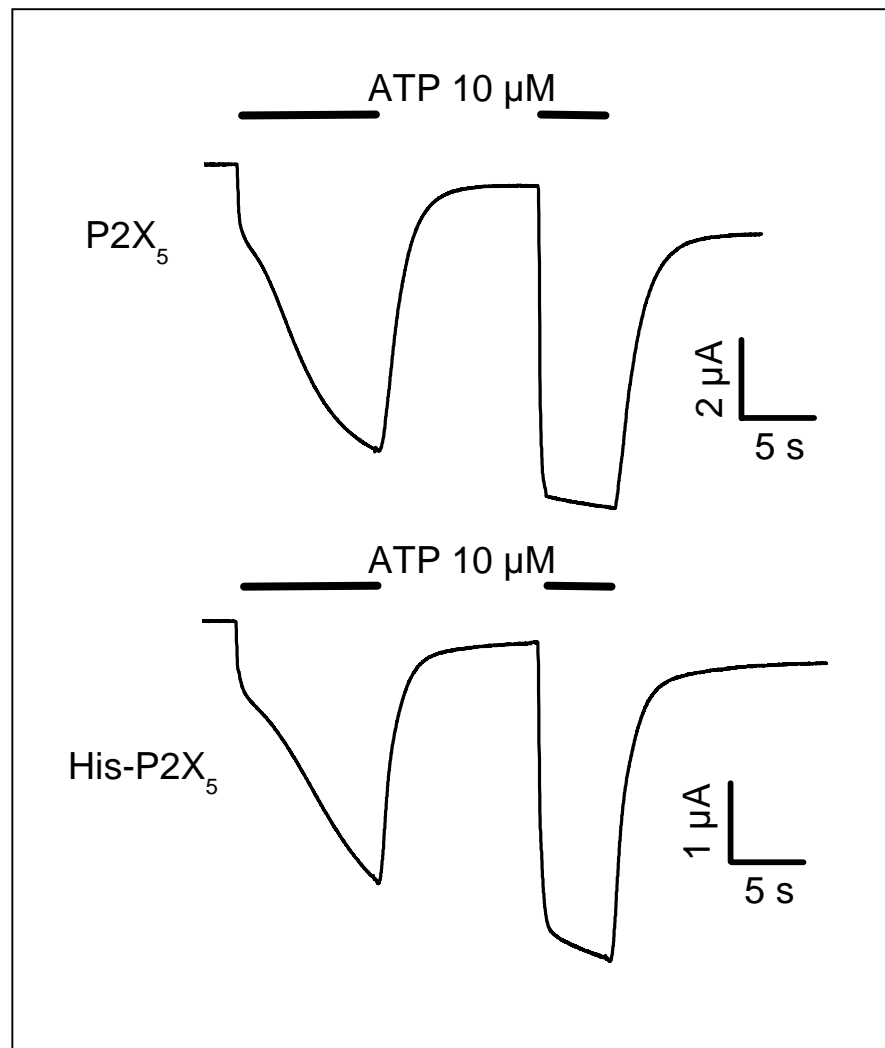


**Fig. 3.9: Comparison of the ATP-elicited currents responses of the wild type rP2X<sub>5</sub> receptor and the hexahistidyl-tagged rP2X<sub>5</sub> receptor.** Oocytes were injected with 25 ng of cRNA for wild type P2X<sub>5</sub> or His-P2X<sub>5</sub>. Two days after injection current responses elicited by 10 μM ATP were measured at -60 mV. The horizontal bar shows the duration of agonist activation. The experiment was performed by Dr. Jürgen Rettinger.

### 3.1.2.2. Biochemical characterization of His-rP2X<sub>5</sub> polypeptides after expression in *Xenopus* oocytes by SDS-PAGE

His-rP2X<sub>5</sub> protein isolated from metabolically labeled oocytes was subjected to SDS-PAGE analysis. His-rP2X<sub>5</sub> subunits yielded one band with approximate molecular masses of 60 kD (Fig. 3.10, lane 2). Treatment with PNGase F reduced the molecular mass by 6-8 kD to ~52 kD (Fig. 3.10, lane 4), close to the mass of the His-tagged protein core computed from the cDNA complex (51.5 kD). Since 6-8 kD corresponds to the mass of three N-linked oligosaccharide side chains, this finding implies that each of the three asparagines for possible N-linked glycosylation

(NXT/S) are occupied by an N-glycan in the His-rP2X<sub>5</sub> subunit. As shown in Fig. 3.10, lane 3, a fraction of metabolically labeled His-rP2X<sub>5</sub> subunit was partially Endo H-resistant, indicating that a significant portion of the His-rP2X<sub>5</sub> subunits leaves the ER and that at least one N-linked carbohydrate chain becomes complex glycosylated in the Golgi apparatus. In addition, the investigation revealed that two days after the injection a part of the synthesized protein was entirely Endo H sensitive and thus was retained in the ER as shown by the samples (Fig. 3.10, lanes 3).

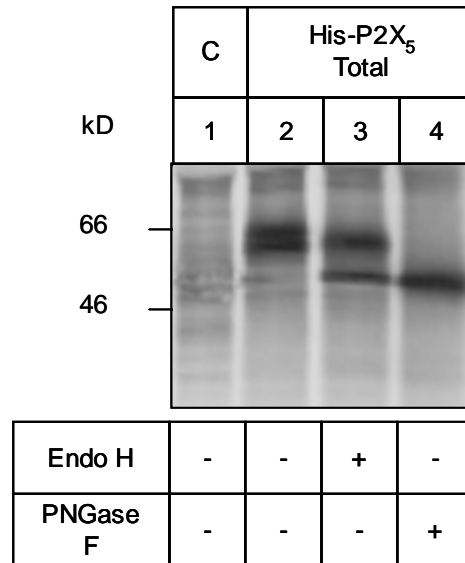


**Fig 3.10: Glycosylation status of His-rP2X<sub>5</sub>.** Oocytes injected with 2.5 ng of cRNA for the His-rP2X<sub>5</sub> were metabolically labeled. His-rP2X<sub>5</sub> was purified by Ni<sup>2+</sup>-NTA affinity chromatography from a 1% digitonin extract of the *Xenopus* oocytes. Samples were eluted under non-denaturing conditions and treated with PNGase F or Endo H and analyzed by SDS-PAGE (8% acrylamide). C indicates samples from non-injected control oocytes.

To reveal the number of N-linked carbohydrate chains that become complex glycosylated *en route* to the plasma membrane, the surface <sup>125</sup>I-labeled His-rP2X<sub>5</sub> polypeptide was first treated with Endo H to release high mannose-type carbohydrates and then subjected to partial deglycosylation with increasing concentrations of PNGase F. Upon treatment with Endo H, the mass of fully processed His-rP2X<sub>5</sub> isolated from surface iodinated oocytes was reduced by 3 kD compared to the untreated His-rP2X<sub>5</sub> polypeptide (Fig. 3.11, lane 3), indicating that only one N-glycan is sensitive to Endo H and hence not complex glycosylated. Treatment with PNGase F generated two additional bands (Fig. 3.11, lanes 4 and 5) besides the protein band representing the Endo H resistant His-rP2X<sub>5</sub> polypeptide. Each of these two bands differed in mass by 2-3 kD, i.e. the mass of an N-linked oligosaccharide side chain. Since these two bands were generated from an Endo H

resistant form of the His-P2X<sub>5</sub> polypeptide, it can be inferred that from the total three N-linked carbohydrate chains, two N-glycans acquire complex-type carbohydrates during transit of the Golgi apparatus.

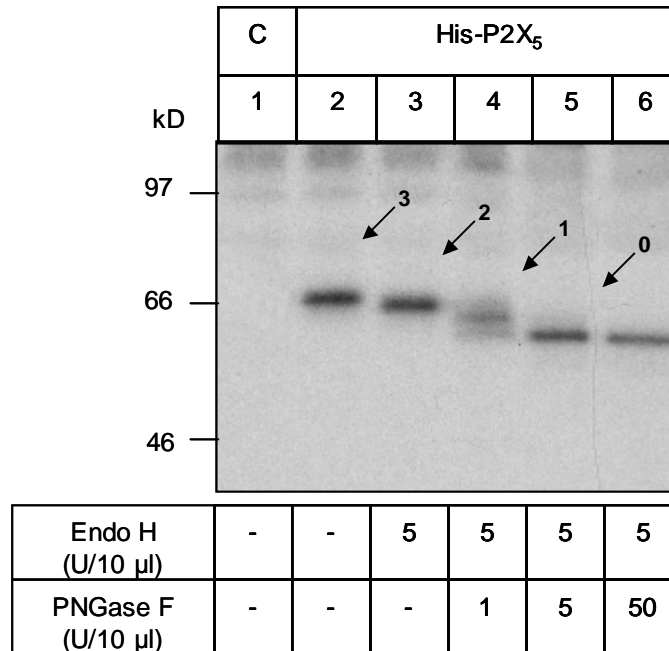


**Fig 3.11: Glycosylation status of surface iodinated His-P2X<sub>5</sub> subunit.** Oocytes injected with 2.5 ng of cRNA for the His-rP2X<sub>5</sub> subunit were left for 3 days at 19°C and then labeled with membrane-impermeant <sup>125</sup>I-sulfo-SHPP. The His-rP2X<sub>5</sub> protein was purified by Ni<sup>2+</sup>-NTA chromatography from 1% digitonin extracts of oocytes, and eluted with non-denaturing elution buffer. Aliquotes of these samples were supplemented with SDS sample buffer, 20 mM DTT, and treated with Endo H or PNGase F as indicated. Samples exposed to both enzymes (lanes 4-6) were first treated with Endo H for 1 h at 37°C, then supplemented with 1% octylglucoside (final concentration) and incubated with PNGase F (1 h at 37°C). After the digestion, proteins were resolved by SDS-PAGE (8% acrylamide), followed by autoradiography. C indicates samples from non-injected control oocytes.

### 3.1.2.3. Biochemical characterization of rP2X<sub>5</sub> constructs after expression in *Xenopus* oocytes using BN-PAGE

The His-rP2X<sub>5</sub> protein that was purified under non-denaturing conditions from metabolically labeled oocytes appeared as one single band at about 340 kD when analyzed by BN-PAGE. In addition, a large amount of aggregated protein in the region of high molecular mass range was observed (Fig. 3.12, lane 1). These aggregations may reflect an incomplete folded or only partially assembled His-rP2X<sub>5</sub> subunits that were retained in the ER two days after injection of the oocytes. To determine the number of subunits incorporated into the defined 340 kD protein, different conditions were elaborated to induce a partial dissociation of the purified

His-rP2X<sub>5</sub> complex. Incubation prior to blue native PAGE of the natively eluted His-rP2X<sub>5</sub> receptor with the strong reductant DTT in the presence of blue native sample buffer had no significant effect (Fig. 3.13, lane 2). When treated with 4 M urea in the presence of blue native sample buffer, two additional protein bands besides the 340 kD His-rP2X<sub>5</sub> complex appeared. These bands of the apparent masses of ~ 100 and 190 kD correspond to the His-rP2X<sub>5</sub> monomer and intermediate dimer, indicating that the non-denatured 340 kD protein band must be a trimer (Fig. 3.12, lanes 2 and 3).

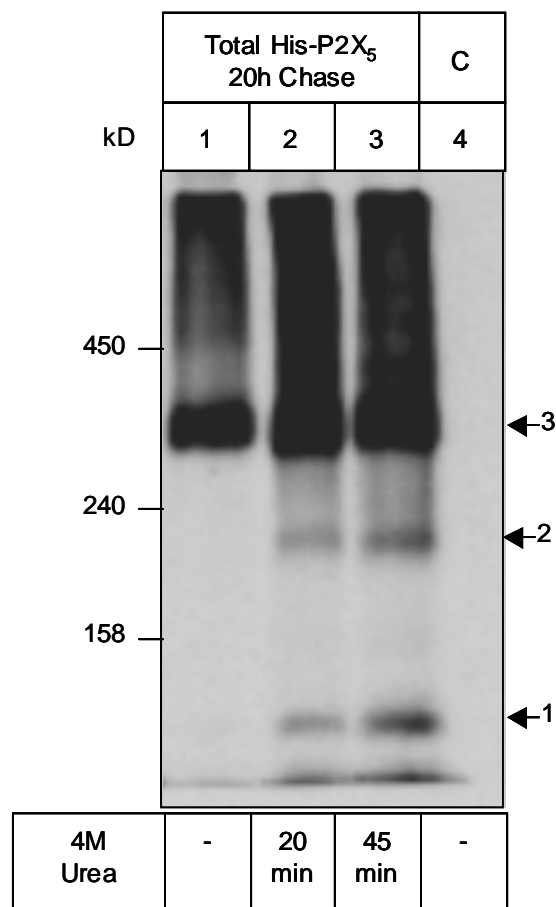


**Fig 3.12: BN-PAGE analysis of total His-rP2X<sub>5</sub> receptor complexes.** Oocytes injected with 2.5 ng of cRNA for His-rP2X<sub>5</sub> subunit were metabolically labeled overnight and then chased for 20 h at 19°C. Cells were extracted with 1% digitonin. The His-rP2X<sub>5</sub> protein was purified by Ni<sup>2+</sup>-NTA affinity chromatography under non-denaturing conditions. Digitonin solubilized His-rP2X<sub>5</sub> receptor was either non-treated (lane 1) or dissociated by incubation at 37°C with 4 M urea in the indicated time (lanes 2 and 3). Samples were supplemented with blue native sample buffer and analyzed by BN-PAGE (4-13% acrylamide gradient gel). C indicates samples from non-injected control oocytes.

Blue native PAGE analysis of the metabolically labeled His-rP2X<sub>5</sub> complex revealed a weak dissociation of the natively eluted protein complex upon treatment with 4 M urea, suggesting that the His-rP2X<sub>5</sub> protein is a rather stable complex.

Likewise, treatment of the natively eluted His-rP2X<sub>5</sub> receptor from surface labeled oocytes with 100 mM DTT in the presence of amino-caproate was not sufficient to cause any dissociation of the protein complex (Fig. 3.13, lane 2). However, when the His-rP2X<sub>5</sub> receptor was treated by both urea and DTT, a partial dissociation occurred, leading to a total of three bands, corresponding to the His-rP2X<sub>5</sub> monomer at ~100 kD, the intermediate dimer at ~190 kD and the non-dissociated, trimeric complex at 340 kD (Fig. 3.13, lanes 3 and 4).

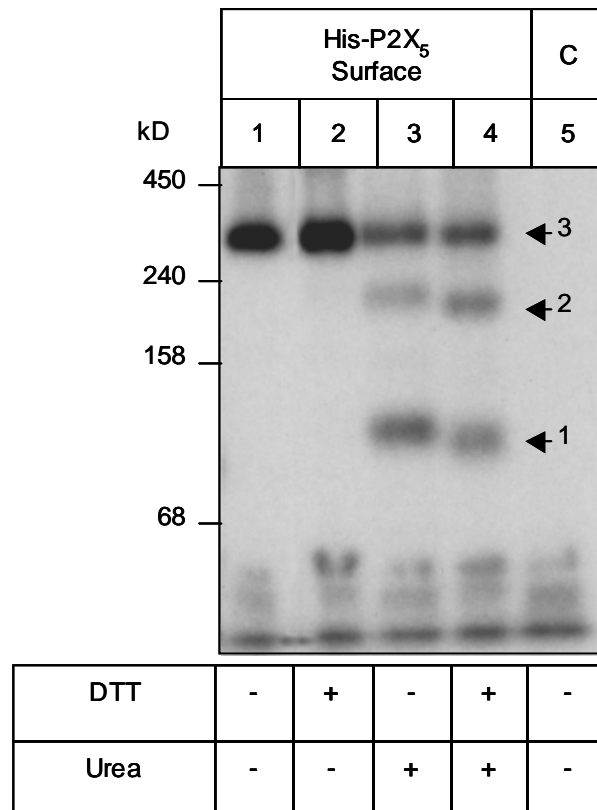


**Fig 3.13: Oligomeric state of the surface-iodinated His-rP2X<sub>5</sub> receptor.** Oocytes injected with 2.5 ng of cRNA for His-rP2X<sub>5</sub> subunit were left for 3 days at 19°C and then labeled with membrane-impermeant <sup>125</sup>I-sulfo-SHPP. His-rP2X<sub>5</sub> protein was purified by Ni<sup>2+</sup>-NTA affinity chromatography from 1% digitonin extracts of oocytes, and eluted with non-denaturing elution buffer. His-rP2X<sub>5</sub> samples were supplemented with BN sample buffer and analyzed by BN-PAGE (4-13% acrylamide gradient gel) either without incubation or after incubation for 45 min at 37°C with 4 M urea and/or 100 mM DTT as indicated. C indicates samples from non-injected control oocytes.

### 3.1.3. Characterization of His-tagged rP2X<sub>6</sub> subunits after expression in *Xenopus* oocytes

For the investigation of heterologously expressed rat P2X<sub>6</sub> subunits in *Xenopus* oocytes, the cDNA for rP2X<sub>6</sub> was N-terminally labeled with a hexahistidyl sequence (His-rP2X<sub>6</sub>) to allow for purification by affinity chromatography.

#### 3.1.3.1. Electrophysiological analysis of oocytes expressing the rat P2X<sub>6</sub> subunit

In an initial experiment, the function of His-rP2X<sub>6</sub> expressed in *Xenopus* oocytes was tested. Under two-electrode voltage clamp at a holding potential of  $-60$  mV, oocytes injected with His-rP2X<sub>6</sub> cRNA two days earlier showed no response to ATP. This observation was also made by other groups, suggesting that rP2X<sub>6</sub> fails to form a functional ion channel in oocytes and that rP2X<sub>6</sub> subunits may require a partner subunit for functional expression (Collo *et al.*, 1996). Currently, there is evidence for the hetero-polymerization of P2X<sub>6</sub> and P2X<sub>4</sub> subunits, since oocytes expressing both P2X<sub>6</sub> and P2X<sub>4</sub> subunits exhibit larger currents than those expressing homomeric P2X<sub>4</sub> receptors alone (Le *et al.*, 1998).

#### 3.1.3.2. Biochemical characterization of the rP2X<sub>6</sub> subunit after expression in *Xenopus* oocytes using SDS-PAGE

Oocytes injected with the cRNA encoding His-rP2X<sub>6</sub> subunits were metabolically labeled by overnight incubation with [<sup>35</sup>S]methionine. Directly after the pulse or after an additional 24 h chase interval, digitonin extracts were prepared. His-rP2X<sub>6</sub> protein was isolated by Ni<sup>2+</sup>-NTA affinity chromatography, eluted with non-denaturing elution buffer, denatured with SDS-sample buffer, and analyzed by reducing SDS-PAGE. Fig. 3.14 A (lane 1) and B (lane 5) show that His-rP2X<sub>6</sub> polypeptides are synthesized in *Xenopus* oocytes. SDS-PAGE characterization of the metabolically labeled His-rP2X<sub>6</sub> subunits after the overnight pulse period yielded a band with an approximate molecular mass of  $\sim 52$  kD (Fig. 3.14 A, lane 1). Treatment with PNGase F reduced

the molecular mass by 8 kD to ~44 kD (Fig. 3.14 A, lane 3), close to the mass of the His-tagged protein core computed from the cDNA complex (43.5 kD). Since 8 kD corresponds to the mass of three N-linked oligosaccharide side chains, this finding implies that each of the three asparagines for possible N-linked glycosylation (NXT/S) of the His-rP2X<sub>6</sub> subunit is occupied by an N-glycan.

Deglycosylation of the His-rP2X<sub>6</sub> subunit after the pulse and the chase interval with Endo H released all N-linked glycans, indicating that the protein does not acquire complex type carbohydrates and therefore, most likely resides entirely in the ER (Fig. 3.14 A, lane 2, and B, lane 6).

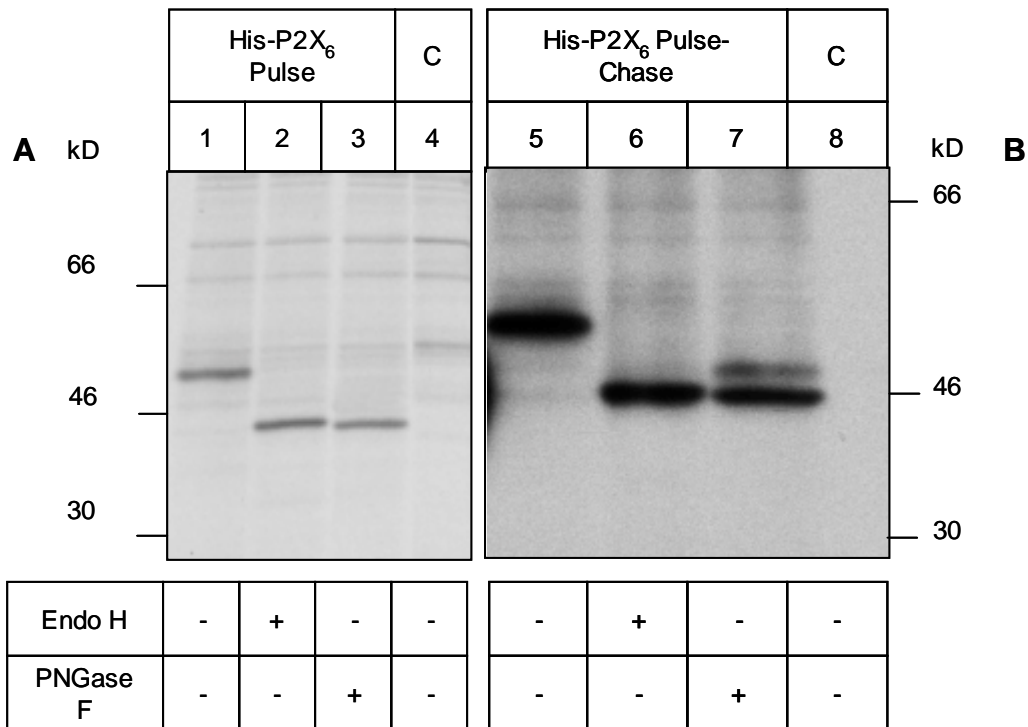


**Fig 3.14: Glycosylation status of the His-rP2X<sub>6</sub> subunit after metabolic labeling.** Oocytes injected with the cRNA for the His-rP2X<sub>6</sub> subunit were metabolically labeled overnight. Cells were either directly extracted with 1% digitonin (**A**) or first chased for 20 h and then extracted (**B**). His-rP2X<sub>6</sub> protein was purified by Ni<sup>2+</sup>-NTA affinity chromatography. Samples were eluted under non-denaturing conditions and treated with PNGase F or Endo H and finally analyzed by SDS-PAGE (8% acrylamide). Lanes 1 and 5 indicate non-injected controls. C indicates samples from non-injected control oocytes.



### 3.1.3.3. Biochemical characterization of the His-rP2X<sub>6</sub> protein after expression in *Xenopus* oocytes by BN-PAGE

To investigate the assembly of His-rP2X<sub>6</sub> subunits, oocytes injected with the cRNA for His-P2X<sub>6</sub> were metabolically labeled. His-P2X<sub>6</sub> protein was then isolated under non-denaturing conditions from a digitonin extract of the oocytes and analyzed by BN-PAGE. The bulk amount of His-rP2X<sub>6</sub> protein migrated at a broad range of high molecular masses indicative of non-defined aggregates (Fig. 3.15. lane 2). Treatment with 0.1 M DTT and 8M Urea (Fig. 3.15, lanes 3 and 4) visualized some intermediate bands that were possibly due to aggregation. These results suggested that His-rP2X<sub>6</sub> subunits alone do not reach a defined assembly status and as suggested by other groups needs the hetero-assembly with other P2X subunits to assemble properly for export to the plasma membrane.

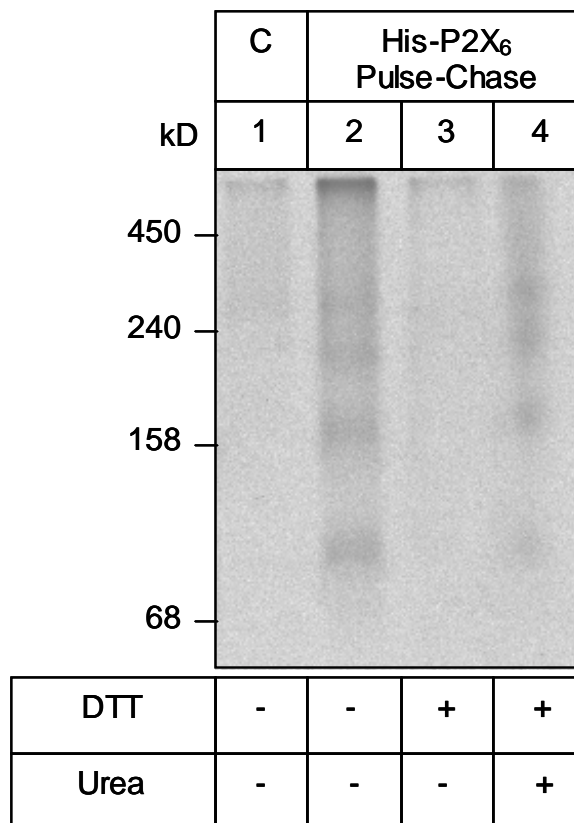


**Fig 3.15: Oligomeric state of metabolically labeled His-rP2X<sub>6</sub> subunits.** Oocytes injected with cRNA for His-rP2X<sub>6</sub> were metabolically labeled overnight following a 20 h chase period at 19°C. Cells were extracted with 1% digitonin. His-rP2X<sub>6</sub> protein was purified by Ni<sup>2+</sup>-NTA affinity chromatography under non-denaturing conditions. Digitonin solubilized His-rP2X<sub>6</sub> protein was analyzed by BN-PAGE (4-13% acrylamide gradient gel) either without further treatment (lane 2) or after 45 min of incubation at 37°C and 100 mM DTT (lane 3) or 100 mM DTT and 8 M urea (lane 4). C indicates samples from non-injected control oocytes.

### 3.1.4. Characterization of rat P2X<sub>1</sub> and P2X<sub>2</sub> subunits after co-expression in *Xenopus* oocytes

#### 3.1.4.1. Biochemical characterization of the rat P2X<sub>1</sub> and P2X<sub>2</sub> polypeptides after co-expression in *Xenopus* oocytes by SDS-PAGE

To examine whether rP2X<sub>1</sub> and rP2X<sub>2</sub> subunits are able to form a heteromultimeric complex, a co-purification assay was exploited, in which the hexahistidyl-tagged rat P2X<sub>2</sub> was co-expressed with non-tagged rP2X<sub>1</sub> and *vice versa* in *Xenopus* oocytes. After digitonin extraction of the cells, the interaction of these subunits was judged from the co-precipitation of the hexahistidyl-tagged subunits with the non-tagged subunits using Ni<sup>2+</sup>-NTA agarose affinity chromatography. The isolated polypeptides were analyzed by SDS-PAGE. To validate this assay, the formation of rP2X<sub>2</sub>/rP2X<sub>3</sub> complexes as a positive control was examined. Co-expression of rP2X<sub>3</sub> subunit with rP2X<sub>2</sub> subunit is known to result in the formation of a hetero-polymerized P2X receptor in *Xenopus* oocytes (Lewis *et al.*, 1995). The rP2X<sub>2</sub> subunit exhibits a higher mass than the P2X<sub>1</sub> or P2X<sub>3</sub> subunits due to its much longer C terminal tail (total length of 472 amino acids vs. 399 amino acids of P2X<sub>1</sub> and 397 amino acids of rP2X<sub>3</sub> polypeptides), and hence exhibits a slower migration in the SDS-polyacrylamide gel. As shown in Fig. 3.16, lanes 3 and 4, co-expression of His-rP2X<sub>2</sub> subunit with non-tagged rP2X<sub>1</sub> or His-rP2X<sub>1</sub> subunit with non-tagged rP2X<sub>2</sub> subunit did not result in a detectable co-isolation of any of the two subunits. In contrast, the non-tagged rP2X<sub>3</sub> subunit was co-purified with the His-rP2X<sub>2</sub> subunit, confirming that this assay is able to correctly display the known physical interaction between rP2X<sub>2</sub> and rP2X<sub>3</sub> subunits (Fig. 3.16, lane 6).

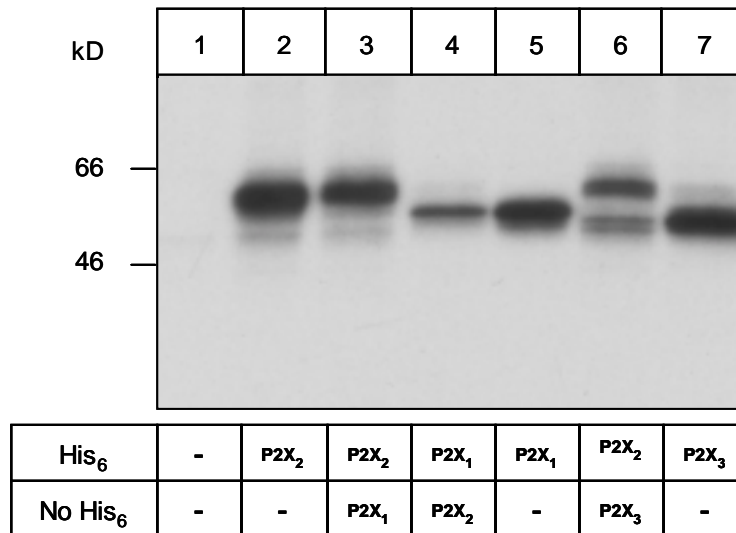


**Fig. 3.16: Co-isolation assay of rP2X<sub>1</sub> with rP2X<sub>2</sub> or rP2X<sub>3</sub> with rP2X<sub>2</sub> subunits after metabolic labeling.** Oocytes were injected with cRNAs for His-rP2X<sub>1</sub> (25 ng), non-tagged rP2X<sub>1</sub> (25 ng), His-rP2X<sub>3</sub> (25 ng), non-tagged rP2X<sub>3</sub> (25 ng), His-rP2X<sub>2</sub> (2.5 ng), or non-tagged rP2X<sub>2</sub> (2.5 ng). The cRNAs were injected either individually or together as indicated. The injected cells were metabolically labeled overnight. Cells were extracted with 1% digitonin after a 20 h chase period. Co-isolation was achieved by Ni<sup>2+</sup>-NTA affinity chromatography. Samples were eluted under non-denaturing conditions, denatured with SDS sample buffer in the presence of 100 mM DTT (10 min at 37°C), and then analyzed by SDS-PAGE (8% acrylamide).

To further investigate a possible co-assembly of the P2X<sub>1</sub> and P2X<sub>2</sub> subunits expressed on the cell surface, oocytes injected with cRNA for His-P2X<sub>2</sub> and non-tagged rP2X<sub>1</sub> and *vice versa* were surface radio-iodinated with <sup>125</sup>I-sulfo-SHPP three days after cRNA injection. The radio-iodinated proteins were then isolated by Ni<sup>2+</sup>-NTA chromatography under non-denaturing conditions from digitonin extracts, denatured with SDS sample buffer, and resolved by SDS-PAGE. Purification of His-P2X<sub>1</sub> protein by Ni<sup>2+</sup>-NTA agarose under non-denaturing conditions resulted in co-purification of non-tagged rP2X<sub>2</sub> subunit from oocytes injected with both cRNAs (Fig. 3.17, lane 5). Likewise, non-tagged rP2X<sub>1</sub> subunits could be co-isolated with His-rP2X<sub>2</sub> protein (Fig. 3.17, lane 4). Proteins isolated from oocytes that were injected with cRNAs for His-rP2X<sub>1</sub> or His-rP2X<sub>2</sub> alone are also shown (Fig. 3.17, lanes 2 and 3). As shown in Fig. 3.17, lane 8, the non-tagged rP2X<sub>3</sub> subunit was co-purified with the His-rP2X<sub>2</sub> subunit, consistent with the presence of rP2X<sub>2</sub>/rP2X<sub>3</sub> heterooligomers. Altogether, these data indicate that rP2X<sub>1</sub> and rP2X<sub>2</sub> subunits can co-assemble into hetero-oligomers like rP2X<sub>2</sub> and rP2X<sub>3</sub> subunits. However, in contrast to rP2X<sub>2</sub>/rP2X<sub>3</sub> heteromultimers, which occur in significant amounts also in the cell interior, the rP2X<sub>1</sub>/rP2X<sub>2</sub> heteromultimers can only be detected at the plasma membrane.

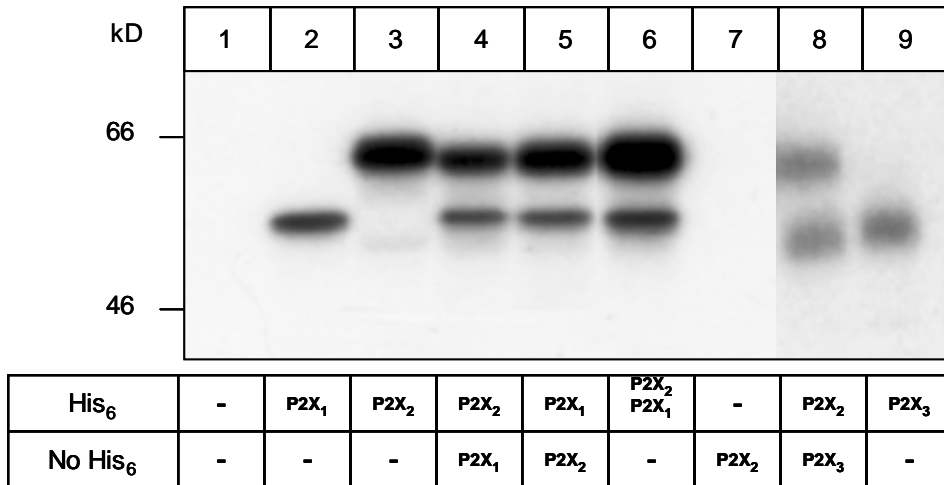


**Fig. 3.17: Plasma membrane-bound rP2X<sub>1</sub> and rP2X<sub>2</sub> can be co-purified after co-expression.**

Oocytes were injected with cRNAs for His-rP2X<sub>1</sub> (25 ng), non-tagged rP2X<sub>1</sub> (25 ng), His-rP2X<sub>3</sub> (25 ng), non-tagged rP2X<sub>3</sub> (25 ng), His-rP2X<sub>2</sub> (2.5 ng), or non-tagged rP2X<sub>2</sub> (2.5 ng). The cRNAs were injected either individually or together as indicated. Cells were kept for 3 days at 19°C and then labeled with membrane-impermeant <sup>125</sup>I-sulfo-SHPP. Proteins were (co-) purified by Ni<sup>2+</sup>-NTA chromatography from 1% digitonin extracts of each oocyte group, eluted with non-denaturing elution buffer and resolved by reducing SDS-PAGE (8% acrylamide) followed by autoradiography.

Next, the glycosylation status of the hetero-oligomerized His-rP2X<sub>2</sub>/rP2X<sub>1</sub> complex from radio-iodinated oocytes was compared with homomultimeric His-rP2X<sub>1</sub> and His-rP2X<sub>2</sub> complexes. SDS-PAGE analysis revealed that the PNGase F-treated rP2X<sub>2</sub> subunit from the hetero-assembled complex migrated at 53 kD like the rP2X<sub>2</sub> subunit from the homomultimeric complex (Fig. 3.18, lanes 6 and 9). Since 53 kD reflects a mass difference in three N-glycans (8 kD) compared to the mass of the non-treated His-rP2X<sub>2</sub> subunit (61 kD), it can be inferred that the number of the acquired N-glycans is not changed by hetero-polymerization of the rP2X<sub>2</sub> subunits. Treatment with Endo H failed to alter the mobility of the homomultimeric His-rP2X<sub>2</sub> subunit and the His-rP2X<sub>2</sub> polypeptide from the heteromultimeric complex, indicating that all three N-glycans are exclusively in the complex-glycosylated form (Fig. 3.18, lane 5 and 8).

Endo H treatment diminished the molecular mass of homomultimeric His-rP2X<sub>1</sub> subunit by 8 kD, but was unable to release all N-glycans, indicating that at least one N-linked oligosaccharide side chain of the subunit must have been complex glycosylated in the Golgi and thus acquired Endo H resistance (Fig. 3.18, lane 2). The same result was obtained for the co-isolated rP2X<sub>1</sub> subunit. Endo H clearly reduced the molecular mass of hetero-assembled rP2X<sub>1</sub> subunit, but in contrast to

PNGase F, was unable to release all N-glycans, indicating that the rP2X<sub>1</sub> subunit is also complex-glycosylated in one site (Fig. 3.18, lane 8).

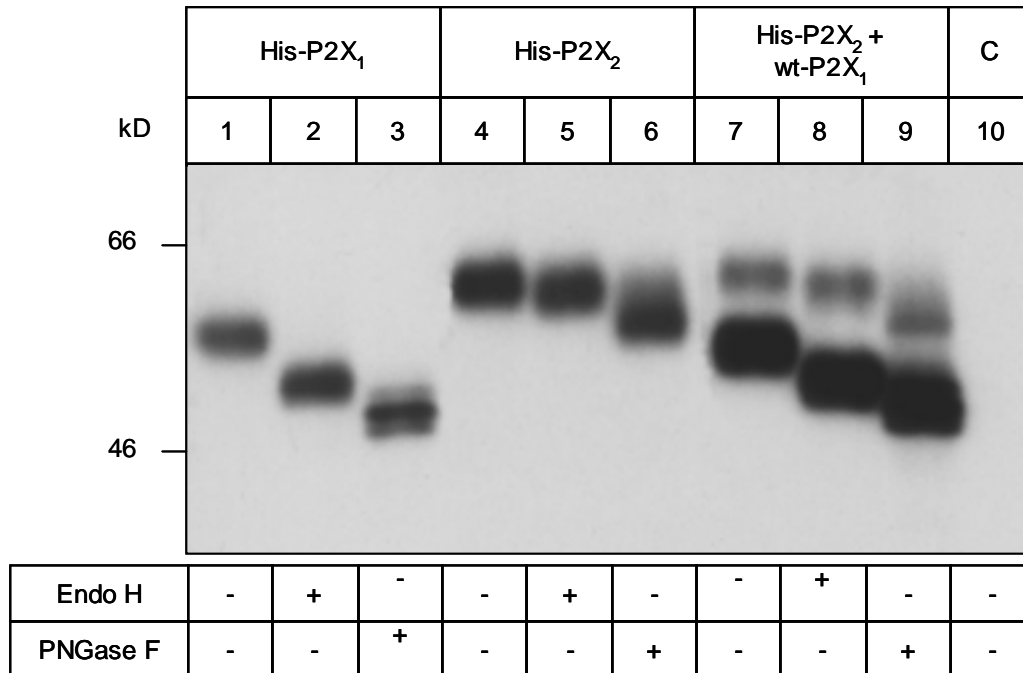


**Fig. 3.18: Glycosylation status of homomultimeric and heteromultimeric rP2X<sub>1</sub> and rP2X<sub>2</sub> subunits on the cell surface.** Oocytes were injected with cRNAs for His-rP2X<sub>1</sub> (25 ng), non-tagged rP2X<sub>1</sub> (25 ng), or non-tagged rP2X<sub>2</sub> (2.5 ng). The cRNAs were injected either individually or together as indicated. Cells were kept for 3 days at 19°C and then labeled with membrane-impermeant <sup>125</sup>I-sulfo-SHPP. Proteins were purified by Ni<sup>2+</sup>-NTA chromatography from 1% digitonin extracts of each oocyte group and eluted with non-denaturing elution buffer. Aliquots of these samples were supplemented with SDS sample buffer and DTT and then incubated in the absence or presence of PNGase F or Endo H as indicated. Samples were resolved by SDS-PAGE (8% acrylamide) followed by autoradiography. C indicates samples from non-injected control oocytes.

### 3.1.4.2. Investigation of the quaternary structure of the rP2X<sub>2</sub>/rP2X<sub>1</sub> complex

#### 3.1.4.2.1. Cross-linking analysis

Analogous to the investigation of the quaternary structure of the homotrimeric His-rP2X<sub>2</sub> receptor (chapter 3.1.1.3), the cross-linker glutardialdehyde was used to investigate the quaternary structure of the hetero-assembled rP2X<sub>2</sub>/rP2X<sub>1</sub> complex in the plasma membrane of intact *Xenopus* oocytes. The injected oocytes were surface-labeled with <sup>125</sup>I-sulfo-SHPP and incubated with glutardialdehyde for up to 60 min before digitonin extraction and affinity purification was performed. SDS-PAGE analysis of the chemically cross-linked His-rP2X<sub>2</sub>/rP2X<sub>1</sub> complex revealed two additional bands of ~117 kD and ~175 kD, corresponding to the dimers and trimers of the 57 kD and 61 kD polypeptides of rP2X<sub>1</sub> and rP2X<sub>2</sub>, respectively (Fig. 3.19,

lane 6). Interestingly, these bands of the higher molecular mass migrated in between the dimeric and trimeric protein bands obtained by cross-linking of homomultimeric His-rP2X<sub>1</sub> and His-rP2X<sub>2</sub> subunits (Fig. 3.19, lanes 5 and 7), indicating the chemical cross-linking of rP2X<sub>1</sub> with rP2X<sub>2</sub>. Increasing the incubation time with glutardialdehyde did not increase the number of bands, but resulted in a decrease of their intensity (Fig. 3.19, lanes 8-10). These observations suggested that hetero-assembled rP2X<sub>1</sub> and rP2X<sub>2</sub> exist as trimers in the plasma membrane.

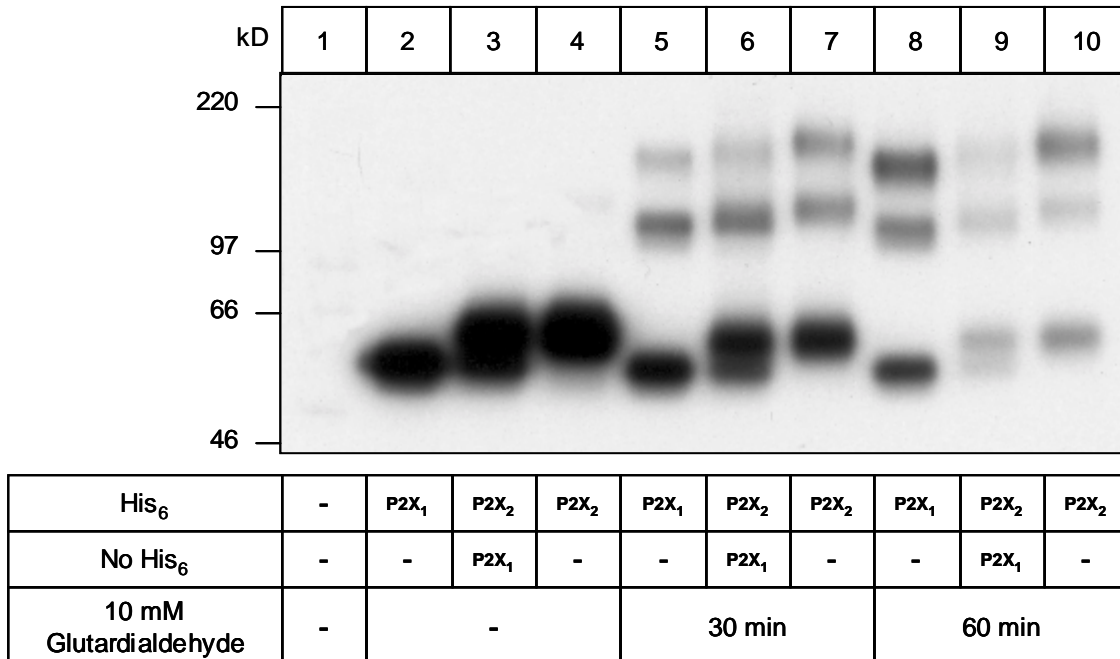


**Fig. 3.19. Cross-linking of rP2X<sub>1</sub>/rP2X<sub>2</sub> complexes by glutardialdehyde in intact *Xenopus* oocytes.** Oocytes were injected with cRNAs for His-rP2X<sub>1</sub> (25 ng), non-tagged rP2X<sub>1</sub> (25 ng), or His-rP2X<sub>2</sub> (2.5 ng). The cRNAs were injected either individually or together as indicated. Cells were kept for 3 days at 19°C and then labeled with <sup>125</sup>I-sulfo-SHPP. Cross-linking was performed on intact oocytes with 10 mM glutardialdehyde for 30 min or 60 min at 4°C. After removing the excess of glutardialdehyde by washing with oocyte-PBS, the oocytes were homogenized in 1% digitonin. Proteins were purified by Ni<sup>2+</sup>-NTA agarose affinity chromatography and eluted with non-denaturing elution buffer and analyzed by reducing SDS-PAGE (4-10% acrylamide gradient gel).

### 3.1.4.2.2. BN-PAGE analysis of the rP2X<sub>2</sub>/rP2X<sub>1</sub> complex

In addition, the oligomeric state of the rP2X<sub>2</sub>/rP2X<sub>1</sub> complex was analyzed by BN-PAGE. To this end, oocytes injected with cRNAs for non-tagged P2X<sub>1</sub> and hexahistidyl-tagged P2X<sub>2</sub> were surface-labeled with <sup>125</sup>I-sulfo-SHPP and then extracted with 1% digitonin and chromatographically purified on Ni<sup>2+</sup>-NTA agarose beads. In parallel, heteromultimeric His-rP2X<sub>2</sub>/rP2X<sub>3</sub> and homomultimeric His-rP2X<sub>1</sub>, His-rP2X<sub>2</sub>, and His-rP2X<sub>3</sub> receptor complexes were surface radio-iodinated and purified under the same conditions. The purified proteins were then analyzed by BN-

PAGE. Proteins isolated from oocytes co-synthesizing rP2X<sub>1</sub> and rP2X<sub>2</sub> subunits migrated as a single protein band at about 320 kD, when resolved by BN-PAGE (Fig. 3.20, lane 3). Homomultimeric His-rP2X<sub>1</sub> and His-rP2X<sub>2</sub> receptors exhibited lower and higher mobility and migrated at 240 kD and 380 kD, respectively (Fig. 3.20, lanes 1 and 2). Likewise, the heteromultimeric rP2X<sub>2</sub>/rP2X<sub>3</sub> receptor appeared as a single band at ~260 kD, slightly larger than the homomultimeric His-rP2X<sub>3</sub> protein at ~240 kD (Fig. 3.20, lanes 4 and 5).

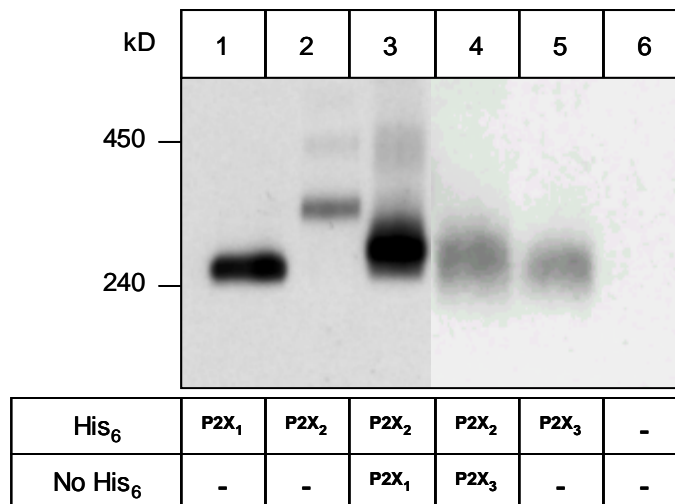


**Fig. 3.20: Rat P2X<sub>1</sub> and P2X<sub>2</sub> subunits co-purified under non-denaturing conditions migrate as one distinct band when resolved by BN-PAGE.** Oocytes were injected with cRNAs for His-rP2X<sub>1</sub> (25 ng), non-tagged rP2X<sub>1</sub> (25 ng), His-rP2X<sub>3</sub> (25 ng), non-tagged rP2X<sub>3</sub> (25 ng), or His-rP2X<sub>2</sub> (2.5 ng). The cRNAs were injected either individually or together as indicated. Cells were kept for 3 days at 19°C and then labeled with membrane-impermeant <sup>125</sup>I-sulfo-SHPP. Proteins were purified by Ni<sup>2+</sup>-NTA chromatography from 1% digitonin extracts of each oocyte group, eluted with non-denaturing elution buffer and resolved by blue native PAGE (4-10% acrylamide) followed by autoradiography.

To determine the number of subunits per complex, the natively eluted rP2X<sub>2</sub>/rP2X<sub>1</sub> complex was incubated with increasing concentration of urea, inducing a partial dissociation of the protein complex prior to the BN-PAGE. Upon denaturing of the rP2X<sub>1</sub>/rP2X<sub>2</sub> complex, blue native PAGE analysis revealed four bands, representing the rP2X<sub>1</sub>/rP2X<sub>2</sub> trimer at ~320 kD, the dimer at ~200 kD, the rP2X<sub>2</sub> monomer at ~120 kD, and the rP2X<sub>1</sub> monomer at ~80 kD (Fig. 3.21, lanes 5 and 6). These results indicate that the hetero-oligomeric rP2X<sub>2</sub>/rP2X<sub>1</sub> complex possesses a trimeric structure like the homomultimeric His-rP2X<sub>1</sub> complex (Fig. 3.21, lanes 1-3) and His-rP2X<sub>2</sub> receptors (Fig. 3.21, lanes 7-9).

When the His-rP2X<sub>2</sub>/rP2X<sub>3</sub> complex was treated with urea in the presence of blue native sample buffer, three protein bands appeared in addition to the non-dissociated 260 kD protein. The bands of the apparent masses of ~80 kD and ~120

kD correspond to the rP2X<sub>3</sub> and rP2X<sub>2</sub> monomers, respectively. The intermediate dimer appeared as a ~170 kD protein band (Fig. 3.21, lanes 11 and 12). Thus, apparently the heteromultimeric His-rP2X<sub>2</sub>/rP2X<sub>3</sub> complex is a trimer like the homomultimeric His-rP2X<sub>2</sub> (Fig. 3.21, lanes 7-9) and His-rP2X<sub>3</sub> (Fig. 3.21, lanes 13-15).

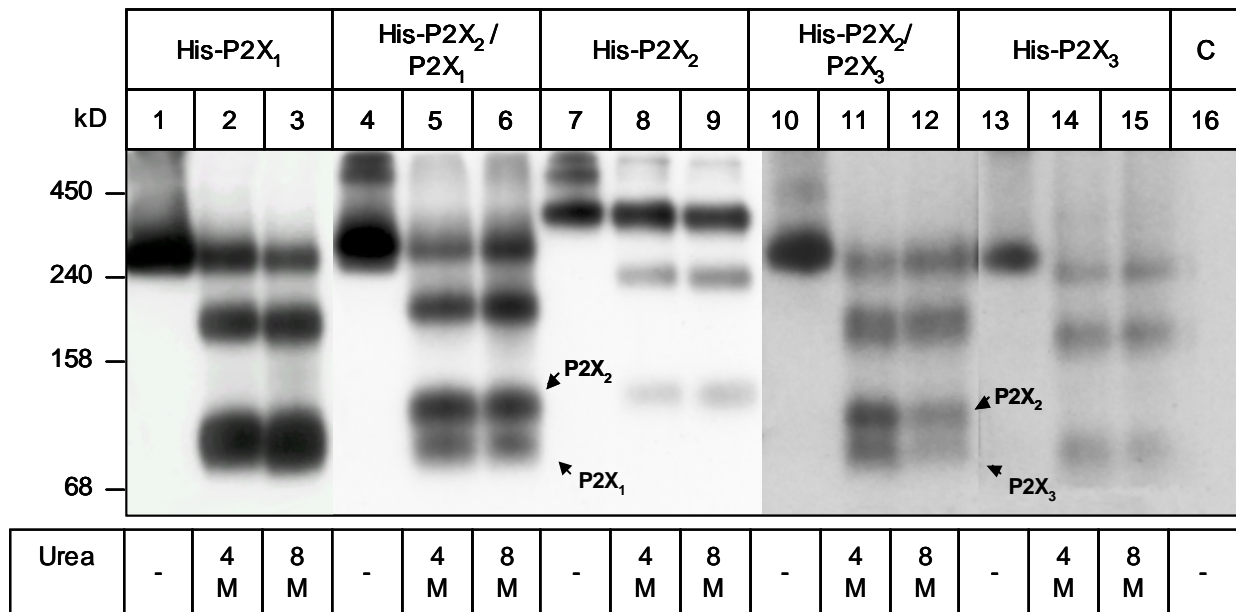


**Fig. 3.21: Partial dissociation of rP2X<sub>1</sub>/rP2X<sub>2</sub> and rP2X<sub>2</sub>/rP2X<sub>3</sub> complexes.** Oocytes were injected with cRNAs for His-rP2X<sub>1</sub> (25 ng), non-tagged rP2X<sub>1</sub> (25 ng), His-rP2X<sub>3</sub> (25 ng), non-tagged rP2X<sub>3</sub> (25 ng), or His-rP2X<sub>2</sub> (2.5 ng). The cRNAs were injected either individually or together as indicated. Cells were kept for 3 days at 19°C and then labeled with <sup>125</sup>I-sulfo-SHPP. Proteins were purified by Ni<sup>2+</sup>-NTA chromatography from 1% digitonin extracts of each oocyte group and eluted with non-denaturing elution buffer. Samples were supplemented with 4 M or 8 M urea in the presence of blue native sample buffer and incubated for 45 min 37°C prior to blue native PAGE (4-13% acrylamide gradient gel). C indicates samples from non-injected control oocytes.

The two-dimensional PAGE analysis was used to confirm that the distinct bands observed by BN-PAGE analysis and ascribed to trimeric and dimeric protein complexes of rP2X<sub>2</sub>/P2X<sub>1</sub> and rP2X<sub>2</sub>/P2X<sub>3</sub> consisted of both P2X isoforms. For this purpose, the partially dissociated protein complexes were excised from the blue native gel (Fig. 3.21, lanes 6 and 12) and reanalyzed in the second dimension by SDS-PAGE. As shown in Fig. 3.22, the higher molecular mass complexes corresponding to the trimeric and dimeric forms of P2X<sub>2</sub>/P2X<sub>1</sub> dissociated into P2X<sub>1</sub> monomers of 57 kD and P2X<sub>2</sub> monomers of 61 kD, when treated with SDS and resolved by SDS-PAGE. Using two-dimensional PAGE, the trimeric and dimeric bands observed for the P2X<sub>2</sub>/P2X<sub>3</sub> complex could also be dissociated into defined P2X<sub>2</sub> and P2X<sub>3</sub> monomers, confirming a hetero-assembly of these subunits in oocytes.



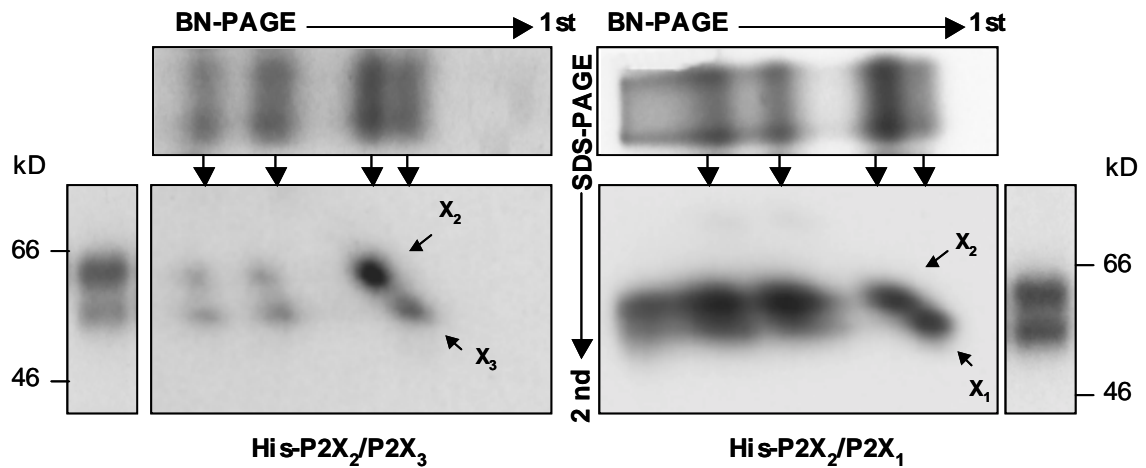


**Fig. 3.22: 2D-PAGE analysis of partially dissociated  $rP2X_1/rP2X_2$  and  $rP2X_2/rP2X_3$  complexes.** Surface radio-iodinated oocytes injected either with the cRNA encoding His- $rP2X_2$  and non-tagged  $rP2X_1$  or His- $rP2X_2$  and non-tagged  $rP2X_3$  were extracted with 1% digitonin. Proteins were purified by  $Ni^{2+}$ -NTA chromatography from extracts of each oocyte group and eluted with non-denaturing elution buffer. Proteins were partially dissociated with 8 M urea in the presence of blue native sample buffer at 37°C for 45 min and resolved on a 4-13% blue native polyacrylamide gradient gel. After BN-PAGE, the lanes carrying the separated proteins were excised and polymerized into the stacking gel of a 8% SDS-polyacrylamide gel. Polypeptides were then resolved in the 2<sup>nd</sup> dimension by SDS-PAGE.

### **3.1.5. Characterization of P2X<sub>1</sub> subunits tagged with green fluorescent protein after expression in *Xenopus* oocytes**

To examine the subcellular localization and membrane targeting of rat P2X<sub>1</sub> receptor by fluorescence microscopy, the His-rP2X<sub>1</sub> receptor subunit was tagged N-terminally (GFP-His-rP2X<sub>1</sub>) or C-terminally (His-rP2X<sub>1</sub>-GFP) with the green fluorescent protein (GFP). These fusion proteins were then expressed in *Xenopus* oocytes.

#### **3.1.5.1. Electrophysiological characterization GFP-tagged His-rP2X<sub>1</sub> constructs after expression in *Xenopus* oocytes**

To test whether both the N- and C- terminally GFP-tagged His-rP2X<sub>1</sub> subunits could assemble into a functional homomultimeric receptors, oocytes expressing one of the two constructs were tested with a two-electrode voltage clamp. Fig. 3.23 shows current responses of parent His-rP2X<sub>1</sub> and C-terminally GFP-tagged His-rP2X<sub>1</sub> receptors, elicited at -60 mV by application of 10 μM ATP. Two days after cRNA injection, His-P2X<sub>1</sub>-GFP produced ATP-elicited currents comparable to that of His-P2X<sub>1</sub> (about 17 μA). Furthermore, the results demonstrate the virtually identical time course of desensitization of both receptors, implying that the electrophysiological properties were not affected by the C-terminal GFP tag. In contrast, only faint signals were detected for the fusion protein consisting of His-P2X<sub>1</sub>, N-terminally tagged with GFP (< 50 nA, results not shown).

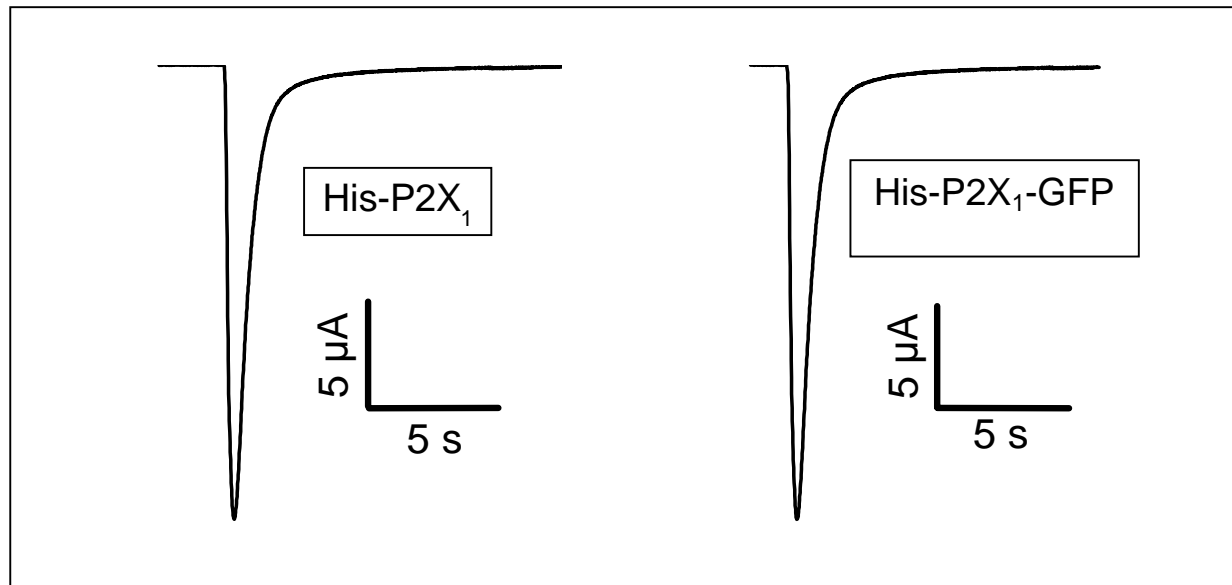


**Fig. 3.23: Comparison of electrophysiological responses to activation of the parent and GFP-tagged His-P2X<sub>1</sub> receptor.** Oocytes were injected with 25 ng of cRNA for His-rP2X<sub>1</sub>, or C-terminally GFP-tagged His-rP2X<sub>1</sub> (His-rP2X<sub>1</sub>-GFP). Two days after injection current responses elicited by 10 μM ATP (applied for 5 s) were measured at holding potential -60 mV. The experiment was performed by Dr. Jürgen Rettinger.

### 3.1.5.2. Visualization of GFP-tagged His-rP2X<sub>1</sub> protein in *Xenopus* oocytes by confocal fluorescence microscopy

The confocal fluorescence microscopy was done by Dr. Bodo Laube (Max-Planck-Institute for Neurology, Frankfurt, Germany). To determine the subcellular distribution of GFP-tagged His-rP2X<sub>1</sub>, oocytes were injected with the cRNA for His-rP2X<sub>1</sub>-GFP and GFP-His-rP2X<sub>1</sub>. Two to three days after injection, the oocytes were examined by confocal fluorescence microscopy for the detection of green fluorescence. Non-injected oocytes showed very low levels of autofluorescence and defined background fluorescence. GFP fluorescence was found throughout the plasma membrane in oocytes that had been injected with His-rP2X<sub>1</sub>-GFP (Fig. 3.24, B). The oocytes also accumulated His-rP2X<sub>1</sub>-GFP in internal membranous structures. These clusters varied in size between 3 μm and 6 μm and formed a continuous web throughout the cytoplasm as shown in oocytes (Fig. 3.24, A). The GFP fluorescence was not observed at the plasma membrane of oocytes injected with GFP-His-rP2X<sub>1</sub>.

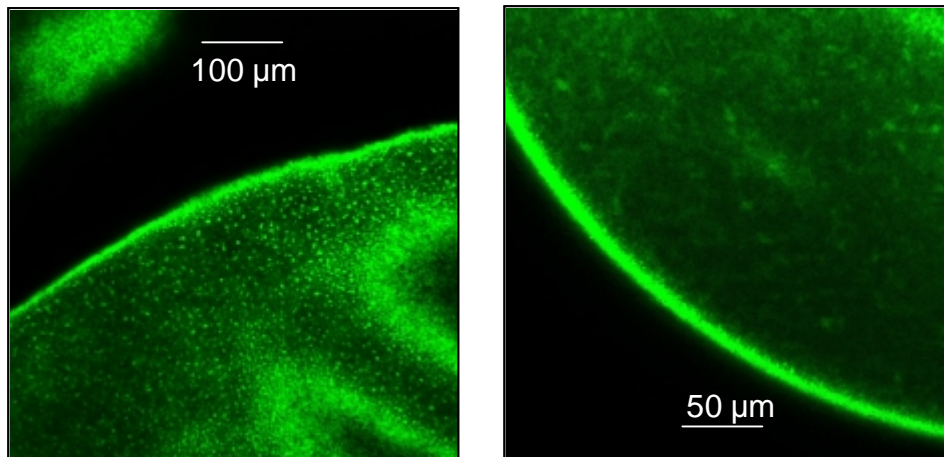


**Fig. 3.24: Visualization of His-rP2X<sub>1</sub> receptor distribution in *Xenopus* oocytes using the GFP-tagged rP2X<sub>1</sub> fusion protein.** Confocal image of oocytes membranes after injection of 25 ng of cRNA encoding His-rP2X<sub>1</sub>-GFP.

### 3.1.5.3. Biochemical characterization of GFP-tagged His-rP2X<sub>1</sub> constructs after expression in *Xenopus* oocytes by SDS-PAGE

For biochemical analysis, oocytes injected with the cRNA for the parent His-P2X<sub>1</sub> subunit or the N- and C- terminally GFP-tagged His-rP2X<sub>1</sub> subunits were metabolically labeled by overnight incubation with [<sup>35</sup>S]methionine. After an additional 20 h chase interval, digitonin extracts were prepared. The fusion proteins were isolated by Ni<sup>2+</sup>-NTA agarose affinity chromatography, and eluted with non-denaturing elution buffer. Samples were incubated in the presence of Endo H or PNGase F and then analyzed by SDS-PAGE. Like the parent His-rP2X<sub>1</sub> subunit, a fraction of the His-rP2X<sub>1</sub>-GFP polypeptide was partially Endo H resistant, indicating that C-terminally GFP-tagged His-rP2X<sub>1</sub> polypeptide is able to leave the ER and that at least one N-linked carbohydrate chain becomes complex glycosylated in the Golgi apparatus (Fig. 3.25, lane 5). In contrast, deglycosylation of N-terminally GFP-tagged His-rP2X<sub>1</sub> polypeptide with Endo H released all N-linked glycans (Fig. 3.25, lane 10), suggesting that this protein does not acquire complex type carbohydrates and, therefore, most likely resides entirely in the ER. Treatment with PNGase F reduced the molecular masses by 10 kD, yielding a ~75 kD band (Fig. 3.25, lanes 6 and 11), close to the 77 kD of the fusion protein computed from the translated cDNA sequence (47 kD for rP2X<sub>1</sub> and 29.4 kD for GFP). His-rP2X<sub>1</sub> C- or N-terminally tagged with GFP both migrated with approximate molecular masses of 87 kD (Fig. 3.25, lanes 4 and 9). As shown in Fig. 3.25, the N-terminally GFP-tagged His-rP2X<sub>1</sub> polypeptide exhibited a decreased expression level as compared with the parent His-

rP2X<sub>1</sub> protein. This observation may be explained by the impaired folding resulting from the N-terminal GFP tag, which may lead to increased degradation through the quality control machinery of the oocytes.

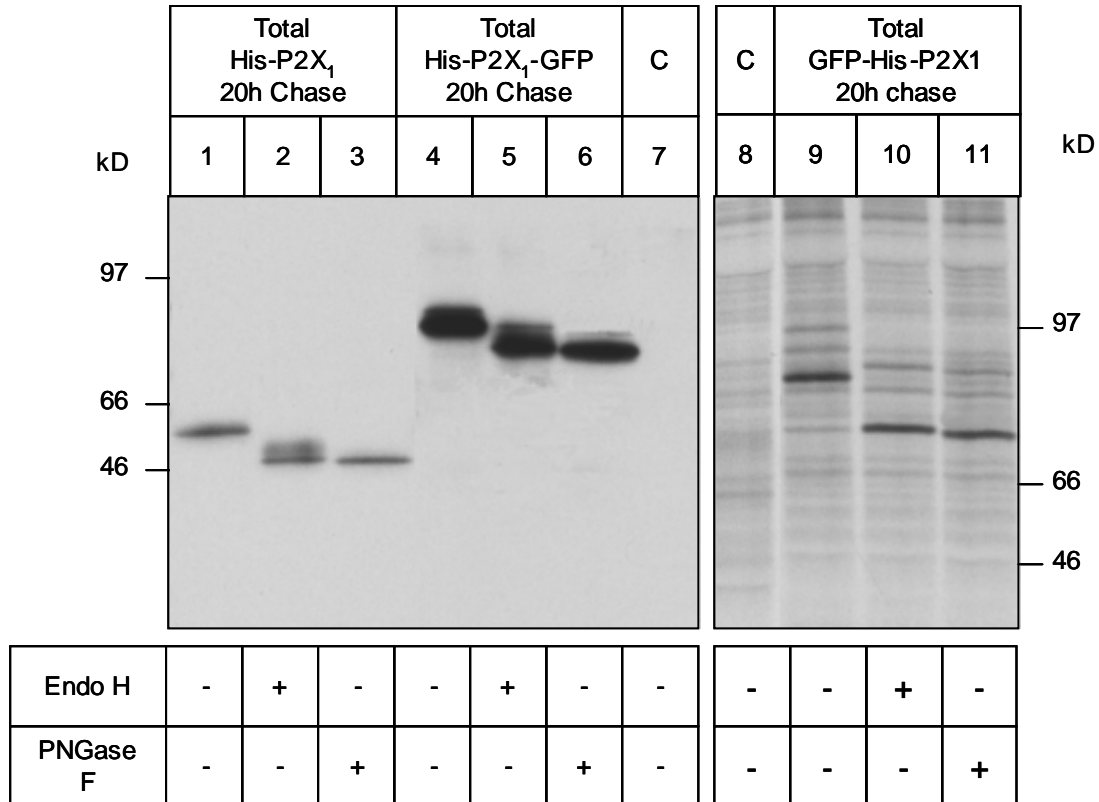


**Fig. 3.25: Glycosylation status of the GFP-tagged His-rP2X<sub>1</sub> polypeptide after metabolic labeling.** Oocytes injected with 25 ng of cRNA for His-rP2X<sub>1</sub>, His-rP2X<sub>1</sub>-GFP or GFP-His-rP2X<sub>1</sub> were metabolically labeled overnight. After a 20 h chase period, cells were extracted with 1% digitonin. Proteins were purified by Ni<sup>2+</sup>-NTA affinity chromatography, eluted under non-denaturing conditions and treated with PNGase F or Endo H and finally analyzed by SDS-PAGE (8% acrylamide). C indicates samples from non-injected control oocytes.

Next, the glycosylation status of the surface-expressed His-P2X<sub>1</sub>-GFP protein was compared with that of the parent His-rP2X<sub>1</sub> protein. Endo H treatment reduced the molecular mass of both the parent His-rP2X<sub>1</sub> subunit and the C-terminally GFP-tagged His-rP2X<sub>1</sub> subunit by 8 kD, but was unable to remove all N-glycans (Fig. 3.26, lane 5). In contrast, PNGase F treatment released all N-glycans of the His-rP2X<sub>1</sub>-GFP polypeptide (Fig. 3.26, lane 6). These results suggest that the His-rP2X<sub>1</sub>-GFP fusion protein like the parent His-rP2X<sub>1</sub> subunit carries four N-linked oligosaccharide side chains, one of which becomes complex glycosylated in the Golgi.

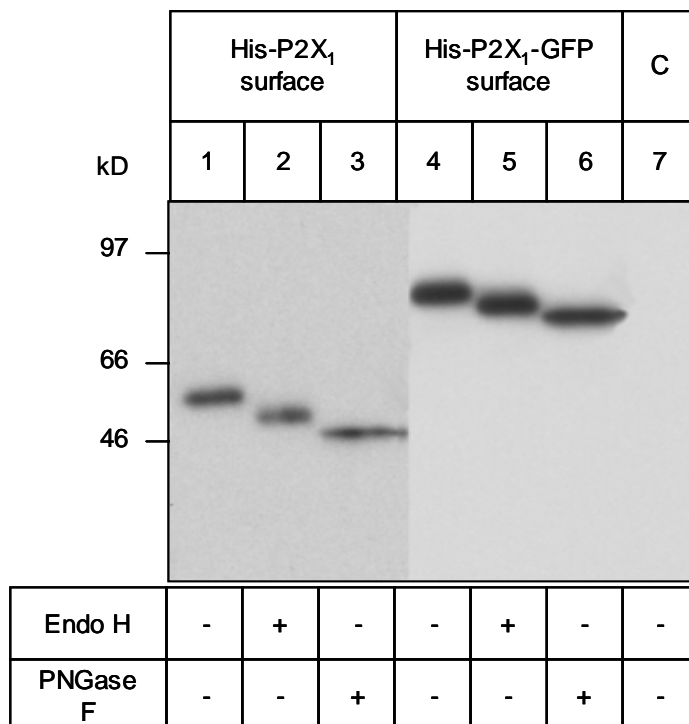


**Fig. 3.26: Glycosylation status of surface His-rP2X<sub>1</sub>-GFP.** Oocytes injected with 25 ng of cRNA for His-rP2X<sub>1</sub> or His-rP2X<sub>1</sub>-GFP were left for 3 days at 19°C and then labeled with membrane-impermeant <sup>125</sup>I-sulfo-SHPP. Proteins were purified by Ni<sup>2+</sup>-NTA chromatography from 1% digitonin extracts of oocytes, and eluted with non-denaturing elution buffer. Aliquots of these samples were supplemented with SDS sample buffer and treated with Endo H or PNGase F as indicated. After the digestion, proteins were resolved by SDS-PAGE (8% acrylamide) followed by autoradiography. C, non-injected control oocytes.

#### 3.1.5.4. Investigation of the quaternary structure of the GFP-tagged rP2X<sub>1</sub> fusion proteins

##### 3.1.5.4.1. Cross-linking analysis of the GFP-tagged rP2X<sub>1</sub> fusion proteins

Oocytes injected with the cRNA for His-rP2X<sub>1</sub>-GFP fusion protein were surface-labeled with <sup>125</sup>I-sulfo-SHPP and then incubated with glutardialdehyde for 60 min. After the cross-linking reaction, the fusion proteins were purified from a digitonin extract of the oocytes by Ni<sup>2+</sup>-NTA agarose affinity chromatography and subjected to reducing SDS-PAGE analysis. In addition to the His-rP2X<sub>1</sub>-GFP monomer, two bands of higher molecular masses were observed (Fig. 3.27, lane 4). These bands corresponded in size to the calculated molecular masses of the His-rP2X<sub>1</sub>-GFP dimer of ~175 kD and trimer of ~260 kD. Incubation of the injected oocytes with

increasing concentrations of glutardialdehyde did not yield bands with higher molecular masses than for a trimer (Fig. 3.27, lanes 5). These results suggest that the His-rP2X<sub>1</sub>-GFP protein, like the parent His-P2X<sub>1</sub> receptor, exists as a trimer in the plasma membrane.

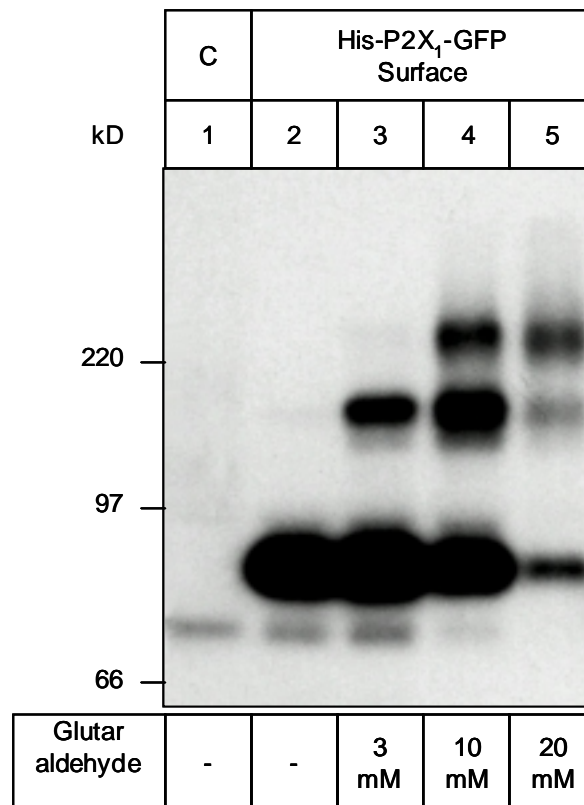


**Fig. 3.27: Cross-linking of the His-rP2X<sub>1</sub>-GFP fusion protein on intact *Xenopus* oocytes.** Oocytes injected with 25 ng of cRNA for His-rP2X<sub>1</sub>-GFP were surface iodinated with <sup>125</sup>I-sulfo-SHPP three days after injection. Cross-linking was performed on intact oocytes with the indicated concentrations of glutardialdehyde for 60 min at 4°C. After removing the excess of glutardialdehyde by washing with oocyte PBS, the oocytes were homogenized in 1% digitonin. His-rP2X<sub>1</sub>-GFP was purified by Ni<sup>2+</sup>-NTA agarose affinity chromatography and eluted with non-denaturing elution buffer and finally analyzed by reducing SDS-PAGE (4-10% acrylamide gradient gel). C indicates samples from non-injected control oocytes.

#### 3.1.5.4.2. BN-PAGE analysis of the GFP-tagged rP2X<sub>1</sub> fusion proteins

The N- or C-terminally GFP-tagged His-rP2X<sub>1</sub> fusion proteins that were purified under non-denaturing conditions from metabolically labeled oocytes migrated as single bands at about 350 kD when analyzed by BN-PAGE (Fig. 3.28, lanes 7 and 10). In addition, a large amount of aggregated protein in the region of high molecular mass range was observed for His-P2X<sub>1</sub>-GFP (Fig. 3.28, lane 7). These aggregations may reflect incompletely folded or only partially assembled fusion protein that was retained in the ER. Due to the mass addition by the GFP tag, the fusion proteins

exhibited a lower mobility in the BN-PAGE system than the parent His-P2X<sub>1</sub> receptor that migrated at 240 kD (Fig. 3.28, lane 4). To determine the number of subunits incorporated into the defined 350 kD fusion protein, a partial dissociation was induced by treatment of the complexes with urea. This treatment led to the appearance of two additional bands besides the non-dissociated complex at 350 kD, corresponding to the monomer at ~120 kD, and the intermediate dimer at ~250 kD (Fig. 28, lanes 9 and 12). These results indicated that the N- or C-terminally GFP-tagged His-rP2X<sub>1</sub> polypeptides adopt a trimeric structure like the parent His-rP2X<sub>1</sub> polypeptide (Fig. 3.28, lanes 4-6).

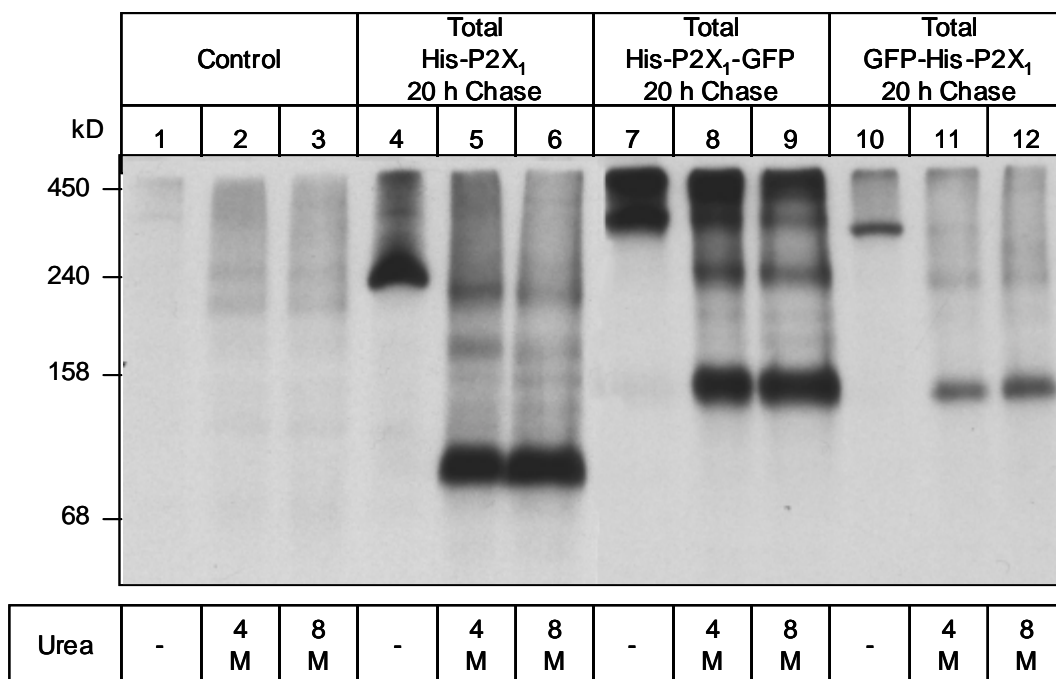


**Fig 3.28: BN-PAGE analysis of N- or C-terminally GFP-tagged His-rP2X<sub>1</sub> protein after metabolic labeling.** Oocytes injected with 25 ng of cRNA for His-P2X<sub>1</sub>, His-rP2X<sub>1</sub>-GFP or GFP-His-rP2X<sub>1</sub> were metabolically labeled overnight and then chased for 20 h at 19°C. Cells were extracted with 1% digitonin. Parent His-P2X<sub>1</sub> or the fusion proteins were purified by Ni<sup>2+</sup>-NTA affinity chromatography under non-denaturing conditions. Digitonin solubilized proteins were supplemented with blue native sample buffer and either directly applied on the gel or first incubated at 37°C with 4 M or 8 M urea in the presence of blue native sample buffer and then applied on the gel (4-13% acrylamide gradient gel).

Blue native PAGE analysis revealed a strong dissociation of the metabolically labeled His-rP2X<sub>1</sub> receptor and the fusion proteins upon treatment with 4 M or 8 M urea, as shown by appearance of the strong monomeric bands (Fig 3.28, lanes 6, 9, and 12). A similar dissociation of the protein complexes could also be produced by treatment with 100 mM DTT in the presence of aminocaproate for the natively eluted His-rP2X<sub>1</sub> or His-rP2X<sub>1</sub>-GFP receptors from surface labeled oocytes (Fig 3.29, lanes



2 and 5). The DTT treatment induced a partial dissociation of the fusion protein and led to the appearance of two additional bands besides the non-dissociated complex at 350 kD, corresponding to the monomer at ~120 kD, and the intermediate dimer at ~250 kD.

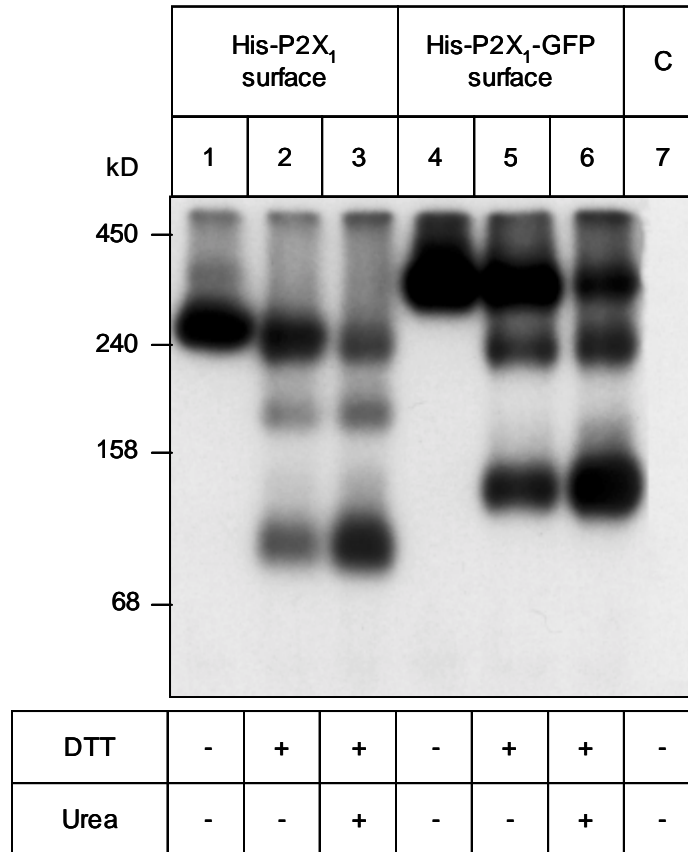


**Fig 3.29: Partial dissociation of surface-iodinated His-rP2X<sub>1</sub>-GFP complex.** Oocytes injected with 25 ng of cRNA for His-rP2X<sub>1</sub> or His-rP2X<sub>1</sub>-GFP were left for 3 days at 19°C and then labeled with membrane-impermeant <sup>125</sup>I-sulfo-SHPP. Proteins were purified by Ni<sup>2+</sup>-NTA affinity chromatography from 1% digitonin extracts of oocytes, and eluted with non-denaturing elution buffer. Samples were supplemented with BN sample buffer and analyzed by BN-PAGE (4-13% acrylamide gradient gel) either without incubation or after incubation for 45 min at 37°C with 4 M urea and/or 100 mM DTT as indicated. C indicates samples from non-injected control oocytes.

### 3.1.6. Characterization of P2X subunit chimeras after expression in *Xenopus* oocytes

Currents evoked by ATP at P2X<sub>1</sub> and P2X<sub>3</sub> receptors undergo marked desensitization within a few hundred milliseconds. In contrast, currents evoked at P2X<sub>2</sub> receptors, similarly expressed, undergo little or no desensitization on this time scale (Valera *et al.*, 1994). The 399 amino acids of P2X<sub>1</sub> subunit are 37% identical with the corresponding portion of the P2X<sub>2</sub> receptor, which has 472 amino acids due to a longer C-terminus. The aim of these studies was to prove or disprove whether P2X receptors with non-desensitizing phenotype have a propensity to assemble to hexamers rather than to trimers. Therefore, the rP2X<sub>2</sub> N-terminal domain was substituted for the corresponding portion of the rP2X<sub>1</sub> and rP2X<sub>3</sub> receptor, which results in a non-desensitizing phenotype in both cases (Werner *et al.*, 1996). Furthermore, the N-terminal domain of human P2X<sub>4</sub> subunit was inserted into the rP2X<sub>1</sub> receptor subunit and the first transmembrane segment of the rP2X<sub>1</sub> receptor subunit was substituted by the first transmembrane region of rP2X<sub>2</sub> receptor subunit (Fig. 3.30). Prior to the electrophysiological characterization of the constructs, the chimeras were analyzed by SDS- and BN-PAGE.

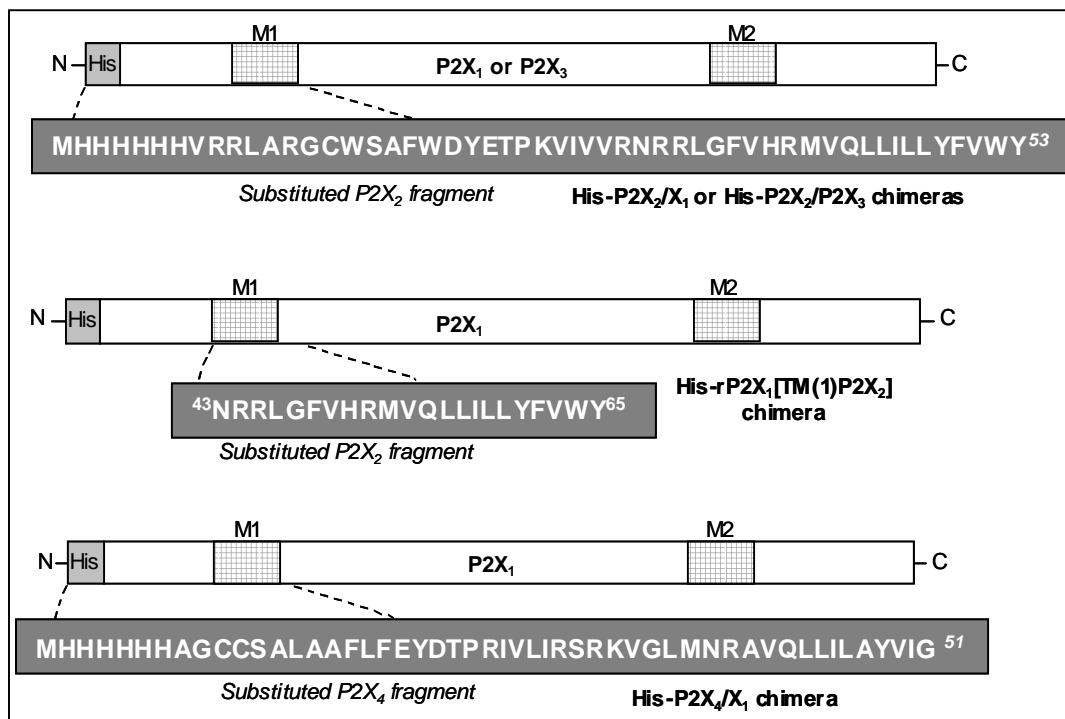


**Fig. 3.30: Schematic representation of the chimeras.** Checkered rectangles indicate positions of putative membrane-spanning regions M1 and M2. White letters in gray rectangles indicate the substituted sequence of segments into the respective P2X subunits. Light gray rectangles show N-terminal hexahistidyl tag.

### 3.1.6.1. Biochemical characterization of P2X subunit chimeras by SDS-PAGE

For biochemical analysis, oocytes injected with the cRNA for the His-rP2X<sub>1</sub> subunit or the N-terminally hexahistidyl-tagged P2X chimeras were metabolically labeled by an overnight incubation with [<sup>35</sup>S]methionine. After the metabolic labeling of the oocytes, digitonin extracts were prepared. The proteins were isolated by Ni<sup>2+</sup>-NTA agarose chromatography, and eluted with non-denaturing elution buffer. Samples were incubated in the presence of Endo H or PNGase F and then analyzed by SDS-PAGE. Fig. 3.31 A shows that like the parent His-P2X<sub>1</sub> subunit, the chimeras consisting of the first 53 amino acids of the rat P2X<sub>2</sub> subunit (His-rP2X<sub>2</sub>/rP2X<sub>1</sub>) or the first 51 amino acids of the human P2X<sub>4</sub> subunit (His-rP2X<sub>4</sub>/rP2X<sub>1</sub>) connected with 352 amino acids of the C terminus of the rat P2X<sub>1</sub> polypeptide could be isolated as 57 kD proteins (lanes 1, 4 and 7). A His-P2X<sub>1</sub> mutant with the amino acid residues for the first transmembrane region substituted with those of the rat P2X<sub>2</sub> subunit (His-rP2X<sub>1</sub>[TM(1)P2X<sub>2</sub>]) migrated as a single polypeptide of an apparent molecular masses of 57 kD (Fig. 3.31 B, lane 4). These manipulations appeared to influence the glycosylation status of the proteins. While the parent His-P2X<sub>1</sub> subunit and the His-hP2X<sub>4</sub>/rP2X<sub>1</sub> chimera were partially Endo H resistant, indicating that at least one N-linked carbohydrate chain becomes complex glycosylated (Fig. 3.31 A, lanes 2 and 8), deglycosylation of the His-rP2X<sub>2</sub>/rP2X<sub>1</sub> and His-rP2X<sub>1</sub>[TM(1)P2X<sub>2</sub>] chimeras with Endo H released all N-linked glycans (Fig. 3.31 A and B, lanes 5), indicating that the rP2X<sub>2</sub>/rP2X<sub>1</sub> chimeras do not acquire complex type carbohydrates.

The His-rP2X<sub>2</sub>/rP2X<sub>3</sub> chimera consisting of the hexahistidyl-tag and the first 47 N-terminal amino acids of rP2X<sub>2</sub> subunit with the C-terminal 356 amino acids of the P2X<sub>3</sub> polypeptide was isolated from *Xenopus* oocytes as a 57 kD protein (Fig. 3.31 B, lane 1). The molecular mass of the metabolically labeled chimera was reduced by 10 kD to 47 kD when this glycoprotein was incubated with PNGase F (Fig. 3.31 B, lane 3). This suggests that His-rP2X<sub>2</sub>/rP2X<sub>3</sub> chimera carries four N-linked oligosaccharide side chains. Upon treatment with Endo H, all N-linked glycans were released, indicating that this chimera does not acquire complex type carbohydrates (Fig. 3.31 B, lane 2).

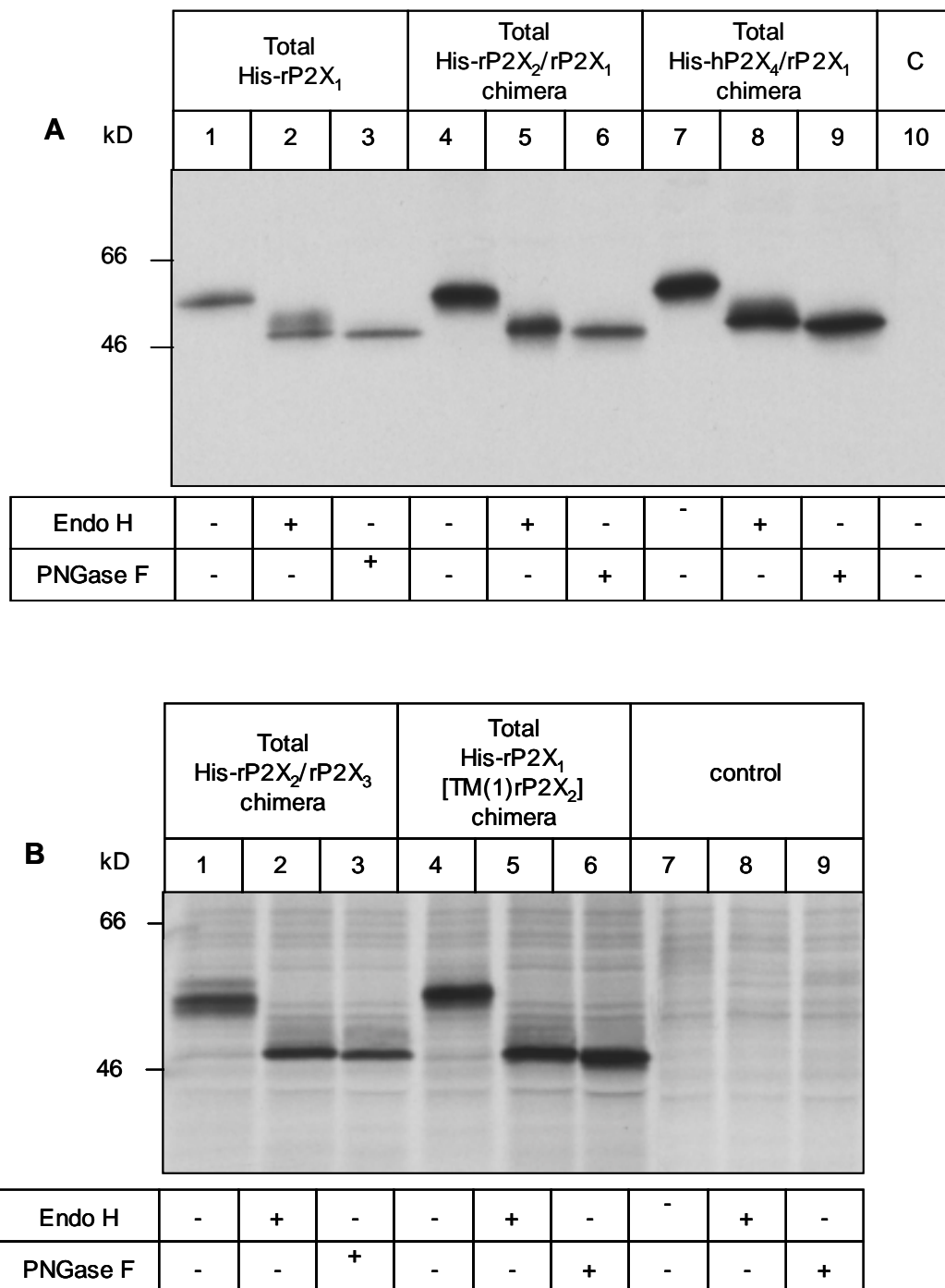


**Fig. 3.31: SDS-PAGE analysis of P2X subunit chimeras after metabolic labeling.** Oocytes injected with 25 ng of cRNA for His-rP2X<sub>1</sub> or the respective P2X chimeras were metabolically labeled overnight. After the metabolic labeling, cells were extracted with 1% digitonin. Proteins were purified by Ni<sup>2+</sup>-NTA affinity chromatography, eluted under non-denaturing conditions and treated with PNGase F or Endo H and analyzed by SDS-PAGE (8% acrylamide) followed by autoradiography. C indicates samples from non-injected control oocytes.

### 3.1.6.2. Blue native PAGE analysis of P2X subunit chimeras

In addition, the oligomeric state of the parent His-rP2X<sub>1</sub> receptor and the respective chimeras was analyzed by BN-PAGE. The parent His-P2X<sub>1</sub> receptor isolated from cRNA injected and [<sup>35</sup>S]methionine-labeled oocytes migrated as a single protein band at about 240 kD, when resolved by BN-PAGE (Fig. 3.32 A, lane 1). His-rP2X<sub>2</sub>/rP2X<sub>1</sub> (Fig. 3.32 A, lane 5), His-hP2X<sub>4</sub>/rP2X<sub>1</sub> (Fig. 3.32 A, lane 9) and rP2X<sub>1</sub>[TM(1)P2X<sub>2</sub>] chimeras (Fig. 3.32 B, lane 7) exhibited a similar mobility and migrated at ~250 kD. For the His-rP2X<sub>2</sub>/rP2X<sub>1</sub> and His-hP2X<sub>4</sub>/rP2X<sub>1</sub> chimeras, an additional band with a high molecular mass of about 450 kD was observed. This band might corresponded in mass to the hexameric form of the chimeras.

To determine the number of subunits per receptor complex, the natively eluted rP2X<sub>1</sub> receptor or the respective chimeras were incubated prior to the BN-PAGE with DTT or urea in the presence of blue native sample buffer to induce a partial dissociation of the protein complexes. As reported already above, blue native PAGE analysis revealed three bands after partial denaturing of the His-rP2X<sub>1</sub> receptor, representing the P2X<sub>1</sub> trimer at ~240 kD, the dimer at ~180 kD, and the P2X<sub>1</sub> monomer at ~80 kD (Fig. 3.32 A, lanes 3 and 4). Treatment with urea in the presence of DTT induced a very strong dissociation, such that almost only His-rP2X<sub>1</sub> monomers of 80 kD are observed (lane 4). When treated with DTT alone in the presence of blue native sample buffer, three protein bands appeared also with His-rP2X<sub>2</sub>/rP2X<sub>1</sub> (lane 7), His-hP2X<sub>4</sub>/rP2X<sub>1</sub> (lane 11) and rP2X<sub>1</sub>[TM(1)P2X<sub>2</sub>] chimeras (Fig. 3.32 B, lane 8). The bands of the apparent masses of ~80 and ~200 kD correspond to the monomers and dimers, respectively. From these results, it is deduced that the chimeras constructed by the connection of complementary regions of the P2X<sub>2</sub> with the P2X<sub>1</sub> polypeptide also assemble to a trimeric complex like the parent His-P2X<sub>1</sub> subunit.

The His-rP2X<sub>2</sub>/rP2X<sub>3</sub> chimera migrated as a single band at ~250 kD when resolved by the blue native PAGE (Fig. 3.32 B, lane 2). Incubation prior to BN-PAGE of the natively eluted His-rP2X<sub>2</sub>/rP2X<sub>3</sub> receptor with DTT and urea in the presence of the blue native sample buffer caused a partial dissociation of the complex into the monomer and dimer of apparent masses of 90 kD and 190 kD, respectively (Fig 3.32 B, lane 5). This observation implies that the non-denatured protein band must be a trimer.

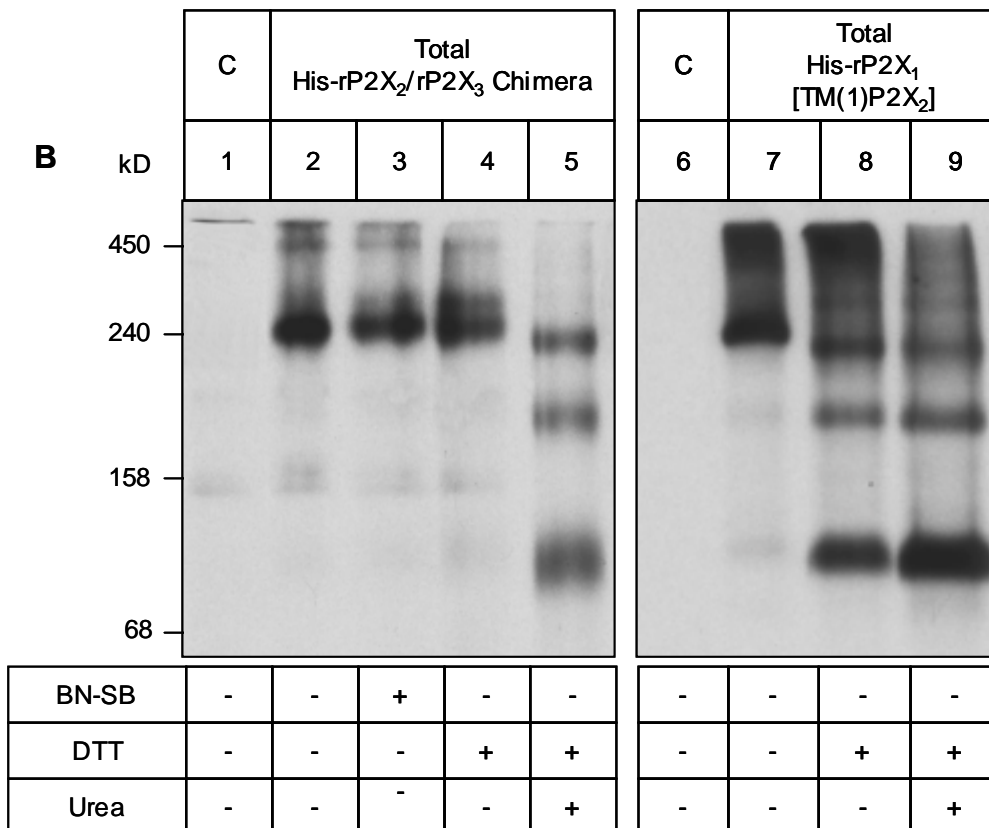
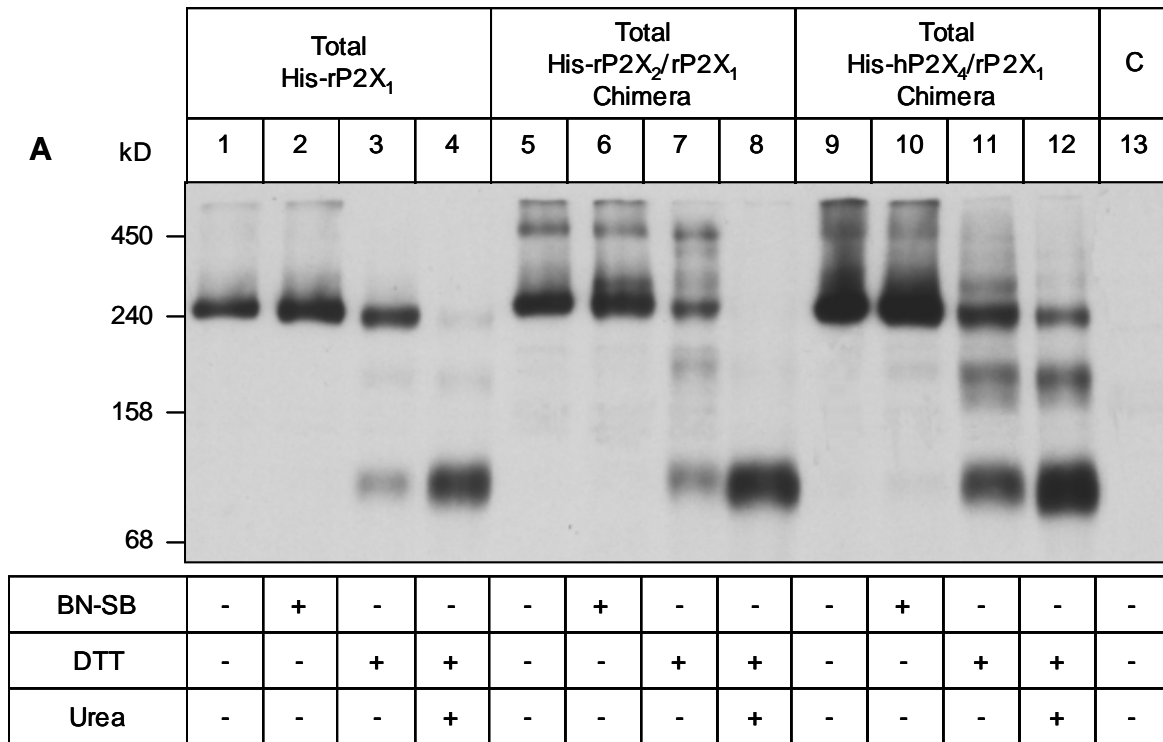


**Fig. 3.32: BN-PAGE analysis of partially dissociated chimeric P2X receptors.** Oocytes injected with 25 ng of cRNA for His-P2X<sub>1</sub> or one of the respective P2X chimeras were metabolically labeled overnight. After the metabolic labeling, digitonin extracts were prepared. Proteins were isolated by Ni<sup>2+</sup>-NTA chromatography and eluted under non-denatured conditions. Samples were analyzed by blue native PAGE (4–13% acrylamide gradient gel) either without further treatment or after incubation with blue native sample buffer in the presence or absence of 100 mM DTT and/or 8 M urea at 37°C for 60 min. C indicates samples from non-injected control oocytes.

### 3.1.6.3. Electrophysiological characterization of P2X subunit chimeras after expression in *Xenopus* oocytes

P2X<sub>1</sub> and P2X<sub>2</sub> receptors are distinguished by their different rates of desensitization (Fig. 3.23 and Fig. 3.1 A). In oocytes expressing P2X<sub>1</sub> or P2X<sub>3</sub> receptors, the current evoked by 10 μM ATP desensitized by around 100% during a 10 s application of ATP. In oocytes expressing the His-rP2X<sub>2</sub> receptor, prolonged application of ATP (30 μM) elicited a large inward current with a rapid onset and slow rate of desensitization. Substitution of the P2X<sub>1</sub> or the P2X<sub>3</sub> subunits with corresponding parts of the intracellular N-terminus and first transmembrane region of P2X<sub>2</sub> receptor segments removes desensitization (Werner *et al.*, 1996) (Fig. 3.33 A and C). At these constructs, ATP (10 μM) evoked a current that declined by only few percents in 10 s. These experiments indicate that exchange of the first 53 amino acid residues fully eliminates desensitization from the P2X<sub>1</sub> or P2X<sub>3</sub> receptors.

Substitution of the corresponding P2X<sub>2</sub> segment into position 43–65 of the P2X<sub>1</sub> receptor provided a channel at which a current was evoked that declined by only few percents during a 10-s application of ATP (10 μM). Thus, Substitution of the residues 43–65 (approximately equivalent to the first transmembrane domain of P2X<sub>2</sub>) into the P2X<sub>1</sub> receptor was effective to remove desensitization from the chimera (Fig. 3.33 B), indicating that a portion of the P2X<sub>1</sub> receptor that is responsible for desensitization is located in this region (Werner *et al.*, 1996).

The analysis of the designed chimeric constructs revealed that two subunits with widely different biophysical and pharmacological properties as P2X<sub>2</sub> and P2X<sub>1</sub> could yield chimeric receptors with unique functional properties as already was reported by others (Werner *et al.*, 1996). Next, instead of P2X<sub>2</sub>, the P2X<sub>4</sub> subunit was chosen. The P2X<sub>4</sub> receptor is known to desensitize partially and it behaves functionally in between P2X<sub>1</sub> and P2X<sub>2</sub> receptors. A chimeric construct was engineered, in which the N-domain including the first transmembrane domain was from P2X<sub>4</sub> and the rest of the flanking protein from P2X<sub>1</sub>. As revealed by the two-voltage clamp measurements, the P2X<sub>1</sub> receptor with the P2X<sub>4</sub> N-domain also exhibits a rapid activation in response to 10 μM ATP followed by a strong desensitization, as also observed for the wild type P2X<sub>1</sub> receptor (Fig. 3.33 D).

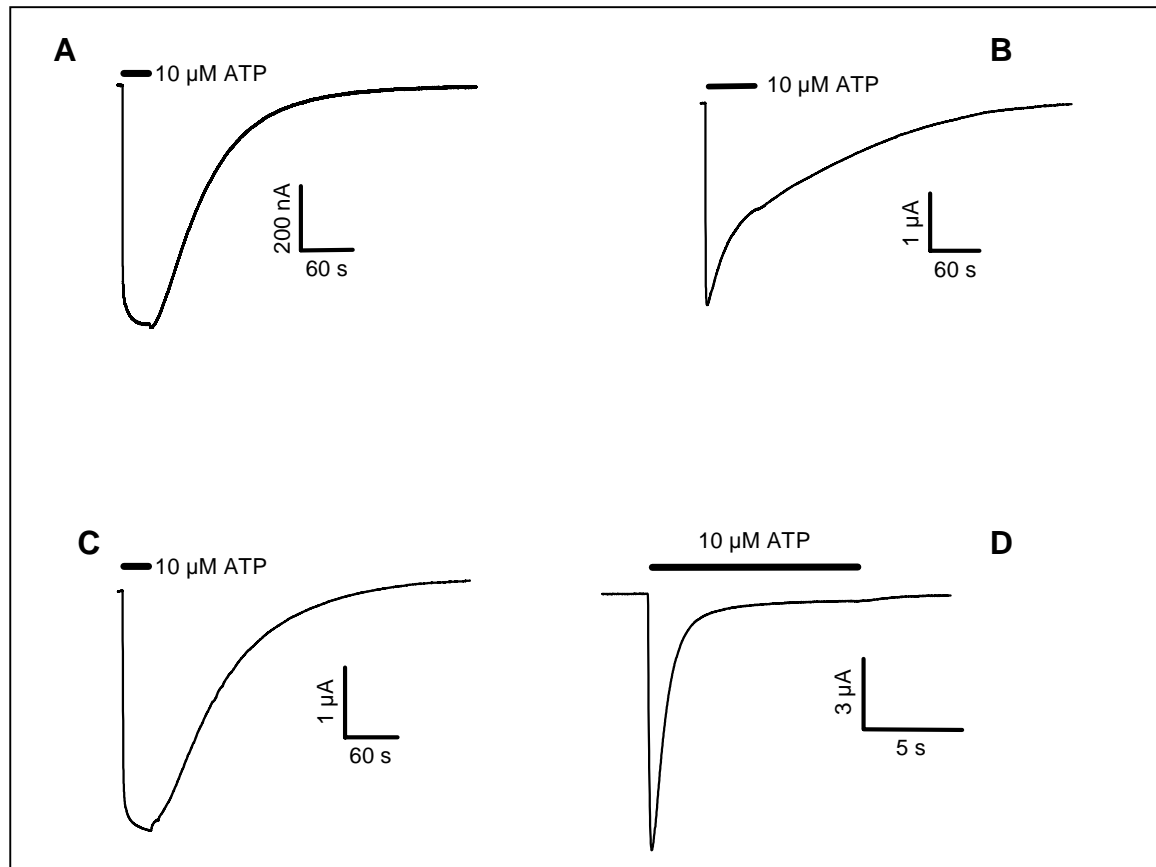


**Fig. 3.33: Comparison of electrophysiological responses to activation of the P2X receptor chimeras.** Oocytes were injected with 23 ng of cRNA for P2X<sub>2</sub>/P2X<sub>1</sub> chimera (A), P2X<sub>1</sub>[TM-P2X<sub>2</sub>] chimera (B), P2X<sub>2</sub>/P2X<sub>3</sub> chimera (C), or P2X<sub>4</sub>/P2X<sub>1</sub> chimera (D). One day after injection current responses elicited by 10 μM ATP were measured at a holding potential -60 mV from oocytes expressing P2X<sub>2</sub>/P2X<sub>1</sub> chimera. Two days after injection current responses elicited by 10 μM ATP were measured at a holding potential -60 mV from oocytes expressing P2X<sub>1</sub>[TM-P2X<sub>2</sub>] chimera, or P2X<sub>2</sub>/P2X<sub>3</sub> chimera. Three days after injection current responses elicited by 10 μM ATP were measured at a holding potential -60 mV from oocytes expressing P2X<sub>4</sub>/P2X<sub>1</sub> chimera. The duration of agonist activation is shown by the horizontal bar. The experiments were performed by Dr. Jürgen Rettinger.



### 3.2. Studies on the role of N-linked glycosylation in the rat P2X<sub>1</sub> receptor function and expression

#### 3.2.1. Identification of the sites of N-linked glycosylation of rat P2X<sub>1</sub> receptor after expression in *Xenopus* oocytes

The His-P2X<sub>1</sub> subunit was isolated from cRNA-injected and [<sup>35</sup>S]methionine-labeled oocytes as a 57 kD glycoprotein (Fig. 3.34 A, lane 1) that carries four N-glycans making up ~18% by mass of the protein (Nicke *et al.*, 1998). The deduced amino acid sequence of the P2X<sub>1</sub> subunit shows five asparagines for possible N-linked glycosylation (NXT/S): <sup>153</sup>NGT, <sup>184</sup>NFT, <sup>210</sup>NGT, <sup>284</sup>NLS, and <sup>300</sup>NGT. Replacement of <sup>153</sup>N, <sup>184</sup>N, <sup>210</sup>N and <sup>300</sup>N by Q, one at a time, resulted in the synthesis of glycoproteins that had a 2-3 kD lower mass than the wild type P2X<sub>1</sub> glycoprotein (Fig. 3.34 A, lanes 2-4, 7). Since 2-3 kD corresponds to the mass of one N-linked oligosaccharide side chain, this finding implies that each of the replaced asparagines is occupied by an N-glycan in the wild type P2X<sub>1</sub> subunit. In contrast, replacement of <sup>284</sup>N by Q had no effect on the mass (Fig. 3.34 A, lane 5), indicating that <sup>284</sup>N of the wild type P2X<sub>1</sub> subunit is the asparagine that is not used as a glycosyl acceptor site.

The inability to glycosylate <sup>284</sup>N of the <sup>284</sup>NLS sequon may be attributed to the leucine residue in the X position, which has been found to impair core glycosylation (Shakin-Eshleman *et al.*, 1996). Alternatively, <sup>287</sup>P immediately following the <sup>284</sup>NLS sequon might be responsible, since proline inhibits core glycosylation not only at the X, but also at the +4 position (Gavel *et al.*, 1990). Indeed, <sup>284</sup>N was efficiently used as a glycosyl acceptor site when alanine was substituted for <sup>287</sup>P, as inferred from the reduced mobility of the His-A<sup>287</sup>-P2X<sub>1</sub> polypeptide, indicating the presence of an additional (fifth) N-glycan (Fig. 3.34 A, lane 6). The occupancy of <sup>284</sup>N by a glycan had no apparent effect on P2X<sub>1</sub> receptor function, as deduced from the magnitude and concentration dependence of ATP-gated currents. The efficient glycosylation at <sup>284</sup>N after elimination of <sup>287</sup>P argues against a significant role of <sup>285</sup>L for the inability to glycosylate <sup>284</sup>N of the parent P2X<sub>1</sub> polypeptide.

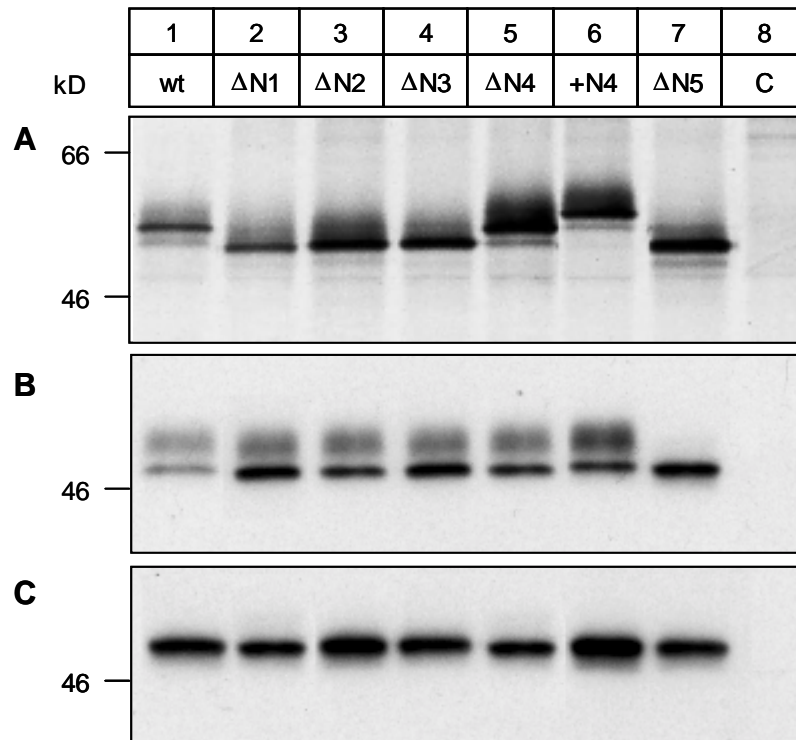


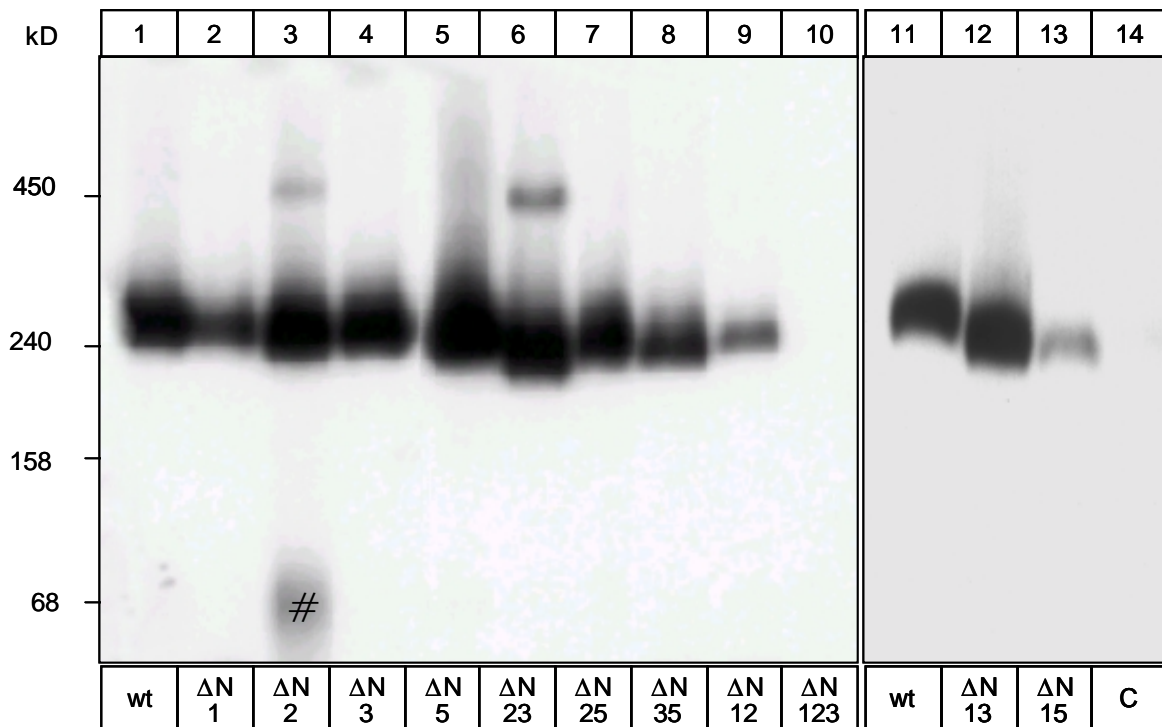
**Fig. 3.34: N-glycosylation of His-P2X<sub>1</sub> mutants each lacking one out of five N-glycosylation sites.** Oocytes injected with 25 ng of the indicated cRNAs were metabolically labeled by overnight incubation with [<sup>35</sup>S]methionine. After an additional 24 h chase interval, digitonin extracts were prepared. Parent His-P2X<sub>1</sub> and the various glycan minus mutants were isolated by Ni<sup>2+</sup>-NTA chromatography, eluted with non-denaturing elution buffer, and then supplemented with SDS sample buffer, 20 mM DTT (final concentration). Samples were incubated for 15 min at 37°C in the absence (A) or for 2 h at 37°C in the presence of Endo H (B) or PNGase F, 1% octylglucoside (C) and then analyzed by SDS-PAGE (10% acrylamide) followed by autoradiography. C indicates samples from non-injected control oocytes.

From the four N-glycans per P2X<sub>1</sub> receptor subunit, only one acquired Endo H resistance during transport to the plasma membrane of *Xenopus* oocytes (Nicke *et al.*, 1998). This suggests that processing by Golgi enzymes of three of the N-glycans is sterically hindered, most likely because of folding and oligomerization of the P2X<sub>1</sub> chains. Fig. 3.34 B shows that like the parent His-P2X<sub>1</sub> receptor (lane 1) all the P2X<sub>1</sub> receptor mutants (lanes 2-6) except  $\Delta$ N5 (lane 7) acquired Endo H-resistant carbohydrates. Since the P2X<sub>1</sub> receptor mutant  $\Delta$ N5 appears at the plasma membrane (*cf.* Figs. 3.35 – 3.37), the absence of Endo H-resistant carbohydrates can be directly conferred to the lack of the sole N-glycan that can acquire complex-type carbohydrates during transit of the Golgi apparatus. This indicates that the glycan at <sup>300</sup>N of the parent His-P2X<sub>1</sub> receptor subunit is the one accessible for complex-glycosylation.

### 3.2.2. Importance of N-glycans for P2X<sub>1</sub> receptor function and assembly

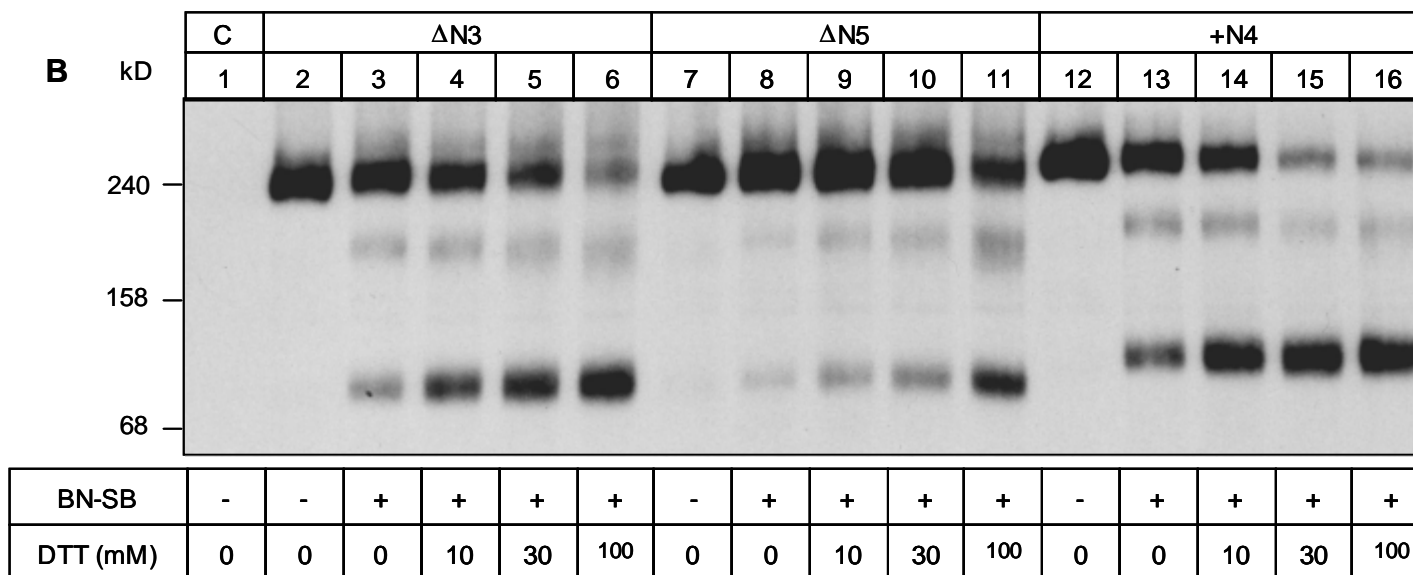
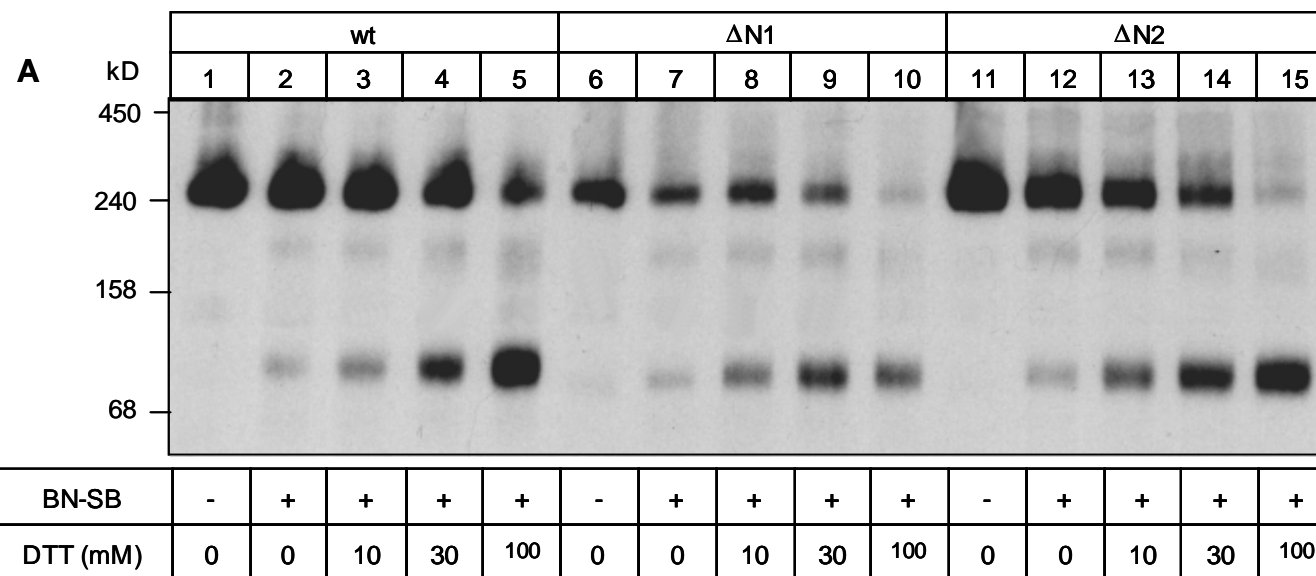
#### 3.2.2.1. BN-PAGE analysis of P2X<sub>1</sub> mutants lacking one or several consensus sequences for N-glycosylation

An additional aim of the study was to examine the influence of carbohydrates on P2X<sub>1</sub> receptor assembly as assessed by blue native PAGE analysis. Parent His-P2X<sub>1</sub> subunits combine rapidly to stable homotrimers that exit the ER, transit the Golgi where complex-glycosylation of  $\Delta N5$  occurs (Fig. 3.34) and finally appear at the plasma membrane. To visualize the plasma membrane form of the His-P2X<sub>1</sub> glycan minus receptor mutants, oocytes surface proteins were radio-iodinated with membrane impermeant <sup>125</sup>I-sulfo-SHPP and then isolated the His-tagged proteins by Ni<sup>2+</sup>-NTA chromatography. When resolved by blue native PAGE, the parent His-P2X<sub>1</sub> receptor migrated at 250-290 kD (Fig. 3.35, lane 1). Overall, elimination of N-glycans resulted in a slight increase in electrophoretic mobility, corresponding maximally to 20 kD when two N-glycans per subunit were lacking. Within the technical limits of receptor quantification by surface radio-iodination, all the receptor mutants lacking one N-glycan (Fig. 3.35, lanes 2-5) and most of the mutants lacking two N-glycans (lanes 12-14) were present at approximately the same density at the plasma membrane as the parent His-P2X<sub>1</sub> receptor.



**Fig. 3.35: Glycan minus mutants migrate as trimers like parent  $2X_1$  when analyzed by blue native PAGE.** Oocytes injected with 25 ng of the indicated cRNA 3 days earlier were surface-labeled with membrane impermeant  $^{125}\text{I}$ -sulfo-SHPP and extracted with digitonin. His-P2X<sub>1</sub> and the His-tagged mutant proteins were then purified by Ni<sup>2+</sup>-NTA chromatography under non-denaturing conditions and after native elution resolved by blue native PAGE (4 –10% acrylamide gradient gel), followed by autoradiography. Shown are samples from two independent experiments. #, contaminating protein not observed in other experiments (cf. lane 3). C indicates samples from non-injected control oocytes.

To display the oligomeric state of these receptor complexes, the natively eluted His-P2X<sub>1</sub> mutant receptors were exposed to DTT in the presence of Coomassie blue and sodium 6-amino-*n*-caproate. This treatment caused a partial dissociation of the parent His-P2X<sub>1</sub> receptor to the monomer and dimer of apparent masses similar to 80 kD and 170 kD, respectively, indicating that the non-denatured 240 kD protein band must be a His-P2X<sub>1</sub> homotrimer (Fig 3.36 A, lanes 1-5). Likewise, also the His-P2X<sub>1</sub> glycan minus receptor mutants lacking one or two N-glycans per subunit dissociated into dimers and monomers when exposed to DTT (Fig. 3.36 A-C).



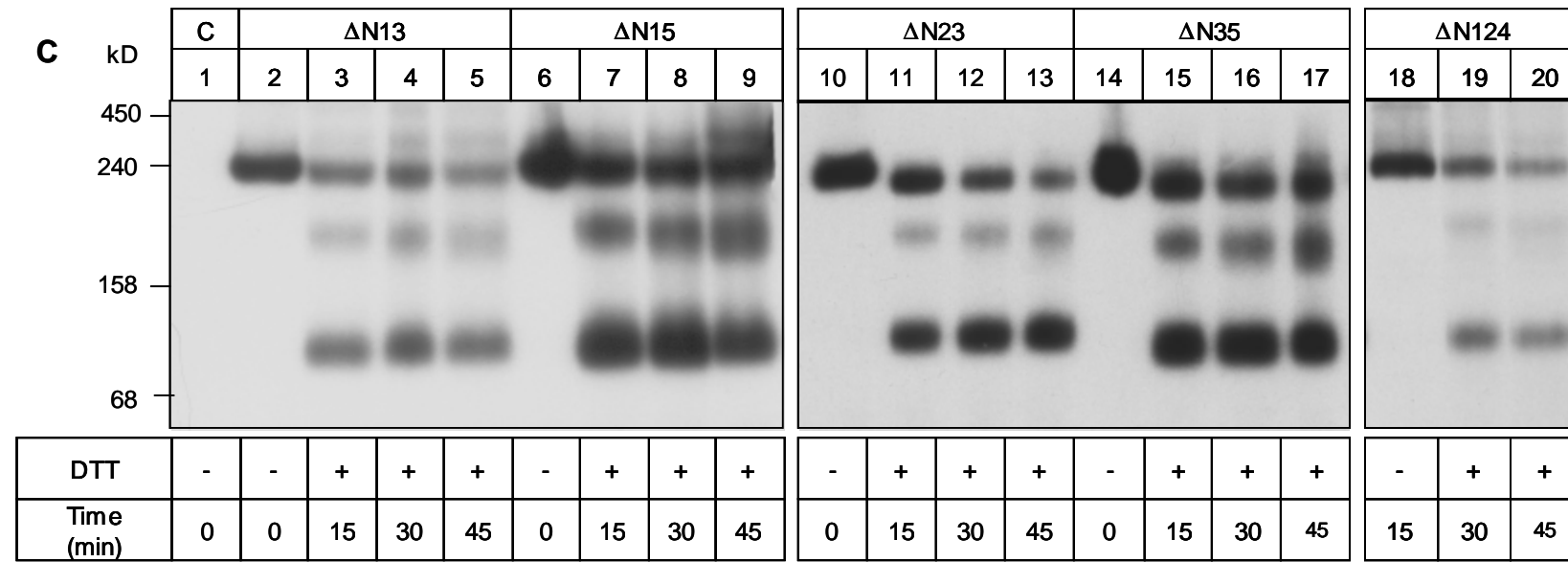


**Fig. 3.36: Partial dissociation of glycan minus mutants.** Oocytes injected with 25 ng of the indicated cRNA were metabolically labeled by overnight incubation with [<sup>35</sup>S]methionine (**C**), or alternatively, oocytes injected with 25 ng of the indicated cRNA were kept for 3 days at 19°C and then labeled with <sup>125</sup>I-sulfo-SHPP (**A** and **B**). Proteins were purified by Ni<sup>2+</sup>-NTA chromatography from 1% digitonin extracts of each oocyte group and eluted with non-denaturing elution buffer. Digitonin solubilized proteins were non-treated or alternatively dissociated by incubation with blue native sample buffer in the presence of indicated amounts of DTT (37°C, 45 min) (**A** and **B**), or dissociated by incubation with 100 mM DTT in the presence of blue native sample buffer for the indicated time at 37°C (**C**) and finally analyzed by BN-PAGE (4-13% acrylamide gradient gel). C indicates samples from non-injected control oocytes.

### 3.2.3. Electrophysiological analysis of oocyte-expressed P2X<sub>1</sub> mutants lacking one or several consensus sequences for N-glycosylation

To examine whether the elimination of a particular N-glycan affects the expression level of functional P2X<sub>1</sub> receptors, current responses to 30 μM ATP at -40 mV were recorded. This ATP concentration elicited different yet maximum responses at the parent P2X<sub>1</sub> receptor and all receptor mutants, since activation with 100 μM ATP did not result in a further increase of currents. Like the parent P2X<sub>1</sub> receptor, also all receptor mutants lacking one N-glycan per subunit exhibited large ATP-gated currents, indicating that no particular N-glycan is essential for receptor function (Fig. 3.37). There are, however, marked positional effects of the N-glycans. While the glycans at ΔN2 or ΔN5 were without significant effect on the expression level of functional receptors, elimination of the glycan at ΔN1 or ΔN3 resulted in a 30% decrease or 70% increase, respectively, of the current response (Fig. 3.37). Likewise, reduced currents were recorded from double mutants that lacked ΔN1 together with ΔN2 or ΔN5, whereas elimination of ΔN3 consistently resulted in increased currents even when ΔN1 was simultaneously eliminated (Fig. 3.37). These findings suggest that the glycans at ΔN1 and ΔN3 play opposing roles for the expression level of functional P2X<sub>1</sub> receptors.

Elimination of any three N-glycans did also not prevent P2X<sub>1</sub> receptor formation, but the functional expression level decreased markedly to < 10% of that of the parent P2X<sub>1</sub> receptor. The currents were particularly low when the three acceptor sites that were eliminated included ΔN1 (Fig. 3.37). No ATP-induced currents could be recorded from oocytes after removal of all canonical N-glycosylation sites. Taken together, these results implicate that despite their marked positional effects, only one N-glycan at any locus is required for the formation of functional P2X<sub>1</sub> receptors and two such sites are sufficient for robust functional expression.

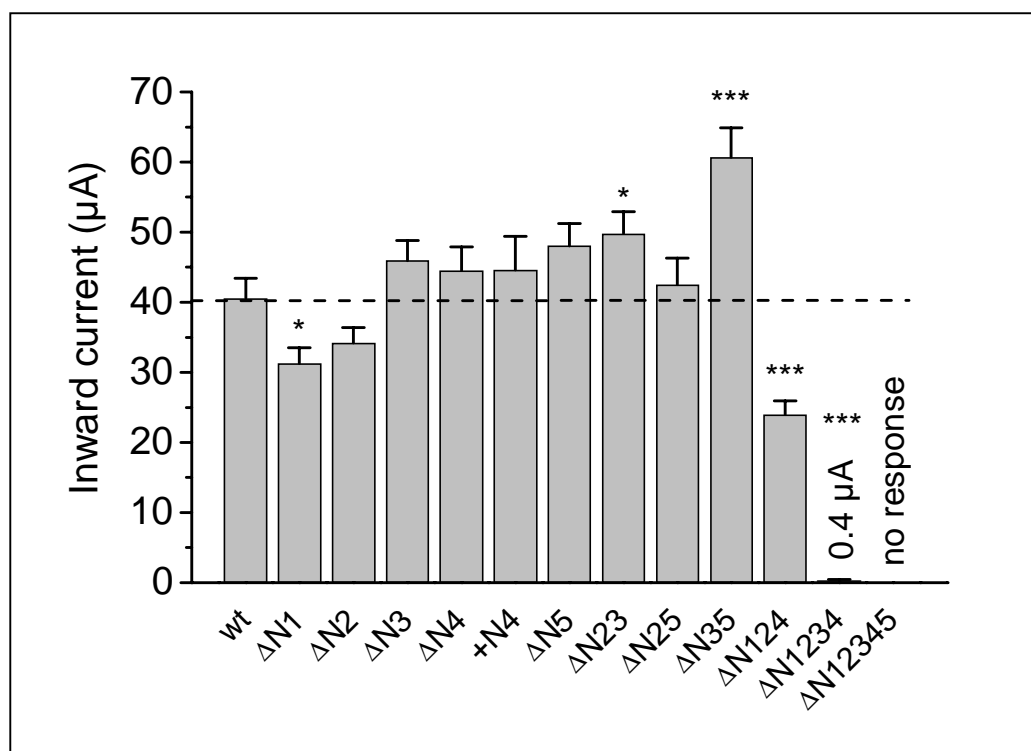


**Fig. 3.37: Comparison of maximum inward current responses generated by parent P2X<sub>1</sub> and glycan minus mutants.** Oocytes were injected with 25 ng of the indicated cRNAs. After three days at 19°C, currents were activated at a holding potential of -40 mV by 30 µM ATP, which elicits maximum responses at parent His-P2X<sub>1</sub> and each mutants. Currents were normalized to the response of the parent His-P2X<sub>1</sub> receptor. Data are given as means ± SEM from 20-48 oocytes per column of 2-6. The experiment was performed by Dr. Jürgen Rettinger.

Since N-glycans are bulky and can shield a large section of the protein surface, the effects on ATP potency by the elimination of N-glycans was investigated. To this end, receptor currents elicited by 0.3 µM and 30 µM ATP were recorded and the ratio of the current responses at these two ATP concentrations were determined. As apparent from Fig. 3.38 C, all the receptor mutants lacking ΔN3 (<sup>210</sup>N) showed a current ratio of 5-7% independent of simultaneous elimination of additional N-glycosylation sites. In contrast, all glycan minus receptor mutants that contained N-glycan ΔN3 showed a ratio of 26-37% similar to the 32% for the parent His-P2X<sub>1</sub> receptor. Since ΔN3 turned out to be crucial for the reduced potency, concentration response curves for ATP of ΔN3 and parent His-P2X<sub>1</sub> were recorded. Fitting the Hill equation to the data for the parent His-P2X<sub>1</sub> receptor yielded an EC<sub>50</sub> value for ATP of 0.7 µM (Fig. 3.38 D). In contrast, the glycan minus receptor mutant ΔN3 exhibited an EC<sub>50</sub> value of 2.1 µM, *i.e.* a threefold-reduced potency for ATP. The Hill coefficients (1.1 vs. 1.3) were not significantly different.



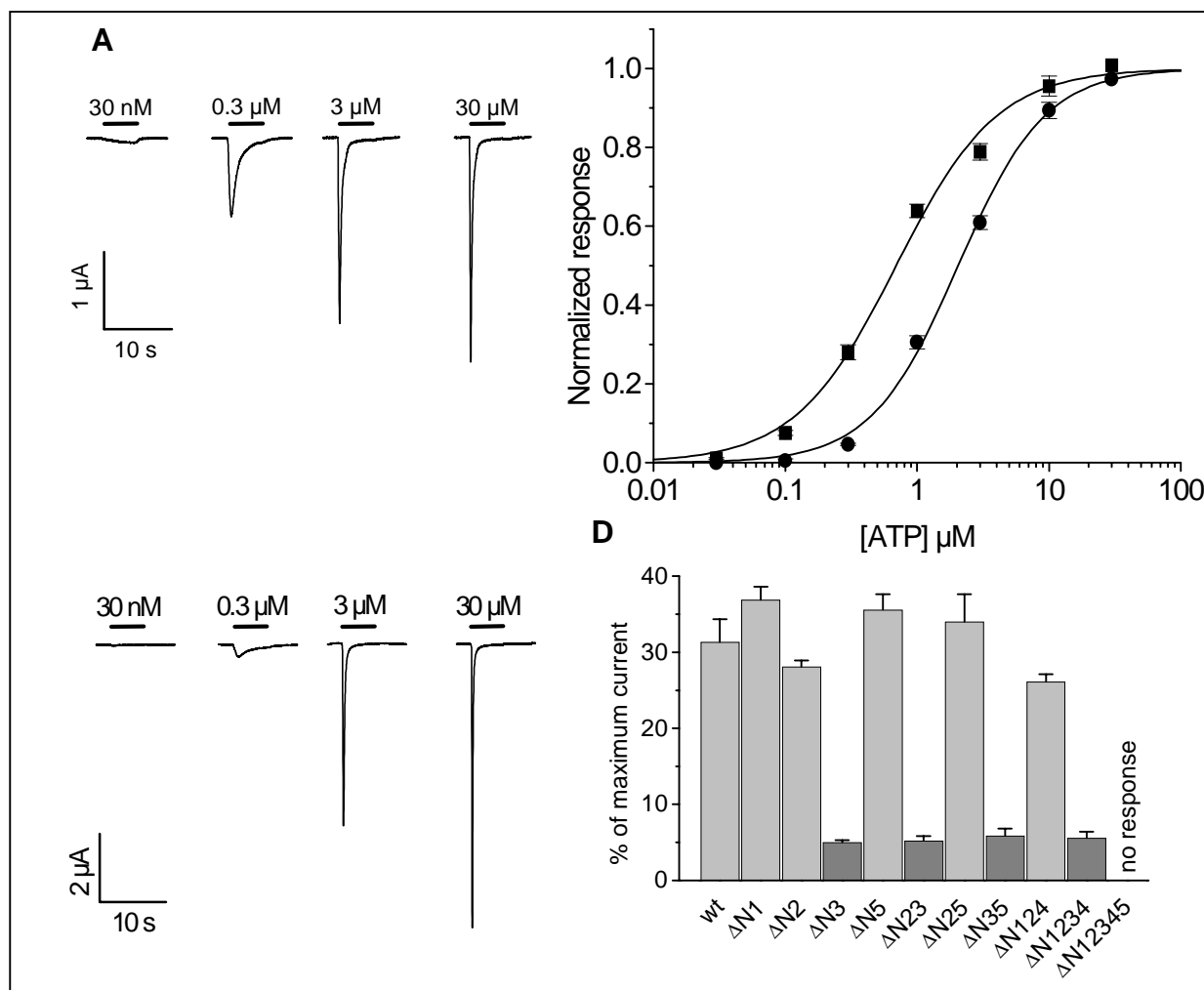


**Fig. 3.38: Comparison of ATP potency of the parent His-P2X<sub>1</sub> receptor and the glycan minus mutants.** Inward current traces were recorded at the indicated ATP concentrations and a holding potential -40 mV from oocytes injected three days earlier with 25 ng of cRNA for parent His-P2X<sub>1</sub> (**A**) or the glycan minus mutant ΔN3 (**B**). **C**, ATP dose-response curve for parent P2X<sub>1</sub>-His (■) and mutant ΔN3 (●). Currents were elicited by the respective ATP-concentration in 1 min intervals. Continuous lines represent least squares fits of the Hill-equation to the data points, yielding EC<sub>50</sub> values of 0.7 ± 0.1 μM (Hill-coefficient of 1.1 ± 0.1) and 2.1 ± 0.2 μM (Hill-coefficient of 1.3 ± 0.1) for the parent His-P2X<sub>1</sub> receptor and mutant ΔN3, respectively (*n* = 6-7, mean ± SEM); **D**, The ratio between currents activated at -40 mV by 0.3 μM and 30 μM ATP was calculated as a measure of the ATP potency at the various glycan minus mutants (*n* = 5-6, mean ± SEM). Note that all mutants lacking N-glycosylation site N3 exhibit a markedly decreased current ratio indicative of a reduced ATP potency. The experiment was performed by Dr. Jürgen Rettinger.

### 3.3. Role of conserved cysteine residues for the function and expression of rat P2X<sub>1</sub> receptor

#### 3.3.1. P2X<sub>1</sub> receptor expression, subunit folding, and intracellular transport: effects of DTT in *Xenopus* oocytes.

The P2X<sub>1</sub> receptors are membrane glycoproteins with large ectodomains that fold inside the ER lumen. The ectodomain contains ten conserved cysteine residues that may contribute to the generation of five intrachain disulfide bonds. From other membrane proteins it is known that the formation of disulfide bonds begins cotranslationally in the ER and is a prerequisite for correct folding of the entire polypeptide (Green & Wanamaker, 1997).

The reducing agent DTT can permeate across cellular membranes and prevent the formation of disulfide bonds of nascent proteins in the ER of living cells (Braakman *et al.*, 1992). Here, this approach was used to study the contribution of the ER redox environment to the posttranslational processing and intracellular transport of oocyte-expressed P2X<sub>1</sub> receptors. Oocytes injected with the cRNA for the His-P2X<sub>1</sub> subunit were pulse-labeled overnight with [<sup>35</sup>S]methionine in the absence or presence of DTT.

As shown in Fig. 3.39, His-P2X<sub>1</sub> subunits were synthesized in the presence of DTT as 57 kD polypeptides (lane 5) like the His-P2X<sub>1</sub> subunits that were synthesized under non-reducing conditions (lane 2). Incubation with PNGase F reduced the molecular masses of the polypeptides to 47 kD (lanes 4 and 7), implying that His-P2X<sub>1</sub> subunits carried four N-glycans irrespective of whether DTT was present during synthesis or not. In contrast, the single Endo H resistant N-glycan was only observed on His-P2X<sub>1</sub> subunits from oocytes that were pulse-labeled in the absence of the reducing agent (Fig. 3.39, lane 6). This indicates that the His-P2X<sub>1</sub> protein does not acquire a complex type carbohydrate in the presence of DTT and, therefore, most likely resides entirely in the ER. If DTT was present only during pulse labeling and was omitted from the chase medium, then His-P2X<sub>1</sub> receptors acquired Endo H resistance (lane 9), implying that the effect exerted by the presence of DTT was reversible. Apparently, His-P2X<sub>1</sub> that was synthesized in the presence of DTT was able to commence proper folding and assembly and eventually to reach the Golgi upon removal of the reducing agent.

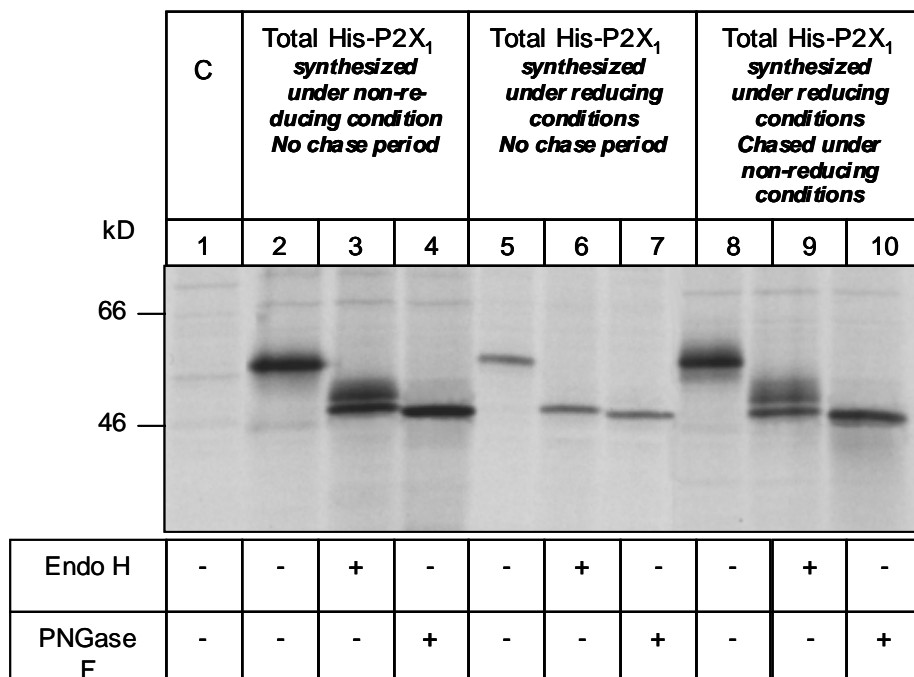


**Fig. 3.39: His-P2X<sub>1</sub> subunits synthesized in the presence of DTT do not acquire complex-type carbohydrates.** Oocytes injected with 25 ng of cRNA for His-P2X<sub>1</sub> were metabolically labeled overnight in the presence or absence of 5 mM DTT as indicated. Cells were either directly extracted with 1% digitonin or first chased for 24 h and then extracted. His-P2X<sub>1</sub> was purified by Ni<sup>2+</sup>-NTA affinity chromatography. Samples were eluted under non-denaturing conditions and treated with PNGase or Endo H and analyzed by SDS-PAGE (8% acrylamide). C indicates samples from non-injected control oocytes.

To determine whether the assembly of His-P2X<sub>1</sub> subunits is affected by DTT treatment, metabolically labeled and natively purified His-P2X<sub>1</sub> protein was subjected to BN-PAGE. His-P2X<sub>1</sub> receptors that were synthesized under reducing or non-reducing conditions migrated like a trimer at 240 kD when resolved by BN-PAGE (Fig 3.40, lanes 2 and 5). Incubation prior to BN-PAGE of the natively eluted His-P2X<sub>1</sub> receptor with DTT in the presence of the blue native sample buffer caused a partial dissociation of the His-P2X<sub>1</sub> receptor into the monomer and dimer of apparent masses of 80 and 170 kD, respectively (Fig 3.40, lanes 7). This observation implies that the formation of His-P2X<sub>1</sub> to a homotrimer is not hindered by the presence of DTT during the synthesis.

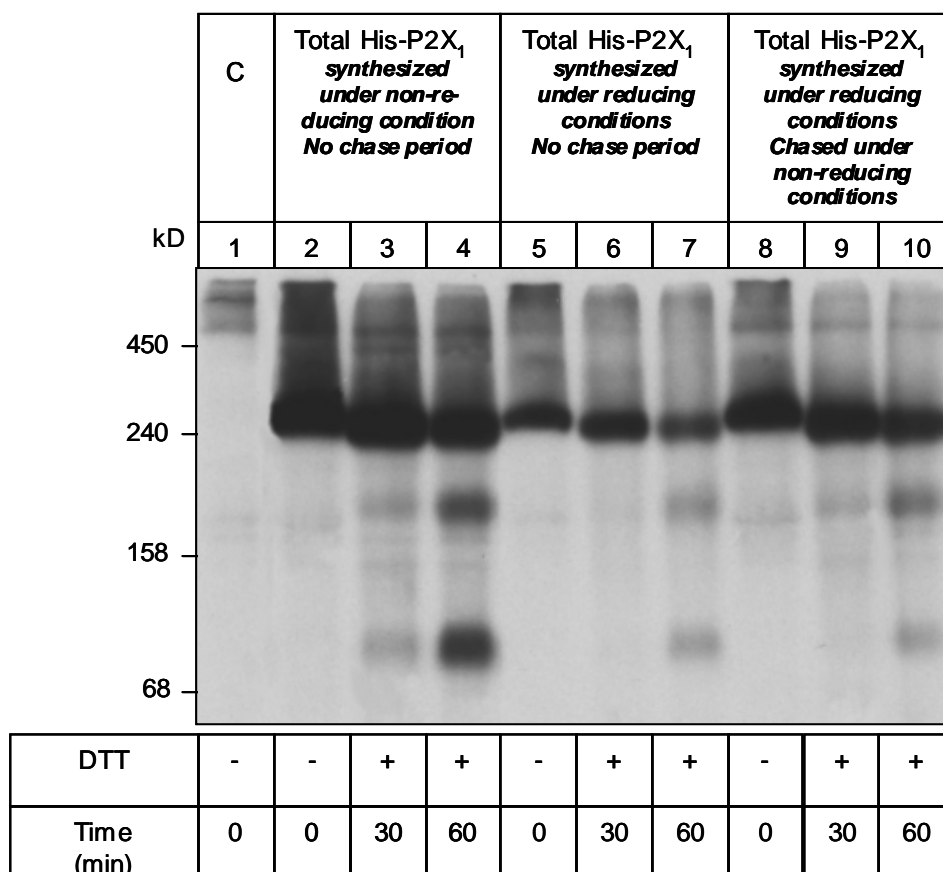


**Fig. 3.40: Effect of DTT on P2X<sub>1</sub> subunit assembly.** Oocytes injected with 25 ng of cRNA for His-P2X<sub>1</sub> were metabolically labeled overnight in the presence or absence of 5 mM DTT. Cells were either directly extracted with 1% digitonin or first chased for 24 h and then extracted. His-P2X<sub>1</sub> protein was purified by Ni<sup>2+</sup>-NTA affinity chromatography. Samples were eluted under non-denaturing conditions and directly analyzed by BN-PAGE (4-13% acrylamide) or incubated at 37°C with 100 mM DTT in the presence of blue native sample buffer for 30 or 60 min prior to BN-PAGE. C indicates samples from non-injected control oocytes.

### 3.3.2. Mutational analysis of the importance of conserved cysteine residues for the generation of P2X<sub>1</sub> receptors in *Xenopus* oocytes

#### 3.3.2.1. Effects of single cysteine substitutions on P2X<sub>1</sub> receptor expression and processing

Rat P2X<sub>1</sub> receptor subunit possesses 11 cysteine residues, from which 10 are located on the extracellular region of the subunit and one (<sup>353</sup>C) is located on the second transmembrane segment. To determine the relative importance of each native cysteine residue in the rat P2X<sub>1</sub> receptor, each of these residues was individually mutated to serine. The cysteine to serine conversion results in a relatively small change in the size of the amino acid side chain, but changes the residue to a more hydrophilic one without the ability to form covalent cross-links.

Oocytes injected with the cRNA for the parent or the mutated His-P2X<sub>1</sub> subunits were pulse-labeled overnight with [<sup>35</sup>S]methionine. After an additional 24 h chase interval, digitonin extracts were prepared. Proteins were isolated by Ni<sup>2+</sup>-NTA agarose affinity chromatography, eluted with non-denaturing elution buffer, then supplemented with SDS sample buffer. Samples were incubated in the presence of Endo H or PNGase F and then analyzed by SDS-PAGE. As shown in Fig 3.31 A, the parent His-P2X<sub>1</sub> subunit and the respective cysteine minus mutants were isolated from the oocytes as 57 kD polypeptides. Apparently, the substitution of an individual cysteine residue by serine did not hinder the synthesis of the respective mutant polypeptide, but influenced the amount of protein synthesized. While serine substitutions at the positions <sup>117</sup>C (ΔC1), <sup>165</sup>C (ΔC6) and <sup>353</sup>C (ΔC11) did not reduce the amount of the protein made, the mutations at the positions <sup>126</sup>C (ΔC2), <sup>132</sup>C (ΔC3), <sup>149</sup>C (ΔC4), <sup>159</sup>C (ΔC5), <sup>217</sup>C (ΔC7), <sup>227</sup>C (ΔC8), <sup>261</sup>C (ΔC9), and <sup>270</sup>C (ΔC10) markedly reduced the amount of the synthesized protein.

Fig. 3.41 B shows that like the parent His-P2X<sub>1</sub> subunit (lane 2), the receptor mutants ΔC1 - ΔC6 and ΔC11 (lanes 3-8, and 13) acquired Endo H-resistant carbohydrates. This finding implies that these mutants like the parent His-P2X<sub>1</sub> receptor can leave the ER and acquire complex-type carbohydrates during transit of the Golgi apparatus. In contrast, Endo H deglycosylation of the cysteine minus mutants ΔC7 - ΔC10 (Fig. 3.41 B, lanes 9-12) released all N-linked glycans, indicating that these mutants do not acquire complex type carbohydrates and most likely reside entirely in the ER.

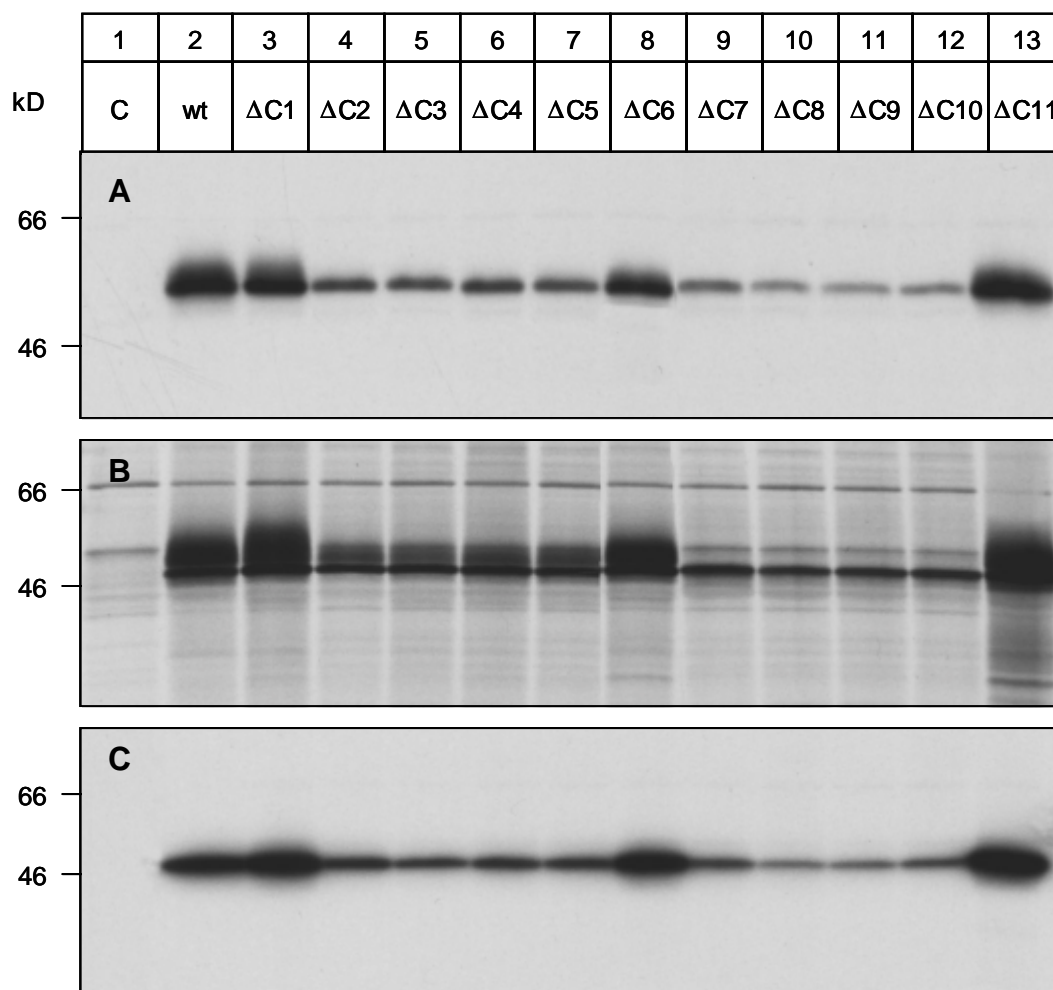


**Fig. 3.41: Carbohydrate status of His-P2X<sub>1</sub> mutants each lacking one out of 11 cysteine residues.** Oocytes injected with 25 ng of the indicated cRNAs were metabolically labeled by overnight incubation with [<sup>35</sup>S]methionine. After an additional 24 h chase interval, digitonin extracts were prepared. Parent His-P2X<sub>1</sub> and the various cysteine minus mutants were isolated by Ni<sup>2+</sup>-NTA chromatography, eluted with non-denaturing elution buffer, and then supplemented with SDS sample buffer. Samples were incubated for 15 min at 37°C in the absence (A) or for 2 h at 37°C in the presence of Endo H (B) or PNGase F (C), and then analyzed by reducing SDS-PAGE (10% acrylamide) followed by autoradiography. C indicates samples from non-injected control oocytes.

Next, the appearance of the various mutants at the cell surface was investigated. To this end, surface protein of intact oocytes injected with the cRNAs for the different cysteine minus mutants was radio-iodinated and subsequently purified by Ni<sup>2+</sup>-NTA chromatography. On oocytes injected with the cRNA for the cysteine minus mutants  $\Delta$ C7 -  $\Delta$ C10, no P2X<sub>1</sub> subunit-specific protein band could be detected by SDS-PAGE. Apparently, these receptor mutants were retained in the ER. This observation is in agreement with the glycan status of the metabolically labeled cysteine minus mutants, showing that the receptor mutants  $\Delta$ C7 -  $\Delta$ C10 do not acquire complex type carbohydrates. In contrast to mutants  $\Delta$ C7 -  $\Delta$ C10, mutants  $\Delta$ C1 -  $\Delta$ C6 could be detected at the cell surface (Fig. 3.42 A and B). Treatment of the cysteine minus mutants  $\Delta$ C1 -  $\Delta$ C6 with Endo H diminished the molecular mass of these glycoproteins by 8 kD, indicating that three minus mutants also acquired three

high mannose type carbohydrates (Fig. 3.42 A, lanes 2, 5, 8, 11 and Fig. 3.42 B, lanes 2, 5) like the parent His-P2X<sub>1</sub>. Endo H was unable to release all N-glycans of these mutant receptors, indicating that the asparagine<sup>300</sup>N of the respective cysteine minus mutants has acquired complex type carbohydrates in the Golgi and thus exhibits Endo H resistance (Fig. 3.42 A, lanes 3, 6, 9, 12 and Fig. 3.42 B, lanes 3, 6).

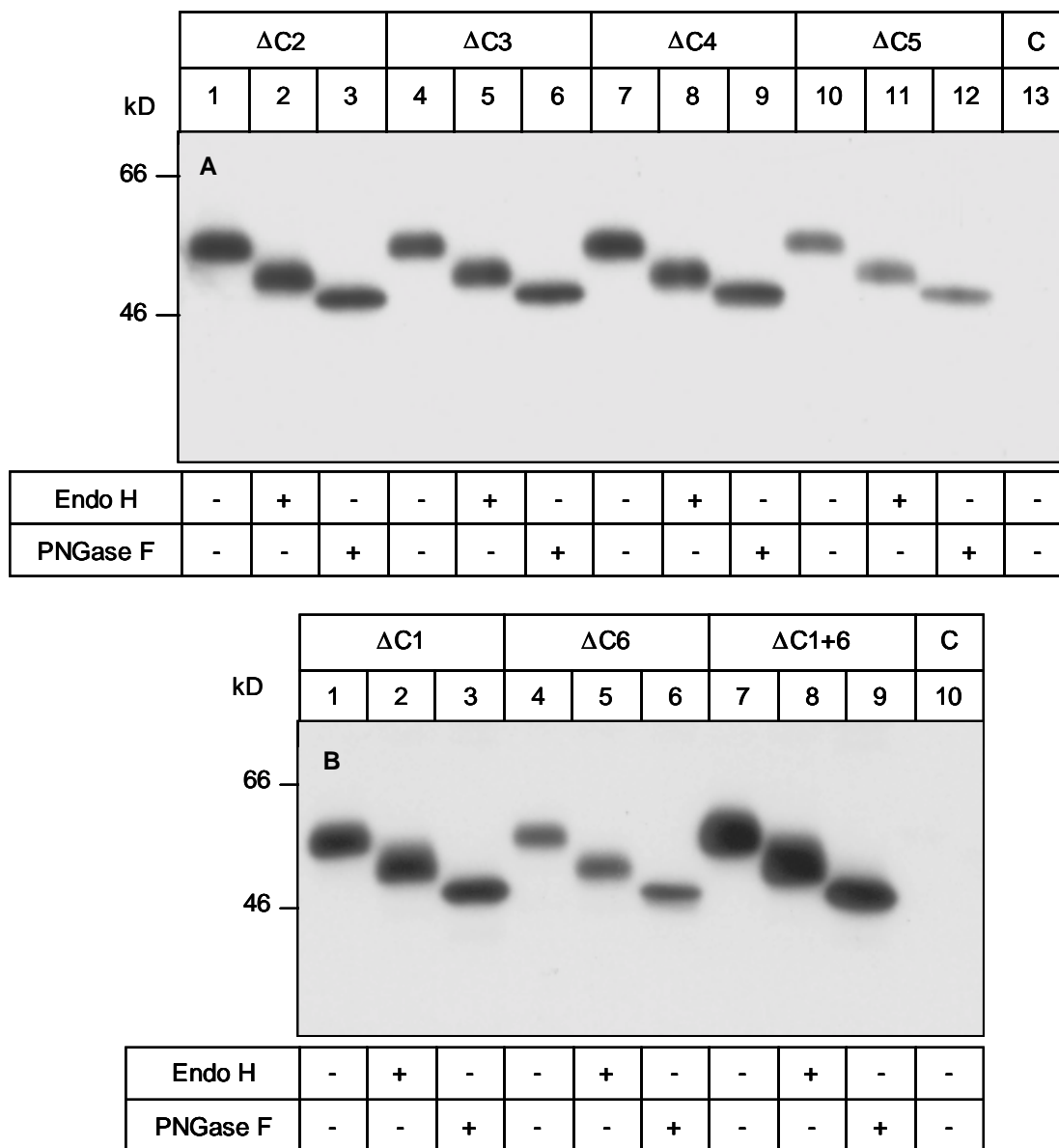


**Fig. 3.42: Glycosylation status of surface iodinated cysteine minus mutants.** Oocytes injected with 25 ng of cRNA for His-P2X<sub>1</sub> or the indicated cysteine minus mutants were left for 3 days at 19°C and then labeled with membrane-impermeant <sup>125</sup>I-sulfo-SHPP. The proteins were purified by Ni<sup>2+</sup>-NTA chromatography from 1% digitonin extracts of oocytes, and eluted with non-denaturing elution buffer. Aliquotes of these samples were supplemented with SDS sample buffer, 20 mM DTT, and treated with Endo H or PNGase F as indicated. After the digestion, proteins were resolved by SDS-PAGE (8% acrylamide) followed by autoradiography. C indicates samples from non-injected control oocytes.

### 3.3.2.2. BN-PAGE analysis of P2X<sub>1</sub> mutants lacking one cysteine residue

To examine the influence of single cysteine residues on P2X<sub>1</sub> receptor assembly, the natively eluted parent P2X<sub>1</sub> receptor and the respective cysteine single mutants were analyzed by BN-PAGE. Like the metabolically labeled parent His-P2X<sub>1</sub> receptor, the cysteine minus mutants  $\Delta C1 - \Delta C6$  and  $\Delta C11$  migrated as one distinct band at 240 kD (Fig. 3.43 A, lanes 2-8, and 13). Thus, elimination of one cysteine residue at a time did not influence the assembly of the respective minus mutants. In contrast to the [<sup>35</sup>S]methionine-labeled  $\Delta C1 - \Delta C6$  and  $\Delta C11$  mutants, the appearance of the mutants  $\Delta C7 - \Delta C10$  differed markedly when these cysteine minus mutants were resolved by BN-PAGE analysis. Besides a smear of aggregated protein, a total of five to six bands were resolved when these mutants were subjected to the BN-PAGE (Fig. 3.43 B, lanes 2-5). The ladder of bands that appeared corresponded in size to multiples of the monomer, which by itself migrates at 80 kD, up to the pentamer and hexamer. Taken together, these results suggest that single exchange of C7, C8, C9, or C10 against S hindered the proper assembly and ER exit of the respective mutant His-P2X<sub>1</sub> receptors. In contrast, the substitution of one of the proximal six cysteine residues of the ectodomain, C1 - C6, or C11 in the second transmembrane segment did not affect assembly and processing of the respective minus mutants.

To display the oligomeric state of the cysteine minus mutants  $\Delta C1 - \Delta C6$  and  $\Delta C11$ , the natively eluted His-P2X<sub>1</sub> mutant receptors were exposed to Coomassie blue and sodium 6-amino-*n*-caproate in the presence or absence of DTT. This treatment caused a partial dissociation of the parent His-P2X<sub>1</sub> receptor and the respective cysteine minus mutants into the monomer and dimer of apparent masses similar to 80 kD and 180 kD, respectively, indicating that the non-denatured 240 kD protein bands observed must be homotrimers (Fig 3.44 A and B).



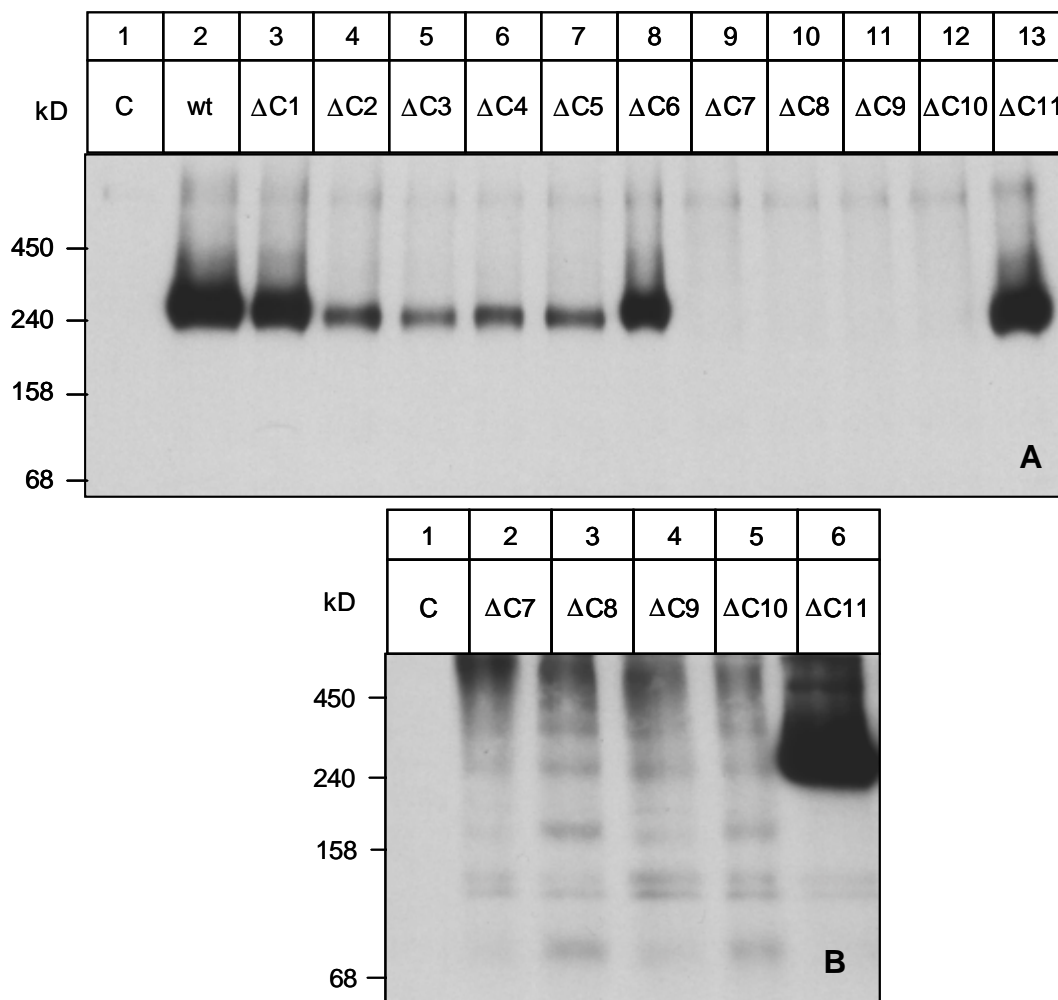


**Fig. 3.43: BN-PAGE analysis of cysteine minus mutants.** Oocytes injected with 25 ng of the indicated cRNAs were metabolically labeled by overnight incubation with [ $^{35}$ S]methionine. After an additional 24 h chase interval, digitonin extracts were prepared. The parent His-P2X<sub>1</sub> receptor and the various cysteine mutants were isolated by Ni<sup>2+</sup>-NTA chromatography, and after native elution resolved by blue native PAGE (4 –10% acrylamide gradient gel) followed by autoradiography. **(B)** Shown are samples from a second independent experiment, in which a BN-polyacrylamide gel (4 –10% acrylamide gradient gel) was autoradiographed for 10 days to make the cysteine minus mutants  $\Delta$ C7 –  $\Delta$ C10 visible. C in lane 1 indicates samples from non-injected control oocytes.

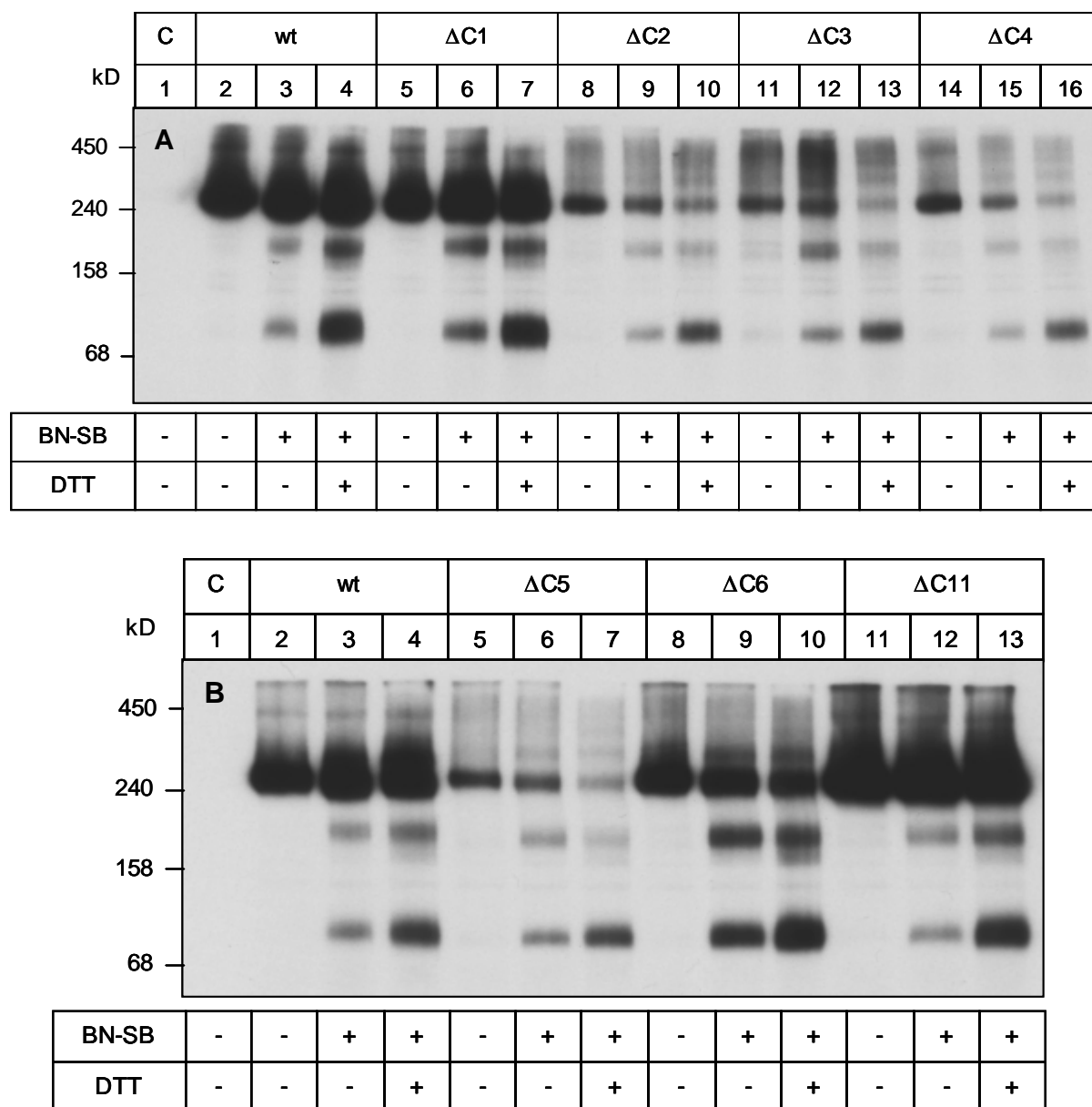


**Fig. 3.44: Oligomeric state of the cysteine minus mutants  $\Delta C1$  -  $\Delta C6$ , and  $\Delta C11$ .** Oocytes injected with 25 ng of the indicated cRNAs were metabolically labeled by overnight incubation with [ $^{35}$ S]methionine. After an additional 24 h chase interval, digitonin extracts were prepared. The parent His-P2X<sub>1</sub> receptor and the cysteine mutants were isolated by Ni<sup>2+</sup>-NTA chromatography and eluted under non-denatured conditions. Proteins were analyzed by blue native PAGE (4 –13% acrylamide gradient gel) either without further treatment or after incubation with blue native sample buffer in the presence or absence of 100 mM DTT at 37°C for 60 min. C in lane 1 indicates samples from non-injected control oocytes.

### 3.3.2.3. Analysis of cell surface expressed P2X<sub>1</sub> receptor mutants lacking two or three cysteine residues

In view of the strong conservation of all cysteine residues, the apparently unimpaired surface-appearance of homotrimeric P2X<sub>1</sub> receptors lacking individual cysteine residues was unexpected. Therefore, additional mutants were generated lacking two or three of the proximal 6 cysteine residues in various combinations to examine whether these mutations affected cell surface appearance and function. Remarkably, also these mutants appeared at the cell surface, as revealed by surface radioiodination combined with Ni<sup>2+</sup>-NTA agarose chromatography and SDS-PAGE. Mutants lacking two or three cysteine residues migrated with apparent masses of 57 kD. Endo H treatment reduced the molecular mass of the cysteine double mutants  $\Delta$ C1+6,  $\Delta$ C2+5,  $\Delta$ C3+5, and  $\Delta$ C2+4 by 8 kD (Fig. 3.45. A-C), consistent with the removal of three high mannose type carbohydrate side chains. An 8 kD shift was also observed for the parent His-P2X<sub>1</sub> subunit and all the cysteine single mutants (Fig. 3.42 A and B). A 3 kD larger shift to 47 kD was produced by PNGase F treatment, indicating that these cysteine minus mutants acquire a single complex-type carbohydrate side chain during transit of the Golgi apparatus.

The molecular masses of the <sup>125</sup>I-labeled cysteine double mutants  $\Delta$ C2+3,  $\Delta$ C3+4,  $\Delta$ C4+5,  $\Delta$ C5+6 and all the cysteine triple mutants ( $\Delta$ C1+2+6,  $\Delta$ C2+3+4 and  $\Delta$ C2+4+5) were reduced by 6 kD only upon Endo H treatment, whereas PNGase F treatment induced a 10 kD shift to 47 kD. This observation suggests that these cysteine minus mutants carry four N-linked oligosaccharide side chains like the parent His-P2X<sub>1</sub>, yet that the mutants acquired two instead of one complex type carbohydrates in the Golgi. This result can best be reconciled with a change of structural conformation induced by the removal of the respective cysteine residues, leading to access of one additional N-glycan for the Golgi enzymes responsible for attachment of complex type carbohydrates (Fig. 3.45 A-C).

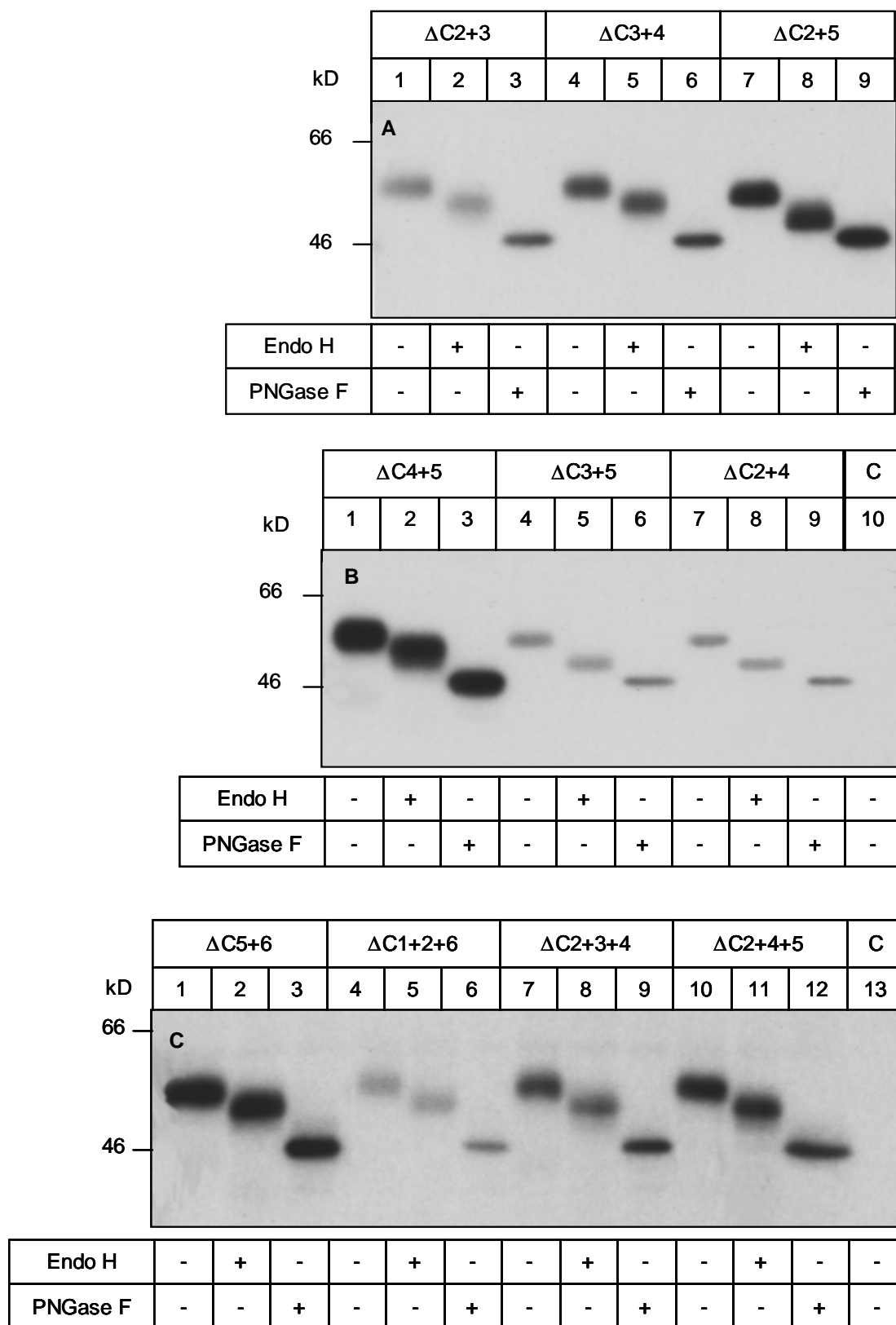


**Fig. 3.45: Glycosylation status of surface iodinated cysteine double and triple mutants.** Oocytes injected with 25 ng of cRNA for His-P2X<sub>1</sub> or the indicated cysteine minus mutants were left for 3 days at 19°C and then labeled with membrane-impermeant <sup>125</sup>I-sulfo-SHPP. The proteins were purified by Ni<sup>2+</sup>-NTA chromatography from 1% digitonin extracts of oocytes, and eluted with non-denaturing elution buffer. Aliquots of these samples were supplemented with SDS sample buffer, 20 mM DTT, and treated with Endo H or PNGase F as indicated. After treatment, proteins were resolved by SDS-PAGE (8% acrylamide) followed by autoradiography. C in lane 13 indicates samples from non-injected control oocytes.

### 3.3.2.4. BN-PAGE analysis of P2X<sub>1</sub> mutants lacking two or three cysteine residues

Upon surface labeling, all cysteine minus mutants lacking two cysteine residues appeared as one single band at about 240 kD when analyzed by BN-PAGE (Fig.3.46, lanes 1-9). The mutants were present at the plasma membrane and exhibited a mobility that corresponded to the migration observed for the parent His-P2X<sub>1</sub> receptor (lane 10). Apparently, elimination of two cysteine residues from the first cysteine rich domain of the extracellular region of the rat P2X<sub>1</sub> receptor does not influence the assembly of the respective minus mutants.

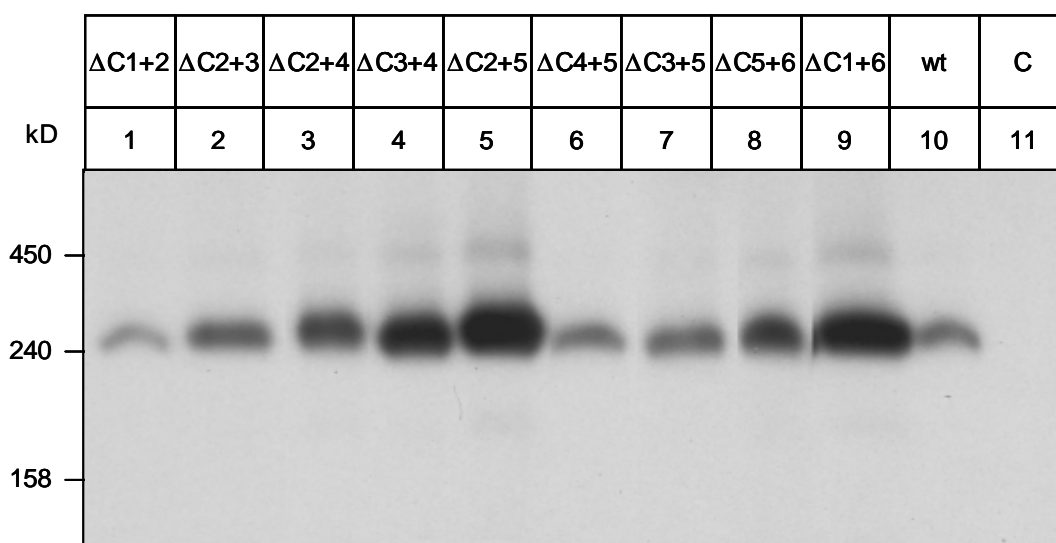


**Fig. 3.46: BN-PAGE analysis of cysteine mutants lacking two cysteine residues.** Oocytes injected with 25 ng of the indicated cRNAs were left for 3 days at 19°C and then labeled with <sup>125</sup>I-sulfo-SHPP. Parent His-P2X<sub>1</sub> and the various cysteine mutants were isolated by Ni<sup>2+</sup>-NTA chromatography, and after native elution resolved by blue native PAGE (4–10% acrylamide gradient gel) followed by autoradiography. C in lane 11 indicates samples from non-injected control oocytes. Shown are samples from independent experiments, in which the digitally scanned autoradiograms of respective protein bands were joined together using the software Paint Shop Pro 5. Samples from the lanes 1, 2, 6, and 7, and lanes 8 through 11, and lanes 3 and 4 were from identical experiments, respectively.

To determine the number of subunits incorporated into the defined 240 kD proteins detected by BN-PAGE, the various surface-expressed mutants lacking two cysteine residues were treated with DTT to induce a partial dissociation of the protein complex. Fig. 3.47 A shows that this treatment of the cysteine minus mutants  $\Delta C2+4$  (lanes 3 and 4),  $\Delta C3+4$  (lanes 6 and 7),  $\Delta C4+5$  (lanes 9 and 10), and  $\Delta C2+3$  (lanes 12 and 13) led in each case to the appearance of two additional bands, corresponding to the monomer at ~80 kD, and the intermediate dimer at ~170 kD

besides the non-dissociated 240 kD complex. These results indicated that these cysteines minus mutants are inserted into the plasma membrane as trimeric complexes like the parent His-P2X<sub>1</sub> receptor. Identical results were obtained for the cysteine minus mutants lacking three cysteine residues ( $\Delta$ C1+2+6,  $\Delta$ C2+3+4, and  $\Delta$ C2+4+5). When a partial dissociation was induced by DTT, the non-dissociated 240 kD complexes were also dissociated into the monomer and dimer of apparent masses similar to 80 kD and 180 kD, indicating that the non-denatured 240 kD protein bands of the mutants  $\Delta$ C1+2+6 (Fig. 3.47 B, lanes 3 and 4),  $\Delta$ C2+3+4 (lanes 6 and 7) and  $\Delta$ C2+4+5 (lanes 9 and 10) must be homotrimers.

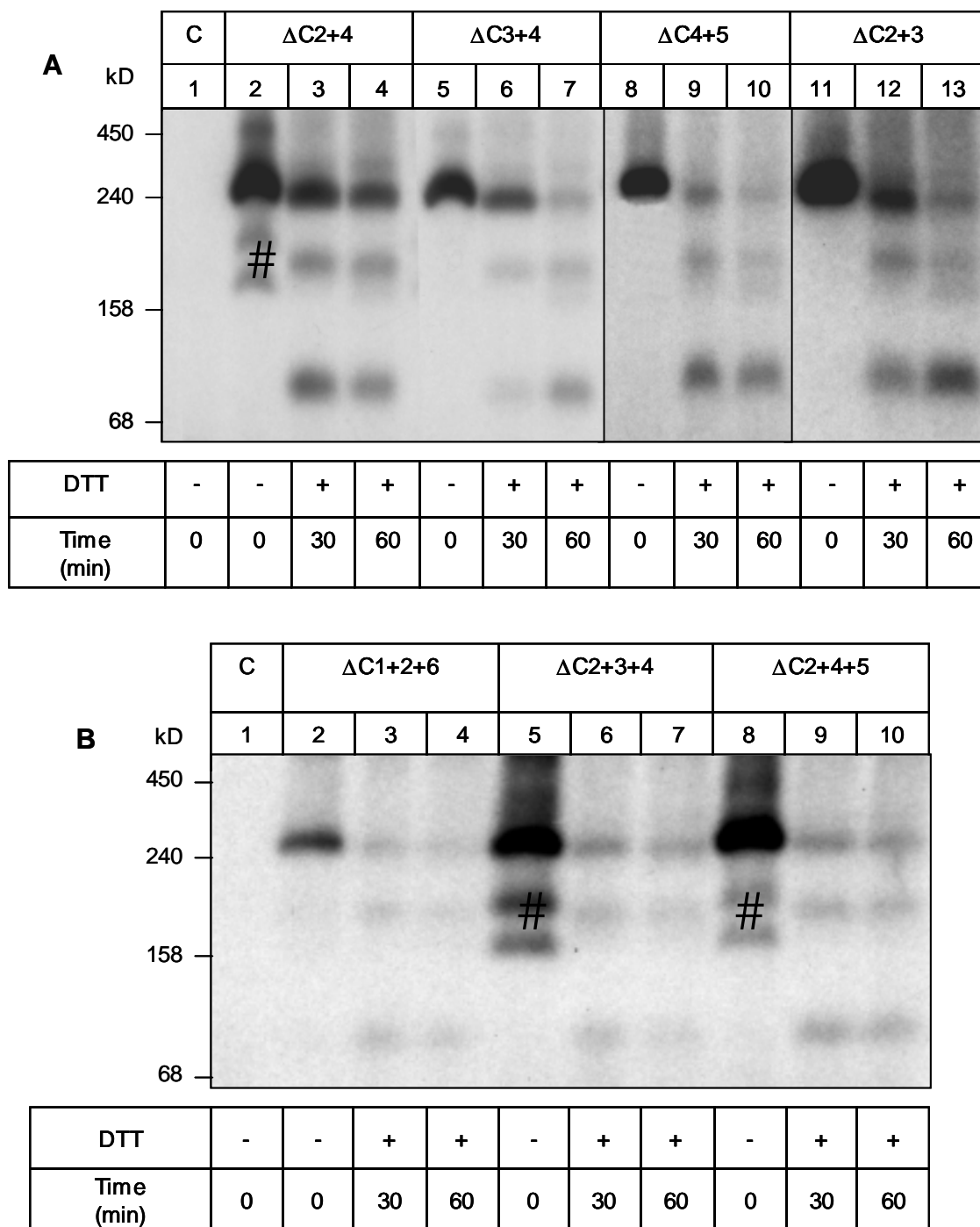


**Fig. 3.47: Oligomeric state of the cysteine minus mutants lacking two or three cysteine residues.** Oocytes injected with 25 ng of cRNA for His-P2X<sub>1</sub> or the indicated cysteine minus mutants were left for 3 days at 19°C and then labeled with <sup>125</sup>I-sulfo-SHPP. The parent His-P2X<sub>1</sub> receptor and the cysteine mutants were isolated by Ni<sup>2+</sup>-NTA chromatography and eluted under non-denatured conditions. Proteins were analyzed by blue native PAGE (4 –13% acrylamide gradient gel) either without further treatment or after incubation with 100 mM DTT in the presence of blue native sample buffer at 37°C for 30 or 60 min. #, contaminating protein not observed in other experiments (cf. A, lane 2; B, lanes 5 and 8). C in lane 1 indicates samples from non-injected control oocytes. Shown are samples from independent experiments, in which the digitally scanned autoradiograms of respective protein bands were joined together using the software Paint Shop Pro 5.

### 3.3.2.4. Functional analysis of P2X<sub>1</sub> receptor mutants lacking one, two, or three cysteine residues

The conservation of the extracellular cysteines among all the members of P2X receptor family suggests the potential importance of the corresponding cysteine residues in the function of P2X subunits. To verify this hypothesis, the cysteine minus mutants were expressed in *Xenopus* oocytes. Subsequently, current responses to 30 mM ATP at -40 mV were recorded to examine whether the elimination of particular cysteine residues affect the expression level of functional P2X<sub>1</sub> receptors. Like the parent P2X<sub>1</sub> receptor, the cysteine minus mutants  $\Delta$ C1- $\Delta$ C6 exhibited large ATP-gated currents, indicating that no particular cysteine residue from this domain is essential for receptor function (Fig. 3.46). There are, however, marked positional effects of the cysteine substitution from this region. While the cysteines at C1, C2, and C6 were without significant effect on the expression level of functional receptors, elimination of the cysteines at C3, C4, and C5 resulted in a 30-60% decrease of the current response (Fig. 3.48). In contrast, currents recorded were markedly decreased to near undetectable levels for oocytes expressing the cysteine minus mutants  $\Delta$ C7- $\Delta$ C10 (Fig. 3.48). The possible mechanisms which could explain the decreased cell surface expression of the these cysteine mutants are a complete blockade of routing to the cell surface by misfolding during translation, as also revealed by the SDS-PAGE analysis after Endo H treatment of the minus mutants, implying a crucial role of this cysteine (C6-C10) containing domain for protein assembly and stability.



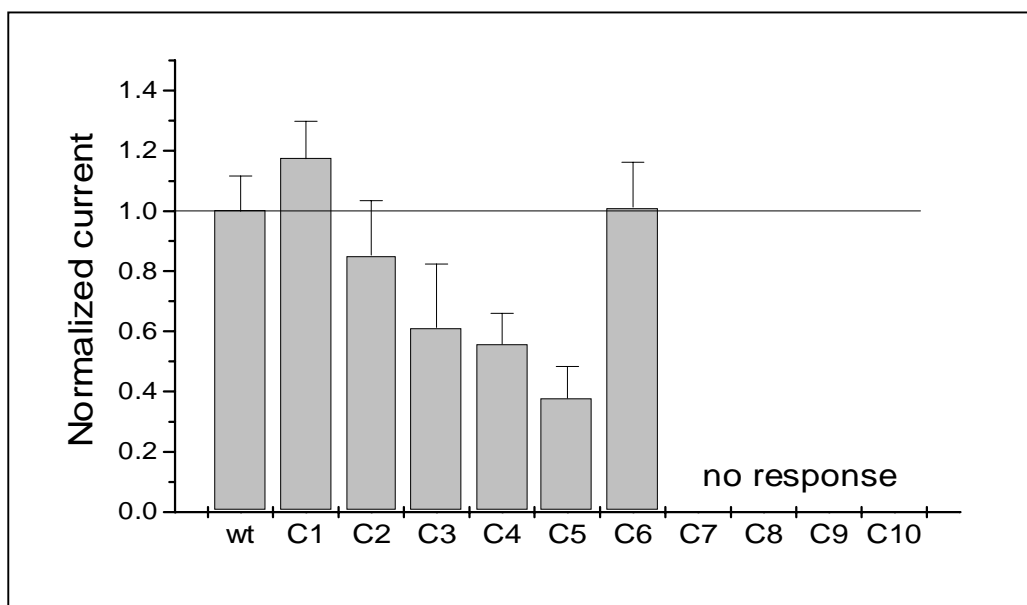


**Fig. 3.46: Comparison of maximum inward current responses of parent His-P2X<sub>1</sub> and cysteine minus mutants.** Oocytes were injected with 23 ng of the indicated cRNAs. After 3 days at 19°C, currents were activated at a holding potential of -40 mV by 30 mM ATP, which elicits maximum responses at parent His-P2X<sub>1</sub> and each mutants. Currents were normalized to the response of the parent His-P2X<sub>1</sub> receptor. Data are given as means  $\pm$  S.E. from 20–48 oocytes per column of two to six experiments with 6–10 oocytes per experimental condition. The experiment was performed by Dr. Jürgen Rettinger.

#### 3.3.2.4.1. Effects of cysteine substitution on ATP concentration response of P2X<sub>1</sub> Receptors

ATP evoked concentration-dependent P2X<sub>1</sub> receptor-mediated currents from parent receptors with an EC<sub>50</sub> value of 0.8  $\mu$ M (Rettinger *et al.*, 2000) (Fig. 3.49). The ability of ATP to evoke functional responses, its potency, is the result of two steps: 1) the binding of ATP to the receptor (affinity) and 2) the ability of bound ATP to open the ion channel (efficacy) (Ennion *et al.*, 2000). Therefore, in the present study, it is referred to the potency of ATP and can only make inferences about the effects of the mutations on the affinity of ATP for the receptor. Point mutants at conserved cysteine C1, C2, C4, C6 had only a small (2-3-fold) decrease in ATP potency. However, when the cysteine residue C3 was removed, the potency was decreased by 5-fold, and even a 10-fold decrease was observed for the Mutations at C5.

Additionally, various double and triple mutants originated from cysteines C1 – C6 were measured after expression in oocytes to verify their effect on the EC<sub>50</sub> for ATP (Fig 3.49). While no EC<sub>50</sub> value could be assessed for the cysteine mutants  $\Delta$ C12,  $\Delta$ C13,  $\Delta$ C14,  $\Delta$ C15,  $\Delta$ C36,  $\Delta$ C46,  $\Delta$ C126, due to a substantial decrease in cell surface expression, double and triple mutations of the most other cysteine residues

led to an 15–50-fold decrease in ATP potency at the P2X<sub>1</sub> receptor. For most double cysteine mutants, so far measurable, the ATP potency was markedly decreased in comparison to their respective cysteine single mutants. This observation was not made for three cysteine double mutants only. The minus mutants  $\Delta$ C16,  $\Delta$ C24,  $\Delta$ C35 showed a small (2-3-fold) decrease in ATP potency like that observed for the single minus mutants. These data indicate that the C1 and C6 in on the one hand and the C2 and C4 in on the other hand as well as C3 and C5 participate in the formation of three different disulfide bridge of this domain of P2X<sub>1</sub> subunit.

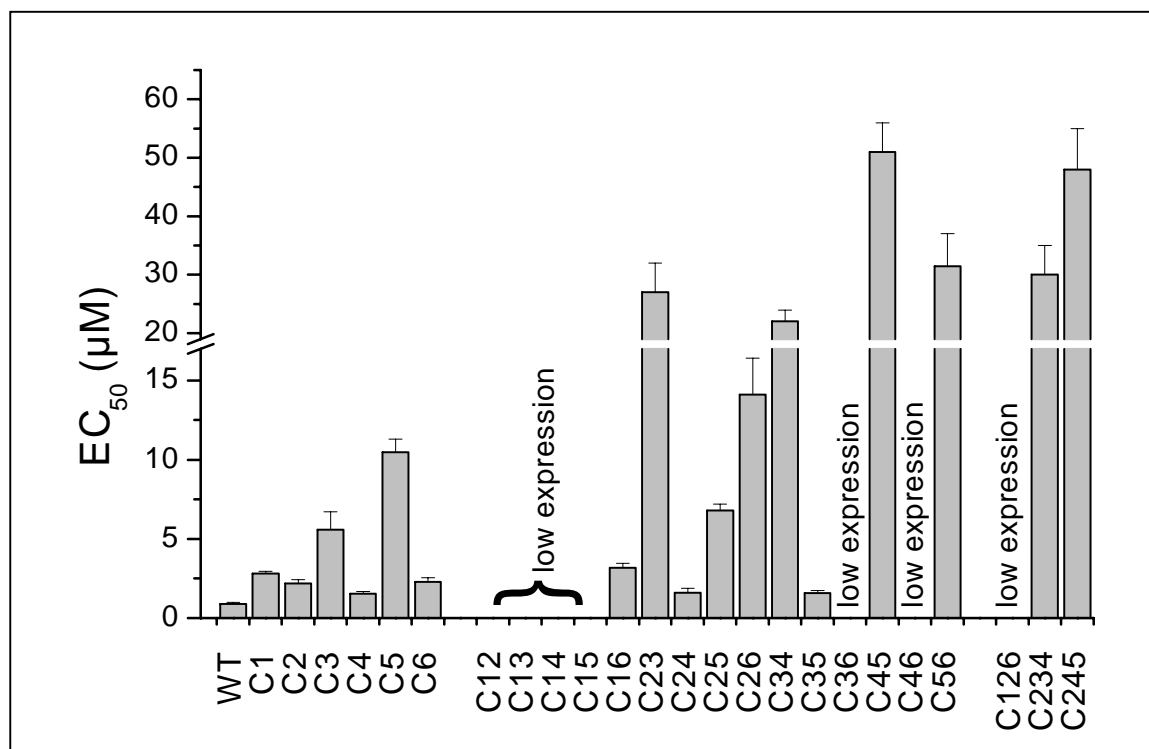


**Fig. 3.49: Comparison of ATP potency between parent His-P2X<sub>1</sub> and cysteine minus mutants.** ATP dose-response curves were elicited at holding potential -40 mV from oocytes injected 3 days earlier with 23 ng of cRNA for parent His-P2X<sub>1</sub> or the indicated cysteine minus mutants. Currents were elicited by the respective ATP concentration in 1-min intervals. Continuous lines represent least squares fits of the Hill equation to the data points, yielding EC<sub>50</sub> values for parent His-P2X<sub>1</sub> and cysteine minus mutants. The experiment was performed by Dr. Jürgen Rettinger.

## 4. Discussion

### 4.1. Investigation of P2X receptors after expression in *Xenopus* oocytes

#### 4.1.1. Homomultimeric assembly of P2X receptors after expression in *Xenopus* oocytes

The most common methods used to assess the expression of fully assembled ion channels are either the electrophysiological assay or flux measurements (for reviews see [Sheng & Deutsch, 1998](#)). In the present study, P2X receptor assembly was assayed by BN-PAGE analysis after metabolic labeling of *Xenopus* oocytes injected with the respective cRNA for the P2X constructs. By first pulse-labeling the subunits, and then chasing the labeled subunits, folding and oligomerization of P2X subunits was assayed by subjecting the purified proteins to blue native PAGE ([Schägger & von Jagow, 1991](#)). Alternatively, *Xenopus* oocytes injected with the respective cRNA for the P2X subunits were surface-labeled using  $^{125}\text{I}$ -sulfo-SHPP prior to the BN-PAGE. The radio-iodination method has the advantage that only completely assembled proteins are labeled that are at the cell surface, i.e. the same proteins that are amenable to electrophysiological analysis. These investigations provide strong evidence for a trimeric architecture of the homomultimeric His-P2X<sub>2</sub>, and His-P2X<sub>5</sub> receptors. The results obtained by BN-PAGE analysis could be corroborated by chemical cross-linking using glutardialdehyde. The observations made are in agreement with the results obtained by [Nicke et al. \(1998\)](#), who were the first to describe a trimeric architecture for His-P2X<sub>1</sub> and His-P2X<sub>3</sub> receptors. By investigating single channel properties of the P2X<sub>2</sub> receptor, [Ding & Sachs \(1999\)](#) found that the channel proceeds through three ATP binding steps before opening and that the three ATP binding sites are not independent, but positively cooperative, supporting the view for a trimeric structure for this receptor. In contrast, [Kim and coworkers \(1997\)](#) suggested a tetrameric structure for the extracellular domain of P2X<sub>2</sub>, which was purified from bacteria. However, a proper folding of the extracellular domain of the P2X<sub>2</sub> subunit appears to be rather unlikely, since [Torres \(Torres et al., 1999\)](#) showed that the transmembrane domains in addition to the extracellular domain are critical for productive P2X subunit assembly.

The P2X receptors that were investigated by BN-PAGE migrated quantitatively as trimers when extracted with digitonin and purified by Ni<sup>2+</sup>-NTA agarose chromatography. Nevertheless, beside trimers also protein bands of higher molecular masses were observed that corresponded in size to hexamers (P2X<sub>1</sub> and P2X<sub>2</sub>) or even nanomers (P2X<sub>2</sub>), when resolved by BN-PAGE. These observations may be interpreted to show that P2X receptors are complexes of six identical subunits. Recently, Surprenant and coworkers identified by using BN-PAGE and Western blotting that native P2X<sub>7</sub> receptors from peritoneal macrophage and bone marrow cells exist as hexa- or nanomeric complexes (Kim *et al.*, 2001). Under physiological conditions, the assembly of P2X receptors into larger complexes might be a possible mechanism for the formation of large pores observed upon repeated stimulation of P2X<sub>7</sub> or P2X<sub>2</sub> with ATP (for P2X<sub>7</sub> see Klapperstück *et al.*, 2000; for P2X<sub>2</sub> see Virginio *et al.*, 1999), as initially suggested by Nicke *et al.* (1998). Dissociation of hexameric complexes into trimeric complexes could be a possible mechanism for the known long lasting desensitization of some P2X subtypes. In addition, it may be considered that digitonin which was used to solubilize membranes is unable to preserve weak protein-protein interactions, such that an actually hexameric P2X<sub>2</sub> receptor dissociates into two trimeric complexes, which by themselves are rather stable. However, from the observation that hexamers became more abundant when P2X receptors were extracted with octylglucoside or dodecylmaltoside, it was concluded that the hexamers represent aggregates of two trimers rather than authentic hexamers of P2X trimers (Nicke *et al.*, 1998).

#### 4.1.2. Role of carboxyl-terminal domain for the assembly of the P2X<sub>2</sub> receptor

In an additional study, the role of cytoplasmic domains of P2X<sub>2</sub> in subunit assembly was investigated. Since a previous study had already ruled out the amino-terminal domain as being critical for assembly (Torres *et al.*, 1999), this investigation was restricted to the carboxyl terminus. To biochemically investigate the role of this region in P2X<sub>2</sub> receptor assembly, a deletion mutant of the His-P2X<sub>2</sub> receptor subunit was constructed, designated His-P2X<sub>2</sub><sup>1-409</sup> lacking the uttermost 63 C-terminal amino acids by introducing a stop codon behind <sup>409</sup>G. The investigation of the metabolically labeled deletion mutant after expression in oocytes revealed that, like full length His-P2X<sub>2</sub> subunit, the C-terminally truncated mutant failed to fully

assemble and that part of this protein was located intracellularly as aggregates. However, surface radio-iodination of oocytes expressing this His-P2X<sub>2</sub> deletion mutant revealed that the deletion mutant, like the parent P2X<sub>2</sub> receptor, was detectable on the surface of *Xenopus* oocytes. His-P2X<sub>2</sub><sup>1-409</sup> migrated as a distinct protein band like the parent P2X<sub>2</sub> receptor when resolved by BN-PAGE, but with a lower apparent molecular mass of about 270 kD (Fig 3.7). This protein band corresponded in size approximately to the size of the protein band detected for the His-P2X<sub>1</sub> complex on the BN-PAGE. Since both proteins consist of approximately the same number of amino acids, this observation indirectly suggests that the P2X<sub>2</sub><sup>1-409</sup> mutant receptor exists also as a trimer. The fact that this carboxyl-terminal mutant was detected on the cell surface indicate that it retained the ability to form homomultimers. This result therefore provides direct evidence that the intracellular carboxyl-terminal tail of P2X<sub>2</sub> is not absolutely required for subunit assembly. The P2X<sub>2</sub> deletion mutant was not studied by electrophysiological techniques, yet it was reported by other laboratories that removal of the entire intracellular carboxyl-terminal domain did not result in loss of channel function (Torres *et al.*, 1999). The P2X<sub>2</sub> C terminal tail consists of a proline-rich site with similarity to a consensus SH3 binding domain. This may provide a functional role for the P2X<sub>2</sub> such as directing subcellular localization, as has been shown for a similar region of the epithelial sodium channel (Rotin *et al.*, 1994). Association of P2X receptors with cellular proteins has been suggested in a study that examined an effect of the state of the actin cytoskeleton on P2X<sub>1</sub> receptor function (Parker, 1998). Phosphorylation of the P2X<sub>2</sub> receptor C terminal tail has also been implicated in the control of its function (Chow & Wang, 1998).

#### 4.1.3. Heteropolymerization of P2X<sub>1</sub> and P2X<sub>2</sub> subunits in *Xenopus* oocytes

A novel and interesting finding of this study is that the P2X<sub>1</sub> and P2X<sub>2</sub> subunits can exist as heteromultimeric protein complexes in the plasma membrane of *Xenopus* oocytes. In all of the surface-labeling experiments employing <sup>125</sup>I-sulfo-SHPP, hetero-oligomeric P2X<sub>1</sub> and P2X<sub>2</sub> receptors were detected, directly demonstrating a physical interaction between P2X<sub>1</sub> and P2X<sub>2</sub> subunits. Purification of surface-expressed His-P2X<sub>2</sub> on nickel-binding agarose beads under non-denaturing conditions allowed the co-purification of co-expressed non-tagged P2X<sub>1</sub> subunits.

Likewise, His-P2X<sub>1</sub> showed detergent-stable association with P2X<sub>2</sub> subunits. These protein-protein interactions were sufficiently strong, and were detected only when cells were surface labeled. When lysates from radio-iodinated cells expressing either subunit were mixed, no interaction was detected, suggesting that the interaction on the cell surface was the result of specific co- or posttranslational processing mechanisms and not the result of random interactions within the plasma membrane. Surprisingly, when co-assembly was assayed in metabolically labeled oocytes, no interaction was detected. One possible reason for this finding can be that the interaction of the two subunit isoforms is stable only when the subunits are in the plasma membrane of the cells and thus only detectable when the receptors have reached the surface of the cell.

Incubation with the bifunctional reagent glutardialdehyde led to the cross-linking of P2X<sub>2</sub> and P2X<sub>1</sub> subunits to dimers and trimers. Interestingly, the cross-linked heteromultimeric complexes migrated in between the dimeric and trimeric protein bands observed for the respective homomultimeric complexes, as expected for chemically cross-linked P2X<sub>1</sub> and P2X<sub>2</sub> subunits. Analysis of P2X<sub>2</sub>/P2X<sub>1</sub> receptor complexes by blue native PAGE yielded results that are consistent with the cross-linking experiments. BN-PAGE analysis of the P2X<sub>2</sub>/P2X<sub>1</sub> complex isolated under non-denaturing conditions from surface-labeled oocytes yielded one distinct band corresponding to a trimeric complex, as also observed for homomultimeric P2X<sub>2</sub> and P2X<sub>1</sub> receptors. The band for the heteromultimeric complex migrated in between the trimeric protein bands obtained for homomultimeric His-P2X<sub>1</sub> or His-P2X<sub>2</sub> receptors, as expected for a heterotrimer consisting of 56 kD P2X<sub>1</sub> subunits and the 66 kD larger P2X<sub>2</sub> subunits. Treatment with urea prior to BN-PAGE induced the partial dissociation of the complex, yielding bands corresponding to dimers and monomers of P2X<sub>1</sub> and P2X<sub>2</sub> subunits. Physical interactions of the subunits were further investigated by SDS-PAGE analysis of the partially dissociated His-P2X<sub>2</sub>/P2X<sub>1</sub> complex in the second dimension, leading to a complete dissociation of the protein complexes observed in the BN-PAGE. The partial dissociation of heteromultimeric complex induced by urea treatment and the complete dissociation observed by denaturing SDS in the second dimension indicated that the association of both subunits is in a non-covalent manner as also observed for homomultimeric His-P2X<sub>1</sub> and His-P2X<sub>2</sub> receptors.

Although the investigations showed the interaction of both subunits, the analysis failed to reveal the ratio of the subunits in the assembly of the observed

phenotype. By mixing different concentrations of P2X<sub>1</sub> and P2X<sub>2</sub> cRNAs prior to injection, it was intended to vary the subunit stoichiometry of the two subunits that form the heteromultimeric complex. Unfortunately, this investigation failed to give an appropriate result. Even when the cRNA coding for His-P2X<sub>2</sub> was injected with a concentration hundred times less than the concentration for cRNA coding for His-P2X<sub>1</sub>, a significant higher amount of His-P2X<sub>2</sub> protein than of His-P2X<sub>1</sub> protein was detected on the surface of radio-iodinated oocytes when analyzed by BN-PAGE.

The results suggested that P2X<sub>1</sub> and P2X<sub>2</sub> receptor subunits could form hetero-oligomeric assemblies that exist as trimeric complexes, properties that might have important influences on the characteristics of ATP signaling. Thus, extension of the biochemical experiments to functional studies is needed in order to determine the physiological significance of P2X<sub>1</sub>/P2X<sub>2</sub> subunit co-assembly. *In situ* hybridization studies suggested that different P2X<sub>1</sub> and P2X<sub>2</sub> receptor subunits are co-expressed in the same tissues and may be co-localized to the same cells (Lewis *et al.*, 1995, Nori *et al.*, 1998). In a paper by Lewis *et al.* (1995), it was reported that co-transfection of HEK 293 cells with of rat P2X<sub>1</sub> and P2X<sub>2</sub> cDNA did not lead to the formation of receptors with novel phenotypes, suggesting that the subunits did not co-assemble. Although in the present investigation no evidence for distinct function can be provided, the results indicate co-assembly of the subunit pair P2X<sub>1</sub> and P2X<sub>2</sub>. The lack of a novel phenotype does not necessarily mean that two subunits do not interact to form a hetero-oligomeric channel complex. When two receptor subunits participate to form a complex, one subunit type can dominate the phenotype of the resulting channel, and thus only a single phenotype is observed. This phenomenon is observed in the ionotropic glutamate receptor family, where the presence of the GluR- $\beta$  subunit dominates hetero-oligomeric receptor assemblies with regard to both rectification and calcium permeability properties (Seeburg, 1993). Even if there is no significant effect on the biophysical phenotype of a receptor, heteromultimeric assembly could still have important impact on receptor function; e.g., by altering the responsiveness of a complex to intracellular regulation.

The first study examining P2X co-assembly was for P2X<sub>2</sub> and P2X<sub>3</sub> subunits, which were shown to form a hetero-oligomeric channel with a novel phenotype when co-expressed in HEK 293 cells (Lewis *et al.*, 1995). The phenotype for the heteromultimeric receptor correlated well with the receptors described in some sensory neurons, where the two proteins are co-expressed, suggesting that this subunit interaction occurred in the native cells as well. Additional evidence for

hetero-oligomeric assembly of P2X subunits was shown by [Le et al. \(1998\)](#), providing functional evidence for a channel formed between P2X<sub>4</sub> and P2X<sub>6</sub> subunits, and furthermore, it was reported that the co-expression of P2X<sub>1</sub> and P2X<sub>5</sub> subunits also resulted in a channel with a novel phenotype ([Torres et al., 1998](#)). Hetero-polymerization of channel subunits has been suggested as a means of generating functional and molecular diversity ([Green & Millar, 1995](#)). Indeed, the formation of heteromultimeric channels has been demonstrated for many members of the transmitter-gated ion channel family such as nicotinic receptors ([Ragozzino et al., 1997](#); [Yu & Role, 1998](#)) and ionotropic glutamate receptors ([Boulter et al., 1990](#)).

#### 4.1.4. Investigation of P2X<sub>6</sub> after expression in *Xenopus* oocytes

In the present study, the homomultimeric (P2X<sub>1</sub>, P2X<sub>2</sub>, P2X<sub>5</sub>) and heteromultimeric assembly (P2X<sub>1</sub> with P2X<sub>2</sub>) of various P2X receptor subunits after expression in *Xenopus* oocytes was investigated. A lack of functional expression was observed for the P2X<sub>6</sub> receptors that were synthesized in oocytes. This result can be explained by the inability of the P2X<sub>6</sub> subunits to form a homomultimeric receptor complex. As demonstrated by BN-PAGE analysis of His-P2X<sub>6</sub> after metabolic labeling with [<sup>35</sup>S]methionine, the His-P2X<sub>6</sub> protein migrated as an amorphous aggregate rather than a protein complex of well-defined stoichiometry and failed to exit the ER. The results reported in the present work are in agreement with findings from two other laboratories that have examined expression of the P2X<sub>6</sub> subunit using *Xenopus* oocytes ([Le et al., 1998](#); [Soto et al., 1996](#)). These findings are in contrast to the report describing that the homomultimeric P2X<sub>6</sub> receptor desensitizes only slowly and does not respond to  $\alpha\beta$ -met-ATP when heterologously expressed in HEK 293 cells ([Collo et al., 1996](#)). The observed lack of assembly and function suggests that differences in the source of cells can influence some cellular features that are crucial for the homomultimeric assembly of these subunits. Such factors may play an important role for the regulation of functional P2X receptor formation in different cell types and/or tissues.

For the P2X subunits abundant in the CNS (namely P2X<sub>2</sub>, P2X<sub>4</sub>, and P2X<sub>6</sub>), epitope-tagged P2X<sub>2</sub> and P2X<sub>6</sub> subunits or P2X<sub>4</sub> and P2X<sub>6</sub> subunits have been shown to form heteromultimeric receptors ([Collo et al., 1996](#)). In addition, the functional properties of the P2X<sub>4/6</sub> heteromers ([Le et al., 1998](#)) and P2X<sub>2/6</sub>



heteromers (King *et al.*, 2000) have been examined, and their phenotype has been characterized. The finding that P2X<sub>6</sub> subunits can co-assemble into heteromultimeric complexes with other P2X subunit isoforms but not with itself, suggests that P2X<sub>6</sub> subunits play a regulatory role within heteromultimeric assembly, similar to the role played by the  $\beta$  and  $\gamma$  subunits of the epithelial sodium channel (Canessa *et al.*, 1994; Cheng *et al.*, 1998), or the  $\beta$  subunit of the inhibitory glycine receptors (Kuhse *et al.*, 1995)

#### 4.1.5. Factors that regulate assembly and folding of P2X receptors

The assembly of P2X receptors shares many features with other proteins produced in the secretory pathway. A large variety of membrane proteins have been studied including viral envelope proteins (Hammond & Helenius, 1995). It has been shown that particular mechanisms exist, which support the folding and assembly of proteins formed in the secretory pathway. To begin with, mRNA is linked to the ER membrane where assembly starts. The early assembly events occur cotranslationally. When the polypeptide chains are inserted into the membrane, the core N-linked glycans are attached to them, and the initial rapid folding takes place. These cotranslational events are followed by slower folding reactions where different domains interact and the disulfide bonds are arranged. This posttranslational folding and processing takes place in the ER and is a requirement for subunit oligomerization, which provides “quality control” by identifying and degrading any misassembled proteins (Hurtley & Helenius, 1989; Helenius *et al.*, 1992; Kopito, 1997). Most likely, the same mechanisms apply also to P2X receptors. In the present study it was shown that the posttranslational modification of P2X receptor subunits, namely attachment of N-linked glycans and disulfide bond formations are crucial for proper oligomerization of P2X receptors.

For intracellular degradation of membrane proteins currently two systems are known, a vacuolar system including lysosomes (Mortimore *et al.* 1983; Urade & Kito 1992; Dunn 1994), and a cytoplasmic system involving ubiquitin and proteasomes (Hershko & Ciechanover, 1992; Bonifacino & Weissman, 1998). It has been described that cells degrade various materials such as internalized ion channels (Silverstein *et al.*, 1977) by the vacuolar system. In addition, in the cytoplasmic

system, secretory and membrane proteins (Ellgaard *et al.*, 1999) are degraded by proteasomes, by which differential turnover of the proteins is controlled (Rechsteiner 1987; Hershko & Ciechanover 1992; Rivera *et al.*, 2000). Many proteins that are not correctly folded or misassembled in the ER are polyubiquitinated and degraded in this pathway by a process known as ER-associated degradation (Haas & Siepmann 1997; Kopito 1997; Sommer & Wolf 1997; Ellgaard *et al.*, 1999). These mechanisms of degradation are likely to be used by *Xenopus* oocytes expressing N-glycan or cysteine minus mutants of P2X<sub>1</sub> receptor. As was shown in this study, many of these mutants failed to fully assemble into functional receptors and the amount of the isolated protein was markedly decreased compared with the wild type receptor.

Some nicotinic receptors are correctly assembled only in cells of neuronal origin containing additional factors (Cooper & Millar, 1997; Rangwala *et al.*, 1997). Chaperone proteins are likely to be some of the cellular factors required for assembly. The ER chaperone proteins BiP (Blount & Merlie, 1991; Paulson *et al.*, 1991; Forsayeth *et al.*, 1992) and calnexin (Gelman *et al.*, 1995; Keller *et al.*, 1996, 1998) associate with unassembled AChR subunits and may directly aid the assembly process. Furthermore, NSF and SNAPS associate with AMPA receptors in the dendrites of hippocampal pyramidal cells (Osten *et al.*, 1998) and appear to function as “chaperones” that are required for channel function or recycling (Nishimune *et al.*, 1998).

#### 4.1.6. Methods used to investigate the quaternary structure of P2X receptors

##### 4.1.6.1. Cross-linking of P2X receptors

Using the potent cross-linker glutardialdehyde, purified His-P2X<sub>1</sub>, His-P2X<sub>1</sub>-GFP, His-P2X<sub>2</sub> receptors, and the P2X<sub>2</sub>/P2X<sub>1</sub> complexes of surface-labeled, intact oocytes could be cross-linked to dimers and trimers. It is assumed that glutardialdehyde via its aldehyde groups forms Schiff bases with lysine residues leading to the cross-linking of the subunits. However, cross-linking could not exclude the existence of complexes higher than a trimer, because the cross-linking reaction was not very efficient. Increasing the concentration of glutardialdehyde or the incubation time led to a decrease of the amount of isolated protein. A possible explanation is the

formation of non-specific aggregates at high concentrations of the cross-linker, which inhibited the accessibility of respective hexa-histidyl tag to the Ni<sup>2+</sup>- agarose beads.

#### 4.1.6.2. Biochemical analysis of the P2X receptor complexes by BN-PAGE

Using polyacrylamide gel electrophoresis, proteins can be separated depending on their net charge and their size as well as on the density of the acrylamide gel. In the present study, two electrophoresis methods, SDS-PAGE and BN-PAGE were applied to biochemically explore the proteins isolated from *Xenopus* oocytes. Both methods are “charge shift methods”, in which the individual proteins receive additional negative charges by binding of SDS or Coomassie blue G in case of SDS-PAGE or BN-PAGE, respectively.

In the SDS-PAGE system, the detergent SDS unfolds proteins and forms SDS/protein micelles. Thereby the intrinsic charges of the proteins are masked by SDS and an excess of negative charges is conferred to them, such that the charge/mass ratio becomes roughly constant for most proteins. Therefore, SDS-PAGE allows for the determination of the molecular mass of migrating proteins, because the charge density is almost equal for all proteins, thus separation of the proteins depends only on the effective molecular radius, which approximates the relative molecular mass. In the BN-PAGE system, Coomassie dye binds to hydrophilic segment of the protein exterior and is believed to have no dissociating effects to bound proteins (Schägger & von Jagow, 1991). The capability of binding Coomassie dye and therefore the charge densities vary between different proteins (Schägger, Cramer & von Jagow, 1994). In the BN-PAGE system, the separating principle is the molecular sieving effect of a polyacrylamide gel within a relatively steep acrylamide gradient. The molecular masses of proteins are determined at their individual end points of migration corresponding to the acrylamide concentration, where they reach their pore edge. Schägger demonstrated that a calibration curve can be established from migration distances in BN-PAGE and known molecular masses of various soluble and membrane proteins (Schägger, Cramer & von Jagow, 1994). Since appropriate membrane proteins of known molecular mass were not available, a set of water-soluble proteins (ferritin, catalase, aldolase, bovine serum albumin and ovalbumin) was utilized in the present study as molecular weight standards for BN-PAGE. Using these proteins as references, BN-PAGE analysis of

all P2X complexes revealed apparent masses of approximately 250-450 kD, far higher than the calculated molecular masses of trimers, which should be in the range of 170-230 kD. This discrepancy might be due to one or more of the following reasons. Generally, the following conditions must be fulfilled to allow for determination of molecular masses by BN-PAGE: the protein must either have an isoelectric point (IP) at or below 5.4 or it must be able to bind Coomassie blue G and have an IP below 8.6 (Schägger, Cramer & von Jagow, 1994). Since most P2X complexes are rather basic (IP of the rat P2X<sub>1</sub> polypeptide: 8.54), the charge shift introduced by Coomassie dye could be insufficient, thus leading to a particularly low electrophoretic mobility and a comparably long electrophoresis time until the end point of migration is reached. The same effect would occur if the P2X proteins were unable to bind enough Coomassie dye to induce an adequate charge shift.

The apparent molecular masses of the BN-PAGE separated P2X complexes might not be those of the pure glycoproteins, but of complexes including detergent. Moreover, since protein complexes are considered to remain in their native state during BN-PAGE, the shape of the P2X receptors could influence its hydrodynamic properties: for example a tightly folded globular protein would exhibit a greater electrophoretic mobility than a funnel shaped ion channel. In addition, the N-glycans exert a small effect on the mobility of the P2X receptors as shown by the slightly faster migration of glycan minus mutants of the His-P2X<sub>1</sub> receptor.

#### 4.1.7. Identification of regions that regulate desensitization of P2X receptors

Desensitization can be removed from the P2X<sub>1</sub> or P2X<sub>3</sub> receptor by replacing the cytoplasmic N-terminal domain including parts of the first transmembrane domain with corresponding parts of the domain from P2X<sub>2</sub> receptor (Werner *et al.*, 1996). The domains play a role in P2X receptor desensitization include the most hydrophobic segments of the molecules, which are known to be membrane-spanning segments. However, they additionally include segments of 11–15 amino acids that are located at the immediate cytoplasmic side of the membrane; these segments have an abundance of positively charged residues, as is commonly found in such a location (von Heijne, 1992). Although these regions were not systematically shortened or mutated, it appears from the results that the first charged region (pre-M1) of P2X<sub>2</sub> is needed for desensitization of P2X<sub>1</sub> or P2X<sub>3</sub>. The amino acid

sequences of the first transmembrane domains of the three receptors P2X<sub>1</sub>, P2X<sub>2</sub> and P2X<sub>3</sub> are compared in Fig. 4.1; they are 26–48% pairwise identical and the positions of all positively charged amino acids are highly conserved. This alignment does not imply that single amino acid substitutions might not have effects on desensitization, but it makes it unlikely that a difference in one or a few amino acids could account for the large differences between P2X<sub>1</sub> and P2X<sub>2</sub>. In homomultimeric  $\alpha$ 7 nicotinic AchR and 5-HT<sub>3</sub> receptors, mutationally induced changes at a single position in the amphipathic M2 (pore-lining) domain can considerably alter the rate of desensitization (Revahet *et al.*, 1991; Yakelet *et al.*, 1993), while glutamate receptors can fine-tune their kinetic properties with the help of alternative splicing (Mosbacher *et al.*, 1994).

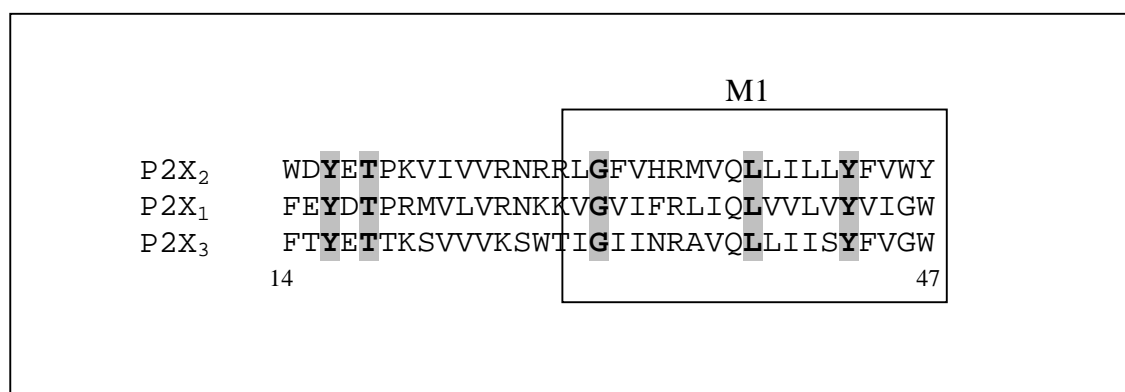


**Fig. 4.1: The domains required for desensitization are the same in P2X<sub>3</sub> and P2X<sub>1</sub> receptors.** Domains required to transfer desensitization include the hydrophobic, presumed first membrane-spanning domain (M1) and 11–15 residues of the cytoplasmic region. Identical amino acids are indicated by shaded boxes.

The alteration of the desensitization of the wild-type P2X<sub>1</sub> receptor by replacing the cytoplasmic N-terminal domain including parts of the first transmembrane domain suggests that it may result from intrinsic conformational changes of the receptor protein. The portions of the molecule that are directly involved in this conformational change appear not to include the large extracellular loop (Werner *et al.*, 1996).

BN-PAGE analysis of the chimeras revealed a trimeric complex for all chimeras, although differences between the acquired types of carbohydrate residue have been observed. Like the parent P2X receptors, the chimeras migrated as one distinct band that could be partially dissociated into dimers and monomers by

treatment with DTT and/or urea. Thus, a change of desensitization does not have an impact to the oligomeric states of the respective chimeras.

## 4.2. Investigation of P2X<sub>1</sub>-GFP fusion proteins

Expression of a C-terminally GFP-tagged His-P2X<sub>1</sub> subunit in oocytes results in proteins that migrated quantitatively as trimers when purified in digitonin and analyzed by BN-PAGE. In addition, cross-linking of His-P2X<sub>1</sub>-GFP on intact oocytes indicated that the fusion protein exists as a trimer on the cell surface consistent with the quaternary structure analysis of the parent His-P2X<sub>1</sub> receptor. Moreover, electrophysiological measurements showed that the C-terminally GFP-tagged His-P2X<sub>1</sub> receptor exhibits a phenotype similar to the parent His-P2X<sub>1</sub> receptor in *Xenopus* oocytes. These results indicated that the GFP tag is functionally silent even though it is much larger than most other protein tags and, with 238 amino acid residues, has approximately half the size of a P2X<sub>1</sub> receptor subunit. Despite this, the addition of this relatively large protein to the C-terminus of the His-P2X<sub>1</sub> subunit does not appear to interfere or alter subunit folding, oligomeric assembly, membrane targeting, or the physiological properties of the receptor.

An N-terminally GFP-tagged His-P2X<sub>1</sub> (designated GFP-His-P2X<sub>1</sub>) subunit was also capable of assembling into trimers, as shown by BN-PAGE. However, most of the protein was retained in the core-glycosylated form in the ER. Likewise, no GFP-His-P2X<sub>1</sub> protein could be detected by surface labeling of oocytes injected with the cRNA for N-terminally GFP tagged His-P2X<sub>1</sub> and no response to ATP was measured when these oocytes were analyzed electrophysiologically. This result indicates the importance of an uncapped N terminal domain for routing of the P2X<sub>1</sub> receptor to the plasma membrane. However, elongation of the N terminal domain does not seem to have an impact on assembly, as shown by BN-PAGE analysis, but rather on routing of the protein complex to the cell surface.

### 4.2.1. Clustering of His-P2X<sub>1</sub>-GFP receptors

Confocal fluorescence microscopy of oocytes injected with the cRNA for His-P2X<sub>1</sub>-GFP revealed small clusters of the fusion protein, approximately 4–6 μm in diameter

in intracellular membranes of *Xenopus* oocytes. During development of striated muscle fibers, small acetylcholine receptor clusters less than 2  $\mu\text{m}$  in diameter appear in the membrane independently of the arrival of motor nerves (Phillips *et al.*, 1985). It seems that there is an intrinsic tendency for receptors to induce the formation of clusters and that these clusters are in a size class of 1–6  $\mu\text{m}$ . However, once the nerve terminal arrives, such large receptor clusters become confined to sites immediately beneath the terminal (Phillips & Bennett, 1987 & 1989). A similar restriction of large P2X<sub>1</sub> receptor clusters to varicosities has been observed during formation of the autonomic neuromuscular junction (Dutton *et al.*, 1999). It is likely that a decrease in extra-junctional receptor insertion occurs at the developing autonomic junction similar to that observed at the somatic neuromuscular junction.

#### 4.2.2. Anchoring of P2X receptors in the membrane

Acetylcholine receptor clustering in striated muscle cells is determined by a 43 kD cytoplasmic protein called rapsyn. Rapsyn interacts with each of the  $\alpha$ ,  $\beta$ ,  $\gamma$ , and  $\delta$  subunits to precisely localize them to the postsynaptic membrane of the motor nerve terminal (Maimone & Merlie, 1993; Glass & Yancopoulos, 1997; Feng *et al.*, 1998). Such a process has been followed in detail by fusing rapsyn to GFP (Ramarao & Cohen, 1998). Injection of cRNA encoding AchR subunits together with the RNA for rapsyn leads to the formation of receptor clusters of 0.5–1.5  $\mu\text{m}$  in diameter (Froehner *et al.*, 1990), i.e. at the lower end of the size range of the P2X<sub>1</sub>–GFP clusters observed in the present study. Another anchoring protein for receptors that has been isolated to date is the 93 kD protein gephyrin that clusters glycine receptors (Kirsch & Betz, 1998). Whether rapsyn or gephyrin can anchor P2X receptors is not yet known. In addition, it is not known whether the clustering of His-P2X<sub>1</sub>–GFP observed in oocytes involves an anchoring mechanism. It seems possible that this anchor system may involve a clustering agent that is not cell specific. This observation is strengthened by data that demonstrate a role for the actin cytoskeleton in the control of the turnover of P2X<sub>1</sub> receptors following agonist exposure (Parker, 1998).

### 4.3. Role of N-glycans for the functional expression and assembly of the rat P2X<sub>1</sub> receptor

The P2X<sub>1</sub> receptor influences its own N-glycosylation at two levels, (i) at the level of its primary sequence and (ii) the level of its three-dimensional structure. First, the <sup>284</sup>NLS tripeptide (N4) is not used as a site for N-glycosylation because of a proline residue in the +4 position. Replacement by alanine resulted in unimpaired N-glycosylation at this site. This observation agrees well with previous reports that the presence of proline immediately following a sequon can inhibit core glycosylation (Gavel *et al.*, 1990; Bause, 1983). A sequon with a proline in +4 position is also present on the P2X<sub>4</sub> polypeptide, but not on the other P2X isoforms. Second, from the four N-glycans that are cotranslationally attached per P2X<sub>1</sub> subunit, only the one at <sup>300</sup>N (N5) acquires complex-type carbohydrates during passage of the Golgi apparatus, whereas the others remain in an Endo H-sensitive form. This observation can best be reconciled with constraints imposed by the three-dimensional structure of the P2X<sub>1</sub> receptor, which apparently restricts the access of individual N-glycans to processing by Golgi enzymes. We considered that the restricted accessibility of the N-glycans results from a lectin-like subunit interaction. However, present findings exclude this possibility, since a P2X<sub>1</sub> triple mutant devoid of the three inaccessible N-glycans ( $\Delta$ N123) acquired the same homotrimeric configuration like the correctly glycosylated parent P2X<sub>1</sub> receptor and formed a functional P2X<sub>1</sub> receptor at the plasma membrane though with low efficiency.



#### 4.3.1. N-glycans and membrane folding of P2X<sub>1</sub>

The two-dimensional orientation of P2X subunits in the plasma membrane has been predicted from hydrophathy plots, usage of natural N-glycosylation sites and N-glycan scanning mutagenesis studies (Newbolt *et al.*, 1998, Torres *et al.*, 1998). The five putative N-glycosylation sites of the P2X<sub>1</sub> polypeptide are all located in the predicted ectodomain. As noted previously, the demonstration that four of the five natural sites are occupied by sugars confirms the membrane topology deduced from hydrophathy analysis, since N-glycosylation sites occur always on the extracellular portion of a protein. Additional important information about membrane folding can be deduced from the observation that <sup>300</sup>N (N5) is not only used, but also fully accessible to Golgi enzymes to acquire complex type carbohydrates. N5 is located only eight residues upstream of the conserved lipophilic domain, which has been postulated to constitute a reentry loop immediately before M2 like the H5 domain of K<sup>+</sup> channels and hence to contribute to the pore (Brake, 1994). Using a cell-free translation system, it has been demonstrated that oligosaccharide transfer occurs only when 12-14 amino acids downstream to a sequon have been translocated (Nilsson & Von Heijne, 1993). The efficient N-glycosylation of N5 and its ready accessibility for Golgi enzymes, *i.e.* within the fully assembled P2X<sub>1</sub> receptor argues against a significant membrane embedding of this lipophilic domain. The glycan may serve to shield a hydrophobic surface at this locus.

#### 4.3.2. Positional effects of N-glycans on surface expression of P2X<sub>1</sub> receptor

The most proximal glycan (N1) appears to be especially important for high surface expression levels of functional P2X<sub>1</sub> receptors, whereas N2 and N5 are dispensable in this respect. The surprising observation that the expression level of functional receptors increased upon elimination of N3 may be correlated with an increased number of P2X<sub>1</sub> receptors at the plasma membrane, as evident from most though not all surface radio-iodination experiments (results not shown), rather than by altered receptor function. The mechanism of this increase is not clear yet. The peculiar role of the glycan at N3 for ATP potency is discussed below.

If the modulatory roles of individual N-glycans are neglected, it becomes obvious that the elimination of two of the four canonical N-glycosylation sites per

subunit is quite well tolerated. This suggests that the number of N-glycans per P2X<sub>1</sub> subunit is redundant, at least for robust expression. A large decline of the expression level occurs only after elimination of three sites per subunit both in terms of maximum current amplitudes and receptor protein at the cell surface. Taking the trimeric architecture of P2X receptors into account, this means that a total of six N-glycans are required per receptor complex for robust functional expression. A reduction of surface appearance has been observed for the non-glycosylated forms of a large variety of glycoproteins, but the mechanisms that account for this phenomenon appear to be different. Many non-glycosylated forms of glycoproteins accumulate in the ER, aggregate, and do not exit (Helenius, 1994). Others exit the ER, but are retained in the Golgi apparatus, apparently because N-linked oligosaccharides are required for efficient transport from the Golgi apparatus to the cell surface (Gut, 1998). Since non-glycosylated His-P2X<sub>1</sub> receptor subunits or complexes accumulate neither in the ER nor in the Golgi apparatus, rapid degradation soon after synthesis is likely to account for the low functional expression levels and low amounts of receptor protein at the cell surface of mutants carrying solely one N-glycan. Elimination of all four glycosyl acceptor sites abolished the appearance of His-P2X<sub>1</sub> at the cell surface. An essential role of N-glycans has been also described for the formation of functional P2X<sub>2</sub> receptors in HEK293 cells (Torres, 1998). This raises the possibility that interaction with lectin-like chaperones such as calnexin and/or calreticulin (Trombetta & Helenius, 1998) is crucial at certain stages of the folding process and for oligomerization of P2X subunits, for instance by providing additional time to allow for productive collisions between P2X monomers. Incompletely folded monomers that lack N-glycans as functional tags may no longer be retained in the ER and eventually get degraded (Hebert *et al.*, 1996).

#### 4.3.3. Conservation of N-glycosylation sites among P2X isoforms

The four N-glycans of P2X<sub>1</sub> are distributed over two thirds of the ectodomain like the ten cysteine residues that are assumed to be involved in disulfide formation. In contrast to the cysteines, however, which are totally conserved among all P2X isoforms, only P2X<sub>3</sub> exhibits a N-glycan distribution that overlaps exactly with that of the P2X<sub>1</sub> subunit. Sequons corresponding to N1 and N2 of P2X<sub>1</sub> are present on

almost all isoforms, whereas the sequon corresponding to N5 (N300) is found on P2X<sub>1</sub>-P2X<sub>3</sub> only. The number of N-glycosylation sites likely to be used amount to three (P2X<sub>2</sub>, P2X<sub>5</sub>, P2X<sub>6</sub>), four (P2X<sub>1</sub>, P2X<sub>3</sub>), six (P2X<sub>7</sub>), and seven (P2X<sub>4</sub>), *i.e.* all isoforms carry at least three N-glycans. Since only two such sites are actually required for robust receptor formation and no particular N-glycan is absolutely important, variation in acceptable positions of glycans can occur. Hence, the redundancy in the number of N-glycans provides at least a partial explanation for the imperfect conservation of the number and positions of N-glycans among the P2X isoforms.

#### 4.3.4. N-glycans and ligand recognition

Elimination of N-glycans has only occasionally been observed to be associated with altered ligand recognition. Lack of N-glycosylation of the glucose transporter GLUT1 decreased its apparent affinity for glucose (Asano *et al.*, 1993). In contrast, the non-glycosylated transporter for serotonin (Tate & Blakely, 1994) or norepinephrine (Melikian *et al.*, 1996) like the Na<sup>+</sup>/glucose symporter SGLT1 (Wu *et al.*, 1994) exhibited no alteration of substrate recognition. Elimination of the four N-glycosylation sites of the insulin receptor  $\beta$  subunit did also not affect the affinity for insulin, but blocked signal transduction (Leconte *et al.*, 1992). The single N-glycan of the human T-cell surface glycoprotein CD2 was first suggested by cell adhesion assays to be required for binding of the counter receptor CD58. However, structure resolution by NMR revealed that this N-glycan is not directly involved in ligand binding, but crucial for the stabilization of the folded protein structure (Wyss *et al.*, 1995). Presence of a glycan in the vicinity of the  $\alpha$ -bungarotoxin binding surface has been demonstrated to confer  $\alpha$ -bungarotoxin resistance to the nicotinic acetylcholine receptor (Kreienkamp *et al.*, 1994). Most likely, the bulky glycan moiety imposes steric hindrance for toxin binding. Referred to the present work, one would expect a gain of function, *i.e.* an increase in ATP potency, once a bulky N-glycan is removed in the vicinity of the ligand-binding site. The observation of a decrease in the potency for ATP, *i.e.* a loss of function, makes it more likely that the glycan at N210 imposes structural alterations, which may act to stabilize a folded domain essential for ATP binding. A contribution of this region to the ATP binding site can be inferred from the recent observation that neutralization of the conserved residues K190 and K215 by

alanine substitution produced also a slight (2-5fold) decrease of ATP potency (Ennion *et al.*, 2000).

#### **4.4. Role of individual cysteine residues for the functional expression and assembly of the rat P2X<sub>1</sub> receptor**

##### **4.4.1. Effects of the reducing agent DTT on His-P2X<sub>1</sub> expression and assembly**

In this study, the effects of the reducing agent DTT on synthesized His-P2X<sub>1</sub> were investigated. The results demonstrate that DTT treatment blocked the appearance of newly synthesized His-P2X<sub>1</sub> receptors at the plasma membranes of *Xenopus* oocytes. In addition, a marked reduction in the amount of isolated protein was observed. The pulse-labeling experiments in the presence of DTT suggest that disulfide bond formation is fundamental for the transport and maturation of the His-P2X<sub>1</sub> receptor. By blocking the disulfide bonds formation, the reducing agent most likely prevented oxidative folding and affected the protein maturation process. As a consequence, His-P2X<sub>1</sub> subunits synthesized in the presence of DTT does not reach the trans-Golgi compartment and therefore does not acquire complex oligosaccharides. Apparently, the amount of isolated His-P2X<sub>1</sub> protein is markedly affected under reducing conditions. In addition, immaturely folded His-P2X<sub>1</sub> subunit in its fully reduced conformation cannot escape the ER quality control system and is probably eliminated by the mechanisms adopted for misfolded proteins. The present study revealed that the described effects of DTT on His-P2X<sub>1</sub> receptor biogenesis are fully reversible. Removal of the reducing agent leads to the resumption of disulfide bond formation of the arrested subunits, with subsequent folding and assembly into trimeric His-P2X<sub>1</sub> receptor complexes, followed by transport to the cell surface as deduced from the capability of the protein to acquire complex-type carbohydrates. These results indicate that DTT treatment does not cause irreversible misfolding or aggregation of the subunits. It appears that subunit conformational maturation is suspended until the oxidizing environment in the ER is restored. It is possible that the prevention of irreversible misfolding of proteins reduced by DTT is mediated by one or more ER-resident molecular chaperones such as calnexin (Gelman & Prives, 1996), which facilitates correct folding of nascent polypeptides.

#### 4.4.2. Investigation of P2X<sub>1</sub> receptor mutants lacking cysteine residues

One of the peculiar features of the P2X receptor family is its membrane topology, which predicts that more than 70% of the protein mass is exposed to the extracellular space. Since the natural ligand ATP is a highly polar and strongly charged molecule, it is self-evident that the extracellular loop has a potential role in ligand-receptor interaction. The extracellular loop of P2X receptor family proteins has been proposed to possess two cysteine-rich domains (CRDs) (Hanson *et al.*, 1997). It has been demonstrated that during protein folding and maturation, extracellular cysteine residues are rapidly oxidized, and that enzyme-catalyzed disulfide exchange continues until the thermodynamically most stable conformation is achieved. For membrane proteins, the formation of disulfide bonds in the extracellular loop of the protein is critical for proper co-translational folding of the protein and subsequent assembly and oligomerization in the ER compartment (Firsov *et al.*, 1999).

The dissociation of the P2X<sub>1</sub> receptor complex into monomers by DTT treatment may suggest that the subunits are covalently linked by disulfide bridges. However, the intersubunit bonding of these proteins can be excluded for the following reason: although dissociation of P2X<sub>1</sub> complexes into monomers was caused by DTT in the presence of sodium aminocaproate, there are a variety of denaturing treatments, which by themselves will not affect disulfide bonds, such as addition of urea or SDS as was visualized by BN-PAGE analysis. Moreover, and even more importantly, there is no evidence from reducing SDS-PAGE for disulfide intersubunit cross-linking of P2X polypeptides. From these results it is concluded that the most probable structural feature of the conserved cysteines is the formation of intrasubunit disulfide bonds. Thus, native P2X receptor complexes are maintained by non-covalent interactions and not by interchain disulfide linkages.

Several approaches are usually used in order to determine the exact pattern of disulfide bond formation for membrane proteins. A possible biochemical approach uses the differential electrophoretic mobility by SDS-PAGE of the wild type and the mutant proteins in their non-reduced forms. However, for the P2X<sub>1</sub> receptor, the shift in the electrophoretic mobility between the parent subunit in its reduced and nonreduced state was not large enough in the present experiments to identify a total of up to five possible disulfide bonds (data not shown). The approach used in the present study is based on the assumption that the effect of Cysteine → Serine mutations is limited to the elimination of disulfide bonds, which involved the mutated

C residue. Therefore, mutation of either one or both cysteine residues involved in a given disulfide bond may be expected to result in channel mutants with the same phenotype. To this end, a series of cysteine double mutants was generated, which included mutations of C1 – C6 of the His-P2X<sub>1</sub> subunit. From the similarity of the decrease in sensitivity to ATP, it is deduced that C1 and C6, C2 and C4 and C3 and C5 are cysteine residues, which might be covalently linked by each other in each P2X<sub>1</sub> subunit.

Interestingly, despite of the absolute conservation of C1 through C6 among all P2X subunits, the substitution of one or more cysteine residues of the CRD1 region with serine did not substantially decrease channel function, as judged from electrophysiological measurements in *Xenopus* oocytes. BN-PAGE characterization of cysteine minus mutants from this domain indicates that the cysteine substitutions do not have a major effect on assembly of the mutant subunits, or on subunit stoichiometry with regard to the trimerization. It seems likely that the modest changes of ATP potency observed by substituting individual cysteines result from small conformational changes rather than from disruption of any specific function of the involved cysteine. The absence of marked functional effects by cysteine substitution could signify that they do not participate in formation of protein structures necessary for intrinsic channel activity. However, from the effect of the cysteine substitutions on ATP potency, an important role of these cysteines in stabilization of the three-dimensional structure of the ligand-binding site can be deduced. Like the number of N-glycans per P2X<sub>1</sub> subunit, also the number of cysteine bonds in the CRD1 region appears to be redundant, since elimination of more than one cysteine was necessary to significantly reduce channel function. Interestingly, North and coworker identified a region distal to the first transmembrane domain, which contained two lysine residues (<sup>69</sup>Lys and <sup>71</sup>Lys) that were critical for the action of ATP. These residues are located close to the domain, in which the first cysteine rich domain is located ([Jiang et al., 2000](#)). In conclusion, present results suggest that replacement of the cysteine residues located in the first CRD introduces structural changes, which affect ion channel characteristics, but that these cysteines (C1-C6) are not absolutely needed for the assembly of the receptor.

The mutational investigation of the four cysteine residues (C7 – C10) of CRD2 demonstrated their critical importance in functional surface expression of the P2X<sub>1</sub> receptor. Biochemical analysis revealed that all the cysteine minus mutants of CRD2 were entirely retained in the ER. Moreover, these mutants existed solely as

aggregates as judged by BN-PAGE analysis. This result suggests that P2X<sub>1</sub> subunits lacking one of the cysteines of CRD2 are incorrectly folded or mis-assembled. Likewise, mutations of one or two cysteines involved in the formation of a disulfide bond in the N-terminus of either the  $\alpha$  or  $\beta$  subunit of the AchR abolished subunit assembly and ligand binding (Green & Wanamaker, 1997). The possible mechanisms which could explain the abolished cell surface expression of these cysteine mutants are the following: (i) misfolding during translation, (ii) lack of proper oligomerization due to abnormal conformations of assembled complexes, (iii) disruption of the normal transport of the mutant proteins from ER to Golgi and/or from Golgi to the cell surface, or (iv) increased rate of degradation of the mutant proteins leading to a decrease of the total channel protein pool.

## 5. Summary

P2X receptor subunits assemble in the ER of *Xenopus* oocytes to homomultimeric or heteromultimeric complexes that appear as ATP-gated cation channels at the cell surface. In this work it was intended to investigate the posttranslational modifications such as N-linked glycosylation and disulfide bond formation that is undergone by P2X<sub>1</sub> receptors. In addition, the aim of this study was to examine the expression and the quaternary structure of selected P2X receptor isoforms in *Xenopus* oocytes.

The investigation of the quaternary structure of the metabolically or surface labeled His-P2X<sub>2</sub> receptor by BN-PAGE revealed that, while the protein complex is only partially assembling in oocytes, the plasma membrane form of the His-P2X<sub>2</sub> receptor assembled into trimeric and even hexameric complex as was shown by the BN-PAGE analysis. Besides this finding, it is shown that the His-P2X<sub>5</sub> protein that was purified from metabolically or surface labeled oocytes appeared as one single band corresponding to a trimer when analyzed by BN-PAGE. The present study signified that His-P2X<sub>6</sub> alone does not reach a defined assembly status and possibly needs the hetero-polymerisation with other P2X subunits to assemble properly for insertion into the plasma membrane. Another finding of this study is that the P2X<sub>1</sub> and P2X<sub>2</sub> subunits could exist as heteromultimeric protein complexes in the plasma membrane of cells. Purification of surface expressed His-P2X<sub>2</sub> subunit allowed the detection of co-injected P2X<sub>1</sub> subunit and *vice versa* in *Xenopus* oocytes. Incubation with glutardialdehyde led to the cross-linking of P2X<sub>2</sub> and P2X<sub>1</sub> subunits to dimers and trimers. BN-PAGE analysis of the P2X<sub>2</sub>/P2X<sub>1</sub> complex isolated under non-denaturing conditions from surface-labeled oocytes yielded one distinct band corresponding to a trimeric complex.

The analysis of a C-terminally GFP tagged His-P2X<sub>1</sub> fusion protein by confocal fluorescence microscopy revealed small clusters of the protein complexes, approximately 4–6 μm in diameter from a diffuse distribution of the protein in the plasma membranes of *Xenopus* oocytes. The cross-linking or BN-PAGE analysis of the fusion protein resulted in proteins that migrated quantitatively as trimers when purified in digitonin.

The analysis of some chimeric constructs confirmed the results of others, which showed that desensitization can be removed from the P2X<sub>1</sub> or P2X<sub>3</sub> receptor by providing the N-domain from the P2X<sub>2</sub> receptor (Werner *et al.*, 1996) The exchange



of this domain did not alter the quaternary structure of the chimeras, which showed to be present as trimers when expressed in oocytes.

In addition, glycan minus mutants of His-P2X<sub>1</sub> receptor were analyzed to examine whether carbohydrate side chains are important for P2X<sub>1</sub> subunit assembly, surface expression, or ligand recognition. SDS-PAGE analysis of glycan minus mutants carrying Q instead of N at five individual NXT/S sequons reveals that <sup>284</sup>N remains unused because of a proline in the +4 position. The four other sites (<sup>153</sup>Asn, <sup>184</sup>N, <sup>210</sup>N, and <sup>300</sup>N) carry N-glycans, but solely <sup>300</sup>N acquires complex-type carbohydrates. Like parent P2X<sub>1</sub> receptor, glycan minus mutants migrate as homotrimers when resolved by blue native PAGE. Recording of ATP-gated currents revealed that elimination of <sup>153</sup>N or <sup>210</sup>N diminishes or increases functional expression levels, respectively. In addition, elimination of <sup>210</sup>N causes a 3-fold reduction of the potency for ATP. If three or all four N-glycosylation sites are simultaneously eliminated, formation of P2X<sub>1</sub> receptors is severely impaired or abolished, respectively. It is concluded that at least one N-glycan per subunit of either position is absolutely required for the formation of P2X<sub>1</sub> receptors.

The SDS-PAGE analysis of surface-labeled His-P2X<sub>2</sub> and His-P2X<sub>5</sub> receptors revealed that, while the His-P2X<sub>2</sub> subunit acquires three complex-type carbohydrates, in case of His-P2X<sub>5</sub> polypeptide, only two of the three N-glycans could obtain complex-type carbohydrates during transit of the Golgi apparatus.

Furthermore, it was shown that DTT treatment blocked the appearance of newly made His-P2X<sub>1</sub> at the plasma membranes of *Xenopus* oocytes. Also, it was revealed that the effects of DTT on His-P2X<sub>1</sub> biogenesis are fully reversible. Removal of the reducing agent leads to subsequent folding and assembly into His-P2X<sub>1</sub> receptor complex, followed by transport to the cell surface.

The characterization of cysteine minus mutants by SDS PAGE and BN-PAGE demonstrated that, the cysteine substitution in the first cysteine rich domain (C1 - C6) does not have a major effect on assembly for the mutant receptors. In contrast, the replacement of the four cysteine residues (C7 – C10) from the second cysteine rich domain demonstrate a critical importance of this domain for the functional surface expression of P2X<sub>1</sub> receptor. The investigations of several double cysteine mutants revealed that according to a similarity in the sensitivity to ATP, the C1 and C6, as well as C2 and C4 and finally C3 and C5 are pairs forming two disulfide bonds in each P2X<sub>1</sub> subunit.

## 6. Zusammenfassung

P2X-Rezeptoren stellen ligandengesteuerte Ionenkanäle dar, die nach ATP-Bindung innerhalb weniger Millisekunden eine intrinsische Pore öffnen, die nicht-selektiv permeabel für kleine Kationen ist. Ziel meiner Arbeit war es, Tertiär- und Quartärstruktur der P2X-Rezeptoren mit molekularbiologischen Methoden zu charakterisieren. Hierbei wurde der Einfluss von Kohlenhydrat-Seitenketten und die Rolle der Disulfidbrücken auf die Expression und Assemblierung des P2X<sub>1</sub>-Rezeptors untersucht.

Die Analyse der Quartärstruktur von metabolisch markierten His-P2X<sub>2</sub>-Rezeptoren ergab, dass die Proteinkomplexe nach der Expression in Oozyten hauptsächlich als Dimere und Trimere vorliegen. Zusätzlich wies ein Teil der isolierten Proteine keinen definierten Oligomerisierungszustand auf, was darauf hindeutet, dass His-P2X<sub>2</sub> in intrazellulären Kompartimenten der Oozyten nicht vollständig assembliert. Die Untersuchung von plasmamembranständigen His-P2X<sub>2</sub>-Rezeptorkomplexen mittels BN-PAGE zeigte neben Proteinbanden für eine trimere Struktur auch Banden, die einer hexameren und einer nanomeren Strukturen entsprechen könnten. Die BN-PAGE-Analyse von P2X<sub>5</sub>-Rezeptoren, die heterolog in Oozyten exprimiert wurden, ergab, dass die Rezeptoren sowohl intrazellulär als auch an der Zelloberfläche hauptsächlich als Trimere vorliegen. Ferner wurde in den Untersuchungen gezeigt, dass die His-P2X<sub>6</sub>-Rezeptoren hauptsächlich als hochmolekulare Komplexe erscheinen und somit keinen definierten Oligomerzustand aufweisen. Diese Resultate deuten daraufhin, dass die P2X<sub>6</sub>-Rezeptoruntereinheit nicht imstande ist, einen homo-oligomeren Ionenkanal zu bilden, und auf die Assemblierung mit anderen P2X- Rezeptoruntereinheiten angewiesen ist.

Ein weiteres Ziel meiner Arbeit war der proteinchemische Nachweis der Bildung von P2X<sub>1</sub> und P2X<sub>2</sub> Heteromultimeren durch Koisolierung. Die cRNA für diese zwei P2X-Isoformen mit oder ohne der jeweiligen Hexahistidylsequenz wurden in *Xenopus*-Oozyten injiziert und die Proteine nach entsprechender radioaktiver Markierung mittels Ni<sup>2+</sup>-Chelat-Chromatographie koisoliert. Die Untersuchung ergab, dass die binäre Kombination von P2X<sub>1</sub> und P2X<sub>2</sub> zur Bildung von stabilen Heteromultimeren führt. Des Weiteren wurde mit Hilfe von Cross-linking-Experimenten und BN-PAGE-Analyse gezeigt, dass diese Proteinkomplexe eine trimere Struktur aufweisen.

Um die zelluläre Lokalisation des P2X<sub>1</sub>-Rezeptors zu bestimmen, wurden die *Xenopus*-Oozyten mit der cRNA eines gentechnisch hergestellten Fusionsproteins, bestehend aus dem P2X<sub>1</sub>-Rezeptor und dem grünfluoreszierenden Protein (GFP), injiziert. An intakten Oozyten erkennt man in den fluoreszenzmikroskopischen Aufnahmen eine Fluoreszenz an der Plasmamembran, sowie kleine, etwa 4-6 µm große Vesikel unterhalb der Plasmamembran. Die Quartärstrukturanalyse dieses Proteins mittels Cross-linking-Experimenten und BN-PAGE ergab, dass dieses Fusionsprotein wie der Wildtyp-P2X<sub>1</sub>-Rezeptor eine trimere Struktur besitzt.

Proteinchemische Analysen der durch gerichtete Mutagenese hergestellten Glycan-Minus-Mutanten des His-P2X<sub>1</sub> Rezeptors zeigten, dass (1) <sup>284</sup>N keine Kohlenhydrat-Seitenkette trägt, weil ein Prolin (<sup>287</sup>P) auf das Glykosylierungsmotiv N-L-S folgt; (2) dass nur die Oligosaccharid-Seitenkette an <sup>300</sup>N auf dem Weg des trimeren Rezeptors an die Plasmamembran im Golgi-Apparat komplex-glykosyliert wird; (3) dass die Deletion von zwei Glykosylierungsstellen gut toleriert wird, dass aber bei der Deletion von drei Stellen die Expression drastisch abnimmt, und (4) dass bei der Deletion aller vier Stellen weder intrazellulär noch an der Plasmamembran P2X<sub>1</sub>-Rezeptoren nachweisbar sind. Elektrophysiologisch zeigte sich, dass die Mutation N<sup>210</sup>Q eine Abnahme der scheinbaren ATP-Affinität um den Faktor drei gegenüber dem Wildtyp-P2X<sub>1</sub> bewirkt, die vermutlich auf dem Ausbleiben der N-Glykosylierung in dieser Position beruht.

Ferner zeigte die proteinchemische Analyse des His-P2X<sub>2</sub>-Rezeptors durch SDS-PAGE, dass alle drei Kohlenhydrat-Seitenketten des P2X<sub>2</sub>-Rezeptors auf dem Weg zur Plasmamembran in die komplex-glykosylierte Form überführt werden, unterdessen aber nur zwei der drei Kohlenhydrat-Seitenketten der P2X<sub>5</sub>-Rezeptoruntereinheit auf dem Weg zur Plasmamembran in die komplex-glykosylierte Form überführt werden.

Untersuchungen zur Rolle der Disulfidbrücken bei der Expression und Assemblierung von P2X-Rezeptoren ergaben, dass die P2X<sub>1</sub>-Rezeptoruntereinheit offenbar über zwei Cystein-faltungsdomänen, CRD1 und CRD2, verfügt. CRD1 umfasst die N-terminal gesehen ersten sechs Cysteine, CRD2 die letzten vier Cysteine der Ektodomäne. Die Disulfidbrücken in CRD1 scheinen redundant angelegt zu sein, da hier der Austausch eines einzelnen Cysteins gegen Serin keinen nennenswerten Einfluss auf die Expression und Assemblierung hat. Bei Mutationen von Cysteinen im CRD2-Bereich kommt es dagegen zu massiven Störungen der Assemblierung.

Aufgrund der Ähnlichkeit der ATP-Empfindlichkeit bei den untersuchten Cysteindoppelmutanten lässt sich schlussfolgern, dass zwischen den Cysteinenresten C1 und C6, C2 und C4 sowie zwischen C3 und C5 Disulfidbrücken gebildet werden.

## 7. Reference List

- ACKERMAN M.J. & CLAPHAM D.E. (1997) Ion channels--basic science and clinical disease. *N.Engl.J.Med.* **336**, 1575-1586.
- ALBERTS B., BRAY D., LEWIS J., RAFF M., ROBERTS K., & WATSON J.D. (1998) *Molecular Biology of the Cell*. Published by Garland
- ANFINSEN C.B. (1973) Principles that govern the folding of protein chains. *Science* **181**, 223-230.
- ATKINSON L., BATTEN T.F. & DEUCHARS J. (2000) P2X(2) receptor immunoreactivity in the dorsal vagal complex and area postrema of the rat. *Neuroscience* **99**, 683-696.
- BARDONI R., GOLDSTEIN P.A., LEE C.J., GU J.G. & MACDERMOTT A.B. (1997) ATP P2X receptors mediate fast synaptic transmission in the dorsal horn of the rat spinal cord. *J.Neurosci.* **17**, 5297-5304.
- BAUSE E. (1983) Structural requirements of N-glycosylation of proteins. Studies with proline peptides as conformational probes. *Biochem.J.* **209**, 331-336.
- BEAN B.P. (1992) Pharmacology and electrophysiology of ATP-activated ion channels. *Trends Pharmacol.Sci.* **13**, 87-90.
- BENHAM C.D. & TSIEN R.W. (1987) A novel receptor-operated Ca<sup>2+</sup>-permeable channel activated by ATP in smooth muscle. *Nature* **328**, 275-278.
- BERGFELD G.R. & FORRESTER T. (1992) Release of ATP from human erythrocytes in response to a brief period of hypoxia and hypercapnia. *Cardiovasc.Res.* **26**, 40-47.
- BLAND-WARD P.A. & HUMPHREY P.P. (1997) Acute nociception mediated by hindpaw P2X receptor activation in the rat. *Br.J.Pharmacol.* **122**, 365-371.
- BLOUNT P. & MERLIE J.P. (1991) BIP associates with newly synthesized subunits of the mouse muscle nicotinic receptor. *J.Cell Biol.* **113**, 1125-1132.
- BO X., ZHANG Y., NASSAR M., BURNSTOCK G. & SCHOEPFER R. (1995) A P2X purinoceptor cDNA conferring a novel pharmacological profile. *FEBS Lett.* **375**, 129-133.
- BO X. & BURNSTOCK G. (1995) Characterization and autoradiographic localization of [<sup>3</sup>H] alpha, beta- methylene adenosine 5'-triphosphate binding sites in human urinary bladder. *Br.J.Urol.* **76**, 297-302.
- BODIN P. & BURNSTOCK G. (1996) ATP-stimulated release of ATP by human endothelial cells. *J.Cardiovasc.Pharmacol.* **27**, 872-875.
- BONIFACINO J.S. & WEISSMAN A.M. (1998) Ubiquitin and the control of protein fate in the secretory and endocytic pathways. *Annu.Rev.Cell Dev.Biol.* **14**, 19-57.

- BOUE-GRABOT E., ARCHAMBAULT V. & SEGUOLA P. (2000) A protein kinase C site highly conserved in P2X subunits controls the desensitization kinetics of P2X(2) ATP-gated channels. *J.Biol.Chem.* **275**, 10190-10195.
- BOULTER J., HOLLMANN M., O'SHEA-GREENFIELD A., HARTLEY M., DENERIS E., MARON C. & HEINEMANN S. (1990) Molecular cloning and functional expression of glutamate receptor subunit genes. *Science* **249**, 1033-1037.
- BOULTER J., O'SHEA-GREENFIELD A., DUVOISIN R.M., CONNOLLY J.G., WADA E., JENSEN A., GARDNER P.D., BALLIVET M., DENERIS E.S., MCKINNON D. & . (1990) Alpha 3, alpha 5, and beta 4: three members of the rat neuronal nicotinic acetylcholine receptor-related gene family form a gene cluster. *J.Biol.Chem.* **265**, 4472-4482.
- BRAAKMAN I., HELENIUS J. & HELENIUS A. (1992) Manipulating disulfide bond formation and protein folding in the endoplasmic reticulum. *EMBO J.* **11**, 1717-1722.
- BRAKE A.J., WAGENBACH M.J. & JULIUS D. (1994) New structural motif for ligand-gated ion channels defined by an ionotropic ATP receptor. *Nature* **371**, 519-523.
- BRANDLE U., SPIELMANN S., OSTEROTH R., SIM J., SURPRENANT A., BUELL G., RUPPERSBERG J.P., PLINKERT P.K., ZENNER H.P. & GLOWATZKI E. (1997) Desensitization of the P2X(2) receptor controlled by alternative splicing. *FEBS Lett.* **404**, 294-298.
- BUELL G., LEWIS C., COLLO G., NORTH R.A. & SURPRENANT A. (1996) An antagonist-insensitive P2X receptor expressed in epithelia and brain. *EMBO J.* **15**, 55-62.
- BURNSTOCK G., CAMPBELL G., BENNETT M., & HOLMAN M.E. (1963) The effects of drugs on the transmission of inhibition from autonomic nerves to the smooth muscle of the guinea pig taenia coli. *Biochem Pharmacol* ,134–135.
- BURNSTOCK G., MCLEAN J.R. & WRIGHT M. (1971) Noradrenaline uptake by non-innervated smooth muscle. *Br.J.Pharmacol.* **43**, 180-189.
- BURNSTOCK G. (1972) Purinergic nerves. *Pharmacol Rev* **24**, 509–581.
- BURNSTOCK G. (1978) A basis for distinguishing two types of purinergic receptors. *Cell Membrane Receptors for Drugs and Hormones: a Multidisciplinary Approach*,107–108.
- BURNSTOCK G., COCKS T., KASAKOV L. & WONG H.K. (1978) Direct evidence for ATP release from non-adrenergic, non-cholinergic ("purinergic") nerves in the guinea-pig taenia coli and bladder. *Eur.J.Pharmacol.* **49**, 145-149.
- BURNSTOCK G. (1996) Development and perspectives of the purinoceptor concept. *J.Auton.Pharmacol.* **16**, 295-302.
- BÜTTNER C. (2001) Identifizierung und Klonierung der P2X-Rezeptorisoformen humaner B-Lymphozyten. Dissertationsschrift:

- CANESSA C.M., MERILLAT A.M. & ROSSIER B.C. (1994) Membrane topology of the epithelial sodium channel in intact cells. *Am.J.Physiol* **267**, C1682-C1690
- CHANCELLOR M.B., KAPLAN S.A. & BLAIVAS J.G. (1992) The cholinergic and purinergic components of detrusor contractility in a whole rabbit bladder model. *J.Urol.* **148**, 906-909.
- CHANG G., SPENCER R.H., LEE A.T., BARCLAY M.T., & REES D.C. (1998) Structure of the MscL homolog from Mycobacterium tuberculosis: a gated mechanosensitive ion channel. *Science* **18**, 282(5397):2220-6.
- CHANG K., HANAOKA K., KUMADA M. & TAKUWA Y. (1995) Molecular cloning and functional analysis of a novel P2 nucleotide receptor. *J.Biol.Chem.* **270**, 26152-26158.
- CHEN C.C., AKOPIAN A.N., SIVILOTTI L., COLQUHOUN D., BURNSTOCK G. & WOOD J.N. (1995) A P2X purinoceptor expressed by a subset of sensory neurons. *Nature* **377**, 428-431.
- CHENG C., PRINCE L.S., SNYDER P.M. & WELSH M.J. (1998) Assembly of the epithelial Na<sup>+</sup> channel evaluated using sucrose gradient sedimentation analysis. *J.Biol.Chem.* **273**, 22693-22700.
- CHESSELL I.P., MICHEL A.D. & HUMPHREY P.P. (1997) Properties of the pore-forming P2X7 purinoceptor in mouse NTW8 microglial cells. *Br.J.Pharmacol.* **121**, 1429-1437.
- CHEVET E., JAKOB C.A., THOMAS D.Y. & BERGERON J.J. (1999) Calnexin family members as modulators of genetic diseases. *Semin.Cell Dev.Biol.* **10**, 473-480.
- CHOW Y.W. & WANG H.L. (1998) Functional modulation of P2X2 receptors by cyclic AMP-dependent protein kinase. *J.Neurochem.* **70**, 2606-2612.
- CLOUES R., JONES S. & BROWN D.A. (1993) Zn<sup>2+</sup> potentiates ATP-activated currents in rat sympathetic neurons. *Pflugers Arch.* **424**, 152-158.
- COCKCROFT S. & GOMPERTS B.D. (1979) ATP induces nucleotide permeability in rat mast cells. *Nature* **279**, 541-542.
- COCKCROFT V.B., ORTELLS M.O., THOMAS P. & LUNT G.G. (1993) Homologies and disparities of glutamate receptors: a critical analysis. *Neurochem.Int.* **23**, 583-594.
- COLLO G., NORTH R.A., KAWASHIMA E., MERLO-PICH E., NEIDHART S., SURPRENANT A. & BUELL G. (1996) Cloning OF P2X5 and P2X6 receptors and the distribution and properties of an extended family of ATP-gated ion channels. *J.Neurosci.* **16**, 2495-2507.
- COLLO G., NORTH R.A., KAWASHIMA E., MERLO-PICH E., NEIDHART S., SURPRENANT A. & BUELL G. (1996) Cloning OF P2X5 and P2X6 receptors and the distribution and properties of an extended family of ATP-gated ion channels. *J.Neurosci.* **16**, 2495-2507.

- COLLO G., NEIDHART S., KAWASHIMA E., KOSCO-VILBOIS M., NORTH R.A. & BUELL G. (1997) Tissue distribution of the P2X7 receptor. *Neuropharmacology* **36**, 1277-1283.
- COMMUNI D., MOTTE S., BOEYNAEMS J.M. & PIROTTON S. (1996) Pharmacological characterization of the human P2Y4 receptor. *Eur.J.Pharmacol.* **317**, 383-389.
- COMMUNI D., PARMENTIER M. & BOEYNAEMS J.M. (1996) Cloning, functional expression and tissue distribution of the human P2Y6 receptor. *Biochem.Biophys.Res.Commun.* **222**, 303-308.
- COMMUNI D. & BOEYNAEMS J.M. (1997) Receptors responsive to extracellular pyrimidine nucleotides. *Trends Pharmacol.Sci.* **18**, 83-86.
- COOK S.P., RODLAND K.D. & MCCLESKEY E.W. (1998) A memory for extracellular Ca<sup>2+</sup> by speeding recovery of P2X receptors from desensitization. *J.Neurosci.* **18**, 9238-9244.
- COOPER S.T. & MILLAR N.S. (1997) Host cell-specific folding and assembly of the neuronal nicotinic acetylcholine receptor alpha7 subunit. *J.Neurochem.* **68**, 2140-2151.
- COUTINHO-SILVA R. & PERSECHINI P.M. (1997). P2Z purinoceptor-associated pores induced by extracellular ATP in macrophages and J774 cells. *Am J Physiol Cell Physiol* **273**, C1793-C1800.
- DEAN D.M. & DOWNIE J.W. (1978) Contribution of adrenergic and "purinergic" neurotransmission to contraction in rabbit detrusor. *J.Pharmacol.Exp.Ther.* **207**, 431-445.
- DEAN D.M. & DOWNIE J.W. (1978) Interaction of prostaglandins and adenosine 5'-triphosphate in the noncholinergic neurotransmission in rabbit detrusor. *Prostaglandins* **16**, 245-251.
- DEMOLOMBE S. & ESCANDE D. (1996) ATP-binding cassette proteins as targets for drug discovery. *Trends Pharmacol.Sci.* **17**, 273-275.
- DENNIS J.W., GRANOVSKY M. & WARREN C.E. (1999) Protein glycosylation in development and disease. *Bioessays* **21**, 412-421.
- DI VIRGILIO F. (1995) The P2Z purinoceptor: an intriguing role in immunity, inflammation and cell death. *Immunol.Today* **16**, 524-528.
- DI VIRGILIO F., MUTINI C., CHIOZZI P., FALZONI S., DI SUSINO M., SANZ J.M. & FERRARI D. (1996) A purinergic hypothesis for immunomodulation. *Ital.J.Biochem.* **45**, 195-203.
- DILL K.A. (1990) Dominant forces in protein folding. *Biochemistry* **29**, 7133-7155.
- DING S. & SACHS F. (1999) Single channel properties of P2X2 purinoceptors. *J.Gen.Physiol* **113**, 695-720.



- DOUPNIK C.A., DAVIDSON N. & LESTER H.A. (1995) The inward rectifier potassium channel family. *Curr.Opin.Neurobiol.* **5**, 268-277.
- DRIESSEN B., VON K., I, BULTMANN R., ELRICK D.B., CUNNANE T.C. & STARKE K. (1994) The fade of the purinergic neurogenic contraction of the guinea-pig vas deferens: analysis of possible mechanisms. *Naunyn Schmiedebergs Arch.Pharmacol.* **350**, 482-490.
- DRURY A.B. & SZENT-GYORGY A. (1929) The physiological activity of adenine compounds with special reference to their action upon the mammalian heart. *J Physiol (Lond)* **68**, 213-237.
- DUBYAK G.R. (1991) Signal transduction by P2-purinergic receptors for extracellular ATP. *Am.J.Respir.Cell Mol.Biol.* **4**, 295-300.
- DUBYAK G.R. & EL MOATASSIM C. (1993) Signal transduction via P2-purinergic receptors for extracellular ATP and other nucleotides. *Am.J.Physiol* **265**, C577-C606
- DUNN P.M., ZHONG Y. & BURNSTOCK G. (2001) P2X receptors in peripheral neurons. *Prog.Neurobiol.* **65**, 107-134.
- DUTTON J.L., HANSEN M.A., BALCAR V.J., BARDEN J.A. & BENNETT M.R. (1999) Development of P2X receptor clusters on smooth muscle cells in relation to nerve varicosities in the rat urinary bladder. *J.Neurocytol.* **28**, 4-16.
- EDWARDS F.A., GIBB A.J. & COLQUHOUN D. (1992) ATP receptor-mediated synaptic currents in the central nervous system. *Nature* **359**, 144-147.
- EGAN T.M., HAINES W.R. & VOIGT M.M. (1998) A domain contributing to the ion channel of ATP-gated P2X2 receptors identified by the substituted cysteine accessibility method. *J.Neurosci.* **18**, 2350-2359.
- ELLSGAARD L., MOLINARI M. & HELENIUS A. (1999) Setting the standards: quality control in the secretory pathway. *Science* **286**, 1882-1888.
- EMBDEN C. & ZIMMERMAN G. (1927) Ueber die Bedeutung der Adenylsaeure. *Hoppe-Seyler's Z Physiol Chem* **167**, 137-140.
- ENNION S., HAGAN S. & EVANS R.J. (2000) The role of positively charged amino acids in ATP recognition by human P2X1 receptors. *J.Biol.Chem.* **275**, 35656
- EVANS R.J., LEWIS C., VIRGINIO C., LUNDSTROM K., BUELL G., SURPRENANT A. & NORTH R.A. (1996) Ionic permeability of, and divalent cation effects on, two ATP-gated cation channels (P2X receptors) expressed in mammalian cells. *J.Physiol (Lond)* **497 ( Pt 2)**, 413-422.
- FIELDS R.D. & STEVENS B. (2000) ATP: an extracellular signaling molecule between neurons and glia. *Trends Neurosci.* **23(12)**:625-33.
- FIRSOV D., GAUTSCHI I., MERILLAT A.M., ROSSIER B.C. & SCHILD L. (1998) The heterotetrameric architecture of the epithelial sodium channel (ENaC). *EMBO J.* **17**, 344-352.

- FIRSOV D., ROBERT-NICOUD M., GRUENDER S., SCHILD L. & ROSSIER B.C. (1999) Mutational analysis of cysteine-rich domains of the epithelium sodium channel (ENaC). Identification of cysteines essential for channel expression at the cell surface. *J.Biol.Chem.* **274**, 2743-2749.
- FORSAYETH J.R., GU Y. & HALL Z.W. (1992) BiP forms stable complexes with unassembled subunits of the acetylcholine receptor in transfected COS cells and in C2 muscle cells. *J.Cell Biol.* **117**, 841-847.
- FROEHNER S.C., LUETJE C.W., SCOTLAND P.B. & PATRICK J. (1990) The postsynaptic 43K protein clusters muscle nicotinic acetylcholine receptors in *Xenopus oocytes*. *Neuron* **5**, 403-410.
- GARCIA-GUZMAN M., SOTO F., LAUBE B. & STUHMER W. (1996) Molecular cloning and functional expression of a novel rat heart P2X purinoceptor. *FEBS Lett.* **388**, 123-127.
- GARCIA-GUZMAN M., STUHMER W. & SOTO F. (1997) Molecular characterization and pharmacological properties of the human P2X3 purinoceptor. *Brain Res.Mol.Brain Res.* **47**, 59-66.
- GARTY H. (1994) Molecular properties of epithelial, amiloride-blockable Na<sup>+</sup> channels. *FASEB J.* **8**, 522-528.
- GAVEL Y. & VON HEIJNE G. (1990) Sequence differences between glycosylated and non-glycosylated Asn-X- Thr/Ser acceptor sites: implications for protein engineering. *Protein Eng* **3**, 433-442.
- GELMAN M.S., CHANG W., THOMAS D.Y., BERGERON J.J. & PRIVES J.M. (1995) Role of the endoplasmic reticulum chaperone calnexin in subunit folding and assembly of nicotinic acetylcholine receptors. *J.Biol.Chem.* **270**, 15085-15092.
- GELMAN M.S. & PRIVES J.M. (1996) Arrest of subunit folding and assembly of nicotinic acetylcholine receptors in cultured muscle cells by dithiothreitol. *J.Biol.Chem.* **271**, 10709-10714.
- GLASS D.J. & YANCOPOULOS G.D. (1997) Sequential roles of agrin, MuSK and rapsyn during neuromuscular junction formation. *Curr.Opin.Neurobiol.* **7**, 379-384.
- GLOOR S., PONGS O. & SCHMALZING G. (1995) A vector for the synthesis of cRNAs encoding Myc epitope-tagged proteins in *Xenopus laevis* oocytes. *Gene* **160**, 213-217.
- GORDON J.L. (1986) Extracellular ATP: effects, sources and fate. *Biochem.J.* **233**, 309-319.
- GREEN W.N. & MILLAR N.S. (1995) Ion-channel assembly. *Trends Neurosci.* **18**, 280-287.
- GREEN W.N. & WANAMAKER C.P. (1997) The role of the cystine loop in acetylcholine receptor assembly. *J.Biol.Chem.* **272**, 20945-20953.

- GUO A., VULCHANOVA L., WANG J., LI X. & ELDE R. (1999) Immunocytochemical localization of the vanilloid receptor 1 (VR1): relationship to neuropeptides, the P2X3 purinoceptor and IB4 binding sites. *Eur.J.Neurosci.* **11**, 946-958.
- GUT A., KAPPELER F., HYKA N., BALDA M.S., HAURI H.P. & MATTER K. (1998) Carbohydrate-mediated Golgi to cell surface transport and apical targeting of membrane proteins. *EMBO J.* **17**, 1919-1929.
- HAAS A.L. & SIEPMANN T.J. (1997) Pathways of ubiquitin conjugation. *FASEB J.* **11**, 1257-1268.
- HAMILTON S.G., WADE A. & MCMAHON S.B. (1999) The effects of inflammation and inflammatory mediators on nociceptive behaviour induced by ATP analogues in the rat. *Br.J.Pharmacol.* **126**, 326-332.
- HAMMOND C. & HELENIUS A. (1995) Quality control in the secretory pathway. *Curr.Opin.Cell Biol.* **7**, 523-529.
- HANSEN M.A., BARDEN J.A., BALCAR V.J., KEAY K.A. & BENNETT M.R. (1997) Structural motif and characteristics of the extracellular domain of P2X receptors. *Biochem.Biophys.Res.Commun.* **236**, 670-675.
- HASHIMOTO M., SHINOZUKA K., BJUR R.A., WESTFALL D.P., HATTORI K. & MASUMURA S. (1995) The effects of age on the release of adenine nucleosides and nucleotides from rat caudal artery. *J.Physiol* **489 ( Pt 3)**, 841-848.
- HEBERT D.N., FOELLMER B. & HELENIUS A. (1996) Calnexin and calreticulin promote folding, delay oligomerization and suppress degradation of influenza hemagglutinin in microsomes. *EMBO J.* **15**, 2961-2968.
- HELENIUS A. (1992) Unpacking the incoming influenza virus. *Cell* **69**, 577-578.
- HELENIUS A. (1994) How N-linked oligosaccharides affect glycoprotein folding in the endoplasmic reticulum. *Mol.Biol.Cell* **5**, 253-265.
- HENNING R.H., DUIN M., DEN HERTOOG A. & NELEMANS A. (1993) Activation of the phospholipase C pathway by ATP is mediated exclusively through nucleotide type P2-purinoceptors in C2C12 myotubes. *Br.J.Pharmacol.* **110**, 747-752.
- HERSHKO A. & CIECHANOVER A. (1992) The ubiquitin system for protein degradation. *Annu.Rev.Biochem.* **61**, 761-807.
- HOLLMANN M. & HEINEMANN S. (1994) Cloned glutamate receptors. *Annu.Rev.Neurosci.* **17**, 31-108.
- HOLMSEN H. (1985) Nucleotide metabolism of platelets. *Annu.Rev.Physiol* **47**, 677-690.
- HOUSLEY G.D., GREENWOOD D., BENNETT T. & RYAN A.F. (1995) Identification of a short form of the P2xR1-purinoceptor subunit produced by alternative splicing in the pituitary and cochlea. *Biochem.Biophys.Res.Commun.* **212**, 501-508.

- HUCHO F., OBERTHUR W. & LOTTSPREICH F. (1986) The ion channel of the nicotinic acetylcholine receptor is formed by the homologous helices M II of the receptor subunits. *FEBS Lett.* **205**, 137-142.
- HUMPHREYS B.D. & DUBYAK G.R. (1996) Induction of the P2z/P2X7 nucleotide receptor and associated phospholipase D activity by lipopolysaccharide and IFN-gamma in the human THP-1 monocytic cell line. *J Immunol.* **15**;157(12):5627-37.
- HURTLEY S.M. & HELENIUS A. (1989) Protein oligomerization in the endoplasmic reticulum. *Annu.Rev.Cell Biol.* **5**, 277-307.
- HUTH J.R., MOUNTJOY K., PERINI F. & RUDDON R.W. (1992) Intracellular folding pathway of human chorionic gonadotropin beta subunit. *J.Biol.Chem.* **267**, 8870-8879.
- ILLES P., FINTA E.P., & NIEBER K. (1993) Neuropeptide Y potentiates via Y2-receptors the inhibitory effect of noradrenaline in rat locus coeruleus neurones. *Naunyn Schmiedebergs Arch Pharmacol.* **348**(5):546-8.
- JAENICKE R. (1991) Protein stability and protein folding. *Ciba Found.Symp.* **161**, 206-216.
- JIANG L.H., RASSENDREN F., SURPRENANT A. & NORTH R.A. (2000) Identification of amino acid residues contributing to the ATP binding site of a purinergic P2X receptor. *J.Biol.Chem.*
- JIANG L.H., RASSENDREN F., SPELTA V., SURPRENANT A. & NORTH R.A. (2001) Amino acid residues involved in gating identified in the first membrane-spanning domain of the rat P2X2 receptor. *J.Biol.Chem.*
- JO Y.H. & SCHLICHTER R. (1999) Synaptic corelease of ATP and GABA in cultured spinal neurons. *Nat.Neurosci.* **2**, 241-245.
- KARLIN A. (1993) Structure of nicotinic acetylcholine receptors. *Curr.Opin.Neurobiol.* **3**, 299-309.
- KATSURAGI T., TOKUNAGA T., OGAWA S., SOEJIMA O., SATO C. & FURUKAWA T. (1991) Existence of ATP-evoked ATP release system in smooth muscles. *J.Pharmacol.Exp.Ther.* **259**, 513-518.
- KHAKH B.S., PROCTOR W.R., DUNWIDDIE T.V., LABARCA C. & LESTER H.A. (1999) Allosteric control of gating and kinetics at P2X(4) receptor channels. *J.Neurosci.* **19**, 7289-7299.
- KHAKH B.S. & HENDERSON G. (2000) Modulation of fast synaptic transmission by presynaptic ligand-gated cation channels. *J.Auton.Nerv.Syst.* **81**, 110-121.
- KHAKH B.S. (2001) Molecular physiology of P2X receptors and ATP signalling at synapses. *Nat.Rev.Neurosci.* **2**, 165-174.
- KHAKH B.S., BURNSTOCK G., KENNEDY C., KING B.F., NORTH R.A., SEGUELA P., VOIGT M. & HUMPHREY P.P. (2001) International union of pharmacology. XXIV. Current status of the nomenclature and properties of P2X receptors and their subunits. *Pharmacol.Rev.* **53**, 107-118.

- KIM M., RAO M.V., TWEARDY D.J., PRAKASH M., GALILI U. & GORELIK E. (1993) Lectin-induced apoptosis of tumour cells. *Glycobiology* **3**, 447-453.
- KIM M., YOO O.J. & CHOE S. (1997) Molecular assembly of the extracellular domain of P2X<sub>2</sub>, an ATP-gated ion channel. *Biochem.Biophys.Res.Commun.* **240**, 618-622.
- KIM M., SPELTA V., SIM J., NORTH R.A. & SURPRENANT A. (2001) Differential assembly of rat purinergic p2x7 receptor in immune cells of the brain and periphery. *J.Biol.Chem.* **276**, 23262-23267.
- KING B.F., TOWNSEND-NICHOLSON A., WILDMAN S.S., THOMAS T., SPYER K.M. & BURNSTOCK G. (2000) Coexpression of rat P2X<sub>2</sub> and P2X<sub>6</sub> subunits in *Xenopus* oocytes. *J.Neurosci.* **20**, 4871-4877.
- KIRSCH J. & BETZ H. (1998) Glycine-receptor activation is required for receptor clustering in spinal neurons. *Nature* **392**, 717-720.
- KLAPPERSTUCK M., BUTTNER C., BOHM T., SCHMALZING G. & MARKWARDT F. (2000) Characteristics of P2X<sub>7</sub> receptors from human B lymphocytes expressed in *Xenopus* oocytes. *Biochim.Biophys.Acta* **1467**, 444-456.
- KOBATA A. (1992) Structures and functions of the sugar chains of glycoproteins. *Eur.J.Biochem.* **209**, 483-501.
- KOPITO R.R. (1997) ER quality control: the cytoplasmic connection. *Cell* **88**, 427-430.
- KOSHIMIZU T., KOSHIMIZU M. & STOJILKOVIC S.S. (1999) Contributions of the C-terminal domain to the control of P2X receptor desensitization. *J.Biol.Chem.* **274**, 37651-37657.
- KOZAK M. (1994) Features in the 5' non-coding sequences of rabbit alpha and beta-globin mRNAs that affect translational efficiency. *J.Mol.Biol.* **235**, 95-110.
- KREIENKAMP H.J., SINE S.M., MAEDA R.K. & TAYLOR P. (1994) Glycosylation sites selectively interfere with alpha-toxin binding to the nicotinic acetylcholine receptor. *J.Biol.Chem.* **269**, 8108-8114.
- KUHSE J., BETZ H. & KIRSCH J. (1995) The inhibitory glycine receptor: architecture, synaptic localization and molecular pathology of a postsynaptic ion-channel complex. *Curr Op Neurobiol.* **5**, 318-323.
- KUJAWA M., TEDDE-PIRAS A., & TEDDE G. (1984) Ultrastructural morphometric characteristics of the cumulus oophorus and corona radiata cells in antral follicles of the rat ovary. *Arch Ital Anat Embriol.* **89**(3-4):167-82.
- LAMBRECHT G., RETTINGER J., BAUMERT H.G., CZECH S., DAMER S., GANSO M., HILDEBRANDT C., NIEBEL B., SPATZ-KUMBEL G., SCHMALZING G. & MUTSCHLER E. (2000) The novel pyridoxal-5'-phosphate derivative PPNSD potently antagonizes activation of P2X<sub>1</sub> receptors. *Eur.J.Pharmacol.* **387**, R19-R21

- LAMMAS D.A., STOBER C., HARVEY C.J., KENDRICK N., PANCHALINGAM S. & KUMARARATNE D.S. (1997) ATP-induced killing of mycobacteria by human macrophages is mediated by purinergic P2Z(P2X7) receptors. *Immunity* **7**, 433-444.
- LE NOVERE N. & CHANGEUX J.P. (1999) The Ligand Gated Ion Channel Database. *Nucleic Acids Res.* **27**, 340-342.
- LE K.T., BABINSKI K. & SEQUELA P. (1998) Central P2X4 and P2X6 channel subunits coassemble into a novel heteromeric ATP receptor. *J.Neurosci.* **18**, 7152-7159.
- LECONTE I., AUZAN C., DEBANT A., ROSSI B. & CLAUSER E. (1992) N-linked oligosaccharide chains of the insulin receptor beta subunit are essential for transmembrane signaling. *J.Biol.Chem.* **267**, 17415-17423.
- LEITE J.F. & CASCIO M. (2001) Structure of ligand-gated ion channels: critical assessment of biochemical data supports novel topology. *Mol.Cell Neurosci.* **17**, 777-792.
- LEWIS C., NEIDHART S., HOLY C., NORTH R.A., BUELL G. & SURPRENANT A. (1995) Coexpression of P2X2 and P2X3 receptor subunits can account for ATP-gated currents in sensory neurons [see comments]. *Nature* **377**, 432-435.
- LUSTIG K.D., SHIAU A.K., BRAKE A.J. & JULIUS D. (1993) Expression cloning of an ATP receptor from mouse neuroblastoma cells. *Proc.Natl.Acad.Sci.U.S.A* **90**, 5113-5117.
- MAIMONE M.M. & MERLIE J.P. (1993) Interaction of the 43 kd postsynaptic protein with all subunits of the muscle nicotinic acetylcholine receptor. *Neuron* **11**, 53-66.
- MCLEAN J.S., KRUGER H., SWIFT D., TANG E.K. & BRENNAND J.C. (1995) Cell-based assay for functional screening of compounds active at the human endothelin A receptor. *J.Cardiovasc.Pharmacol.* **26**, 978-982.
- MELIKIAN H.E., RAMAMOORTHY S., TATE C.G. & BLAKELY R.D. (1996) Inability to N-glycosylate the human norepinephrine transporter reduces protein stability, surface trafficking, and transport activity but not ligand recognition. *Mol.Pharmacol.* **50**, 266-276.
- MERLIE J.P. & LINDSTROM J. (1983) Assembly in vivo of mouse muscle acetylcholine receptor: identification of an alpha subunit species that may be an assembly intermediate. *Cell* **34**, 747-757.
- MICHALAK M., CORBETT E.F., MESAELI N., NAKAMURA K. & OPAS M. (1999) Calreticulin: one protein, one gene, many functions. *Biochem.J.* **344 Pt 2**, 281-292.
- MORTIMORE G.E., HUTSON N.J. & SURMACZ C.A. (1983) Quantitative correlation between proteolysis and m. *Proc.Natl.Acad.Sci.U.S.A* **80**, 2179-2183.
- MOSBACHER J., SCHOEPFER R., MONYER H., BURNASHEV N., SEEBURG P.H. & RUPPERSBERG J.P. (1994) A molecular determinant for submillisecond desensitization in glutamate receptors. *Science* **266**, 1059-1062.

- MULRYAN K., GITTERMAN D.P., LEWIS C.J., VIAL C., LECKIE B.J., COBB A.L., BROWN J.E., CONLEY E.C., BUELL G., PRITCHARD C.A. & EVANS R.J. (2000) Reduced vas deferens contraction and male infertility in mice lacking P2X1 receptors. *Nature* **403**, 86-89.
- NAKAZAWA K., INOUE K. & OHNO Y. (1998) An asparagine residue regulating conductance through P2X2 receptor/channels. *Eur.J.Pharmacol.* **347**, 141-144.
- NEARY J.T., RATHBONE M.P., CATTABENI F., ABBRACCHIO M.P. & BURNSTOCK G. (1996) Trophic actions of extracellular nucleotides and nucleosides on glial and neuronal cells. *Trends Neurosci.* **19**, 13-18.
- NEWBOLT A., STOOP R., VIRGINIO C., SURPRENANT A., NORTH R.A., BUELL G. & RASSENDREN F. (1998) Membrane topology of an ATP-gated ion channel (P2X receptor). *J.Biol.Chem.* **273**, 15177-15182.
- NEWMAN E.A. & ZAHS K.R. (1997) Calcium waves in retinal glial cells. *Science* **275**, 844-847.
- NICKE A., BAUMERT H.G., RETTINGER J., EICHELE A., LAMBRECHT G., MUTSCHLER E. & SCHMALZING G. (1998) P2X1 and P2X3 receptors form stable trimers: a novel structural motif of ligand-gated ion channels. *EMBO J.* **17**, 3016-3028.
- NICKE A., RETTINGER J., BUTTNER C., EICHELE A., LAMBRECHT G. & SCHMALZING G. (1999) Evolving view of quaternary structures of ligand-gated ion channels. *Prog.Brain Res.* **120**, 61-80.
- NILSSON I.M. & VON HEIJNE G. (1993) Determination of the distance between the oligosaccharyltransferase active site and the endoplasmic reticulum membrane. *J.Biol.Chem.* **268**, 5798-5801.
- NISHIMUNE A., ISAAC J.T., MOLNAR E., NOEL J., NASH S.R., TAGAYA M., COLLINGRIDGE G.L., NAKANISHI S. & HENLEY J.M. (1998) NSF binding to GluR2 regulates synaptic transmission. *Neuron* **21**, 87-97.
- NORI S., FUMAGALLI L., BO X., BOGDANOV Y. & BURNSTOCK G. (1998) Coexpression of mRNAs for P2X1, P2X2 and P2X4 receptors in rat vascular smooth muscle: an in situ hybridization and RT-PCR study. *J.Vasc.Res.* **35**, 179-185.
- NORTH R.A. (1996) Families of ion channels with two hydrophobic segments. *Curr.Opin.Cell Biol.* **8**, 474-483.
- NOVAKOVIC S.D., KASSOTAKIS L.C., OGLESBY I.B., SMITH J.A., EGLEN R.M., Ford A.P., HUNTER J.C. (1999) Immunocytochemical localization of P2X3 purinoceptors in sensory neurons in naive rats and following neuropathic injury. *Pain.* **80**(1-2):273-82.
- OSTEN P., SRIVASTAVA S., INMAN G.J., VILIM F.S., KHATRI L., LEE L.M., STATES B.A., EINHEBER S., MILNER T.A., HANSON P.I. & ZIFF E.B. (1998) The AMPA receptor GluR2 C terminus can mediate a reversible, ATP- dependent interaction with NSF and a. *Neuron* **21**, 99-110.

- PARKER K.E. (1998) Modulation of ATP-gated non-selective cation channel (P2X1 receptor) activation and desensitization by the actin cytoskeleton. *J.Physiol* **510** (Pt 1), 19-25.
- PARODI A.J. (1999) Reglucosylation of glycoproteins and quality control of glycoprotein folding in the endoplasmic reticulum of yeast cells. *Biochim.Biophys.Acta* **1426**, 287-295.
- PAULSON H.L., ROSS A.F., GREEN W.N. & CLAUDIO T. (1991) Analysis of early events in acetylcholine receptor assembly. *J.Cell Biol.* **113**, 1371-1384.
- PHILLIPS W.D., LAI K. & BENNETT M.R. (1985) Spatial distribution and size of acetylcholine receptor clusters determined by motor nerves in developing chick muscles. *J.Neurocytol.* **14**, 309-325.
- PHILLIPS W.D. & BENNETT M.R. (1987) Elimination of distributed acetylcholine receptor clusters from developing fast-twitch fibres in an avian muscle. *J.Neurocytol.* **16**, 1-10.
- PHILLIPS W.D. & BENNETT M.R. (1989) The distribution of intracellular acetylcholine receptors and nuclei in developing avian fast-twitch muscle fibres during synapse elimination. *J.Neurocytol.* **18**, 241-255.
- PINNA C., PUGLISI L. & BURNSTOCK G. (1998) ATP and vasoactive intestinal polypeptide relaxant responses in hamster isolated proximal urethra. *Br.J.Pharmacol.* **124**, 1069-1074.
- PINTOR J., DIAZ-HERNANDEZ M., BUSTAMANTE C., GUALIX J., DE TERREROS F.J. & MIRAS-PORTUGAL M.T. (1999) Presence of dinucleotide and ATP receptors in human cerebrocortical synaptic terminals. *Eur.J.Pharmacol.* **366**, 159-165.
- RADFORD K.M., VIRGINIO C., SURPRENANT A., NORTH R.A. & KAWASHIMA E. (1997) Baculovirus expression provides direct evidence for heteromeric assembly of P2X2 and P2X3 receptors. *J.Neurosci.* **17**, 6529-6533.
- RAGOZZINO D., FUCILE S., GIOVANNELLI A., GRASSI F., MILEO A.M., BALLIVET M., ALEMA S. & EUSEBI F. (1997) Functional properties of neuronal nicotinic acetylcholine receptor channels expressed in transfected human cells. *Eur.J.Neurosci.* **9**, 480-488.
- RALEVIC V. & BURNSTOCK G. (1998) Receptors for purines and pyrimidines. *Pharmacol.Rev.* **50**, 413-492.
- RAMARAO M.K. & COHEN J.B. (1998) Mechanism of nicotinic acetylcholine receptor cluster formation by rapsyn. *Proc.Natl.Acad.Sci.U.S.A* **95**, 4007-4012.
- RANGWALA F., DRISDEL R.C., RAKHILIN S., KO E., ATLURI P., HARKINS A.B., FOX A.P., SALMAN S.S. & GREEN W.N. (1997) Neuronal alpha-bungarotoxin receptors differ structurally from other nicotinic acetylcholine receptors. *J.Neurosci.* **17**, 8201-8212.



- RASSENDREN F., BUELL G., NEWBOLT A., NORTH R.A. & SURPRENANT A. (1997) Identification of amino acid residues contributing to the pore of a P2X receptor. *EMBO J.* **16**, 3446-3454.
- RASSENDREN F., BUELL G.N., VIRGINIO C., COLLO G., NORTH R.A. & SURPRENANT A. (1997) The permeabilizing ATP receptor, P2X7. Cloning and expression of a human cDNA. *J.Biol.Chem.* **272**, 5482-5486.
- RECHSTEINER M. (1987) Ubiquitin-mediated pathways for intracellular proteolysis. *Annu.Rev.Cell Biol.* **3**, 1-30.
- RETTINGER J., ASCHRAFI A. & SCHMALZING G. (2000) Roles of Individual N-glycans for ATP Potency and Expression of the Rat P2X1 Receptor. *J.Biol.Chem.*
- REVAH F., BERTRAND D., GALZI J.L., DEVILLERS-THIERY A., MULLE C., HUSSY N., BERTRAND S., BALLIVET M. & CHANGEUX J.P. (1991) Mutations in the channel domain alter desensitization of a neuronal nicotinic receptor. *Nature* **353**, 846-849.
- ROBITAILLE R. (1995) Purinergic receptors and their activation by endogenous purines at perisynaptic glial cells of the frog neuromuscular junction. *J.Neurosci.* **15**, 7121-7131.
- ROTIN D., BAR-SAGI D., O'BRODOVICH H., MERILAINEN J., LEHTO V.P., CANESSA C.M., ROSSIER B.C. & DOWNEY G.P. (1994) An SH3 binding region in the epithelial Na<sup>+</sup> channel (alpha rENaC) mediates its localization at the apical membrane. *EMBO J.* **13**, 4440-4450.
- RUPPELT A., MA W., BORCHARDT K., SILBERBERG S.D., & SOTO F. (2001) Genomic structure, developmental distribution and functional properties of the chicken P2X(5) receptor. *J Neurochem.* **77**(5):1256-65.
- SAWYNOK J. & REID A. (1997) Peripheral adenosine 5'-triphosphate enhances nociception in the formalin test via activation of a purinergic p2X receptor. *Eur.J.Pharmacol.* **330**, 115-121.
- SCHAGGER H. & VON JAGOW G. (1991) Blue native electrophoresis for isolation of membrane protein complexes in enzymatically active form. *Anal.Biochem.* **199**, 223-231.
- SCHAGGER H., CRAMER W.A. & VON JAGOW G. (1994) Analysis of molecular masses and oligomeric states of protein complexes by blue native electrophoresis and isolation of membrane protein complexes by two-dimensional native electrophoresis. *Anal.Biochem.* **217**, 220-230.
- SCHMALZING G., GLOOR S., OMAI H., KRONER S., APPELHANS H. & SCHWARZ W. (1991) Up-regulation of sodium pump activity in *Xenopus laevis* oocytes by expression of heterologous beta 1 subunits of the sodium pump. *Biochem.J.* **279** ( Pt 2), 329-336.
- SCHMIDT J.W. & CATTERALL W.A. (1986) Biosynthesis and processing of the alpha subunit of the voltage-sensitive sodium channel in rat brain neurons. *Cell* **46**, 437-444.

- SEEBURG P.H. (1993) The TINS/TIPS Lecture. The molecular biology of mammalian glutamate receptor channels. *Trends Neurosci.* **16**, 359-365.
- SEGAL M.S., BYE J.M., SAMBROOK J.F. & GETHING M.J. (1992) Disulfide bond formation during the folding of influenza virus hemagglutinin. *J.Cell Biol.* **118**, 227-244.
- SHAKIN-ESHLEMAN S.H., SPITALNIK S.L. & KASTURI L. (1996) The amino acid at the X position of an Asn-X-Ser sequon is an important determinant of N-linked core-glycosylation efficiency. *J.Biol.Chem.* **271**, 6363-6366.
- SHENG Z. & DEUTSCH C. (1998) Assembly of ion channels. *Methods Enzymol.* **293**, 17-32.
- SILVERSTEIN S.C., STEINMAN R.M. & COHN Z.A. (1977) Endocytosis. *Annu.Rev.Biochem.* **46**, 669-722.
- SIMON J., KIDD E.J., SMITH F.M., CHESSELL I.P., MURRELL-LAGNADO R., HUMPHREY P.P. & BARNARD E.A. (1997) Localization and functional expression of splice variants of the P2X2 receptor. *Mol.Pharmacol.* **52**, 237-248.
- SMITH F.M., HUMPHREY P.P. & MURRELL-LAGNADO R.D. (1999) Identification of amino acids within the P2X2 receptor C-terminus that regulate desensitization. *J.Physiol* **520 Pt 1**, 91-99.
- SOMMER T. & WOLF D.H. (1997) Endoplasmic reticulum degradation: reverse protein flow of no return. *FASEB J.* **11**, 1227-1233.
- SOTO F., GARCIA-GUZMAN M., KARSCHIN C. & STUHMER W. (1996) Cloning and tissue distribution of a novel P2X receptor from rat brain. *Biochem.Biophys.Res.Commun.* **223**, 456-460.
- SOTO F., GARCIA-GUZMAN M. & STUHMER W. (1997) Cloned ligand-gated channels activated by extracellular ATP (P2X receptors). *J.Membr.Biol.* **160**, 91-100.
- SOUSLOVA V., RAVENALL S., FOX M., WELLS D., WOOD J.N., AKOPIAN A.N. (1997) Structure and chromosomal mapping of the mouse P2X3 gene. *Gene.* **195(1)**:101-
- STEVENS B. & FIELDS R.D. (2000) Response of Schwann cells to action potentials in development. *Science* **287**, 2267-2271.
- STOJILKOVIC S.S. & KOSHIMIZU T. (2001) Signaling by extracellular nucleotides in anterior pituitary cells. *Trends Endocrinol.Metab* **12**, 218-225.
- SUKHAREV S.I., BLOUNT P., MARTINAC B., BLATTNER F.R. & KUNG C. (1994) A large-conductance mechanosensitive channel in E. coli encoded by mscL alone. *Nature* **368**, 265-268.
- SUKHAREV S.I., SCHROEDER M.J., & MCCASLIN D.R. (1999) Stoichiometry of the large conductance bacterial mechanosensitive channel of E. coli. A biochemical study. *J Membr Biol.* **171(3)**:183-93.

- SURPRENANT A. (1996) Functional properties of native and cloned P2X receptors. *Ciba Found. Symp.* **198**:208-222.
- SURPRENANT A., RASSENDREN F., KAWASHIMA E., NORTH R.A. & BUELL G. (1996) The cytolitic P2Z receptor for extracellular ATP identified as a P2X receptor (P2X7). *Science* **272**, 735-738.
- TANAKA J., MURATE M., WANG C.Z., SEINO S., & IWANAGA T. (1996) Cellular distribution of the P2X4 ATP receptor mRNA in the brain and non-neuronal organs of rats. *Arch Histol Cytol.* **59**(5):485-90.
- THOMPSON J.A., LAU A.L. & CUNNINGHAM D.D. (1987) Selective radiolabeling of cell surface proteins to a high specific activity. *Biochemistry* **26**, 743-750.
- TORRES G.E., HAINES W.R., EGAN T.M. & VOIGT M.M. (1998) Co-expression of P2X1 and P2X5 receptor subunits reveals a novel ATP-gated ion channel. *Mol.Pharmacol.* **54**, 989-993.
- TORRES G.E., EGAN T.M. & VOIGT M.M. (1998) N-Linked glycosylation is essential for the functional expression of the recombinant P2X2 receptor. *Biochemistry* **37**, 14845-14851.
- TORRES G.E., EGAN T.M. & VOIGT M.M. (1999) Identification of a domain involved in ATP-gated ionotropic receptor subunit assembly. *J.Biol.Chem.* **274**, 22359-22365.
- TOWNSEND-NICHOLSON A., KING B.F., WILDMAN S.S. & BURNSTOCK G. (1999) Molecular cloning, functional characterization and possible cooperativity between the murine P2X4 and P2X4a receptors. *Brain Res.Mol.Brain Res.* **64**, 246-254.
- TROADEC J.D., THIRION S., NICAISE G., LEMOS J.R., & DAYANITHI G. (1998) ATP-evoked increases in  $[Ca^{2+}]_i$  and peptide release from rat isolated neurohypophysial terminals via a P2X2 purinoceptor. *J Physiol.* **511** ( Pt 1):89-103.
- TROMBETTA E.S. & HELENIUS A. (1998) Lectins as chaperones in glycoprotein folding. *Curr.Opin.Struct.Biol.* **8**, 587-592.
- TROMBETTA E.S. & HELENIUS A. (2000) Conformational requirements for glycoprotein reglucosylation in the endoplasmic reticulum. *J.Cell Biol.* **148**, 1123-1129.
- URADE R. & KITO M. (1992) Inhibition by acidic phospholipids of protein degradation by ER-60 protease, a novel cysteine protease, of endoplasmic reticulum. *FEBS Lett.* **312**, 83-86.
- VALERA S., HUSSY N., EVANS R.J., ADAMI N., NORTH R.A., SURPRENANT A. & BUELL G. (1994) A new class of ligand-gated ion channel defined by P2x receptor for extracellular ATP [see comments]. *Nature* **371**, 516-519.
- VALERA S., TALABOT F., EVANS R.J., GOS A., ANTONARAKIS S.E., MORRIS M.A. & BUELL G.N. (1995) Characterization and chromosomal localization of a human P2X receptor from the urinary bladder. *Receptors.Channels* **3**, 283-289.

- VASSILAKOS A., MICHALAK M., LEHRMAN M.A. & WILLIAMS D.B. (1998) Oligosaccharide binding characteristics of the molecular chaperones calnexin and calreticulin. *Biochemistry* **37**, 3480-3490.
- VASSORT G. (2001) Adenosine 5'-triphosphate: a P2-purinergic agonist in the myocardium. *Physiol Rev.* **81**, 767-806.
- VERKHRATSKY A., ORKAND R.K. & KETTENMANN H. (1998) Glial calcium: homeostasis and signaling function. *Physiol Rev.* **78**, 99-141.
- VIRGINIO C., CHURCH D., NORTH R.A. & SURPRENANT A. (1997) Effects of divalent cations, protons and calmidazolium at the rat P2X7 receptor. *Neuropharmacology* **36**, 1285-1294.
- VIRGINIO C., NORTH R.A. & SURPRENANT A. (1998) Calcium permeability and block at homomeric and heteromeric P2X2 and P2X3 receptors, and P2X receptors in rat nodose neurones. *J.Physiol (Lond)* **510 ( Pt 1)**, 27-35.
- VIRGINIO C., MACKENZIE A., RASSENDREN F.A., NORTH R.A. & SURPRENANT A. (1999) Pore dilation of neuronal P2X receptor channels. *Nat.Neurosci.* **2**, 315-321.
- VLAJKOVIC S.M., THORNE P.R., MUNOZ D.J. & HOUSLEY G.D. (1996) Ectonucleotidase activity in the perilymphatic compartment of the guinea pig cochlea. *Hear.Res.* **99**, 31-37.
- VON HEIJNE G. (1992) Membrane protein structure prediction. Hydrophobicity analysis and the positive-inside rule. *J.Mol.Biol.* **225**, 487-494.
- VULCHANOVA L., RIEDL M.S., SHUSTER S.J., BUELL G., SURPRENANT A., NORTH R.A. & ELDE R. (1997) Immunohistochemical study of the P2X2 and P2X3 receptor subunits in rat and monkey sensory neurons and their central terminals. *Neuropharmacology* **36**, 1229-1242.
- WEBB T.E., SIMON J., KRISHEK B.J., BATESON A.N., SMART T.G., KING B.F., BURNSTOCK G. & BARNARD E.A. (1993) Cloning and functional expression of a brain G-protein-coupled ATP receptor. *FEBS Lett.* **324**, 219-225.
- WERNER P., SEWARD E.P., BUELL G.N. & NORTH R.A. (1996) Domains of P2X receptors involved in desensitization. *Proc.Natl.Acad.Sci.U.S.A* **93**, 15485-15490.
- WILLIAMS C.A. & FORRESTER T. (1983) Possible source of adenosine triphosphate released from rat myocytes in response to hypoxia and acidosis. *Cardiovasc.Res.* **17**, 301-312.
- WU J.S. & LEVER J.E. (1994) N-linked glycosylation is not required for Na<sup>+</sup>/glucose symport activity in LLC-PK1 cells. *Biochim.Biophys.Acta* **1192**, 289-292.
- WYSS D.F., CHOI J.S., LI J., KNOPPERS M.H., WILLIS K.J., ARULANANDAM A.R., SMOLYAR A., REINHERZ E.L. & WAGNER G. (1995) Conformation and function of the N-linked glycan in the adhesion domain of human CD2. *Science* **269**, 1273-1278.

- YAKEL J.L., LAGRUTTA A., ADELMAN J.P. & NORTH R.A. (1993) Single amino acid substitution affects desensitization of the 5- hydroxytryptamine type 3 receptor expressed in *Xenopus* oocytes. *Proc.Natl.Acad.Sci.U.S.A* **90**, 5030-5033.
- YOSHIMURA N. & DE GROAT W.C. (1997) Neural control of the lower urinary tract. *Int.J.Urol.* **4**, 111-125.
- YU C.R. & ROLE L.W. (1998) Functional contribution of the alpha7 subunit to multiple subtypes of nicotinic receptors in embryonic chick sympathetic neurones. *J.Physiol* **509 ( Pt 3)**, 651-665.
- ZHOU Z., MONSMA L.R. & HUME R.I. (1998) Identification of a site that modifies desensitization of P2X2 receptors. *Biochem.Biophys.Res.Commun.* **252**, 541-545.

## 8. Appendix

### 8.1. Oligodeoxynucleotides

#### 8.1.1. Oligodeoxynucleotide primers used for site-directed mutagenesis

(mutated codons are indicated by shaded boxes)

Mutated construct	Primer	Sequence (5'→3')
His-P2X <sub>1</sub> .N153Q (ΔN1)	492	CTGTGTGCCCTTCCAGGGCACTGTGAAG ( <i>sense</i> )
	493	CTTCACAGTGCCCTGGAAGGGCACACAG ( <i>antisense</i> )
His-P2X <sub>1</sub> .N184Q (ΔN2)	494	CTTCGTGAGGCTGAGCAGTTCACCCTCTTC ( <i>sense</i> )
	495	GAAGAGGGTGAAGTCTCAGCCTCACGAAG ( <i>antisense</i> )
His-P2X <sub>1</sub> .N210Q (ΔN3)	506	GTAGAGGAGGTGCAGGGCACCTACATGAAG ( <i>sense</i> )
	507	CTTCATGTAGGTGCCCTGCACCTCCTCTAC ( <i>antisense</i> )
His-P2X <sub>1</sub> .N284Q (ΔN4)	508	CTGTATGGGAGAAGCAGCTGTCTCCAGGC ( <i>sense</i> )
	509	GCCTGGAGACAGCTGCTTCTCCCATACAG ( <i>antisense</i> )
His-P2X <sub>1</sub> .N300Q (ΔN5)	519	GCCAGGCATTTCTGTCAGCAGGGGACAAACCGTCG ( <i>sense</i> )
	520	CGACGGTTTGTCCCCTGCTGCACGAAATGCCTGGC ( <i>antisense</i> )
His-rP2X <sub>1</sub> .C117S (ΔC1)	642	GACTCAAGGCCATTCTGCAGAGAACCCAG ( <i>sense</i> )
	643	CTGGGTTCTCTGCAGAATGGCCTTGAGTC ( <i>antisense</i> )
His-rP2X <sub>1</sub> .C126S (ΔC2)	652	CAGAAGTGGCATATCCAGGATGACAGTG ( <i>sense</i> )
	653	CACTGTCATCCTGGGATATGCCACCTTCTG ( <i>antisense</i> )
His-rP2X <sub>1</sub> .C132S (ΔC3)	654	GGATGACAGTGGCTCCACTCCAGGAAAAG ( <i>sense</i> )
	655	CTTTTCTGGAGTGGAGCCACTGTCATCC ( <i>antisense</i> )
His-rP2X <sub>1</sub> .C149S (ΔC4)	656	CGCACAGGCAACTCTGTGCCCTTCAATG ( <i>sense</i> )
	657	CATTGAAGGGCACAGAGTTGCCTGTGCG ( <i>antisense</i> )
His-rP2X <sub>1</sub> .C159S (ΔC5)	658	GGCACTGTGAAGACATCTGAGATCTTTGGTTGG ( <i>sense</i> )
	659	CCAACCAAAGATCTCAGATGTCTTCACAGTGCC ( <i>antisense</i> )
His-rP2X <sub>1</sub> .C165S (ΔC6)	660	GAGATCTTTGGTTGGTCTCCTGTAGAGGTGG ( <i>sense</i> )
	661	CCACCTCTACAGGAGACCAACCAAAGATCTC ( <i>antisense</i> )
His-rP2X <sub>1</sub> .C217S (ΔC7)	678	GCACCTACATGAAGAAGTCCCTCTATCACAAGATTC ( <i>sense</i> )
	679	GAATCTTGTGATAGAGGGACTTCTTCATGTAGGTGC ( <i>antisense</i> )
His-rP2X <sub>1</sub> .C227S (ΔC8)	680	CAACACCCCTGTCCCCAGTCTTCAAC ( <i>sense</i> )
	681	GTTGAAGACTGGGGACAGGGGGTGTG ( <i>antisense</i> )

Mutated construct	Primer	Sequence (5'→3')
His-rP2X <sub>1</sub> . C261S (ΔC9)	682	CCATTGACTGGAAGTCTGATCTGGACTGGC ( <i>sense</i> )
	683	GCCAGTCCAGATCAGACTTCCAGTCAATGG ( <i>antisense</i> )
His-rP2X <sub>1</sub> . C270S (ΔC10)	684	GGCACGTTCCGGCACTCCAAACCCATCTAC ( <i>sense</i> )
	685	GTAGATGGGTTTGGAGTGCCGAACGTGCC ( <i>antisense</i> )
His-rP2X <sub>1</sub> . C353S (ΔC11)	686	GTGGCCACAGTGCTTTCTGATCTCTTATTGCTC ( <i>sense</i> )
	687	GAGCAATAAGAGATCAGAAAGCACTGTGGCCAC ( <i>antisense</i> )
His-rP2X <sub>2</sub> . N239Q	947	GAGAAGGCAGGAGAGCAATTCACAGAACTGGCAC ( <i>sense</i> )
	948	GTGCCAGTTCTGTGAATTGCTCTCCTGCCTTCTC ( <i>antisense</i> )

### 8.1.2. Oligodeoxynucleotide primers used for sequencing

Sequenced construct	Primer	Sequence (5'→3')
pNKS2	565 or 436 (SP6)	CATACACATACGATTTAGGTGACAC
	52 (T7)	TAATACGACTCACTATAGGG
	72	AACTGTTGGGAAGGGCGATC
P2X <sub>1</sub> . pNKS2	78	AAGAGATCACAAAGCACTGT
	479	ACTCCAGGAAAAGCAGAA
P2X <sub>2</sub> . pNKS2	498	GACGACGACTGTATTGC
	499	CCACTGCTCTGACCTC
	515	GGGATTCGCACAGGGCAC

### 8.1.3. Oligodeoxynucleotide primers used for insertion or deletion of a restriction site into constructs

Construct	Primer	Sequence (5'→3')
Deletion of Nco I from P2X <sub>2</sub> .pNKS2	488	CACTGTGTACCCTATTATCATGGGGACTCCAAG ( <i>sense</i> )
	489	CTTGGAGTCCCCATGATAATAGGGTACACAGTG ( <i>antisense</i> )
Insertion of Sna BI into P2X <sub>4</sub> .pNKS2	513	GGCCTACGTCATCGGGTACGTATTTGTGTGGGAAAAGGGC ( <i>sense</i> )
	514	GCCCTTTTCCCACACAAATACGTACCCGATGACGTAGGCC ( <i>antisense</i> )
Insertion of Sna BI into P2X <sub>1</sub> .pNKS2	502	GTTTCTGGTCTACGTCATTGGGTACGTATTTGTCTATGAAAAA GG ( <i>sense</i> )
	503	CCTTTTTCATAGACAAATACGTACCCAATGACGTAGACCAGAA CC ( <i>antisense</i> )
Insertion of Sna BI into P2X <sub>2</sub> .pNKS2	504	CTTCGTGTGGTACGTATTCATCGTGCAGAAAAGC ( <i>sense</i> )
	505	GCTTTTCTGCACGATGAATACGTACCACACGAAG ( <i>antisense</i> )
Insertion of Sna BI into P2X <sub>3</sub> .pNKS2	527	GCTGCTGATTATCTCCTACTTTGTGGGGTACGTATTCTTGCAT GAG ( <i>sense</i> )
	528	CTCATGCAAGAATACGTACCCACAAAGTAGGAGATAATCAGC AGC ( <i>antisense</i> )
Insertion of Bsp EI into P2X <sub>1</sub> .pNKS2	525	GGATGGTGTGCTGGTCCGGAACAAGAAGGTGGG ( <i>sense</i> )
	526	CCCACCTTCTTGTTCGGACCAGCACCATCC ( <i>antisense</i> )
Insertion of Nco I into P2X <sub>5</sub> .pNKS4	535	GTGAGCTGGAGCCATGGGCCAGGCG ( <i>sense</i> )
	536	CGCCTGGCCCATGGCTCCAGCTCAC ( <i>antisense</i> )



### 8.1.4. Oligodeoxynucleotide primers inserted into constructs

Description	Primer	Sequence (5'→3')
N-terminal hexahistidin tag	496	CGAAGTAGCCACCATGGCACACCACCACCACCA ( <i>sense</i> )
	497	CATGTGGTGGTGGTGGTGGTGTGCCATGGTGGCTACTTCGACGT ( <i>antisense</i> )
First transmembrane domain of P2X <sub>2</sub>	529	CCGGAATCGGCGCCTGGGATTCGTGCACCGCATGGTGCAGCTGCTCATCTGCTTTACTTCGTGTGGTAC ( <i>sense</i> )
	530	GTACCACACGAAGTAAAGCAGGATGAGCAGCTGCACCATGCCGTGCACGAATCCCAGGCGCCGATT ( <i>antisense</i> )
N-terminal hexahistidin tag and Kozak sequence	547	AGCTTCAACAAACAACAAGTCCGACGTCAAGTAGCCACCATGGCACACCACCACCACCA ( <i>sense</i> )
	548	CATGTGGTGGTGGTGGTGGTGTGCCATGGTGGCTACTTCGACGTCCGACTTTGTTGTTTGTGA ( <i>antisense</i> )
Introduction of stop codons into C-terminus of His-P2X <sub>2</sub>	719	ATCAGGTTGATAGTAATAGACTAGT ( <i>sense</i> )
	720	CTAGACTAGTCTATTACTATCAACCTGA ( <i>antisense</i> )
Kozak sequence	423	AGCTAACAACAAGAACAACAACAAGTCCGACGTCGAA GTAGCCAC ( <i>sense</i> )
	424	CATGGTGGCTACTTCGACGTCGGACTTTGTTGTTTGTGTTCT TTGTTGTT ( <i>antisense</i> )

### 8.2. Glossary of Abbreviation

$\alpha,\beta$ -met-ATP	$\alpha,\beta$ -methyleneadenosine-5'-triphosphate
Ach	Acetylcholine
ADP	Adenosine-5'-diphosphate
AMPA	$\alpha$ -Amino-3-hydroxy-5-methyl-4-isoaxole propionic acid
ATP	Adenosine-5'-triphosphate
ATP <sup>4-</sup>	Fully ionized form of Adenosine-5'-triphosphate
Bistris	2,2-Bis-(hydroxyethyl)-(iminotris)-(hydroxymethyl) methane
BN-PAGE	Blue native polyacrylamide gel electrophoresis
BzATP	Benzoylbenzonic-adenosine-5'-triphosphate
C-terminus	carboxyl (COOH) terminus
CHAPS	3-[(3-Cholamidopropyl)dimethylammonio]-1-propane-sulfonate
CNS	Central nervous system

DMSO	Dimethylsulfoxide
DNA	Deoxyribonucleic acid
DRG	Dorsal root ganglion
DTT	Dithiothreitol
EC <sub>50</sub>	Concentration of agonist producing half maximal effect
EDTA	Ethylenediamine tetra-acetic acid
EnaC	Epithelial Na <sup>+</sup> channel
Endo H	Endoglycosidase H
ER	Endoplasmatic reticulum
G protein	Guanine nucleotide-binding protein
GABA	γ-aminobutyric acid
Glu	Glutamate
GluR	Glutamate receptor subunit
GlyR	Glycine receptor
GT	glucosyltransferase
h	hour
HEK cells	Human embryonic kidney cells
HEPES	N-2-Hydroxyethylpiperazine-N'-2-ethansulphonic acid
5-HT <sub>3</sub> R	Ionotropic 5-Hydroxytryptamine (Serotonin) receptor
IP	Isoelectric point
IP3	Inositol-1,4,5-triphosphate
kb	Kilo bases
kD	Kilo Dalton
Kir	Inward-rectifier K <sup>+</sup> channel
LGICS	ligand-gated ion channel superfamily
min	Minute
2-MeSATP	2-Methylthioadenosine-5'-triphosphate
ms	Milliseconds
mscL	Mechanosensitive channel of <i>E. Coli</i>
N-terminus	Amino (NH <sub>2</sub> ) -terminus
NA	Noradrenaline
nAChR	Nicotinic acetylcholine receptor
Ni <sup>2+</sup> -NTA	Ni <sup>2+</sup> .-Nitriloacetic acid
NMDA	N-Methyl-D-aspartate
P2X	Ionotropic receptor for nucleotides

---

P2Y	Metabotropic receptor for nucleotides
PBS	Phosphate buffered saline
PC 12 cells	Rat Phaeochromocytoma cell line
PNGase F	Peptide:N-glycosidase F
PNS	Peripheral nervous system
PPADS	Pyridoxalphosphate-6-azophenyl-2',4'-disulfonic acid
pS	Pico Siemens
RB2	Reactive Blue 2
RNA	Ribonucleic acid
RT-PCR	Reverse transcription polymerase chain reaction
s	Seconds
SDS-PAGE	Sodium dodecyl sulfate polyacrylamide gel electrophoresis
Sulfo-SSHP	Sulfosuccinimidyl-3-(4-hydroxyphenyl)propionate
TM or M	Transmembrane domain
TRIS	Tris(hydroxymethyl)-aminomethane
UDP	Uridine-5'-diphosphate
UTP	Uridine-5'-triphosphate
wt	Wild-type

## 9. Bibliography

### Original Articles

Jürgen Rettinger, Armaz Aschrafi, and Günther Schmalzing  
Roles of individual N-glycans for ATP potency and expression of the rat P2X<sub>1</sub> receptor  
*Journal of Biological Chemistry*, 275, 33542–33547 (2000)

Masahisa Horiuchi, Annette Nicke, Jesus Gomeza, Armaz Aschrafi, Günther Schmalzing, and Heinrich Betz  
Surface-localized glycine transporters 1 and 2 function as monomeric proteins in *Xenopus* oocytes  
*Proc. Natl. Acad. Sci.*, 98, 1448-1453 (2001)

### Posters

#### **40. Frühjahrstagung der DGPT (Deutsche Gesellschaft für Experimentelle und Klinische Pharmakologie und Toxikologie), März 1999, Mainz**

Aschrafi A., Rettinger J., and Schmalzing G.  
N-glycans and P2X<sub>1</sub> receptor function

#### **41. Frühjahrstagung der DGPT, März 2000, Mainz**

Rettinger J., Nicke A., Aschrafi A., and Schmalzing G.  
Electrophysiological analysis of P2X<sub>2</sub>/P2X<sub>1</sub> receptor chimera expressed in *Xenopus* oocytes

Aschrafi A., Rettinger J. and Schmalzing G.  
Role of extracellular cysteine residues for the assembly and surface expression of the P2X<sub>1</sub> receptor

#### **Purines 2000, Juli 2000, Madrid, Spanien**

Aschrafi A., Rettinger J. and Schmalzing G.  
Roles of individual N-glycans for ATP potency and expression of the rat P2X<sub>1</sub> receptor

Büttner C., Sadtler S., Aschrafi A., Markwardt F., and Schmalzing G.  
The rat P2X<sub>7</sub> isoform behaves like a trimer when purified from *Xenopus* oocytes

**Oral Presentations**

**42. Frühjahrstagung der DGPT, März 2001, Mainz**

Aschrafi A., Rettinger J., and Schmalzing G.

Role of extracellular cysteine residues for the assembly and surface expression of the P2X<sub>1</sub> receptor

## 10. Curriculum Vitae

### Sepandarmaz Aschrafi

19.09.1971	Geboren in Teheran, Iran
08/77 – 01/85	Grund- und Volksschule in Teheran, Iran
01/85 – 06/86	Gustav-Heinemann Realschule in Dinslaken
08/86 – 06/88	Städtische Realschule in Wesseling
08/88 – 05/91	Städtisches Gymnasium in Wesseling, Allgemeine Hochschulreife
09/91 – 06/96	Studium der Chemieingenieurwesen, Fachrichtung Biotechnologie an der Fachhochschule Aachen Erlangung des Grades Diplom-Ingenieur (FH)
01/96 – 05/96	Durchführung einer Diplomarbeit in der Firma Basell (vormals R.O.W.) mit dem Thema: <i>Untersuchung von Kunststoff-Additiven mittels spektroskopischer Methoden</i>
09/96 – 08/97	Studium eines Masters of Science Studiumsgangs für Medizinische Biotechnologie an der Demontfort University (Leicester, Grossbritannien) und der Hogeschool West- Brabant (Breda, Niederlande)
03/97 – 08/97	Durchführung einer Diplomarbeit am Slater Institut der Universiteit van Amsterdam mit dem Thema: <i>Purification and characterization of bovine testis-specific Cytochrome c</i>
05/98 – 11/01	Anfertigung einer Dissertation in der Arbeitsgruppe von Prof. Dr. G. Schmalzing am Pharmakologischen Institut für Naturwissenschaftler in Frankfurt am Main mit dem Thema: <i>Charakterisierung der Tertiär- und Quartärstruktur von P2X-Rezeptoren</i>
05/98 – 03/01	Graduiertenstipendiat der Deutschen Forschungsgemeinschaft im Graduiertenkolleg „Arzneimittel: Entwicklung und Analytik“ im Fachbereich Biochemie, Pharmazie und Lebensmittelchemie der J. W. Goethe-Universität in Frankfurt am Main

